Einfluss membranmimetischer Umgebungen auf die Dimerisierung von Glykophorin A

JOHANNES GUTENBERG UNIVERSITÄT MAINZ

Dissertation

zur Erlangung des Grades

"Doktor der Naturwissenschaften"

Im Promotionsfach Chemie

am Fachbereich Chemie, Pharmazie und Geowissenschaften
der Johannes Gutenberg-Universität Mainz

Michael Stangl

geboren in Speyer

Mainz, Januar 2015

D77

Inhaltsverzeichnis

1. Einleitung

1.1 Die Zellmembran eine biologische Grenze

Politische Grenzen sind geographische Markierungen zwischen Staatsgebieten, die Sicherheit und Kontrolle eines Landes ermöglichen. Der Fluß von Waren, das Verhindern des Eindringens von gefährlichen Gütern, die Erhaltung der Stabilität und Rechtsordnung des Staates, all das ermöglicht eine intakte Grenze. Vergleichbare Aufgaben erfüllt die Membran einer biologischen Zelle. Die Zell- oder Plasmamembran eukaryotischer Zellen besteht aus einer Lipiddoppelschicht, welche für wasserlösliche Moleküle eine unüberwindbare Grenze darstellt, während lipophile Stoffe einfach durch die Membran diffundieren können. Die physikalische strukturgebende Grenze stellt die Lipiddoppelschicht dar, welche aus verschiedenen Spezies amphiphiler Lipide gebildet wird und eine Dicke von etwa 6-10 nm aufweist. Der hydrophobe Kern der Membran ist etwa 3 nm dick, der jeweilige Kopfgruppenbereich etwa 1,5 nm [1, 2] (Abb. 1.1). Neben der Plasmamembran sind in eukaryotischen Zellen zahlreiche interne Membransysteme zu finden, welche die Zelle in Organellen unterteilen, wie z. B. das Endoplasmatische Retikulum, das Golgi-Membransystem, die Mitochondrien, die Lysosomen und Peroxisomen sowie Chloroplasten in pflanzlichen Zellen. Diese vielzähligen Membranen sind je nach Organismus, Gewebe oder Kompartiment aus verschiedenen Lipidspezies aufgebaut [3, 4]. Die größte Gruppe dieser Lipide stellen die Phospholipide oder auch Phosphoglyceride dar, welche aus zwei hydrophoben Acylketten verestert mit einem Glycerinmolekül aufgebaut sind. Weiterhin ist die freie Hydroxygruppe über ein Phosphat mit einem weiteren Molekül, wie z. B. Cholin, Inositol, Serin, Ethanolamin, verestert (nicht im Falle von Phosphatidylglycerol), was die hydrophile Kopfgruppe des Lipids darstellt (Abb. 1.1). Des Weiteren kommen in eukaryotischen Zellen Sphingolipide in größeren Mengen vor. Das Grundgerüst der Sphingolipide stellt das Sphingosin dar, ein einfach ungesättigter Aminoalkohol aus insgesamt 18 Kohlenstoffatomen. Sphingosin ist über eine Amidbindung an eine beliebige Fettsäure gebunden, was ein Ceramidmolekül ergibt. Ceramide können über die freie Hydroxygruppe mittels eines Phosphoesters mit Cholin, Serin oder Ethanolamin verknüpft sein, was die Gruppe der Sphingomyeline darstellt (Abb. 1.1). Ist ein Ceramid glykosidisch mit einem Oligosaccharid verbunden, zählen es zu den Glycosphingolipiden (Abb. 1.1). Ein weiteres wichtiges Lipid in vielen eukaryotischen Membranen (vor allem tierischen) ist das Cholesterin (Abb.1.1), welches nicht die typische Struktur der Phospholipide aufweist, aber in hohen Mengen (bis zu 50%) in der Membran vorkommen kann [5-10]. Cholesterin kann aufgrund seiner starren Struktur die Membran stabilisieren, sie aber vorm Kristallisieren schützen, indem es die Acylketten der Phospholipide voneinander separiert und eine gewisse Fluidität erlaubt [11, 12].

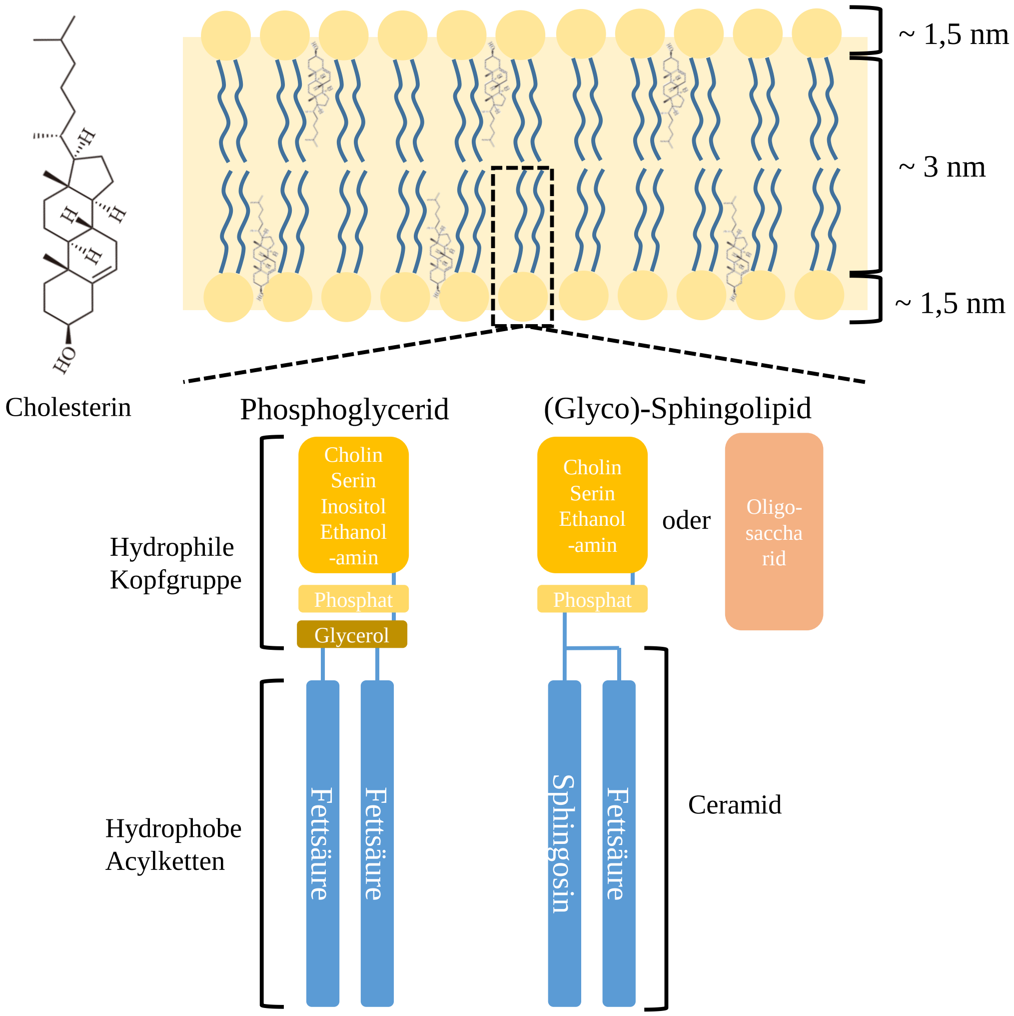

Abb 1.1 Die Lipiddoppelschicht und ihre Lipidklassen
Die Zellmembran besteht aus einer Lipiddoppelschicht mit einer Dicke von etwa 6-10 nm. Der hydophobe Bereich besitzt eine Dicke von etwa 3 nm, wobei die beiden hydrophilen Kopfgruppenbereiche jeweils etwa 1,5 nm dick sind. In einer eukaryotischen Zellmembran befinden sich hauptsächlich Phosphoglyceride, Sphingolipide und Cholesterin in verschiedenen Anteilen. Die Kopfgruppen der Lipide können variieren und können aus Cholin, Serin, Inositol, Ethanolamin oder nur Phosphoglycerol bestehen. Sphingolipide können zudem mit Oligosacchariden glycolysiert sein und gehören dann zu Gruppe der Glycosphingolipide.

Lipiddoppelschichten können je nach Temperatur und Lipidzusammensetzung in unterschiedlichen Phasen vorliegen, die sich in der Packungsdichte und der daraus resultierenden lateralen Beweglichkeit der Lipide unterscheiden. In der Gelphase unterhalb

der Übergangstemperatur (Schmelztemperatur) liegen die Acylketten der Lipide dicht gepackt vor. Oberhalb der Überganstemperatur, in der fluiden Phase, erhöht sich die laterale Bewegungsfreiheit der Lipide ähnlich einer Flüssigkeit [13]. Die verschiedenen Lipidklassen entscheiden über die physico-chemischen Eigenschaften der daraus resultierenden Membran. Fluidität, Dicke, Packungsdichte und der daraus resultierende Lateraldruck, Oberflächenladung sowie die laterale Verteilung der Lipide über die Membran stellen Parameter dar, die eine spezifische Membran genau definieren und die darin eingelagerten Membranproteine stark beeinflussen können (siehe 1.4.1) [14, 15].
Des Weiteren gibt es Lipide, die sich vornehmlich in der äußeren oder der inneren Schicht der Lipiddoppelschicht, wie z. B. Sphingomyelin und Phosphatidylcholin (außen) und Phosphatidylinositol, Phosphatidylserin und Phosphatidylethanolamin (innen), befinden [16-18]. Diese Asymmetrie wird von speziellen Flippasen, Floppasen und Scramblasen aufrechterhalten und beeinflusst eine Vielzahl biologischer Prozesse [19]. Dazu zählen z. B. die Apoptose, die Ausschüttung von Neurotransmittern, die Thrombozytenaggregation oder der Reifungsprozess von Spermien [20]. Eine Störung der Asymmetrie oder der lateralen Lipidverteilung der Membran kann zu schweren Krankheiten führen, indem die eingebetteten Membranproteine in ihrer Struktur und Funktion gestört werden [21, 22].

1.2 Membranproteine

Membranproteine, die in die Membran eingelagert sind, erfüllen eine Vielzahl von Funktionen. Sie können unter anderem als Verbindung zwischen verschiedenen Zellen, Kompartimenten oder dem Cytosol und dem extrazellulären Milieu dienen. Membranproteine repräsentieren etwa 20-30% des Proteoms der meisten Organismen [23] und stellen etwa 60% der gesamten Ansatzpunkte für Medikamente dar [24]. Etwa die Hälfte der Membranproteine durchspannen die Membran mit nur einer Helix [25, 26]. Einen Teil der Membranproteine stellen transmembrane Rezeptoren dar, die Signale in das Zellinnere übertragen. Zu diesen Rezeptoren gehört z. B. die Klasse der G-Protein-gekoppelten Rezeptoren [27], die eine wichtige Rolle bei Signaltransduktionsprozessen in Zellen spielen, oder Rezeptortyrosinkinasen, die mit nur einer transmembranen Helix die Membran durchspannen [28]. Andere Membranproteine, wie z. B. Pumpen, Kanäle oder Transporter, sind wichtig für den Transport von hydrophilen Stoffen über die Membran und den Erhalt des physiologischen Membranpotentials. Bei Prozessen, wie z. B. der Atmungskette, der Photosynthese, dem Sehvorgang in der Retina sowie dem Einstellen des Membranpotentials bei Nervenzellen spielen Membranproteine eine entscheidende Rolle. Trotz der Bedeutung von Membranproteinen ist, im Vergleich zu löslichen Proteinen, wenig über sie bekannt. Im Gegensatz zu löslichen Proteinen sind nur wenige 3D-Strukturen von Membranproteinen aufgeklärt [29, 30]. 2320 der 105268 Einträge (Stand 17.10.2014) in der Protein Data Bank sind integrale Membranproteine, was nur etwa 2% entspricht. Ein Grund dafür ist, dass die Untersuchung von Membranproteinen eine große experimentelle Herausforderung darstellt. Angefangen bei der Expression, ist vor allem die Solubilisierung der Membranproteine, die sich natürlicherweise in einer hauptsächlich hydrophoben Umgebung befinden, schwierig [31]. Zudem wurden viele Methoden für lösliche Proteine entwickelt, die aber nicht auf Membranproteine übertragbar sind. Somit erfordert die Erforschung der Membranproteine oft die Etablierung neuer Methoden [32]. Um isolierte Membranproteine in wässrigen Lösungen zu untersuchen, werden amphiphile Stoffe benötigt, die Membranproteine solubilisieren und stabilisieren können. Dabei sollten chemische und physikalische Eigenschaften der amphiphilen Moleküle die Proteinstruktur und Aktivität des Membranproteins nicht stören [33].

1.2.1 Struktur und Funktion von Membranproteinen

Membranproteine lassen sich in integrale und periphere Membranproteine einteilen. Periphere (monotopische) Membranproteine sind nur an die Membran assoziiert oder mit einem Lipidanker in der Membran verankert [34] (Abb. 1.2).

Integrale Membranproteine durchspannen die Membran komplett und werden deshalb auch Transmembranproteine genannt. Diese Transmembranproteine können wiederum in zwei Klassen eingeteilt werden. Die *β-barrel* Proteine, die eine fassartige Struktur aus β-Faltblättern besitzen, stellen eine Klasse von Proteinen dar, die nur in der äußeren Hüllmembran von Bakterien, Chloroplasten und Mitochondrien zu finden sind [35]. Die zweite und weitaus häufiger vorkommende Klasse von Transmembranproteinen durchspannt die Membran mit einer (bitopisch) oder mehreren (polytopisch) α-helikalen Transmembranhelices, die meist aus 15-30 hydrophoben Aminosäuren (AS) bestehen. Dabei muss die Helix eine Distanz von etwa 30 Å, was etwa der Dicke der hydrophoben Acylketten der Lipiddoppelschicht entspricht, überbrücken [36]. Um solche Transmembranhelices zu identifizieren, genügt oft schon die Kenntnis der Aminosäuresequenz des Proteins. Mittels eines Hydrophathiediagramms ist in vielen Fällen eine Vorhersage einer Transmembranhelix möglich, da die Häufigkeit hydrophober Aminosäuren einen Höhepunkt in der Mitte der

Membran hat [34, 37]. Die niedrige Konzentration von Wassermolekülen in der Membran ermöglicht die Ausbildung einer stabilen α-Helix, die über Wasserstoffbrücken des Peptidrückgrates stabilisiert ist [38].

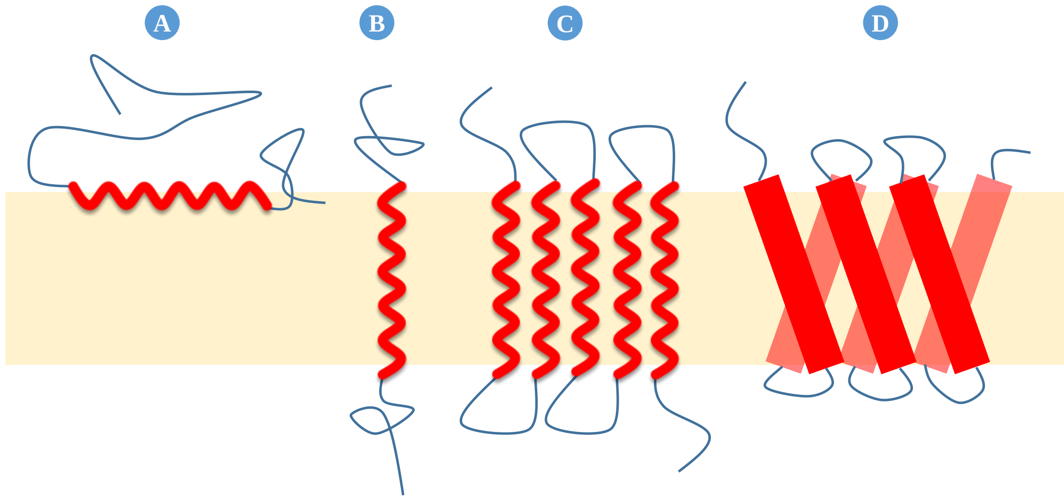

Abb. 1.2 Klassen von Membranproteinen
(A) Monotopische periphere Membranproteine sind an die Membran assoziiert. (B) Bitopische integrale Membranproteine durchspannen die Membran mit einer einzigen α-Helix. (C) Polytopische integrale Membranproteine durchspannen die Membran mit mehreren α-Helices. (D) Polytopische integrale β-Fass-Membranproteine durchspannen die Membran mit mehreren β-Faltblättern und bilden eine Pore aus.

1.2.2 Oligomerisierung von Transmembranhelices

Transmembranhelices bilden in Lipiddoppelschichten oft eine höher geordnete Struktur aus. Die Ausbildung ihrer korrekten Tertiär- und Quartärstruktur hat eine starke Auswirkung auf die Aktivität und Funktion der Membranproteine. Der Assemblierung eines bitopischen oder polytopischen Membranproteins liegen einfache Helix-Helix-Interaktionen zu Grunde [39]. Die Wichtigkeit der Interaktion einzelner Transmembransegmente bitopischer Membranproteine zeigen folgende Beispiele. Die Transmembranhelix von Integrinen, fördert die Ausbildung eines αβ-Dimers, wodurch wichtige Informationen in beiden Richtungen über die Membran gelangen können [40, 41]. Signale aus dem Inneren der Zelle initiieren die Interaktion von Integrinen mit Makromolekülen, die Zell-Zell- und Zell-Matrixkontakte herstellen können. Signale von außen werden über Integrine weitergeleitet und beeinflussen die Zytoskelett-Organisation, die Zellmigration, die Zellproliferation, die Zelldifferenzierung sowie den Vorgang der Apoptose [42]. Ein weiteres wichtiges Beispiel für die Relevanz der Oligomerisierung bitopischer Membranproteine sind Rezeptortyrosinkinasen, die über ihre Transmembranhelix dimerisieren oder höhere Oligomere ausbilden. Dabei ermöglicht die

Dimerisierung die Autphosphorylierung des Rezeptors, wodurch Signale ins Innere der Zelle weitergeleitet werden [43]. Die MHC Klasse-II Moleküle stellen einen Schlüsselinitiator in der Immunantwort einer Zelle dar. Mittels eines speziellen Aminosäuremotivs dimerisieren MHC Klasse-II Moleküle und ermöglichen die Ausbildung des MHC Komplexes [44]. Das Vorläuferprotein der Amyloid β-Peptide, welches in Zusammenhang mit der Alzheimer Erkrankung gebracht wird, APP, besitzt ebenfalls eine dimerisierende Transmembranhelix, wobei der oligomere Zustand des Proteins einen Einfluss auf die Prozessierung durch Proteasen hat [45, 46].

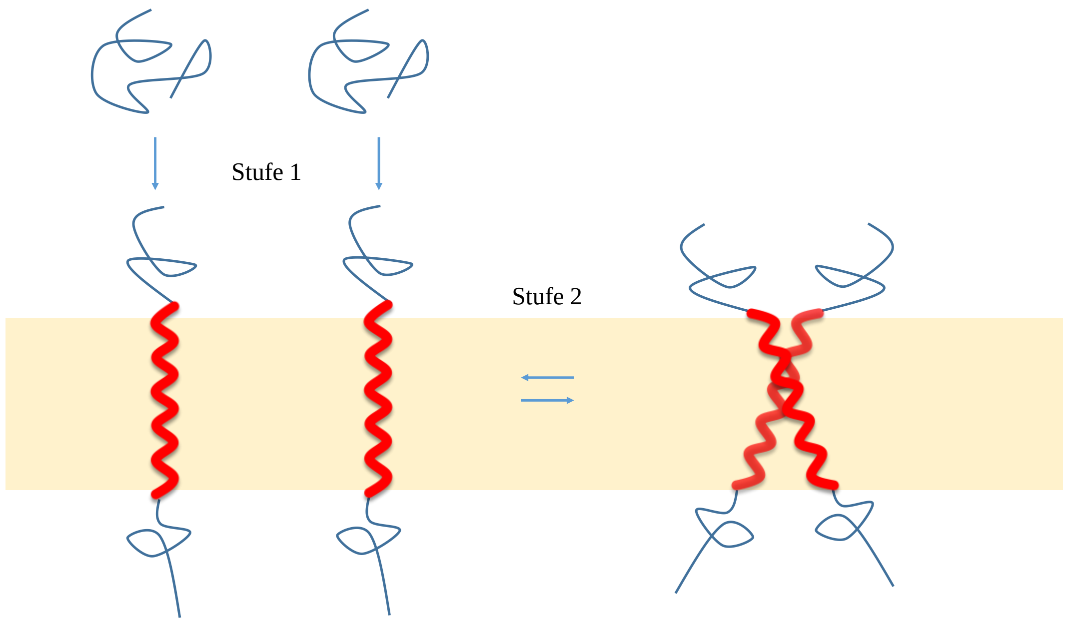

Abb. 1.3 Das 2-Stufen Modell (Popot und Engelmann) zur Faltung von Membranproteinen
In einer ersten Stufe bilden die Membranproteine unabhängig voneinander stabile α-Helices in der Membran aus. In einer zweiten Stufe können diese miteinander interagieren. Bei der Oligomerisierung der Transmembranhelices handelt es sich um einen Gleichgewichtsprozess.

Das mit am besten untersuchte Membranprotein ist Bakteriorhodopsin aus dem Archaeon *Halobacterium salinarium*, welches aus sieben Transmembranhelices besteht, die über kleine Schleifen miteinander verbunden sind [47, 48]. Es konnte gezeigt werden, dass das Protein aus einzelnen Fragmenten rekonstituiert werden kann und dabei seine Funktion nicht verliert. Die durch Proteasen getrennten Schleifen tragen somit nicht entscheidend zur Interaktion der Transmembranhelices bei [49]. Basierend auf diesem und weiteren Versuchen wurde das 2-Stufen-Modell zur Faltung bzw. Assemblierung α-helikaler Transmembranproteine vorgeschlagen [50] (Abb. 1.3). Die erste Stufe beschreibt die unabhängige Ausbildung stabiler Transmembranhelices in einer Membran. In einer zweiten Stufe können diese miteinander interagieren, wobei höher geordnete Strukturen ausgebildet werden. Effekte der löslichen Domänen oder möglicher gebundener Co-Faktoren werden dabei allerdings nicht berücksichtigt. Diese werden aber teilweise in einem erweiterten 3-Stufen-Modell mit eingebunden [51]. Die Interaktion einzelner α-Helices lässt sich allerdings ausreichend durch das 2-Stufen-Modell beschreiben.

Aus der Energiebilanz der Interaktion zwischen Lipiddoppelschicht und Transmembranhelix ergibt sich, dass die Oligomerisierung von Transmembranhelices thermodynamisch meist bevorzugt ist. Die Helix-Helix-Interaktion, beziehungsweise deren Assoziation in Membranen oder membranmimetischen Umgebungen, wird von zwei Energiebeiträgen beeinflusst. Zum einen durch den Enthalpiebeitrag der Helix-Helix-, Lipid-Lipid- und Helix-Lipid-Interaktionen. Hierbei ist die Ausbildung von Van-der-Waals-Kräften zwischen hydrophoben Aminosäuren der dicht gepackten Helices gegenüber der Helix-Lipid-Interaktion energetisch begünstigt. Zum anderen trägt die Entropie des Systems zur Interaktion der Helices bei, indem bei der Helix-Helix-Interaktion Lipide frei werden, die vorher eine Helix-Lipid-Interaktion eingegangen sind und somit nicht frei beweglich waren, was eine erhöhte Entropie des Systems zur Folge hat.

Die Assoziation der Transmembranhelices findet jedoch nicht zufällig statt. Anhand von Mutationsanalysen wurde gezeigt, dass eine spezifische Interaktion von Transmembranhelices durch eine definierte Aminosäuresequenz zustande kommen kann. Für die Interaktion von Transmembrandomänen konnte ein hochspezifisches, für eine starke Interaktion verantwortliches Motiv, das GxxxG-Motiv, identifiziert werden (siehe 1.3) [52-57]. Homo-Interaktionen anderer Transmembrandomänen können aber auch von Serin/Threonin Motiven, QxxS-Motiven, aromatischen Aminosäuren oder Carboxamid-Aminosäuren vermittelt werden [58]. Die Wechselwirkungen zwischen den Helices können somit von Van-der-Waals-Wechselwirkungen, Wasserstoffbrücken, ionischen Wechselwirkungen sowie π-Stapelwechselwirkungen aromatischer Ringe ermöglicht werden. Allerdings hängt die Stärke dieser Wechselwirkungen sehr vom Abstand der Bindungspartner ab. Deshalb ist eine dichte Packung der Helices wichtig. Diese wird durch ein reißverschlussartiges Ineinandergreifen der Aminosäureseitenketten und kleinen Aminosäuren (Gylcin, Alanin) an der direkten Kontaktfläche ermöglicht.

Viele Zellprozesse basieren auf der Dimerisierung von Transmembranhelices, wobei der Effekt äußerer Einflüsse, wie z. B. der Lipidmembran, wenig verstanden ist. In dieser Arbeit wurde die humane Glykophorin A (GpA) Transmembranhelix als Modellprotein verwendet, um den Effekt der direkten Membran- oder membranmimetischen Umgebung auf die Dimerisierung von GpA zu untersuchen.

1.3 Glykophorin A als Modellprotein für Dimerisierungsstudien

Glykophorine sind Sialoglykoproteine, die in der Membran von roten Blutzellen vorkommen [59, 60]. Alle Mitglieder der Glykophorin-Proteinfamilie sind bitopische Transmembranproteine, die am N-Terminus durch eine hohe Zahl von glykosylierten Aminosäuren gekennzeichnet sind. Dabei handelt es sich um den negativ geladenen Zucker Sialinsäure, welcher der Zelloberfläche eine starke negative Ladung verleiht. Ein menschlicher Erythrozyt kann dabei bis zu 20 Millionen Sialinsäuremoleküle pro Zelle tragen. Zu den menschlichen Glykophorinen gehören Glykophorin A, B, C, D und E, wobei GpD eine Variante von GpC ist. GpA, GpB und GpE sind Bestandteile des MNS-Blutgruppensystems [61]. Die genaue biologische Funktion von GpA ist derzeit jedoch noch nicht bekannt. Möglicherweise verhindert die negative Ladung an der Oberfläche der Zelle eine Adhäsion an andere Zellen, um somit die Zirkulation der Erythrozyten in den Blutgefäßen zu erleichtern. Zudem ist bekannt, dass GpA eine wichtige Rolle als Rezeptor für Viren, wie z.B. das Influenza Virus, spielt [62]. Weiterhin scheint GpA dem Malaria Parasiten (*Plasmodium sp.*) das Eindringen in die Zelle zu ermöglichen, da Erythrozyten, die kein GpA exprimieren, immun gegen den Parasiten sind [63-67].

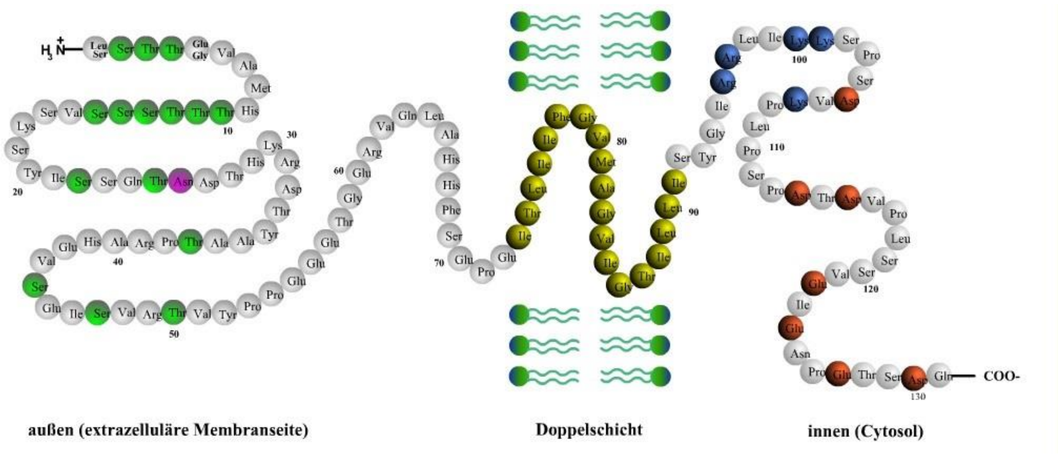

Abb. 1.4 Primärstruktur von GpA
Hydrophobe AS (gelb), negativ geladene AS (rot), positiv geladene AS (blau), O-glykosylierte AS (grün), N-glykosylierte AS (lila) [68].

GpA besteht aus einer einzelnen Polypeptidkette, wobei der N-Terminus außerhalb der Zelle und der C-Terminus im Cytosol liegt. Im Transmembranbereich des Proteins befinden sich 19 unpolare Aminosäuren, welche die Transmembranhelix ausbilden (Abb. 1.4). Die NMR-

Struktur von GpA wurde in Dodecylphosphocholin-Mizellen aufgeklärt (PDB: 2 KPE) [69]. Es handelt sich um eine rechtshändig gedrehte α-Helix, welche in einem Kontaktwinkel von etwa 40° dimerisiert (Abb. 1.5). Die Interaktionsfläche ist leicht zum N-terminalen Ende der Transmembranhelix gerichtet und liegt daher nicht exakt in der Mitte der Lipiddoppelschicht [69]. Die Dimerisierung der GpA-Transmembrandomäne wurde in den letzten Jahren mit vielen biochemischen und biophysikalischen Methoden untersucht, um den molekularen Vorgang bei der Dimerisierung von Transmembranhelices besser zu verstehen. Zu Beginn der Untersuchungen an der GpA-Transmembranhelix wurden die bereits erwähnten Mutationsanalysen durchgeführt, wobei ein Dimerisierungsmotiv in der Transmembrandomäne von GpA identifiziert werden konnte [52-54]. Da die Dimerisierung auf Proteinebene aufgeklärt wurde, stellte sich die Frage, ob die Art der hydrophoben Umgebung der GpA Transmembrandomäne die Dimerisierung beeinflussen kann. Es wurde gezeigt, dass die Transmembranhelices von GpA z. B. in einer SDS-PAGE [52], in künstlichen sowie biologischen Membranen dimerisieren können [70-74].Zahlreiche Studien konnten bereits vor 20 Jahren die Homodimerisierung der Transmembrandomäne des Erythrocyten-Proteins GpA nachweisen [52-54]. In diesen Studien konnte folgendes hochspezifische und eine starke Interaktion ermöglichende Aminosäuremotiv in der GpA-Transmembranhelix identifiziert werden [52-54].

$$^{94}\mathbf{L\text{-}I\text{-}x\text{-}x\text{-}\underline{G}\text{-}V\text{-}x\text{-}x\text{-}\underline{G}\text{-}V\text{-}x\text{-}x\text{-}T}^{106}$$

Dieses Aminosäuremotiv besteht hauptsächlich aus hydrophoben β-verzweigten Aminosäuren, wobei die Aminosäuresequenz GxxxG, in der Mitte des Dimerisierungsmotivs, notwendig für die Dimerisierung von GpA ist. Das GxxxG-Motiv ermöglicht aufgrund der Lage der beiden Glycine auf der gleichen Seite der Helix (Abb. 1.5), und der kleinen Glycinseitenkette, eine planare Kontaktfläche zwischen den beiden Helices. Diese können eine sehr dichte Packung eingehen, die Wasserstoffbrückenbindungen und vor allem eine Vielzahl von Van-der-Waals-Interaktionen zwischen den weiteren Aminosäuren der Helices ermöglicht. Die Vielzahl von Interaktionen ist somit, neben dem Entropiegewinn der Lipide, die treibende Kraft der Helix-Helix-Assoziation. Zudem kommt es bei der Helix-Helix-Interaktion zu einer Abnahme der Entropie der Aminosäureseitenketten, da diese in ihrer Rotation eingeschränkt werden. Dies ist für die beiden wichtigen Glycine, aufgrund der kleinen Seitenkette, nicht der Fall, was erklärt, dass diese oft an der Dimerisierung von α-Helices beteiligt sind und die bereits erwähnte dichte Packung ohne Entropieverlust ermöglichen [75].

Das GxxxG-Motiv konnte bereits in einer Vielzahl von Membranproteinen nachgewiesen werden und dessen Wichtigkeit für die Oligomerisierung der Proteine konnte oft bestätigt werden [76-78]. Allerdings bestimmen weitere Aminosäuren über die Spezifität und Stärke der Interaktion, damit sich unter hunderten Transmembranhelices in derselben Membran die richtigen Interaktionspartner finden.

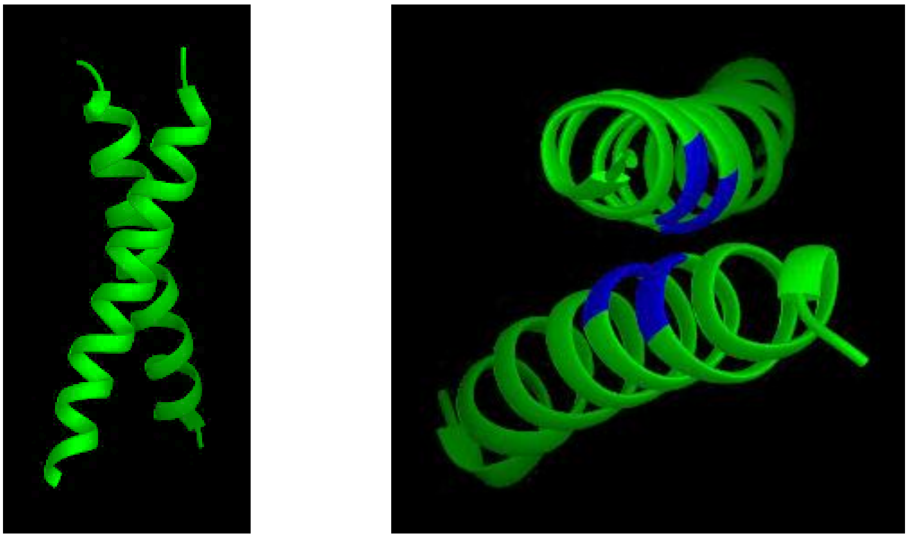

Abb. 1.5 NMR-3D-Struktur des GpA Dimers
Die pdb Struktur 2KPE [69] zeigt das GpA-Dimer gemessen in Dodecylphoscholin Mizellen. Glycine des GxxxG-Motives sind in der rechten Abbildung in blau markiert (Blick von oben auf das Dimer).

Zur Quantifizierung der sequenzspezifischen Dimerisierung von Transmembranhelices wurden sowohl *in vivo* als auch *in vitro* Methoden unter Verwendung der GpA-Transmembranhelix entwickelt. *In vivo* können mit Hilfe der genetischen Systeme GALLEX [79], TOXCAT [80], ToxR [81], POSSYCCAT [82] und BACTH [83] Homo- sowie Heterodimerisierung zweier Helices bestimmt werden [84, 85]. *In vitro* lassen sich Förster-Resonanzenergietransfer (FRET) Studien durchführen, die eine genaue Bestimmung des Verhältnisses von Monomer zu Dimer zulassen [86, 87]. Es konnte gezeigt werden, dass das GpA-Dimer in zwitterionischen Detergenzien (z. B. DPC und DDMAB) doppelt so stabil ist wie in SDS-Mizellen und höhere SDS-Konzentrationen die Dimerisierung der Transmembranhelices vermindert [73, 74]. Dies bedeutet, dass milde und der Natur ähnelnde amphiphile Stoffe besser geeignet sind, um die Dimerisierung von Transmembranproteinen zu stabilisieren. Des Weiteren konnte gezeigt werden, dass in den bisher verwendeten Detergenzien und Lipiden die Dimerisierung unabhängig von der Ausbildung der α-Helix ist, da sich die Sekundärstruktur der GpA-Peptide unter den getesteten Bedingungen nicht verändert. Diese Beobachtungen korrelieren mit dem 2-Stufen-Modell von Popot und

Engelman. In künstlichen Membranen, wie z. B. Liposomen, konnte gezeigt werden, dass die Dicke sowie die Fluidität der Lipiddoppelschicht, die abhängig von der Länge der hydrophoben Ketten der Lipide ist, einen entscheidenden Einfluss auf die Dimerisierung der GpA-Transmembrandomäne hat [72]. Neueste Untersuchungen zeigten jedoch auch, dass eine künstliche Lipidmembran, die der Plasmamembran in ihrer Zusammensetzung nachempfunden ist, sogar eine starke Destabilisierung des GpA Dimers hervorrufen kann [88]. Die GpA-Transmembranhelix besitzt eine Länge von etwa 32 Å und integriert optimal in die Membran, wenn deren hydrophober Kern eine Dicke von etwa 32 Å aufweist. Ändert sich die Dicke der Membran, kann sich die GpA-Transmembranhelix gegebenenfalls mit einem anderen Neigungswinkel in die Membran einlagern, was die Effizienz der Dimerisierung beeinflussen kann. Dieser Effekt wird als *hydrophobic mismatch* bezeichnet [89, 90]. Des Weiteren wirkt sich der Ordnungsgrad einer Membran auf das Dimer-Monomer-Gleichgewicht von GpA aus [72]. Nimmt die Ordnung der Membran und somit die Packungsdichte der Lipide, z. B. durch die Zugabe eines Anästhetikums oder durch das Verkürzen der Lipid Acylkette, ab, reduziert sich der Anteil an GpA-Dimeren deutlich [72]. Dieser Effekt beruht auf veränderten Lipid-Lipid- und Lipid-Protein-Wechselwirkungen, die die Energiebilanz der Helix-Helix-Assoziation beeinflussen. Zudem scheint die Ladung der Lipidkopfgruppen einen Effekt auf das GpA-Dimer zu haben. Interaktionen von cytosolisch lokalisierten positiv geladenen Aminosäuren des GpA mit negativ geladenen Lipidkopfgruppen scheinen die Dimerisierung erheblich zu stören [88].

Da GpA bisher sehr gut charakterisiert wurde, dient die GpA-Transmembranhelix als geeignetes Modell, um vielfältige neue amphiphile Systeme und deren Einfluss auf die Dimerisierung membranständiger α-Helices studieren zu können.

1.4 Amphiphile Stoffe zur Untersuchung von Membranproteinen

Die Charakterisierung von Membranproteinen ist im Vergleich zu löslichen Proteinen ein schwieriges Unterfangen. Membranproteine lösen sich nicht in Wasser, sondern aggregieren, indem sich ihre hydrophoben Bereiche zusammenlagern und dabei Wassermoleküle verdrängen. Um isolierte Membranproteine *in vitro* biochemisch und biophysikalisch untersuchen zu können, muss die natürliche Umgebung der Proteine, die Zellmembran, ersetzt werden. In der Regel dienen dazu Detergenzien, Lipide und neuerdings synthetische amphiphile Copolymere (Abb. 1.6). Zur Charakterisierung isolierter Membranproteine, werden diese meist heterolog in *E. coli* Bakterien, Hefen oder eukaryotischen Zelllinien exprimiert und darauffolgend extrahiert. Um die Membranproteine aus der nativen Membran zu isolieren, werden Detergenzien zugegeben. In einem ersten Schritt destabilisieren die Detergenzmoleküle die Zellmembran und verdrängen anschließend die Lipidmoleküle von den hydrophoben Transmembranbereichen des Membranproteins, wodurch sie selbst mittels der hydrophoben Kette mit dem Protein interagieren. Dabei kann es aber zu Problemen kommen. Das Protein löst sich nicht, aggregiert und ist meist unwiderruflich verloren. Des Weiteren besteht die Möglichkeit, dass sich das Protein zwar löst, aber nicht in seinem nativen, funktionalen Zustand verbleibt, wodurch es nicht für weitere Experimente verwendbar ist. Daher ist es von großer Bedeutung, das richtige Detergenz zur Solubilisierung von Membranproteinen zu wählen. Jedes Membranprotein erfordert unterschiedliche Bedingungen zur Ausbildung seiner funktionalen Konformation in wässriger Lösung [91, 92]. Nach diesem Schritt kann das Membranprotein z.B. in Lipidliposomen oder Copolymere eingebaut und rekonstituiert werden, um es weiter zu untersuchen.

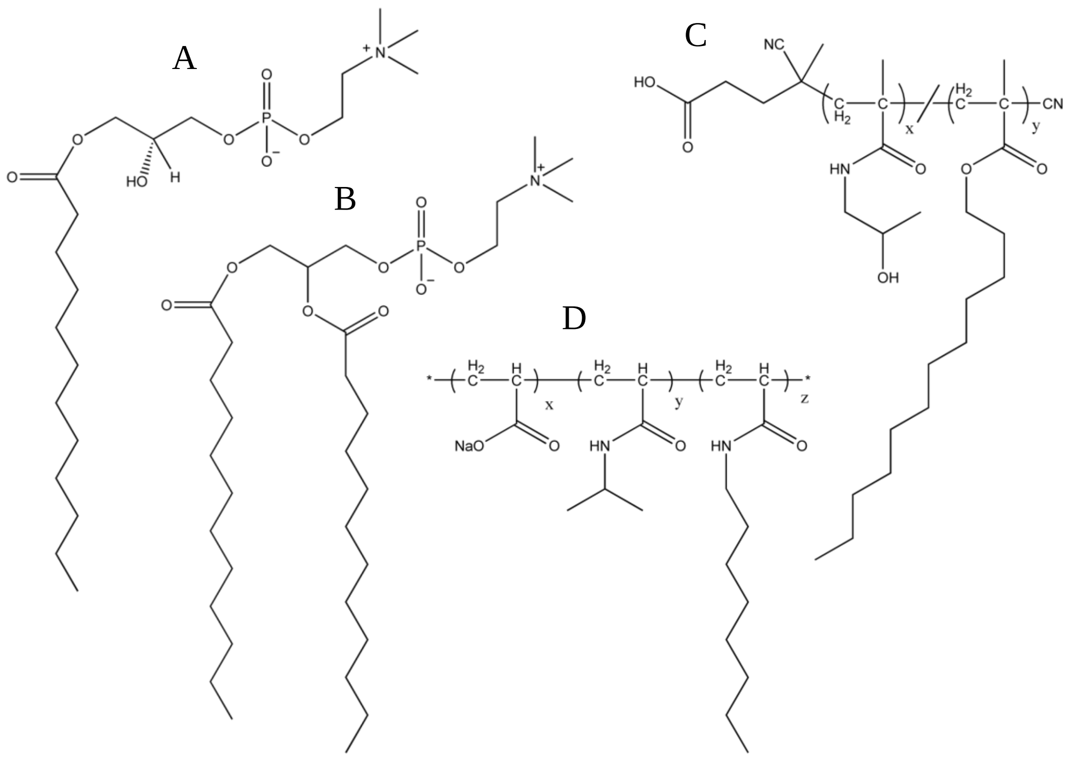

Abb. 1.6 Amphiphile Moleküle zur Solubilisierung von Membranproteinen
Chemische Struktur eines Detergenz (A) Lauryl-Lysophosphocholin, und eines doppelschichtbildenden Lipides (B) Dilaurylphosphocholin. (C) stellt ein amphiphiles HPMA (x)-LMA (y) Copolymer dar wobei die beiden Monomere x und y statistisch über die Polymerkette verteilt sind. (D) Amphipol A8-35 ist ein kommerziell erhältliches Terpolymer mit Monomeranteilen in der Gesamtpolymerkette von x = 0,35; y = 0,25; z = 0,40.

Eine neue Klasse von Polymeren, die sogenannten SMA (Polystyrol-malein-anhydride) Polymere, sind in der Lage, Membranproteine direkt aus ihrer nativen Membran in Form von kleinen Nano-Lipiddiscs herauszulösen, und z.B. eine affinitätschromatographische Reinigung des Proteins kann im Anschluss folgen [93, 94]. Die daraus erhaltenen Nano-Lipiddiscs halten das Membranprotein in seiner natürlichen Umgebung. Diese lassen sich für alle bekannten spektroskopischen Methoden sehr gut verwenden [95, 96]. Somit kann in diesem Fall der Einsatz von Detergenzien vermieden werden, was neue Möglichkeiten in der Membranprotein Forschung ermöglicht. Jedoch sind zum jetzigen Zeitpunkt Detergenzien noch nicht wegzudenken und durch ihre Vielfalt stellen sie ein wichtiges Werkzeug für die Erforschung isolierter Membranproteine dar.

1.4.1 Synthetische Phospholipide zum Nachbau natürlicher Membranen

Um lipidspezifische Effekte auf die Faltung von Membranproteinen zu untersuchen, können Membranen mit synthetisch hergestellten Lipiden in Form von Liposomen imitiert werden.
Im Vergleich zu Detergenzien und Polymeren, die Mizellen (Abb. 1.7A) oder mizellenartige Strukturen (Abb. 1.7C) bilden, formen Phospholipide eine Lipiddoppelschicht (Abb. 1.7B), ähnlich der Zellmembran. Die Phospholipide können in Kettenlänge, Sättigungsgrad sowie der Kopfgruppe variieren. Alle drei Parameter können über die Fluidität der Membran entscheiden. Soll die Dicke der Membran gezielt variiert werden, kann dies durch Änderung der Acylkettenlänge realisiert werden. Fluidität sowie die Dicke der Membran spielen z. B. eine wichtige Rolle bei der Dimerisierung der GpA-Transmembranhelix [72]. Lagert sich eine Transmembranhelix in eine Membran einer bestimmten Dicke ein, so kann es, wenn die Länge der Helix nicht mit der Dicke der Membran übereinstimmt, zu dem bereits erwähnten *hydrophobic mismatch* kommen. Dieser *mismatch* kann Helix-Helix-Interaktionen beeinträchtigen was weitreichende Folgen auf Proteinaktivität, Stabilität, Orientierung, Oligomerisierung, Lokalisierung und Konformation haben kann [90].
Neben den hydrophoben Acylketten kann auch die Chemie der Lipidkopfgruppen variieren. Die Kopfgruppen von Phospholipiden sind meist Cholin, Inositol, Ethanolamin, Phosphoglycerol oder Serin (siehe 1.1) und unterscheiden sich durch ihre verschiedene Ladung und ihre hydrodynamischen Radius. Die Ladungen der Kopfgruppen geben der Lipidoberfläche eine charakteristische Nettoladung, die in natürlichen Membranen meist negativ ist [97, 98]. Diese negativen Ladungen können Ionen, die in der Zelle in verschiedenen Konzentrationen vorkommen, anziehen. Ein wichtiger sekundärer Botenstoff sind z. B. Calciumionen, die bei Signaltransduktionenprozessen eine wichtige Rolle spielen. Es ist naheliegend, dass Calciumionen durch Wechselwirkungen mit Lipidkopfgruppen die

Membran, möglicherweise auch Membranproteine, beeinflussen können. Bereits bekannt ist, dass Calcium an negativ geladene Lipide bindet, die laterale Verteilung verschiedener Lipidspezies verändert und die Fusion von Membranen auslösen kann [99, 100].

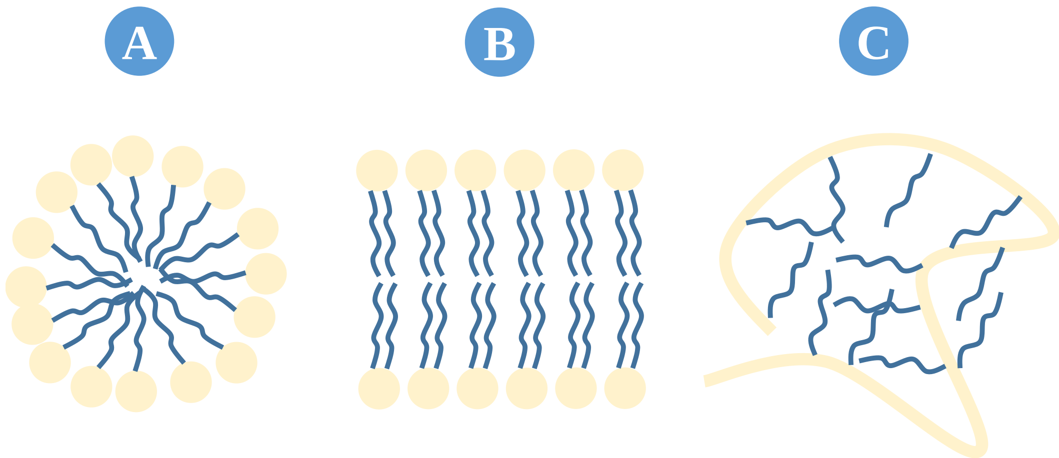

Abb. 1.7 Aggregate amphiphiler Stoffe in Wasser
(A) Detergenzmizelle (hydrophile Kopfgruppe-beige, hydrophobe Acylkette-blau). (B) Lipiddoppelschicht (hydrophile Kopfgruppe-beige, hydrophobe Acylkette-blau). (C) mizellenartiges Polymeraggregat, hydrophiles Polymerrückgrat (beige) umschließt die hydrophoben Polmyerseitenketten (blau).

Ändert sich jedoch die Kopfgruppengröße, so hat dies einen Einfluss auf die Architektur des Lipids und dessen Raumanspruch in der Membran [101]. Befinden sich z. B. Phosphatidlyethanolamin-Lipide in der Membran, erhöht dies den lateralen Druck in der Membran, da bei Phosphatidlyethanolamin-Lipide im Gegensatz zu den meisten anderen Phospholipiden die Acylketten mehr Platz beanspruchen als die Kopfgruppe und diese Lipide alleine keine Lipiddoppelschicht ausbilden würden [102, 103]. Ähnlich wie beim *hydrophobic mismatch* können Membranproteine dadurch stark beeinflusst werden [104, 105]. Lipiddoppelschichten können somit die Membranproteinfaltung abhängig von Dicke, Ladung, Fluidität und Lateraldruck beeinflussen (Abb. 1.8). In Form von Liposomen lassen sich gezielt unzählige Membranzustände simulieren, um die Faltung von Membranproteinen, abhängig von der Lipidumgebung, zu untersuchen.

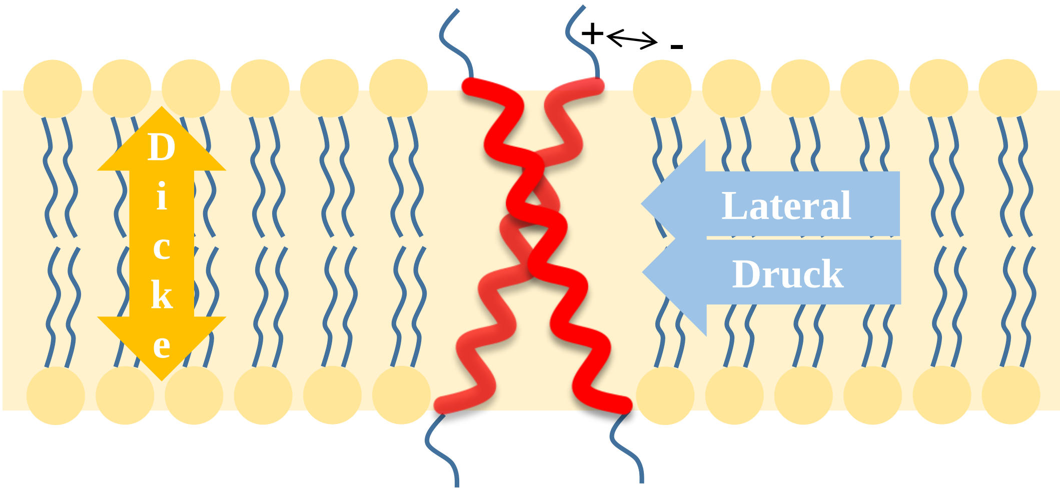

Abb. 1.8 Eigenschaften von Lipiddoppelschichten beeinflussen die Membranproteinfaltung
Die Zusammensetzung der Membran aus verschiedenen Phospholipiden entscheidet über deren Eigenschaften. Lateraldruck (inklusive Membranfluidität) Membrandicke und Ladung können die Faltung und Aktivität von Membranproteinen stark beeinflussen.

1.4.2 Detergenzien als Membranersatz

Detergenzien bestehen in der Regel aus einem hydrophilen Teil, gebunden an einen hydrophoben Bereich, was ihnen einen amphiphilen Charakter gibt. Drei Parameter entscheiden im Allgemeinen über die Eigenschaften eines Detergenz: die Länge der hydrophoben Acylkette, die Größe der hydrophilen Kopfgruppe sowie die Ladung der Kopfgruppe. Diese Parameter sind wiederum ausschlaggebend für die Eigenschaften der Detergenzmizellen, die sich in wässriger Lösung ausbilden. Durch den *Hydrophoben Effekt*, der die Zusammenlagerung unpolarer Stoffe in wässriger Lösung beschreibt, bilden Detergenzmoleküle Mizellen aus. Mizellen sind globuläre Aggregate, deren Kern hydrophob und, deren äußere Hülle hydrophil ist (Abb. 1.7A). Detergenzmoleküle lagern sich ab einer bestimmten Konzentration, *critical micellar concentration* (CMC), zu Aggregaten zusammen, indem die hydrophoben Acylketten Van-der-Waals-Wechselwirkungen ausbilden und Wassermoleküle aus dem hydrophoben Aggregat ausschließen. Die Erhöhung der Entropie der freigewordenen Wassermoleküle ist die treibende Kraft der Mizellenbildung. Der ausgebildete hydrophobe Kern ähnelt dem hydrophoben Bereich einer Lipiddoppelschicht, wodurch sich die hydrophoben Transmembranbereiche der Membranproteine in die Mizelle einlagern können. Die Natur des Detergenz sowie die Pufferbedingungen (pH, Ionenstärke, etc.) bestimmen über die Eigenschaften der Mizellen. Zum einen kann die CMC, die Detergenzkonzentration ab der sich Mizellen bilden, variieren. Des Weiteren kann die Aggregationszahl, die Anzahl der Detergenzmoleküle in einer Mizelle, sowie die äußere

Erscheinungsform (globulär, röhrenförmig, invers), sich je nach Art des Detergenz unterscheiden [106]. Diese Parameter können weiterhin einen starken Einfluss auf die Sekundär-, Tertiär- und Quartärstruktur eines Membranproteins ausüben, da die Mizelle das direkte Lösungsmittel des Membranproteins verkörpert. Aus diesem Grund ist es notwendig, neben der Oligomerisierung des Membranproteins auch die Eigenschaften der Mizellen zu charakterisieren, um genauere Einblicke in den Effekt der amphiphilen Stoffe auf die Faltung des Membranproteins zu bekommen. Diese Erkenntnisse können z. B. sehr wichtig für die Kristallisation von Membranproteinen sein, um nativ gefaltete Membranproteine zu erhalten, aber auch für weitere Untersuchungsmethoden in Detergenz gilt.

1.4.3 Amphiphile Copolymere als Alternative zu Detergenzien

Im Jahre 1996 beschrieb die Forschungsgruppe von Jean-Luc Popot erstmals ein amphiphiles Copolymer namens Amphipol A8-35 (Abb. 1.6D), welches als Ersatz für Detergenzien zur Solubilisierung von Membranproteinen verwendet werden konnte [107]. Dabei handelte es sich um ein Terpolymer bestehend aus einer Polyacrylatkette, die an verschiedenen Stellen mit Isopropylamin und Ocytylamin vernetz ist. Daraus ergeben sich drei verschiedene Monomer Einheiten. Das Acrylat verleiht der Polymerkette eine negativ geladene hydrophile Oberfläche. Die Isopropyleinheiten dienen zur Verminderung der Ladungsdichte der Polymerkette, um Abstoßungseffekte durch die Acrylatgruppen zu vermeiden. Um dem Polymer einen amphiphilen Charakter zu geben, sind Octylketten über die Polymerkette verteilt. A8-35 besitzt eine hohe Wasserlöslichkeit von über 200 g/L und bildet in wässriger Lösung mizellenartige monodisperse Aggregate aus. Diese Aggregate (Abb. 1.7C) setzen sich aus wenigen Polymerketten (~4) zusammen und bilden sich bereits ab Polymerkonzentrationen im nanomolaren Bereich, was einen deutlichen Vorteil gegenüber Detergenzien darstellt [108-110]. Detergenzien haben CMC-Werte im mikromolaren bis millimolaren Bereich, was zur Folge hat, dass viele Detergenzmoleküle als Monomere vorliegen und nicht in Mizellen zu finden sind. Frei vorliegende Detergenzmoleküle oder nicht proteinbeinhaltende Mizellen stellen ein Problem dar, da sie Proteindesaktivierung durch Dissoziation von Proteinkomplex-Untereinheiten, sowie Phasenseparation in Kristallisationsexperimenten oder eine erhöhte Viskosität der Lösung bei NMR-Experimenten, hervorrufen können [107]. Durch die Möglichkeit A8-35 in sehr niedrigen Konzentrationen einsetzen zu können, lässt es sich leicht gegen Detergenz, gebunden an Membranproteine, austauschen, um im Folgenden weitere Untersuchungen durchzuführen.

Des Weiteren sind aufgrund der niedrigen Einsatzkonzentration von A8-35 wenige, nicht an Protein-Polymer-Aggregaten beteiligte, Polymermoleküle in Lösung vorhanden, womit Amphipole wenig denaturierend auf Membranproteine wirken [107]. Neben Amphipol A8-35 gibt es eine Vielzahl von Derivaten, die sich in der statistischen Zusammensetzung, Länge der hydrophoben Kette und Ladung der Polymerkette unterscheiden [110, 111].

Zudem wurden bereits fluoreszenmarkierte Amphipole synthetisiert, um z. B. direkte Amphipol-Membranprotein-Interaktionen untersuchen zu können. Aufgrund der relativ einfachen Synthese sind Funktionalisierungen der Amphipole keine Grenzen gesetzt. Mehr als 30 Membranproteine konnten bisher in Amphipolen solubilisiert werden, wobei deren native Struktur sowie ihre Aktivität erhalten werden konnten [110]. Allerdings stellt eine Polymerkette ein rigides Gerüst dar, welches weit weniger dynamisch als eine Detergenzmizelle ist. Dies wiederrum kann die stabilisierenden Eigenschaften des Amphipols auf Membranproteine erklären. Sind im Protein jedoch große strukturelle Veränderungen für die Aktivität erforderlich, kann der rigide "Gürtel" des Amphipols hinderlich sein. Dies konnte bei der sarkoplasmatischen Calcium-ATPase, deren Aktivität durch eine Amphipol-Umgebung inhibiert wurde, beobachtet werden [112, 113]. Da die Faltung von Membranproteinen letztendlich durch Helix-Helix-Interaktionen bestimmt wird, ist es von Bedeutung, den Effekt von Amphipolen auf die Interaktion einzelner Transmembranhelices zu untersuchen.

Eine weitere Klasse amphiphiler Copolymere, ähnlich zu den Amphipolen, sind p(HPMA)-co-p(LMA)-Copolymere (Abb. 1.6C). In der Arbeitsgruppe von Prof. Dr. Rudolf Zentel an der Universität in Mainz wird die Synthese dieser Polymere ständig verfeinert und eine Vielzahl von Varianten der Polymere kann reproduzierbar synthetisiert werden.

Die Polymere bestehen aus Hydroxypropylmethacrylamid (HPMA) und Laurylmethacrylamid (LMA) Monomeren, die statistisch über die Polymerkette verteilt sind. Die letztendliche Zusammensetzung hängt vom stöchiometrischen Einsatz der Monomervorstufen ab. p(HMPA) ist ein wasserlösliches, ungiftiges und nicht immunaktives Polymer, was einen Einsatz als Therapeutikum ermöglicht [114]. Vor Kurzem wurde es möglich, dieses Polymer monodispers in Lösung zu bringen und mit dem hydrophoben LMA zu koppeln [115]. Daraus ergibt sich ein amphiphiles Polymer, das wie Amphipole eine micellenartige Struktur in Wasser ausbildet und hydrophobe Stoffe zum Transport aufnehmen kann [116]. Es konnte für diese Polymere gezeigt werden, dass sich kleine Aggregate aus wenigen Polymerketten bilden und das bereits ab Konzentrationen im nanomolaren Bereich [115, 117, 118]. Im Gegensatz zu Amphipolen besteht das Copolymer nur aus zwei Monomereinheiten. Die amphiphilen

Eigenschaften des Copolymers lassen sich dadurch bei der Synthese über das stöchiometrische Verhältnis des hydrophilen und des hydrophoben Monomers verändern. Diese Art von Polymere konnte bereits erfolgreich eingesetzt werden, um hydrophobe Stoffe, wie z. B. Domperidon oder Rhodamin, über die Blut-Hirn Schranke zu transportieren, was den Einsatz als *drug carrier* möglich macht [116, 119, 120]. Des Weiteren zeigen Versuche, dass statistische Copolymere dieser Art verstärkt in Walker-256 Karzinomen aufgenommen werden, was sie zu möglichen *drug carriern* in der Krebstherapie macht [120]. Die amphiphilen Eigenschaften sowie die Möglichkeit die p(HPMA)-co-p(LMA)-Copolymere individuell zu gestalten machen diese amphiphilen Polymere interessant für den Einsatz in Membranproteinforschung.

1.5 Ziele der Arbeit

Bei der Untersuchung von Membranproteinen bedarf es der Entwicklung von neuen Methoden, da Standardmethoden, entwickelt für lösliche Proteine, nicht auf Membranproteine angewendet werden können. Das größte Problem besteht in der schlechten Wasserlöslichkeit der Membranproteine, da diese sich *in vivo* in einer hydrophoben Umgebung, der Membran, befinden. Um dennoch isolierte Membranproteine und ihre Faltung *in vitro* charakterisieren zu können, sind membranmimetische Systeme notwendig um die Membranproteine in Lösung zu bringen. In dieser Arbeit sollte der Effekt verschiedener membranmimetischer Umgebungen auf die Dimerisierung der GpA-Transmembranhelix untersucht werden. GpA eigentlich sich dazu als Modellprotein, da die Dimerisierung der Transmembranhelix bereits auf Proteinstrukturebene geklärt werden konnten und gut verstanden ist. Aufgrund eines spezifischen Aminosäuremotives ist GpA befähigt stabile Dimere auszubilden.

In vier unabhängigen Projekten sollten Einfluss von Konzentration und Acylkette von Lysophosphocholin Detergenzmizellen, das kommerziell erhältliche Amphipol A8-35, die stöchiometrische Zusammensetzung von amphiphilen p(HPMA)-co-p(LMA)-Copolymeren sowie der Effekt von Calciumionen auf eine binäre, negativ geladene Lipidmembran, näher untersucht werden. Zu Beginn sollten diese verschiedenen Systeme auf ihr Verhalten in wässriger Lösung getestet werden, um Parameter der Mizellen, Polymeraggregate und Lipidmembranen bei verschiedenen experimentellen Bedingungen, zu erhalten. Mit diesem Erkenntnisgewinn sollten die unterschiedlichen Eigenschaften gezielt genutzt werden, um den Effekt der amphiphilen Stoffe auf die Dimerisierung der GpA-Transmembranhelix, die mittels FRET-Messungen verfolgt und quantifiziert werden kann, zu erklären. Helixdimere können als kleinste strukturgebende Einheit in größeren Membranproteinen oder Oligomerkomplexen angesehen werden. Die Erkenntnisse, die mit Hilfe der GpA-Transmembranhelix über die Helix-Helix-Assoziation und vor allem den Einfluss äußerer Faktoren gewonnen werden, dienen als Grundlage für die Erforschung der Faltung weiterer bitopischer und polytopischer Membranproteine.

2. Ergebnisse und Diskussion

2.1 Detergenzeigenschaften beeinflussen die Stabilität des Glykophorin A Transmembranhelix-Dimers in Lysophosphocholin Mizellen

Michael Stangl, Anbazhagan Veerappan, Anja Kröger, Peter Vogel und Dirk Schneider
Biophysical Journal, Dezember 2012, Volume 103, Issue 12

Detergenzien werden typischerweise zur Extraktion, Reinigung und Strukturanalysen von Membranproteinen, sowie zur Bestimmung thermodynamischer Parameter der Membranproteinfaltung und Stabilität, verwendet. Sie dienen nicht nur als hydrophobe Umgebung zur Solubilisierung des hydrophoben Transmembranbereiches, sondern stellen das direkte Lösungsmittel eines isolierten Membranproteins bei *in vitro* Experimenten dar. Eine Detergenzumgebung kann bei *in vitro* Studien die native Membran ersetzen und Sekundär- und Tertiärstruktur von isolierten Membranproteinen stabilisieren [121]. Sogar Quartärkontakte in Membranproteinkomplexen können in Detergenz natürlich ausgebildet oder erhalten bleiben [122, 123]. Allerdings besteht die Möglichkeit, dass Detergenzien intramolekulare Interaktionen in Membranproteinen verändern, was z. B. am Beispiel von Bakteriorhodopsin gezeigt wurde. Bakteriorhodopsin konnte in Detergenz nur als Monomer kristallisiert werden, obwohl es in der natürlichen Membran als Trimer vorliegt [124, 125]. Dies und weitere Beispiele zeigen, dass die Wahl des Detergenz von hoher Bedeutung ist, um die Struktur und Funktion eines Membranproteins zu bewahren. Welche Detergenzeigenschaften die Faltung von Membranproteinen beeinflussen, wurde hier am Modellsystem einer Helix-Helix-Interaktion (GpA) untersucht.

In dieser Studie wurden der Einfluss der Detergenzkonzentration und der Acylkettenlänge von Lysophosphocholin (Lyso-PC) Detergenzien (Abb. 1.6A) auf die Dimerisierung der GpA-Transmembranhelix untersucht. Lyso-PC ist ein strukturell zu doppelschichtbildenden Phospholipiden ähnliches Detergenz. Es besitzt eine zwitterionische Phosphocholin Kopfgruppe und, im Gegensatz zu Phospholipiden, nur eine Acylkette. Lyso-PCs kommen natürlich in menschlichen Zellen vor. Sie entstehen bei der Hydrolyse von Phosphatidylcholinen und sind in Zellprozessen, wie die Proliferation von T-Lymphozyten und der Proteinkinase C Aktivierung involviert [126, 127]. Zudem zeigen Tumorzellen eine erhöhte Konzentration von Lyso-PC Molekülen [128, 129].

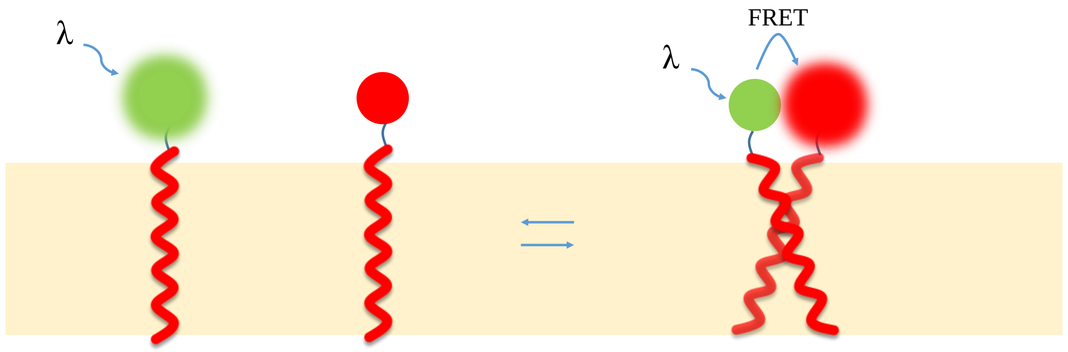

Abb. 2.1 GpA Dimerisierung induziert FRET
Liegen die GpA-Peptide als Monomere vor wird keine Energie übertragen und nur der Donor fluoresziert. Dimerisieren zwei Transmembranhelices, so wird Energie vom Donor auf den Akzeptor übertragen und die Donorfluoreszenz wird gequencht, wobei die Akzeptorfluoreszenz zunimmt. Die Stärke des Donorquenchings kann zur Quantifizierung der Dimerisierung genutzt werden.

Es wurden Lyso-PCs mit der Kettenlänge von 10 bis 16 C-Atomen auf ihre CMC und Aggregationszahl untersucht und weiterhin die Dimerisierung der GpA-Transmembranhelix, solubilisiert in diesen Detergenzien, mittels FRET quantifiziert. Die FRET-Methode setzt voraus, dass im Dimer alle Energie vom donormarkierten GpA-Peptid auf das akzeptormarkierte GpA-Peptid übertragen wird. Diese Annahme ist gerechtfertigt, da die N-Termini (hier wurde der Fluoreszenzfarbstoff gekoppelt) in der GpA NMR-Struktur von MacKenzie *et al.* [69] nur 10 Å auseinander liegen und der Försterradius der beiden Farbstoffe bei 55 Å liegt. D.h., dass nur Energie übertragen wird, sobald die Peptide dimerisieren (Abb. 2.1). Durch die Stärke des Donorquenchings lässt sich folglich der Anteil an GpA-Dimeren in der Probe bestimmen.

Zu Beginn wurde die Integrität der α-helikalen Struktur der Transmembranhelix in den verschiedenen Lyso-PC-Mizellen mittels CD-Spektroskopie überprüft. Alle synthetisierten GpA-Peptide zeigen eine eindeutige α-helikale Struktur (Abb. 2.2) mit einem berechneten α-Helix-Anteil von 78-81%. Nur die Peptide gelöst in Lyso-PC C16, dem Detergenz mit der längsten Acylkette, zeigen eine verminderte α-helikale Struktur mit einem berechneten α-Helix Anteil von 66%. Da bis auf Lyso PC C16 alle Peptide eine vornehmlich α-helikale Sekundärstruktur aufweisen, ist die 1. Stufe des 2-Stufen-Modells, dass die Helices eine stabile α-helikale Struktur in der membranmimetischen Umgebung ausbilden, erfüllt. Somit kann eine sequenzspezifische Helix-Helix-Interaktion stattfinden und eine unspezifische Proteinaggregation ist wenig wahrscheinlich.

Eine Interaktion der Transmembranhelices lässt sich allerdings nicht über CD-Spektroskopie ermitteln, weshalb im Folgenden FRET-Analysen durchgeführt wurden.

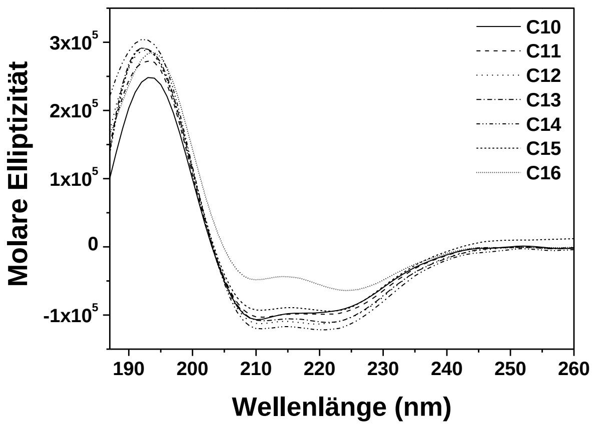

Abb. 2.2 CD-Spektren der GpA-Transmembranpeptide in verschiedenen Lyso-PCs
CD-Spektren von nichtmarkiertem GpA-Transmembranpeptid in 20 mM Lyso-PC der Kettenlängen 10-16. Dabei unterscheidet sich nur das GpA-Transmembranpeptid in Lyso-PC der Kettenlänge 16 von den anderen Spektren. Charakteristische Minima und Maxima für eine α-Helix sind bei 190 nm, 209 nm und 222 nm zu sehen.

Die FRET-Messungen zeigten eine kontinuierliche Abnahme der Dimere mit steigender Acylkettenlänge des Detergenz (20 mM) [148]. Weitere Messungen, beginnend knapp über der CMC des jeweiligen Lyso-PCs, zeigten eine Abhängigkeit der Dimerisierung mit veränderter Detergenzkonzentration (Abb. 2.3). Bei konstanter Peptidkonzentration (in allen Messungen konstant) und steigenden Detergenzkonzentrationen nimmt die Dimerisierung drastisch ab. Je länger die Kettenlänge des Detergenz, desto ausgeprägter ist dieser Effekt.

Dabei ist zu beachten, dass es sich bei der Dimerisierung von Helices immer um ein dynamisches Gleichgewicht zwischen Monomer und Dimer handelt. Monomere Einheiten assoziieren und dissoziieren also ständig. In einem vergleichbaren dynamischen Gleichgewicht stehen auch Mizellen, die sich immer wieder neu formieren, fusionieren oder sich auflösen. Zur weiteren Interpretation der Ergebnisse wurden daher die Detergenzien näher analysiert. Mittels des Fluorophors ANS (1-Anilinonaphtalen-8-sulfonat), das nur in hydrophober Umgebung stark fluoresziert, wurde die jeweilige CMC des Lyso-PCs bestimmt. Die Messungen ergaben, dass die CMC mit steigender Kettenlänge exponentiell abnimmt und sich im Bereich von 6 mM (Lyso-PC C10) und 3 µM (Lyso-PC C16) befindet [148].

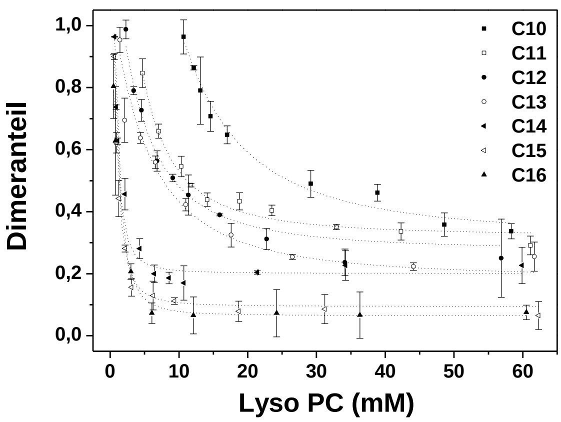

Abb. 2.3 Dimeranteile der GpA-Peptide bei verschiedenen Lyso-PC-Konzentrationen und -Kettenlängen
Die Dimerisierung der GpA-Transmembranhelix (0,5 µM), ermittelt durch FRET-Messungen, nimmt mit steigenden Lyso-PC-Konzentrationen rapide ab. Diese Abnahme ist umso drastischer je länger die Kettenlänge des Detergenz ist.

Aus der folgenden Gleichung, die den Zusammenhang der verschiedenen Mizellenparameter beschreibt ($N_{agg}=([Det]\text{-}CMC)/[M]$), und den CMC-Messungen lässt sich folgern, dass sich bei einer konstanten Detergenzkonzentration (*[Det]*) aller Lyso-PC-Kettenlängen unterschiedlich viele Mizellen (*[M]*) in Lösung befinden, vorausgesetzt die Aggregationszahl (N_{agg}) ist für alle gleich. Die unterschiedliche Mizellenkonzentration kann einen deutlichen Effekt auf die GpA Dimerisierung haben, da die Mizellen das direkte Lösungsmittel darstellen und je mehr Mizellen vorhanden sind, desto mehr effektives Volumen bietet sich den Helices, die dann eher dissoziieren können.

Um die vorherrschenden mizellaren Bedingungen noch näher zu bestimmen, wurde die Aggregationszahl und hydrodynamischer Radius der Detergenzmizellen bestimmt. Dazu wurde eine fluoreszenzspektroskopische Methode, sowie statische Lichtstreuung (SLS und DLS durchgeführt von XXX *et al.*) angewandt. Diese Messungen ergaben, dass die Aggregationszahl sowie der hydrodynamischer Radius der Mizellen mit steigender Kettenlänge ansteigt (Abb. 2.4). Nicht veröffentlichte Daten lassen sogar die Vermutung zu, dass die Aggregationszahl der Mizellen mit steigender Detergenzkonzentration zunimmt (Abb. 2.4C).

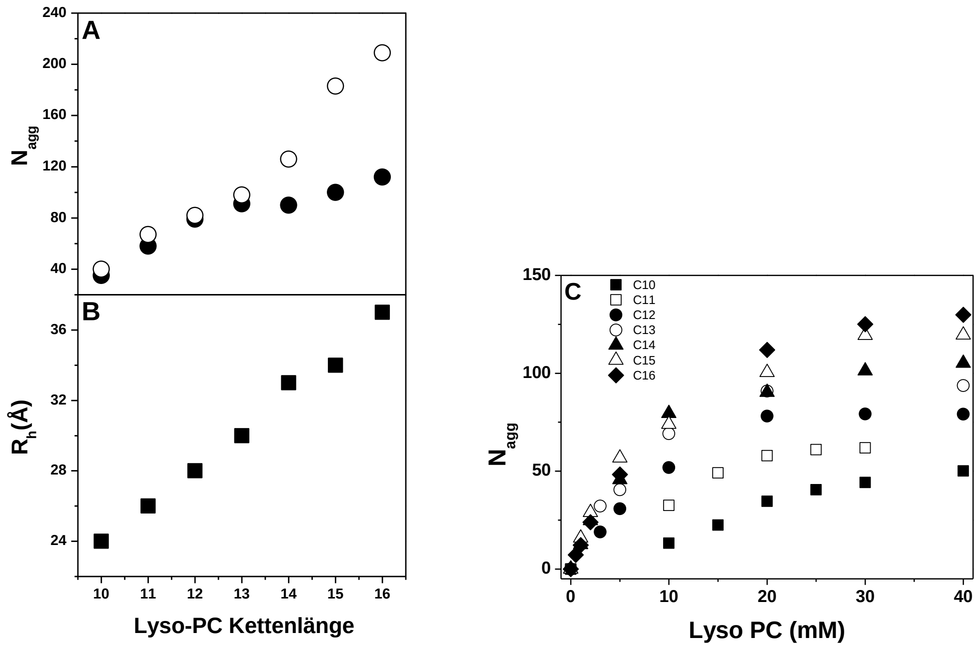

Abb. 2.4 Aggregationszahlen und hydrodynamische Radien der Lyso-PC Mizellen
(A) Aggregationszahl als Funktion der Lyso-PC Acylkettenlänge bei 20 mM Detergenz. Aggregationszahlen wurden mittels Fluoreszenzquenching (●) sowie statischer Lichtstreuung (○) ermittelt. (B) Hydrodynamische Radien der Lyso-PC Mizellen bestimmt mit dynamischer Lichtstreuung (SLS und DLS durchgeführt von XXX *et al.*). (C) Aggregationszahl als Funktion der Lyso-PC Konzentration ermittelt über Fluoreszenzquenching.

In dieser Studie sollte der Einfluss der Lyso-PC Kettenläge und der Konzentration auf das GpA-Dimer bei gleichbleibender Detergenzkopfgruppe untersucht werden. Thermodynamisch gesehen kann die freie Energie der Helix-Helix-Assoziation (ΔG_{ha}) wie folgt formuliert werden:

$$\Delta G_{ha} = \Delta G_{h\text{-}h} + n\ \Delta G_{d\text{-}d} - 2n\ \Delta G_{h\text{-}d}$$

wobei $\Delta G_{h\text{-}h}$, $\Delta G_{d\text{-}d}$, $\Delta G_{h\text{-}d}$ die freien Energien von Helix-Helix-, Detergenz-Detergenz- und Helix-Detergenz-Interaktionen sind. Dimerisieren zwei Helices, so werden $2n$ Helix-Detergenz-Interaktionen aufgehoben und n Detergenz-Detergenz-Interaktionen hinzugewonnen. Dies erhöht die freie Energieänderung der Helix-Helix-Interaktion und begünstigt diese somit thermodynamisch. Erhöht sich nun die Kettenlänge des Detergenz und somit dessen Hydrophobizität, so ist zu erwarten, dass dieses stärker mit der Transmembranhelix interagiert als ein Detergenz mit einer kürzeren Acylkette. Die erhöhte Interaktion mit dem Detergenz könnte mit der Helix-Dimerisierung in Konkurrenz stehen, was im Fall der längerkettigen Detergenzien stärker zum Tragen kommt und die freie Energie der Helix-Helix-Assoziation vermindert.
Ein weiterer Grund für die gezeigten Resultate könnte mit der Detergenzkonzentration erklärt werden. Unabhängig von der Kettenlänge konnte eine starke Reduzierung der Dimerisierung

der GpA-Transmembranhelix mit steigender Detergenzkonzentration beobachtet werden. Diese Art von Destabilisierung wurde bereits von Fisher *et al.* [74] als einfacher Verdünnungseffekt, basierend auf einer entropisch bedingten Dissoziation, beschrieben. Im Idealfall hängt die freie Energie der Helixassoziation linear vom Logarithmus der Lyso-PC-Konzentration, mit einer Steigung von $R*T$ ab. Die Ergebnisse hier zeigen aber eine Abweichung von diesem Idealfall [148]. Nur im Falle von Lyso-PC-C16 ist eine nahezu ideale Verdünnung erkennbar. Die generelle Abweichung vom Idealfall lässt die Vermutung zu, dass die Vorgänge deutlich komplexer sind als beschrieben durch eine einfache Verdünnung und nicht genauer beschrieben werden können.

In der Vergangenheit wurde bei der Integration und Interaktion von Transmembranhelices in Lipiddoppelschichten der *hydrophobic mismatch* diskutiert [89, 90, 130]. Dieser kommt zum Tragen, sobald die Länge der Transmembranhelix nicht mit der Dicke der Membran übereinstimmt, was zu einer starken Destabilisierung der Membranproteinstruktur führen kann. Im Vergleich zu Lipiddoppelschichten sind Mizellen aber deutlich flexibler und dynamischer und sollten sich besser an die Oberfläche des Membranproteins anpassen können. Die Länge des hydrophoben Bereichs des GpA-Dimers beträgt etwa 31 Å. Wäre nun der Radius der Mizellen ausschlaggebend für die Dimerisierung der GpA Helix, sollte, anhand der DLS Ergebnisse (Abb. 2.4B), ein Maximum in Mizellen aus Lyso-PC-C13 oder C14, deren hydrodynamischer Radius 31-33Å ist, zu sehen sein. Dies entspricht aber nicht den dieser Arbeit zu Grunde liegenden Ergebnissen, da GpA in Mizellen aus Lyso-PC-C10 am stabilsten zu sein scheint und deren hydrodynamischer Radius aber nur 24Å beträgt. Demzufolge kann *hydrophobic mismatch* nicht ausschließlich zur Erklärung der verminderten GpA Dimerisierung, mit steigender Lyso-PC-Acylkette, genutzt werden.

Ein genauere Auswertung der Charakterisierung der Mizellen zeigt die Zunahme der Aggregationszahl mit steigender Kettenlänge des Detergenz (Abb. 2.4A). Ein Vergleich der Dimeranteile bei jeweils 20 mM Lyso-PC mit der jeweiligen Aggregationszahl zeigt einen linearer Zusammenhang (Abb. 2.5). Der Anteil von Peptiden zu Detergenzmolekülen innerhalb einer einzelnen Mizelle ist somit bei jedem Fall unterschiedlich. Dies lässt die Vermutung zu, dass neben den bisher erläuterten Interaktionen, möglicherweise die Aggregationszahl der Mizellen auch ein wichtiger Faktor für die Assoziation von Transmembranhelices ist.

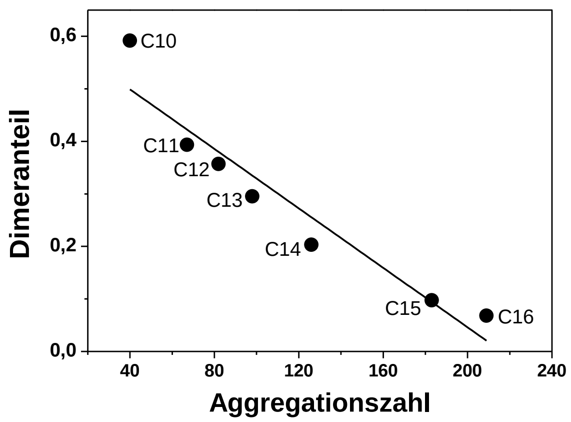

Abb. 2.5 Korrelation zwischen Dimerstabilität und Aggregationszahl
GpA-Dimeranteile bei 20 mM Lyso-PC als Funktion der Aggregationszahl (bestimmt über SLS). Die Aggregationszahl korreliert linear mit den GpA-Dimeranteilen mit R^2=0,9.

Die Ergebnisse dieser Studie zeigen, dass die Acylkettenlänge sowie die Konzentration eines Detergenz den oligomeren Zustand eines Membranproteins stark beeinflussen können. Einerseits spielen Helix-Detergenz-Interaktionen eine entscheidende Rolle, andererseits löst die Konzentrationszunahme an Mizellen eine Dissoziation der Helices aus. Zudem konnte in dieser Studie gezeigt werden, dass der Effekt des *hydrophobic mismatch* in Detergenzumgebung, im Gegensatz zu Lipidmembranen, eher eine untergeordnete Rolle zu spielen scheint. Beim Einsatz von Detergenzien zur Membranproteinanalyse wird in der Regel die Aggregationszahl des Detergenz nicht berücksichtigt. In dieser Studie konnte erstmals gezeigt werden, dass die Aggregationszahl einer Mizelle vermutlich eine entscheidende Rolle bei der Stabilisierung nativer Membranproteinstrukturen in Mizellen spielen kann.

2.2 Sequenz-spezifische Dimerisierung einer Transmembranhelix in Amphipol A8-35

<u>Michael Stangl</u>, Sebastian Unger, Sandro Keller und Dirk Schneider

Plos One, Oktober 2014, Volume 9, Issue 10

Seit einigen Jahren können Detergenzien teilweise durch synthetische amphiphile Copolymere, genannt Amphipole, ersetzt werden. Amphipole wurden erstmals 1996 von der Gruppe von Jean-Luc Popot beschrieben [107]. Aufgrund ihrer guten Wasserlöslichkeit und der niedrigen Einsatzkonzentration können Amphipole Detergenzien nach der Extraktion der Proteine aus der Membran ersetzen. Amphipole bilden ab Konzentrationen im nanomolaren Bereich Aggregate aus wenigen Polymerketten, in deren Innerem sich die hydrophoben Bereiche eines Membranproteins einlagern können, wie es bei Detergenzmizellen bekannt ist. Die niedrige Anzahl von Polymermolekülen pro Aggregat bietet im Gegensatz zu Mizellen, die aus vielen Detergenzmolekülen zusammengesetzt sind, die Möglichkeit, Membranproteine sehr gut zu stabilisieren. Daher wirken Amphipole weniger denaturierend auf Membranproteine. Für die Extraktion von Membranproteinen aus Membranen sind allerdings zunächst noch Detergenzien notwendig, um an die Membranproteine zu gelangen, da Amphipole eine Membran nicht auflösen können.

Bisher wurde bereits der Einfluss von Amphipolen auf die Stabilität von ausgewählten Membranproteinen untersucht. In diesen Studien wurden polytopische Membranproteine untersucht, die von vielzähligen Interaktionen, kurzer und langer Reichweite, stabilisiert sind. In dieser Studie sollte die Stabilität der GpA-Transmembranhelix in Amphipol A8-35, dem ersten und beststudierten Amphipol, untersucht werden.

Zu Beginn wurde die Sekundärstruktur der GpA-Helixpeptide, gelöst in A8-35, mittels CD-Spektroskopie bestimmt (Abb. 2.6). Zum Vergleich wurden die GpA-Peptide in TFE, DDM und SDS gelöst, da diese Substanzen Membranproteine sehr gut in Lösungen bringen können und die Ausbildung von α-Helices fördern. Amphipol A8-35 vermag die GpA-Peptide ähnlich gut zu lösen wie die Kontrollsubstanzen. Die Ausbildung der Transmembranhelix von GpA wird durch A8-35 stabilisiert. Ein Unterschied ist allerdings die eingesetzte Konzentration. Bereits bei einer 1:1 Mischung von Peptid zu Polymer ist das Peptid vollständig gelöst und vorwiegend α-helikal (Abb. 2.6). Dies zeigen die vergleichbaren berechneten α-helikalen Anteile von 67% in A8-35, 62% in TFE, 76% in SDS und 79% in DDM.

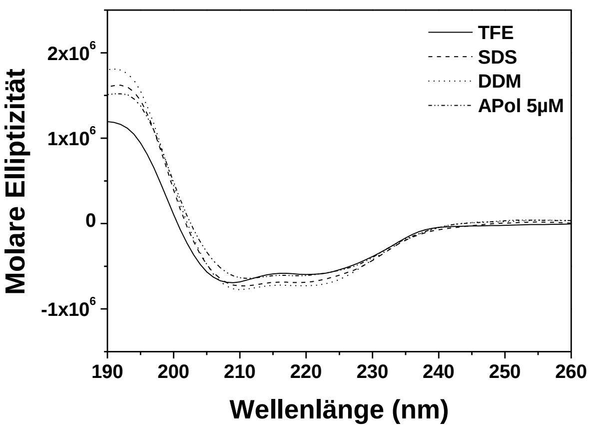

Abb. 2.6 CD-Spektren der GpA-Transmembrandomäne in Amphipol
Unmarkierte GpA-Peptide (5 µM) gelöst in 5 µM A8-35, Trifluorethanol (TFE), 5 mM Dodecylmaltosid (DDM) und 5 mM Natriumdodecylsulfat (SDS).

In einem weiteren Schritt wurde die Stabilität des GpA-Dimers in Amphipol A8-35 mittels FRET-Messungen ermittelt. Hierzu wurde die Peptidkonzentration der markierten Peptide konstant gehalten und die Polymerkonzentration von 5-75 µM erhöht. Diese Messungen zeigen eine hohe Dimerisierung bei niedrigen A8-35 Konzentrationen (Abb 2.7). Eine Erhöhung der Polymerkonzentration führt zu einer Abnahme der Dimerisierung bis zu einem Dimeranteil von etwa 0,65 bei 20 µM Amphipol.

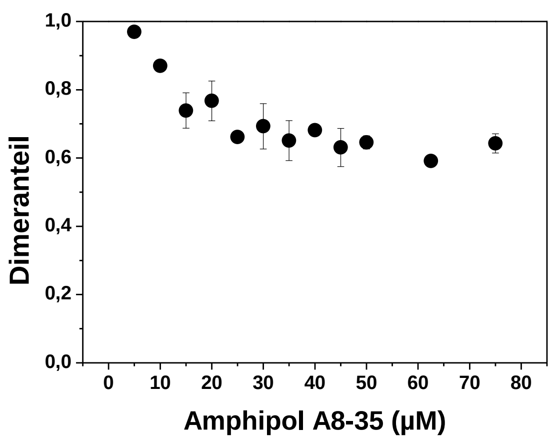

Abb. 2.7 Assoziation der GpA-Transmembranhelix in Amphipol A8-35
FRET-Messungen wurden bei einer konstanten Peptidkonzentration von 0,5 µM durchgeführt. Dimeranteile wurden durch Energietransfereffizienzen von Donor- auf Akzeptorpeptid berechnet.

Eine weitere Erhöhung der Polymerkonzentration beeinflusst die Dimerisierung nur minimal. Im Vergleich dazu können Detergenzien, auch bereits knapp über der CMC, stark dissoziierend auf die GpA-Transmembranhelix wirken. Bei den getesteten Bedingungen in

Amphipol A8-35 sind die Dissoziationskonstanten von GpA unter 0,3 µM und steigen bei Erhöhung der Amphipolkonzentration nicht stark an. Bei manchen Detergenzien (SDS, DDMAB, DPC, Lyso-PC) sind die Dissoziationskonstanten, bei sehr niedrigen Konzentrationen über der CMC, im ähnlichen Bereich von ≤ 0,5 µM. Allerdings können diese sehr stark ansteigen, sobald die Detergenzkonzentration erhöht wird. Amphipol hingegen scheint auch bei höherer Konzentration, relativ zur kritischen Aggregationskonzentration (nanomolar), das GpA-Dimer sehr gut zu stabilisieren. Dies liegt möglicherweise an folgenden Faktoren: (i) Die fehlende Eigenschaft von Amphipolen mit Protein-Protein-Wechselwirkungen zu konkurrieren. (ii) Die verminderte Größe des Faltungstrichters für Membranproteine im Vergleich zu einer Detergenzumgebung, die deutlich denaturierender wirken kann (iii) Der Dämpfungseffekt von möglichen Konformationsänderungen im Protein durch die Viskosität des Polymerrückgrates.

Weitere Versuche zur Stabilität des GpA-Dimers zeigten, dass die Peptide nicht permanent an das Polymer assoziiert sind, sondern ein dynamisches reversibles System vorhanden ist. Dazu wurden Donor- und Akzeptorpeptid getrennt in 20 µM A8-35 solubilisiert und im Verhältnis 50:50, wie es bei den Gleichgewichts-FRET-Messungen der Fall war, gemischt und das FRET-Signal verfolgt. Der Austausch der Peptide in der Polymerlösung findet zwar langsam über mehrere Stunden statt, aber die Energietransfereffizienz aus den Gleichgewichtsmessungen wird schließlich erreicht. Im Gegensatz dazu geschieht der Austausch in DDM-Mizellen in wenigen Minuten. Somit ist die Transmembranhelix nicht im Polymeraggregat "gefangen" und es findet ein kontinuierlicher Austausch von Polymerketten an den hydrophoben Bereichen des Proteins statt, was eine spezifische Interaktion der Transmembranhelices ermöglicht. Die ist eine Voraussetzung für weitere Versuche, da die Untersuchung eines Gleichgewichtes (Monomer-Dimer) eine Flexibilität des Systems voraussetzt. Zudem verdeutlicht der langsame Austausch die Stabilität des GpA-Dimers in A8-35 und könnte ein Grund für dessen stabilisierenden Effekt, durch eine, im Vergleich zu einer Detergenzumgebung, erniedrigte Entropie, sein.

Um die Stabilität und Faltung von Proteinen zu messen, können Denaturierungsstudien durchgeführt werden. Eine thermische Denaturierung hat bei den meisten Membranproteinen eine Aggregation zur Folge, und chemische Denaturierungsagenzien wie Harnstoff oder Guanidiniumchlorid dringen nicht bis zu den Transmembranbereichen durch und sind somit ungeeignet. Deshalb wird bei Membranproteinen häufig eine Entfaltung durch gemischte Mizellen verwendet. Typischerweise werden steigende Mengen des anionische Detergenz SDS zum Protein, gelöst in einem milden Detergenz, wie z. B. DDM, gegeben. SDS eignet sich dazu gut, da es bis in die Transmembranbereiche vordringt und dabei nicht die Sekundärstruktur des Proteins verändert. Es werden lediglich Tertiär- oder Quartärkontakte durch die Abstoßungskräfte der geladenen SDS-Kopfgruppen untereinander destabilisiert. Daher lässt sich die Entfaltung, die in diesem Fall nur die Dissoziation der Transmembranhelices beschreibt, mit gemischten Mizellen verfolgen. Zudem stellen gemischte Mizellen ein wichtiges Intermediat bei der Rekonstitution von Membranproteinen in Amphipolen dar. Detergenzien sind notwendig zur Extraktion von Membranproteinen aus der Membran. Mittels Dialyse werden die Detergenzmoleküle entfernt und das Protein integriert schrittweise in Amphipolaggregate. Als Zwischenstufen kommen gemischte Amphipol/Detergenzmizellen vor, die, falls sie denaturierend auf das Protein wirken, die Faltung stark beeinflussen können und rufen womöglich ein inaktives, fehlgefaltetes Protein hervor.

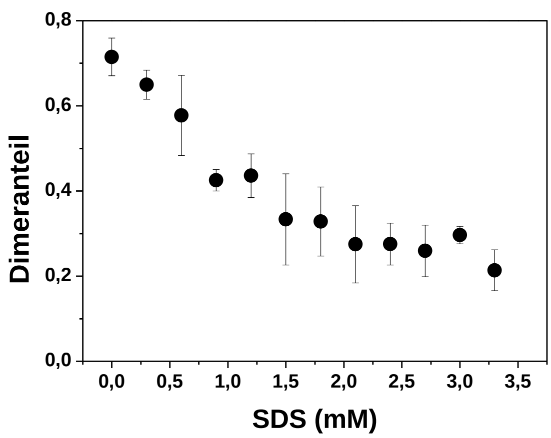

Abb. 2.8 Entfaltung des GpA-Dimers in A8-35 durch Zugabe von SDS
FRET-Messungen wurden bei 20 µM A8-35 und 0.5 µM Peptid und steigenden SDS-Konzentrationen durchgeführt.

Der Einfluss von gemischten A8-35/SDS-Mizellen auf die Dimerisierung der GpA-Transmembranhelix wurde über FRET-Messungen mithilfe der markierten GpA-Peptide untersucht. Steigende SDS-Konzentrationen (unterhalb der CMC) bis etwa 1,5 mM (= CMC bestimmt mittels ANS [131]) rufen eine starke Destabilisierung des Dimers hervor. Der GpA-Dimeranteil ohne SDS-Zugabe reduziert sich um mehr als die Hälfte von ~0,7 auf ~0,3 (Abb. 2.8), wobei die Dissoziationskonstanten um etwa eine 10er Potenz ansteigen. Gemischte Amphipol/SDS-Mizellen destabilisieren das GpA-Dimer ähnlich zu gemischten DDM/SDS-Mizellen. DDM/SDS-Mizellen dissoziieren das GpA-Dimer allerdings vollständig, was bei den hier verwendeten Bedingungen für A8-35/SDS-Mizellen nicht der Fall ist, obwohl SDS bei 3,5 mM in deutlichem Überschuss (175:1) zu A8-35 (20 µM) vorliegt. Ein direkter Vergleich der gemischten Mizellen ist aufgrund der unterschiedlichen chemischen Beschaffenheit von DDM und Polymer allerdings nicht möglich. Zudem erschwert das nicht-ideale Mischungsverhalten von A8-35 mit SDS [149], das stark von den experimentellen Bedingungen abhängt, eine Interpretation der Daten. Allerdings deuten die Ergebnisse erneut auf eine erhöhte Stabilität des GpA-Dimers in Amphipol, im Vergleich zu einem milden Detergenz wie DDM, hin. Darüber hinaus lässt sich durch Verringern der SDS-Konzentration, die Entfaltung des Dimers vollständig rückgängig machen.

Zusammenfassend konnte in dieser Studie konnte gezeigt werden, dass die Integration eines bitopischen Membranproteins in Amphipol A8-35 die Ausbildung von sequenzspezifischen Helix-Helix-Kontakten nicht ausschließt. Die Ausbildung der Sekundärstruktur und die Oligomerisierung der GpA-Transmembranhelix sind in A8-35 möglich. Eine Entfaltung des Dimers mit SDS ist zwar möglich, jedoch nicht in vollem Maße, was belegt, dass Amphipol A8-35 wenig dissoziierend ist. Gemischte Mizellen aus Amphipol und SDS könnten ein nützliches Werkzeug in der Strukturanalyse sein, da der oligomere Zustand eines Proteins durch eine Veränderung der SDS Konzentration leicht beeinflusst werden kann. Amphipole stabilisieren zwar Membranproteine sehr gut, jedoch wurde bei Proteinen, die eine gewisse Flexibilität für ihre Aktivität brauchen, eine durch die rigide Amphipolstruktur hervorgerufene Inhibierung beobachtet [112, 113]. Diese könnte mit der Zugabe von geringen Mengen SDS oder anderen Detergenzien gelockert werden, um Konformationsänderungen, die zur Aktivität des Proteins nötig sind, zuzulassen.

2.3 Eine minimale Hydrophobizität ist erforderlich, um amphiphile p(HPMA)-co-p(LMA) statistische Copolymere erfolgreich in der Membranforschung einzusetzen

Michael Stangl, Mirjam Hemmelmann, Mareli Allmeroth, Rudolf Zentel und Dirk Schneider
Biochemistry, Februar 2014, Volume 53, Issue 9

Die Charakterisierung von Membranproteinen *in vitro* erfordert den Einsatz eines amphiphilen Stoffes, der die Membran imitiert und hydrophobe Bereiche der Membranproteine in Lösung bringen kann. Normalerweise werden dazu Detergenzien oder Lipide verwendet. In letzter Zeit ist das Interesse an amphiphilen Polymeren gewachsen und sie werden bereits in Form von diversen Amphipolen in der Membranproteinforschung genutzt. Das Copolymer p(HPMA)-co-p(LMA) (Abb. 1.6C), synthetisiert in der Gruppe von Prof. Zentel, stellt eine ähnliche Klasse von amphiphilen Polymeren zu klassischen Amphipolen dar. Dabei sind die beiden Monomereinheiten HPMA und LMA statistisch über die Polymerkette verteilt. p(HPMA)-co-p(LMA) Copolymere können in wässriger Lösung spontan mizellenartige Aggregate bilden, was den Einbau hydrophober Substanzen in den hydrophoben Polymerkern erlaubt. Vergleichbar zu Amphipolen sind Polymerkonzentrationen im nanomolaren Bereich ausreichend, um solche Aggregate auszubilden. Die Polymere lassen sich leicht modifizieren, indem die Anteile von hydrophilen und hydrophoben Monomeren bei der Synthese variiert werden, wodurch sich das Aggregationsverhalten in wässriger Lösung ändert. Bisher konnte gezeigt werden, dass Copolymere mit 5% hydrophobem LMA Anteil nur wenige kleine Aggregate bilden und sich diese durch Einbringen einer hydrophoben Substanz stabilisieren lassen. Polymere mit 10% LMA bilden bereits einen stabileren hydrophoben Kern aus. Die genaue Struktur der Polymeraggregate ist nicht bekannt, jedoch sind sie in der Lage, eine hydrophobe Umgebung in wässriger Lösung zu erzeugen. Aufgrund dieser Eigenschaften eignet sich diese Art von Polymeren möglicherweise zur Membranproteinsolubilisierung und Charakterisierung oder zum Transport von pharmazeutisch relevanten hydrophoben Peptiden zu speziellen Zielen eines Organismus. In dieser Studie wurden p(HPMA)-co-p(LMA) statistische Copolymere mit hydrophoben LMA Anteilen von 5% (C5), 15% (C15) und 25% (C25) für einen möglichen Einsatz in der Membranforschung getestet.

Es wird diskutiert, dass p(HPMA)-co-p(LMA)-Copolymere mit geringen LMA Anteilen von 5-15% mit Blutkomponenten, wie z. B. VLDL, und Zellmembranen interagieren können. Dies könnte aber auch durch membranassoziierte oder integrale Membranproteine vermittelt worden sein. Ob die Polymere direkt mit Lipidmembranen interagieren, sollte zunächst geklärt werden. Dazu wurden Phosphatidylcholin-Membranen hergestellt und das fluoreszierende Lipid Laurdan in die Membran integriert. Die Laurdanfluoreszenzemission hängt vom Eindringen von Wassermolekülen und der dadurch veränderten Anisotropie ab [132]. Diese sagt wiederum etwas über die Fluidität der Lipidmembran aus. Somit lassen sich Fluiditätsänderungen der untersuchten Membran mittels der Laurdan-Fluoreszenz betrachten. Interagieren die Polymere mit den Membranen, so sollte sich die Fluidität der Membranen verändern. Die Messungen ergaben, dass durch Zugabe von steigenden Mengen Polymer C5 und C15 die Membran starrer wird, was eine Interaktion der Polymere mit der Membran bedeutet. Vermutlich interagieren die hydrophoben Ketten des Polymers mit der Membran und das starre Polymerrückgrat erhöht die Dichte der Lipidpackung. Bei Zugabe von Polymer C25 und Amphipol A8-35 (Negativkontrolle) ändert sich die Packungsdichte der Membran allerdings nicht, was vermuten lässt das diese Polymere nicht mit Membranen interagieren. Die Messungen ergaben zudem, dass die Interaktion nicht von der Art der Lipide abhängt [133].

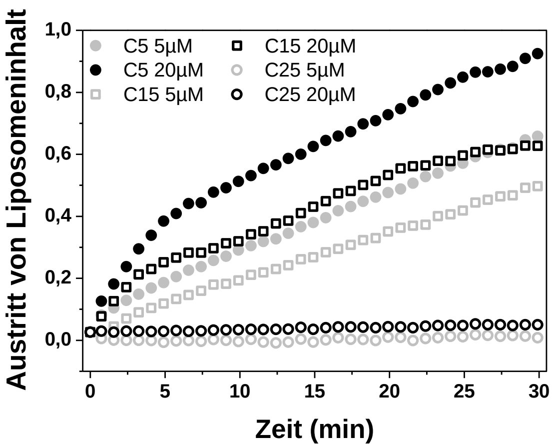

Abb. 2.9 Polymerinduzierter Austritt von Liposomeninhalt
DOPC-Liposomen wurden mit ANTS (Fluorophor) und DPX (Quencher) beladen und die Polymere in zwei verschiedenen Konzentrationen (5 µM und 20 µM) zugegeben. Die ANTS-Fluoreszenz wurde über 30 min bei 530 nm verfolgt und der Anteil an ausgetretenem Inhalt zu jedem Zeitpunkt berechnet (1 ≙ 100%).

Des Weiteren wurde getestet, ob die Zugabe der Copolymere die Stabilität der Membranen beeinflusst oder diese sogar lysieren kann. Dazu wurden Liposomen mit einem Fluoreszenzfarbstoff und einem Quencher beladen. Stören die Polymere die Dichtigkeit der Liposomen, so werden Farbstoff und Quencher in den Umgebungspuffer entlassen und die Fluoreszenz des Farbstoffes steigt an. Die Messungen ergaben, dass bei Zugabe von C25 der Inhalt der Liposomen nicht austritt und daher die Stabilität der Membran nicht beeinflusst wird. Im Gegensatz dazu induzieren die Polymere C5 und C15 einen Austritt des Liposomeninhalts, wobei der Effekt bei C15 schwächer war als bei C5 (Abb. 2.9).

Zusammen mit den Ergebnissen der Laurdan Messungen lässt sich folgern, dass C5 und C15, aber nicht C25, mit Membranvesikeln interagieren und diese sogar destabilisieren können. Möglicherweise ermöglicht der höhere LMA Anteil bei C25 das Ausbilden eines stabileren hydrophoben Kerns der Polymeraggregate, weshalb diese nicht mit Membranen interagieren. Um dies zu überprüfen, wurde der hydrophobe Farbstoff ANS in die Polymeraggregate eingebaut und die thermische Stabilität verfolgt. ANS zeigt in wässriger Lösung kaum Fluoreszenz. Diese steigt in hydrophober Umgebung stark an, weshalb ANS z. B. zur Bestimmung von CMCs genutzt wird. In einer C5-Polymer-Lösung zeigt ANS nur eine schwache Fluoreszenz, die sich mit steigender Temperatur nicht ändert. Dies deutet darauf hin, dass Polymer C5 keine oder nur wenige instabile hydrophobe Kerne ausbildet. C15 hingegen zeigt eine leicht höhere Stabilität der hydrophoben Kerne, ist aber bei weitem nicht so stabil wie der des Polymers C25. Dies zeigt die starke Fluoreszenz von ANS in Polymer C25, die bei steigender Temperatur nur leicht abfällt [133].

Zusammenfassend zeigen die Ergebnisse, dass C25 einen signifikant stabileren hydrophoben Kern ausbilden kann als die beiden weiteren Polymere. Bei C25 Aggregaten sind scheinbar keine oder nur wenige hydrophobe Seitenketten exponiert, wodurch das Polymer nicht mit Membranen wechselwirkt und somit nicht zur Extraktion von Lipiden oder Membranproteinen geeignet ist. Allerdings könnte der stabile hydrophobe Kern vorteilhaft für die Solubilisierung von Membranproteinen sein.

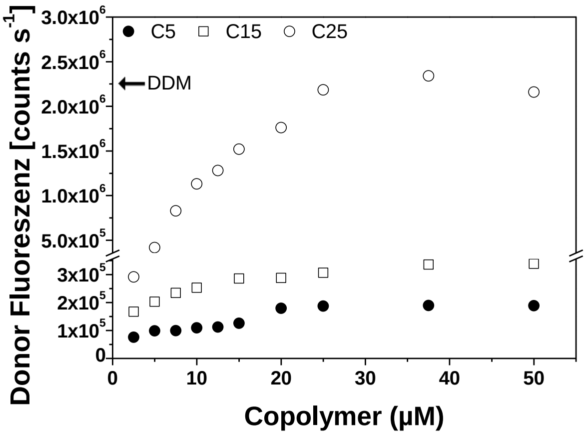

Abb. 2.10 Fluoreszenz der Donor-markierten GpA-Peptide in Polymerlösung
Fluoreszenzintensität der fluoreszein-markierten GpA-Peptide (0,25 µM), gelöst in C5, C15 und C25 bei steigenden Polymerkonzentrationen. Der Pfeil markiert die Fluoreszenzintensität der gleichen Menge GpA-Peptid gelöst in 5 mM DDM.

Im nächsten Schritt wurde daher versucht die sehr hydrophobe Transmembranhelix von GpA in den p(HPMA)-co-p(LMA)-Polymeren zu solubilisieren. Das Fluoreszein markierte GpA-Peptid (0.25 µM) wurde bei verschiedenen Polymerkonzentrationen gelöst und die Fluoreszenzintensität verfolgt. In allen drei Polymerlösungen ist ein nichtlinearer Anstieg der Fluoreszenz bis etwa 20 µM Polymer zu sehen (Abb. 2.10). Höhere Polymerkonzentrationen veränderten das Signal nicht mehr. Die Maximale Fluoreszenz der markierten GpA-Peptide gelöst in C15 ist etwa doppelt so hoch wie in Polymer C5. Das Signal in C25 ist etwa 7fach stärker als in der C15 Polymerlösung und vergleichbar mit der Fluoreszenzintensität in 5 mM DDM Detergenz (Abb. 2.10). Folglich solubilisiert das Polymer C25 eine Transmembranhelix am effizientesten und vergleichbar gut wie das oft genutzte Detergenz DDM. Zudem ist im Vergleich zu einer Detergenzlösung eine nur sehr niedrige Polymerkonzentration erforderlich, um die GpA-Peptide in Lösung zu bringen.

Da dies nichts über die Struktur des Peptides aussagt, wurden CD-Spektroskopie-Messungen mit den unmarkierten GpA-Peptiden und den Copolymeren durchgeführt. Die Messungen zeigen, dass die GpA-Transmembranhelix in allen drei Polymeren korrekt ausgebildet ist und es wurden α-helikale Anteile von im Mittel 90% mathematisch bestimmt. Allerdings zeigen die GpA-Peptide gelöst in niedrigen Konzentrationen C5 und C15 ein schwächeres CD-Signal als in C25- oder DDM-Lösung. Im Falle dieser beiden Polymere wurde eine höhere Konzentration Polymer benötigt, um die Ausbildung der GpA-Transmembranhelix zu unterstützen. Bereits 10 µM C25 reichen aus, um 5 µM GpA-Peptid zu solubilisieren und dieα-helikale Struktur zu stabilisieren.

Ist die α-Helix voll ausgebildet, so können die GpA-Peptide über das GxxxG-Motiv Dimere bilden. Da Helix-Helix-Kontakte in größeren polytopischen Membranproteinen und oligomeren Komplexen eine bedeutende Rolle bei der Ausbildung der nativen 3D-Struktur spielen, wurde überprüft, ob eine p(HPMA)-co-p(LMA)-Polymerumgebung eine Dimerisierung der GpA-Transmembranhelix ermöglicht.

Da die Ausbildung der α-Helices in den Polymeren C5 und C15 ineffizient ist, konnte keine Unterstützung der GpA-Dimerbildung erwartet werden. Die Emissionsspektren der gemischten Donor- und Akzeptorpeptide der GpA-Transmembranhelix bestätigen dies (Abb. 2.11). In Polymer C5 und C15 ist nur eine geringe Fluoreszenz detektierbar. Die Akzeptoremission, die durch die Dimerisierung der GpA-Peptide hervorgerufen wird, ist ebenfalls sehr schwach ausgeprägt (Abb. 2.11). Das Verhältnis von Akzeptorpeak zu Donorpeak entspricht im Fall von C5 etwa dem der reinen Donorprobe, was dafür spricht, dass keine Dimere gebildet werden. Im Vergleich ist das Verhältnis in der C15-Polymer-

Umgebung nur marginal höher. Eine Erhöhung der C5/C15-Polymerkonzentration konnte die Dimerisierung nicht wesentlich verbessern.

Wie in Abbildung 2.11 zu sehen, ist die Akzeptoremission in Polymer C25 deutlich höher im Vergleich zu C5 und C15. Eine Erhöhung der Polymerkonzentration von 2,5 µM auf 10 µM, führt zu einem Anstieg des Dimeranteils in der Probe. Ab 10 µM ändert sich dieser nicht mehr signifikant und ist mit dem Wert in 5 mM DDM-Mizellen oder Amphipol A8-35 zu vergleichen. Kontrollmessungen zeigen, dass die erhöhte Akzeptoremission durch eine spezifische Dimerisierung und nicht durch unspezifische Aggregation der Peptide hervorgerufen wird. Polymer C25 ist somit sehr gut geeignet, um Helix-Helix-Interaktionen zu stabilisieren.

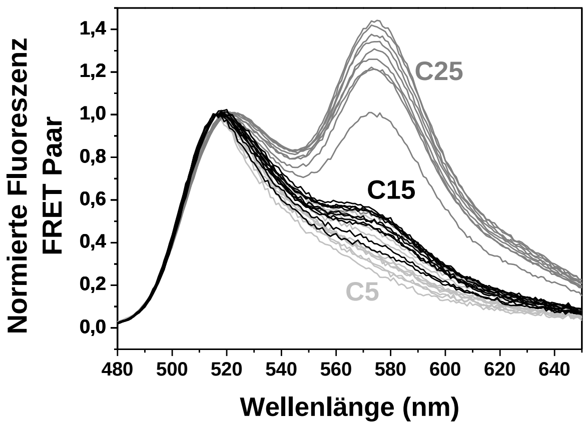

Abb. 2.11 Dimerisierung der GpA-Transmembranhelix in C-5, C15- und C25-Polymerlösungen
GpA Donor- und Akzeptorpeptide wurden 1:1 gemischt und bei verschiedenen Polymerkonzentrationen in Lösung gebracht. Nach Anregung bei 439 nm wurden die Emissionsspektren aufgenommen und bei 520 nm normiert. Eine hohe Akzeptoremission bei ~575 nm ist auf eine Dimerisierung der Peptide zurückzuführen.

In dieser Studie konnte gezeigt werden, dass die p(HPMA)-co-p(LMA)-Polymere C5 und C15 direkt mit Lipidmembranen wechselwirken können, dabei aber nur wenige und instabile hydrophobe Aggregate ausbilden, wobei C15-Aggregate einen vergleichsweise stabileren hydrophoben Kern ausbilden. Vermutlich sind Teile der hydrophoben Bereiche der Polymere nach außen exponiert, wodurch sie hydrophobe Wechselwirkungen mit Lipiden eingehen können, selbst aber keinen oder nur einen instabilen hydrophoben Kern ausbilden.

Das p(HPMA)-co-p(LMA)-Polymer mit 25% Anteil an hydrophobem LMA interagiert allerdings nicht mit Membranen, da es durch den höheren Anteil an hydrophoben Seitenketten eine mizellenartige Struktur mit einem hydrophoben Kern ausbilden kann. Der hydrophobe Kern, der selbst bei hohen Temperaturen von 80°C noch stabil zu sein scheint, ermöglicht den Einsatz des Polymers als "Lösungsmittel" für Membranproteine. Sehr geringe Mengen von

C25 reichen aus, um die hydrophobe Transmembranhelix von GpA zu solubilisieren und zudem die Dimerisierung dieser zu ermöglichen. Die Polymere C5 und C15 sind dazu nicht in der Lage. Die geringen Anteile von LMA reichen nicht aus, um die Struktur eines Membranproteins zu stabilisieren. Die Fähigkeit der Polymere mit der Membran zu interagieren ist antiproportional zu der Fähigkeit, Membranproteine zu solubilisieren und zu stabilisieren. Der Anteil des hydrophoben LMA ist daher ausschlaggebend für den Einsatz der Polymere. Es sind mehr als 15% LMA nötig, um eine Transmembranhelix nativ gefaltet zu inkorporieren. Da diese Polymere (>15% LMA) nicht mit Membranen wechselwirken, können sie z. B. dazu genutzt werden, die Interaktion löslicher Bereiche von Membranproteinen mit Bestandteilen von lebenden Zellen *in vivo* zu untersuchen, ohne biologische Membranen strukturell zu beeinflussen. Somit besteht die Möglichkeit p(HPMA)-co-p(LMA)-Polymere als Ersatzstoffe für Detergenzien in der Membran- und Membranproteinforschung einzusetzen.

2.4 Calciumbindung an Phosphatidylglycerol Membranen steuert die Ausbildung transmembraner Helix-Helix-Interaktionen

Viele Studien beschäftigen sich mit dem Einfluss der Lipidumgebung auf die Faltung, Stabilität und Aktivität von Membranproteinen. Die Eigenschaften einer Membran sind durch ihre spezielle Zusammensetzung aus verschiedenen Lipiden und sich darin befindlicher Proteine gegeben. Verschiedene Parameter, wie Ordnungsgrad, Dicke, Oberflächenladung, Lateraldruck oder die laterale Verteilung von Lipiden, sind charakteristische Eigenschaften einer Membran. Die meisten natürlichen Membranen weisen eine Ladung, erzeugt durch Lipidkopfgruppen, auf. Am häufigsten kommen zwitterionische und negativ geladene Kopfgruppen vor. Typischerweise sind etwa 25% negativ geladene Lipide in einer Membran, die der Membran eine negative Oberflächenladung verleihen [134]. Diese ist in eukaryotischen Zelle vornehmlich in der inneren Hälfte der Lipiddoppelschicht zu finden [135]. Bei diesem komplexen Ladungsmuster der Membranoberfläche stellt sich die Frage, wie die Membran durch die sich in Lösung befindenden Ionen beeinflusst werden könnte. Des Weiteren besteht die Möglichkeit, dass geladene Lipidkopfgruppen über elektrostatische Wechselwirkungen direkt mit Proteinen wechselwirken können, wie es z. B. für die Lipide Phosphatidylinositol-4,5-bisphosphat (PIP_2) und Phosphatidylinositol-3,4,5-triphosphat PIP_3) und dem SNARE-Protein Syntaxin 1A gezeigt wurde [136, 137]. Syntaxin 1A induziert die Akkumulation von PIP2 in der Zellmembran und verändert dadurch die laterale Verteilung und effektive lokale Konzentration der Lipide [137]. Diese spezifischen Interaktionen von Lipidkopfgruppe und Protein könnte in Konkurrenz mit elektrostatischen Interaktionen von Ionen und Lipidkopfgruppe stehen. Somit ist eine Vielzahl von Interaktionen möglich, die die Faltung und Aktivität von Membranproteinen steuern könnten.

Eines der wichtigsten Ionen in zahlreichen biochemischen Prozessen ist Calcium. Bekannt als sekundärer Botenstoff in Signaltransduktionsprozessen steht Calcium möglicherweise mit negativen Lipiden der Zellmembran in Kontakt [138]. Bivalente Calcium Ionen adsorbieren tatsächlich *in vitro* an negative geladene, und zu einem geringeren Ausmaß, an zwitterionische Lipide [139-144]. Monovalente Ionen wie Natrium oder Kalium adsorbieren hingegen kaum an solche Lipide. Vermutlich bindet ein Calcium Ion an zwei Lipidkopfgruppen und erhöht dadurch die Packung der Lipide. Elektrostatische Abstoßung zwischen den geladenen Kopfgruppen kann dadurch minimiert werden. Weiterhin können Calciumionen Lipidaggregation, Lipidphasentrennung und Vesikelfusion auslösen [99, 143, 145-147].

In diesem Projekt sollte der Effekt von Calciumionen auf die Dimerisierung der GpA-Transmembranhelix näher untersucht werden. Es sollte überprüft werden, ob Ca^{2+} einen direkten Effekt auf die Dimerbildung hat oder ob nur die Membran, bestehend aus zwitterionischen und negativ geladenen Lipiden, durch Calciumbindung verändert wird. Vermutet wurde ein sequentieller Effekt, der die GpA-Dimerisierung über veränderte Membraneigenschaften, aufgrund der Calciumbindung, steuert. Zu Beginn sollte überprüft werden, ob die Stabilität des GpA-Dimers direkt von Calcium beeinflusst wird. Dazu wurden die fluoreszenzmarkierten GpA-Peptide in 5 mM DDM-Puffer mit steigender Calciumchlorid Konzentration solubilisiert. Mittels, der bereits beschriebenen FRET-Messungen wurde die Dimerisierung quantifiziert [148, 149]. Die Messungen ergaben eindeutig, dass in Mizellen die Zugabe von Calcium keinen Effekt auf die Dimerisierung der GpA-Transmembranhelix hat und somit ein direkter Einfluss ausgeschlossen werden kann (Abb. 2.12). Daher können Änderungen der GpA-Dimerisierung in folgenden Experimenten auf Veränderungen von Membraneigenschaften zurückgeführt werden. Zur Herstellung von teilweise negativ geladenen Membranen wurde ein Lipidsystem aus Phosphatidylcholin und Phosphatidylglycerol mit verschiedenen Anteilen des negativen Lipids gewählt.

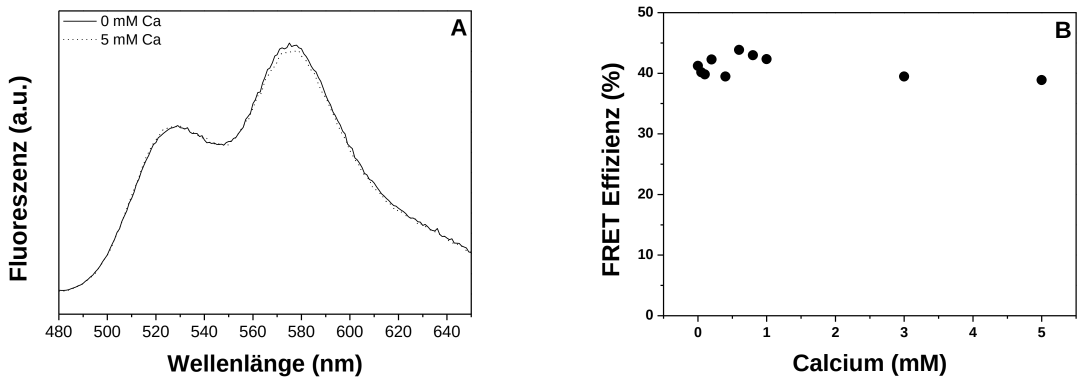

Abb. 2.12 Effekt von Calcium-Ionen auf die GpA-Dimerisierung in DDM-Mizellen
(A) Emissionsspektren der FRET-Paare (GpA-Fluoreszein + GpA-Tetramethylrhodamin 1:1) ohne und mit 5 mM Calcium in 5 mM DDM. (B) FRET-Effizienzen berechnet aus den Emissionsspektren. Zugabe von 0-5 mM Calcium hat keinen Einfluss auf die GpA-Dimerisierung.

Die Lipide wurden in organischem Lösungsmittel zusammen mit dem fluoreszierenden Lipidfarbstoff Laurdan, der die Membranfluidität detektiert, gemischt und mittels des *Freeze-Thaw* Verfahrens große unilamellare Lipsomen (LUVs) hergestellt [150]. Um den Einfluss von Calcium auf das Phasenverhalten der Lipide zu testen, wurden DMPC und DMPG, sowie eine 1:1 Mischung dieser, eingesetzt, da diese Lipide eine Phasenübergangstemperatur von Gelphase zu fluider Phase bei Raumtemperatur haben. Calcium wurde äquimolar zu den

Lipiden hinzugegeben und die Emissionspektren von 10-60°C aufgenommen. Der Wert der *generalized polarization* (GP) ist der Quotient der Fluoreszenzintensität bei 435 nm minus der bei 490 nm und der Gesamtfluoreszenz beider Wellenlängen [133]. Er spiegelt die Fluidität der Membranen über Änderungen der Fluoreszenzintensität bei 435 nm und 490 nm von Laurdan wider. Eine Zunahme des Intensitätspeaks bei 435 nm im Vergleich zu 490 nm, ist die Folge einer starreren Membran. Im umgekehrten Fall ist die Fluidität der Membran erhöht. Die Schmelzkurven der Lipide (DMPC, DMPG, DMPC/DMPG 1:1) zeigen ohne Calciumzugabe die zu erwartende Phasenübergangstemperatur von ~25°C (Abb.2.13). Die Zugabe von Calcium zu DMPC-Membranen zeigt keinen Effekt, was der Erwartung, dass Ca^{2+} nicht oder nur schwach mit zwitterionischen Lipiden wechselwirkt, entspricht.

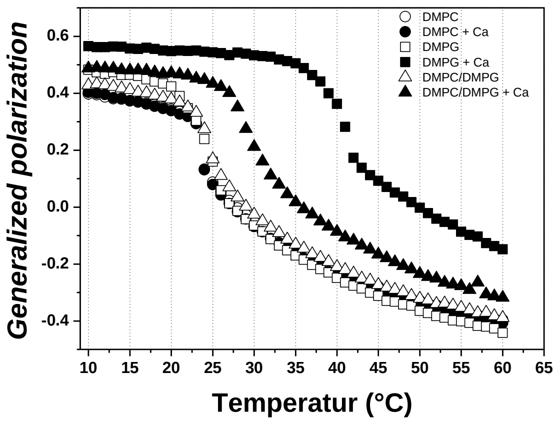

Abb. 2.13 Schmelzkurven von DMPC/DMPG Lipiden unter Zugabe von Calcium
LUVs bestehend aus 0,5 mM DMPC, DMPG und DMPC/DMPG 1:1, beinhalten 1 µM Laurdan. Zu den Lipidproben wurden 0,5 mM Calcium hinzugefügt. Die *generalized polarization* wird aus den Fluoreszenzintensitäten bei 435 nm und 490 nm der Laurdan-Emissionsspektren berechnet [133].

Bei Zugabe von Ca^{2+} zu Membranen mit 50% negativ geladenen Kopfgruppen (DMPG) ist ein Anstieg des Phasenübergangs um ~5°C auf ~30°C zu sehen (Abb. 2.13). Bestehen die Membranen ausschließlich aus DMPG, so steigt die Phasenübergangstemperatur sogar um ~15°C auf ~40°C an (Abb. 2.13). Vermutlich erhöhen die Calciumionen durch Bindung an die Kopfgruppe die Lipidordnung, wodurch sich die Phasenübergangstemperatur dramatisch erhöht. Dieser verstärkte Packungseffekt wurde auch für negative Phosphatidylglycerol-(PG)- und Phosphatidylserin-(PS)-Lipide beobachtet, wobei monovalente Natriumionen keinen Effekt zeigten [151]. Weiterhin wurde mit Lipiden mit den gleichen Kopfgruppen aber längeren, einfach ungesättigten Ölsäureacylketten (18:1) (DOPC/DOPG) gearbeitet, da DMPC (14:0) und DMPG (14:0) nicht die Dicke einer natürlichen Membran widerspiegeln und zudem die GpA-Dimerisierung, durch die zu geringe Membrandicke (*hydrophobic mismatch)*, nicht unterstützen [72].

Die Fluidität der DOPC/DOPG Membranen wurde im Folgenden bei Raumtemperatur nach Zugabe von Calcium mittels Laurdanfluoreszenz bestimmt. Steigende Anteile, des negativen Lipids DOPG, bei konstanter Gesamtlipidkonzentration, erzeugen eine leicht starrere Membran im Vergleich zu reinem DOPC (Abb. 2.14). Die Zugabe von Calcium zu DOPC (Abb. 2.14 100% DOPC ≙ 0) ändert die Membranfluidität nur marginal. Sobald sich aber bereits 10% negative Lipide in der Membran befinden, nimmt nach Zugabe von Calcium, die Fluidität dieser, ab (≙ steigendem GP-Wert). Durch weitere Erhöhung des DOPG Anteils der Membranen nimmt die Fluidität immer stärker ab, wobei die Zugabe von Calcium diesen Effekt verstärkt (Abb. 2.14).

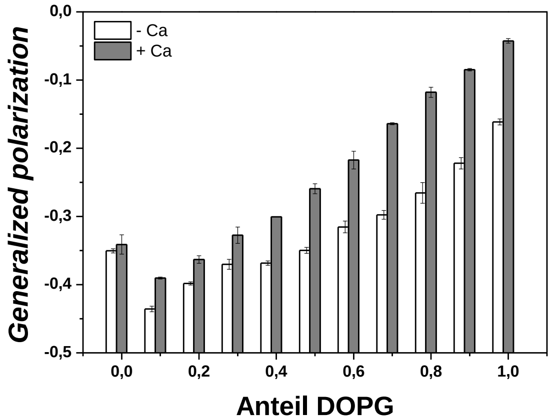

Abb. 2.14 Fluidität von DOPC/DOPG Membranen nach Zugabe von Calcium

LUVs bestehend aus je 0,5 mM DMPC, DMPG und verschiedenen DMPC/DMPG-Mischungen, beinhalten 1 µM Laurdan. Zu den Lipidproben wurden 0,5 mM Calcium hinzugefügt. *Die generalized polarization* wird aus den Fluoreszenzintensitäten bei 435 nm und 490 nm der Laurdan-Emissionsspektren berechnet [133].

So werden vermutlich Membranen, die in der fluiden Phase sind und DOPG enthalten, durch die Zugabe von Ca^{2+} stabilisiert und deren Packungsdichte erhöht. Dieser Effekt scheint spezifisch für die negative geladene Lipidkopfgruppe, und nicht an die Beschaffenheit der Acylkette des Lipides gekoppelt, zu sein. Die Beobachtungen der Laurdanmessungen stimmen mit Ergebnissen von Claessens *et al.* überein [152]. Die Erkenntnis, dass DOPG-Lipide Gegenionen anziehen und diese eine Erhöhung der Lipidpackung hervorrufen, ist für das hier zugrunde liegende Testsystem zu vermuten [152].

Um die Sekundärstruktur und die Löslichkeit der GpA-Peptide in den Lipiden zu testen, wurden CD-Messungen durchgeführt. Die CD-spektroskopischen Messungen zeigen, dass Calcium keinen Effekt auf die Sekundärstruktur der Peptide hat. Jedoch unterscheidet sich die

Sekundärstruktur abhängig von Lipidkopfgruppe. Der α-helikale Anteil der GpA-Transmembranhelix in DOPG entspricht dem Wert, der in mizellarer Umgebung (z. B. SDS, DDM) gefunden wurde. Befinden sich 50% DOPC-Lipide in der Membran, ist der α-helikale Anteil leicht reduziert. Dieser verringert sich noch weiter in Membranen bestehend aus 100% DOPC, was an Form und Intensität der Spektren erkennbar ist (Abb. 2.15).

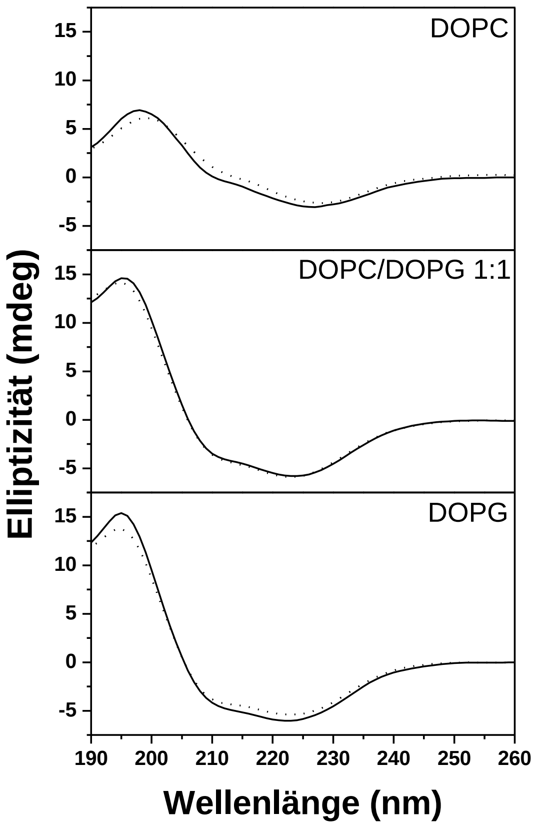

Abb. 2.15 CD-Spektren der GpA-Peptide in DOPC/DOPG Membranen
Peptid/Lipid-Film aus 5 µM GpA und 0,5 mM Lipid, wurde mit 10 mM Phosphatpuffer (pH 7,4) ± 0,5 mM Calcium hydratisiert. Durchgezogene Linien zeigen Spektren ohne Calcium. Gepunktete Linien zeigen Spektren mit 0,5 mM Calcium. Die aus den Spektren berechneten α-helikalen Anteile der Proben ohne Calcium sind: 54% DOPC, 75% DOPC/DOPG, 82% DOPG.

Die weniger ausgeprägten Minima und Maxima der Spektren in DOPC könnten aber auch auf eine verminderte Löslichkeit der Peptide in DOPC hindeuten. Dies sollte allerdings kein Problem bei den FRET-Messungen darstellen, da dort eine zehnfach niedrigere Peptidkonzentration eingesetzt wurde. Für eine vergleichbare Löslichkeit der GpA-Peptide in DOPC und DOPG spricht auch, dass sich die Fluoreszenintensitäten der markierten GpA-Peptide in DOPC und DOPG, bei den FRET-Messung nicht wesentlich unterscheiden. Trotz des geringeren α-helikalen Anteils ist die GpA Transmembranhelix in der Lage, in DOPC-Dimere zu bilden, was in den folgenden Experimenten zu sehen ist (Abb. 2.16, 2.17).

Zur Bestimmung der GpA-Dimerisierung in DOPC/DOPG Membranen wurden FRET-Messungen in Abhängigkeit von Calcium durchgeführt. Hierzu wurden wiederum 0,5 µM Peptid (0,25 µM GpA-FL und 0,25 µM GpA TAMRA) in 0,5 mM Lipid solubilisiert und Emissionsspektren der Donor-, Donor- mit Akzeptor- und Akzeptor-Proben, ohne und mit 0,5 mM Ca^{2+}, aufgenommen. Kontrollen zu den FRET-Messungen zeigten, dass bei allen getesteten Bedingungen ausschließlich eine Dimerisierung der GpA Transmembranhelix zum FRET-Signal beigetragen hat. Der lineare Zusammenhang der FRET-Effizienz ist auf eine ausschließliche Dimerisierung zurückzuführen, sodass keine höheren Oligomere die Messungen beeinflusst haben könnten (Abb. 2.16) [70, 73, 86].

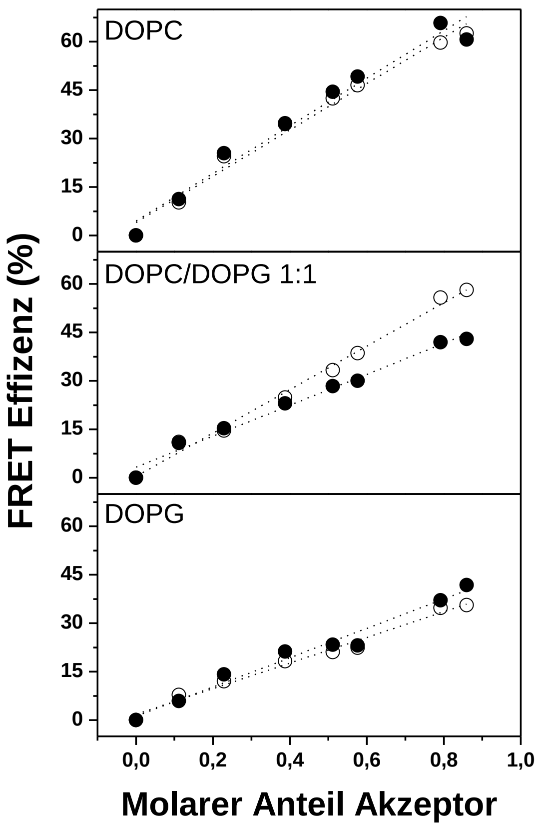

Abb. 2.16 Stöchiometrie der GpA-Oligomerisierung
Der Lineare Verlauf der FRET-Effizienz, mit steigendem Anteil an Akzeptorpeptiden bei konstanter Peptid- und Lipidkonzentration, zeigt, dass ausschließlich Dimere das FRET-Signal erzeugen. (●) mit 0,5 mM Calcium. (○) ohne Calcium

Bei niedrigen Lipid-zu-Peptid-Verhältnissen kann eine unspezifische Colokalisation der Peptide ein FRET-Signal erzeugen [72]. Aus diesem Grund wurden für die FRET-Messungen verschiedene Lipid-zu-Peptid-(L/P)-Verhältnisse überprüft und ein L/P-Verhältnis von 1000:1 gewählt. Dabei sind die Peptide stark in der Membran verdünnt, damit eine zufällige Co-lokalisation nahezu ausgeschlossen werden kann. Es kann somit angenommen werden, dass die gemessene FRET-Effizienz ausschließlich einer spezifischen Dimerisierung der GpA-Transmembranhelix zuzuordnen ist. Eine FRET-Effizienz von 50% bedeutet, dass alle Peptide als Dimere vorliegen, da Donor und Akzeptor in der FRET-Paar-Probe im Verhältnis 1:1 vorliegen [71, 87].

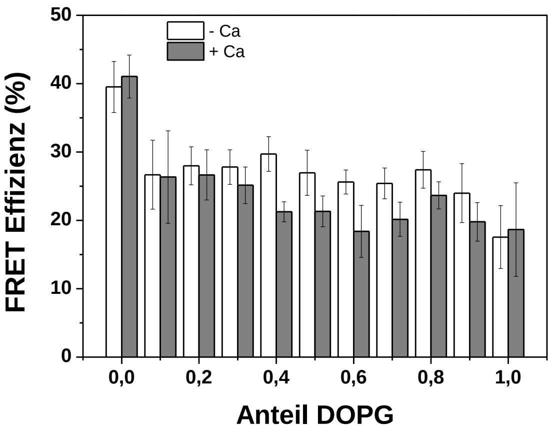

Abb. 2.17 Effekt von Calcium auf die GpA-Dimerisierung in DOPC/DOPG-Membranen
FRET-Messungen wurden bei einer Peptid-Konzentration von 0,5 µM und 0,5 mM Lipid durchgeführt. Es wurde je 0,5 mM Calcium dem Puffer zugefügt. Anteil von 0 DOPG entspricht reinen DOPC Membranen. 50% FRET-Effizienz bedeutet, dass alle Peptide als Dimere vorliegen.

Die FRET-Messungen zeigen eine deutliche Reduktion der Dimerisierung bei Zunahme der negativ geladenen PG-Lipide. Bereits 10% PG reichen aus, um die FRET-Effizienz um ca. 15% zu reduzieren (Abb. 2.17). Eine weitere Steigerung des DOPG-Anteils in der Membran beeinflusst die FRET-Effizienz bis zu 90% DOPG nur marginal (Abb. 2.17). Damit lässt sich direkt folgern, dass die negativen Kopfgruppen der PG-Lipide das GpA-Dimer destabilisieren. Der destabilisierende Effekt von negativ geladenen Lipidkopfgruppen wurde auch von Hong *et al.* beobachtet [88]. Es wird vermutet, dass die negativen Ladungen mit den basischen Aminosäuren, Arg96, Arg97, Lys100 und Lys101 am C-terminalen Ende der GpA-Transmembranhelix wechselwirken und dadurch die Helix-Helix-Interaktion stören. Die Mutation dieser Aminosäuren gegen neutrale polare Aminosäuren ermöglicht GpA wieder eine starke Interaktion, auch in Gegenwart negativ geladener Lipide [88].
Bei Zugabe von äquimolaren Mengen Calcium (im Vgl. zur Lipidkonzentration) ist ein nicht-linearer Verlauf der FRET-Effizienz zu erkennen (Abb. 2.17). In reinen DOPC- oder DOPG-Membranen ist ein leichter Anstieg der Dimere zu sehen, welcher aber innerhalb der Standardabweichung der Messungen liegt und somit nicht signifikant ist. Bei Mischungen der Lipide ist zu erkennen, dass Calcium eine Reduktion der Dimerisierung hervorruft und sich die FRET-Effizienzen bei niedrigen DOPG-Anteilen mit Calcium dem Wert in reinen DOPG-

Membranen annähern. Der größte signifikante Unterschied zwischen Proben mit 0,5 mM und ohne Calcium ist im Bereich von 0,4-0,6 Anteilen DOPG zu sehen, wo dieser etwa 10% Energietransfer, also etwa 20% Dimeranteil, ausmacht. Es scheint, dass die Zugabe von Calcium den destabilisierenden Effekt von DOPG auf die GpA-Dimerisierung verstärkt (Abb 2.17). Da, wie bereits gezeigt, Calcium keinen direkten Effekt auf die Dimerisierung hat, stellt sich die Frage, auf welche Art Calcium die Membranen beeinflusst und dadurch die Dimerisierung der GpA-Transmembranhelix verändert.

Wie zuvor gesehen, verändert Calcium die Fluidität der Membranen (Abb. 2.14). Diese nimmt mit steigendem DOPG-Anteil sowie nach Zugabe von Calcium ab. Es wurde beschrieben, dass in starreren Membranen die GpA-Dimerisierung erhöht ist, da die laterale Diffusion der Transmembranhelices verringert ist [72, 153]. Der Trend der FRET-Messungen ist allerdings gegenläufig, was bedeutet, dass die Membranfluidität hier wohl eine untergeordnete Rolle spielt. Allerdings detektiert die Laurdan-Methode nur die Gesamtheit der Fluiditätsänderung in der Membran [154]. Liegt eine heterogene Membran vor, so können sich Membraneigenschaften lokal stark unterscheiden, wobei diese Heterogenität durch die Laurdanmessung, die nur einen Durchschnittswert liefert, nicht erfasst werden kann. Bilden sich z. B. durch Zugabe von Calcium geordnete, komprimierte Lipidnanodomänen, so bietet dies den daran nicht beteiligten Lipiden mehr Platz in der Membran und deren Fluidität erhöht sich. Aus diesem Grund besteht die Möglichkeit, dass sich die Membranfluidität anhand der Laurdanmessungen zwar ändert, sich die direkte Umgebung der GpA-Transmembranhelix aber komplett entgegengesetzt verhält.

Möglicherweise bilden DOPC/DOPG-Membranen nach Calciumzugabe geordnete Nanodomänen, die die Dimerisierung der GpA-Transmembranhelix beeinflussen. Calciuminduzierte Lipidnanodomänen wurden bereits in Membranen beobachtet und werden mit Mechanismus der proteingetriebenen Membranunterteilung in Verbindung gebracht, da z. B. Calcium-, PIP2- und Aktinkonzentration zusammen in Mastzellen oszillieren [155, 156]. In Mischungen von etwa 50% DOPC und 50% DOPG ist eine deutliche Verringerung der Dimerisierung nach Zugabe von Calcium zu sehen (Abb. 2.17). Möglicherweise induziert Calcium geordnete DOPG-Nanodomänen, in denen die effektive DOPG Konzentration höher ist als tatsächlich angenommen. Da die FRET-Effizienz bei 50% DOPG + Calcium bereits fast so gering wie in reinen DOPG-Membranen ist (Abb. 2.17), befinden sich die GpA-Peptide vielleicht mehrheitlich in den DOPG-Nanodomänen wodurch sie mehr destabilisierende Wechselwirkungen durch die Lipide erfahren. Andererseits befinden sich die Peptide vielleicht in der DOPC-Phase, die durch die komprimierten DOPG-Nanodomänen mehr Platz einnimmt und somit eine höhere Fluidität aufweisen könnte. Somit würde die erhöhte Fluidität der DOPC-Phase eine Dissoziation der GpA-Dimere hervorrufen [4, 5].

Ein elektrostatischer Effekt, der besagen würde, dass Calcium-Lipid- und Protein-Lipid-Wechselwirkungen in Konkurrenz stehen könnten, scheint auf Grund der hier erhaltenen Ergebnisse eher unwahrscheinlich. Wäre dieser der Fall, könnte erwarten werden, dass die GpA-Dimerisierung in DOPG mit Calcium auf das Niveau von DOPC ansteigt, da die destabilisierenden negativen Ladungen der Lipide durch Calcium abgeschirmt werden könnten. Ein Anstieg ist aber nicht zu beobachten (Abb. 2.17).

Der komplexe Effekt von Calcium auf die Ausbildung von Helix-Helix-Interaktionen kann anhand der Daten nicht vollkommen geklärt werden. Calcium zeigt einen starken Einfluss auf partiell geladene Membranen, deren Fluidität sich vermindert. Calcium induziert möglicherweise die Bildung geordneter Lipidnanodomänen in der Membran und steuert dadurch Helix-Helix-Interaktionen.

Es konnte aber eindeutig gezeigt werden, dass geringe Mengen negativ geladener PG-Lipide ausschlaggebend für die Dissoziation der GpA-Helices sind, was durch Wechselwirkungen zwischen Lipidkopfgruppen und basischen Aminosäuren im Protein vermittelt wird. Das GpA-Dimer dimerisiert mit einem Kontaktwinkel von etwa 40° [69]. Die Wechselwirkungen zwischen Lipidkopfgruppe und Transmembranhelix verhindern möglicherweise die richtige Ausrichtung der Helices, wodurch keine Interaktion zustande kommen kann.

Die Ergebnisse zeigen, dass neben dem Einfluss von verschiedenen Lipiden, die Interaktion von Transmembranhelices durch weitere externe Faktoren, wie z. B. Ionen, beeinflusst werden kann und diese Faktoren Steuerelemente für die Faltung von Membranproteinen darstellen können.

2.5 Zusammenfassung

Bei der Untersuchung von Membranproteinen bedarf es der Entwicklung von neuen Methoden, da Standardmethoden, entwickelt für lösliche Proteine, meist nicht auf Membranproteine angewendet werden können. Das größte Problem besteht in der schlechten Wasserlöslichkeit der Membranproteine, da diese sich *in vivo* in einer hydrophoben Umgebung, der Membran, befinden. Um dennoch isolierte Membranproteine und ihre Faltung *in vitro* charakterisieren zu können, sind membranmimetische Systeme notwendig um Membranproteine in Lösung zu bringen. Dazu werden häufig Detergenzien verwendet, deren amphiphiler Charakter die Ausbildung von Detergenzmizellen ermöglicht. Eine solche Mizelle besteht aus einem hydrophoben Kern, sowie einem äußeren hydrophilen Bereich, der dem wässrigen Milieu zugewendet ist. Diese Merkmale ermöglichen die Solubilisierung von Membranproteinen durch Detergenzien, wodurch die Membranproteine näher studiert werden können. Allerdings kann die Faltung von Membranproteinen, das Ausbilden der nativen räumlichen Struktur des Proteins, durch Detergenzien verschiedener Art gestört werden, was die Aktivität der Proteine stark beeinflussen kann. Deshalb ist es notwendig, die richtigen Bedingungen, sowie die richtige membranmimetische Umgebung auszuwählen, um Membranproteine erfolgreich zu rekonstituieren um detailliertere Untersuchungen durchführen zu können. In letzter Zeit wurden zudem Alternativen zu Detergenzien entwickelt, sogenannte amphiphile Copolymere, die ähnlich wie Detergenzien hydrophile und hydrophobe Bereiche besitzen und je nach Zusammensetzung, die individuell angepasst werden kann, mizellenartige Aggregate in wässriger Lösung bilden. Daher können diese Polymere auch zur Solubilisierung von Membranproteinen verwendet werden. In dieser Arbeit wurden Lysophosphocholin Detergenzien, die Copolymere Amphipol A8-35, p(HMPA)-co-p(LMA) sowie synthetische Membranen aus Phospholipiden auf Ihre Eigenschaften in wässriger Lösung untersucht, und deren Auswirkungen auf die Solubilisierung und Dimerisierung der GpA-Transmembranhelix mittels *Förster*-Resonanz-Elektronentransfer verfolgt. Es konnte erstmals gezeigt werden, dass sowohl die Acylkettenlänge als auch die Einsatzkonzentration der Detergenzien einen starken Einfluss auf die Dimerisierung der GpA-Transmembranhelix hat, und dies auf veränderte Mizelleneigenschaften, wie der Aggregationszahl, zurückzuführen ist. Amphipol A8-35 ist in der Lage die Transmembranhelix sehr effizient zu solubilisieren und unterstützt dabei die Dimerisierung von GpA. Eine Zugabe des Detergenz SDS, was normalerweise zur Dissoziation von Transmembranhelices führt und daher zu Entfaltungsstudien verwendet wird, konnte in A8-35 gelöstes GpA allerdings nicht komplett dissoziieren, was auf die erhöhte Stabilität der Dimere in Amphipol zurückzuführen ist. Die Copolymere p(HMPA)-co-p(LMA), synthetisiert im AK Zentel, wurden auf den möglichen Einsatz in der Membranproteinforschung hin getestet. In dieser Arbeit wurde gezeigt, dass steigende Anteile des hydrophoben Monomers LMA die Ausbildung eines hydrophoben Kerns begünstigen, wobei eine Interaktion der Polymere mit Membranen abnimmt. Ein Anteil von > 15% LMA ist Voraussetzung für die effiziente Solubilisierung der GpA-Transmembranhelix. Zudem wird auch die Ausbildung des GpA-Dimers von p(HMPA)-co-p(LMA) Polymeren mit mehr als 15% LMA begünstigt. In einem weiteren Projekt wurde der Einfluss von Calcium-Ionen auf teilweise negativ geladene Membranen und der sich darin befindlichen GpA-Transmembranhelix untersucht. Es wurde gezeigt, dass negative Lipide die Dimerisierung der Helices behindern. Die Zugabe von Calcium verstärkt diesen Effekt in Membranen mit mittlerem Anteil an negativ geladenen Lipiden. Calcium bindet an negative geladene Lipide und verringert dadurch die Fluidität der Membranen. Möglicherweise ruft Calcium zudem eine veränderte laterale Verteilung der Lipide in der Membran hervor, was die Dimerisierung der GpA-Transmembranhelix beeinflussen könnte.

3. Referenzen

1. White, S.H. and W.C. Wimley, *Membrane protein folding and stability: Physical principles.* Annual Review of Biophysics and Biomolecular Structure, 1999. **28**: p. 319-365.
2. Wiener, M.C. and S.H. White, *Structure of a Fluid Dioleoylphosphatidylcholine Bilayer Determined by Joint Refinement of X-Ray and Neutron-Diffraction Data .2. Distribution and Packing of Terminal Methyl-Groups.* Biophysical Journal, 1992. **61**(2): p. 428-433.
3. Spector, A.A. and M.A. Yorek, *Membrane Lipid-Composition and Cellular Function.* Journal of Lipid Research, 1985. **26**(9): p. 1015-1035.
4. van Meer, G., D.R. Voelker, and G.W. Feigenson, *Membrane lipids: where they are and how they behave.* Nat Rev Mol Cell Biol, 2008. **9**(2): p. 112-24.
5. Evans, W.H. and W.G. Hardison, *Phospholipid, cholesterol, polypeptide and glycoprotein composition of hepatic endosome subfractions.* Biochem J, 1985. **232**(1): p. 33-6.
6. Zambrano, F., S. Fleischer, and B. Fleischer, *Lipid composition of the Golgi apparatus of rat kidney and liver in comparison with other subcellular organelles.* Biochim Biophys Acta, 1975. **380**(3): p. 357-69.
7. Mitra, K., et al., *Modulation of the bilayer thickness of exocytic pathway membranes by membrane proteins rather than cholesterol.* Proc Natl Acad Sci U S A, 2004. **101**(12): p. 4083-8.
8. Andreyev, A.Y., et al., *Subcellular organelle lipidomics in TLR-4-activated macrophages.* J Lipid Res, 2010. **51**(9): p. 2785-97.
9. Wood, W.G., M. Cornwell, and L.S. Williamson, *High performance thin-layer chromatography and densitometry of synaptic plasma membrane lipids.* J Lipid Res, 1989. **30**(5): p. 775-9.
10. Daum, G., *Lipids of mitochondria.* Biochim Biophys Acta, 1985. **822**(1): p. 1-42.
11. Feinstein, M.B., S.M. Fernandez, and R.I. Shaafi, *Fluidity of Natural Membranes and Phosphatidylserine and Ganglioside Dispersions - Effects of Local-Anesthetics, Cholesterol and Protein.* Biochimica Et Biophysica Acta, 1975. **413**(3): p. 354-370.
12. Chen, Q., et al., *Excess membrane cholesterol alters human gallbladder muscle contractility and membrane fluidity.* Gastroenterology, 1999. **116**(3): p. 678-685.
13. Eeman, M. and M. Deleu, *From biological membranes to biomimetic model membranes.* Biotechnologie Agronomie Societe Et Environnement, 2010. **14**(4): p. 719-736.
14. Subczynski, W.K. and A. Wisniewska, *Physical properties of lipid bilayer membranes: relevance to membrane biological functions.* Acta Biochim Pol, 2000. **47**(3): p. 613-25.
15. Lee, A.G., *Functional properties of biological membranes: a physical-chemical approach.* Prog Biophys Mol Biol, 1975. **29**(1): p. 3-56.
16. Ikeda, M., A. Kihara, and Y. Igarashi, *Lipid asymmetry of the eukaryotic plasma membrane: functions and related enzymes.* Biol Pharm Bull, 2006. **29**(8): p. 1542-6.
17. Quinn, P.J., *Plasma membrane phospholipid asymmetry.* Subcell Biochem, 2002. **36**: p. 39-60.
18. Verkleij, A.J. and J.A. Post, *Membrane phospholipid asymmetry and signal transduction.* J Membr Biol, 2000. **178**(1): p. 1-10.
19. Heinrich, P.C., Müller, Matthias, Graeve, Lutz, *Löffler/Petrides Biochemie und Pathobiochemie.* Springer Verlag, 2014. **9. Auflage**.
20. Marino, G. and G. Kroemer, *Mechanisms of apoptotic phosphatidylserine exposure.* Cell Res, 2013. **23**(11): p. 1247-8.
21. Fadeel, B. and D. Xue, *The ins and outs of phospholipid asymmetry in the plasma membrane: roles in health and disease.* Crit Rev Biochem Mol Biol, 2009. **44**(5): p. 264-77.
22. Schroeder, F., *Role of membrane lipid asymmetry in aging.* Neurobiol Aging, 1984. **5**(4): p. 323-33.
23. Krogh, A., et al., *Predicting transmembrane protein topology with a hidden Markov model: application to complete genomes.* J Mol Biol, 2001. **305**(3): p. 567-80.
24. Overington, J.P., B. Al-Lazikani, and A.L. Hopkins, *How many drug targets are there?* Nat Rev Drug Discov, 2006. **5**(12): p. 993-6.

25. Wallin, E. and G. von Heijne, *Genome-wide analysis of integral membrane proteins from eubacterial, archaean, and eukaryotic organisms.* Protein Sci, 1998. **7**(4): p. 1029-38.
26. Worch, R., et al., *Focus on composition and interaction potential of single-pass transmembrane domains.* Proteomics, 2010. **10**(23): p. 4196-208.
27. Katritch, V., V. Cherezov, and R.C. Stevens, *Structure-function of the G protein-coupled receptor superfamily.* Annu Rev Pharmacol Toxicol, 2013. **53**: p. 531-56.
28. Lemmon, M.A. and J. Schlessinger, *Cell signaling by receptor tyrosine kinases.* Cell, 2010. **141**(7): p. 1117-34.
29. Carpenter, E.P., et al., *Overcoming the challenges of membrane protein crystallography.* Curr Opin Struct Biol, 2008. **18**(5): p. 581-6.
30. Lacapere, J.J., et al., *Determining membrane protein structures: still a challenge!* Trends Biochem Sci, 2007. **32**(6): p. 259-70.
31. Seddon, A.M., P. Curnow, and P.J. Booth, *Membrane proteins, lipids and detergents: not just a soap opera.* Biochim Biophys Acta, 2004. **1666**(1-2): p. 105-17.
32. Baker, M., *Making membrane proteins for structures: a trillion tiny tweaks.* Nat Methods, 2010. **7**(6): p. 429-34.
33. Arachea, B.T., et al., *Detergent selection for enhanced extraction of membrane proteins.* Protein Expr Purif, 2012. **86**(1): p. 12-20.
34. von Heijne, G., *Membrane-protein topology.* Nat Rev Mol Cell Biol, 2006. **7**(12): p. 909-18.
35. Wimley, W.C., *The versatile beta-barrel membrane protein.* Curr Opin Struct Biol, 2003. **13**(4): p. 404-11.
36. Popot, J.L. and D.M. Engelman, *Helical membrane protein folding, stability, and evolution.* Annu Rev Biochem, 2000. **69**: p. 881-922.
37. Ulmschneider, M.B., M.S. Sansom, and A. Di Nola, *Properties of integral membrane protein structures: derivation of an implicit membrane potential.* Proteins, 2005. **59**(2): p. 252-65.
38. Kovacs, H., et al., *The effect of environment on the stability of an integral membrane helix: molecular dynamics simulations of surfactant protein C in chloroform, methanol and water.* J Mol Biol, 1995. **247**(4): p. 808-22.
39. White, S.H. and W.C. Wimley, *Membrane protein folding and stability: physical principles.* Annu Rev Biophys Biomol Struct, 1999. **28**: p. 319-65.
40. Li, R., et al., *Dimerization of the transmembrane domain of Integrin alphaIIb subunit in cell membranes.* J Biol Chem, 2004. **279**(25): p. 26666-73.
41. Gottschalk, K.E., et al., *Transmembrane signal transduction of the alpha(IIb)beta(3) integrin.* Protein Sci, 2002. **11**(7): p. 1800-12.
42. Kim, M., C.V. Carman, and T.A. Springer, *Bidirectional transmembrane signaling by cytoplasmic domain separation in integrins.* Science, 2003. **301**(5640): p. 1720-5.
43. Cymer, F. and D. Schneider, *Transmembrane helix-helix interactions involved in ErbB receptor signaling.* Cell Adh Migr, 2010. **4**(2): p. 299-312.
44. King, G. and A.M. Dixon, *Evidence for role of transmembrane helix-helix interactions in the assembly of the Class II major histocompatibility complex.* Mol Biosyst, 2010. **6**(9): p. 1650-61.
45. Song, Y., et al., *Competition between homodimerization and cholesterol binding to the C99 domain of the amyloid precursor protein.* Biochemistry, 2013. **52**(30): p. 5051-64.
46. Song, Y., et al., *Impact of bilayer lipid composition on the structure and topology of the transmembrane amyloid precursor C99 protein.* J Am Chem Soc, 2014. **136**(11): p. 4093-6.
47. Tastan, O., et al., *Retinal proteins as model systems for membrane protein folding.* Biochimica Et Biophysica Acta-Bioenergetics, 2014. **1837**(5): p. 656-663.
48. Luecke, H., et al., *Structure of bacteriorhodopsin at 1.55 A resolution.* J Mol Biol, 1999. **291**(4): p. 899-911.
49. Marti, T., *Refolding of bacteriorhodopsin from expressed polypeptide fragments.* J Biol Chem, 1998. **273**(15): p. 9312-22.
50. Popot, J.L. and D.M. Engelman, *Membrane protein folding and oligomerization: the two-stage model.* Biochemistry, 1990. **29**(17): p. 4031-7.
51. Engelman, D.M., et al., *Membrane protein folding: beyond the two stage model.* FEBS Lett, 2003. **555**(1): p. 122-5.

52. Lemmon, M.A., et al., *Glycophorin A dimerization is driven by specific interactions between transmembrane alpha-helices.* J Biol Chem, 1992. **267**(11): p. 7683-9.
53. Lemmon, M.A., et al., *Sequence specificity in the dimerization of transmembrane alpha-helices.* Biochemistry, 1992. **31**(51): p. 12719-25.
54. Lemmon, M.A., et al., *A dimerization motif for transmembrane alpha-helices.* Nat Struct Biol, 1994. **1**(3): p. 157-63.
55. Sternberg, M.J. and W.J. Gullick, *A sequence motif in the transmembrane region of growth factor receptors with tyrosine kinase activity mediates dimerization.* Protein Eng, 1990. **3**(4): p. 245-8.
56. Langosch, D. and J. Heringa, *Interaction of transmembrane helices by a knobs-into-holes packing characteristic of soluble coiled coils.* Proteins, 1998. **31**(2): p. 150-9.
57. Brosig, B. and D. Langosch, *The dimerization motif of the glycophorin A transmembrane segment in membranes: importance of glycine residues.* Protein Sci, 1998. **7**(4): p. 1052-6.
58. Kirrbach, J., et al., *Self-interaction of transmembrane helices representing pre-clusters from the human single-span membrane proteins.* Bioinformatics, 2013. **29**(13): p. 1623-1630.
59. Stoddart, R.W. and S.M. Metcalfe, *Studies on sialoglycoprotein complexes of human erythrocyte membranes.* Biochem J, 1969. **115**(5): p. 57P-58P.
60. Liljas, L., P. Lundahl, and S. Hjerten, *The major sialoglycoprotein of the human erythrocyte membrane. Release with a non-ionic detergent and purification.* Biochim Biophys Acta, 1976. **426**(3): p. 526-34.
61. Reid, M.E., *MNS blood group system: a review.* Immunohematology, 2009. **25**(3): p. 95-101.
62. Ohyama, K., et al., *Isolation and influenza virus receptor activity of glycophorins B, C and D from human erythrocyte membranes.* Biochim Biophys Acta, 1993. **1148**(1): p. 133-8.
63. Pasvol, G., et al., *Inhibition of malarial parasite invasion by monoclonal antibodies against glycophorin A correlates with reduction in red cell membrane deformability.* Blood, 1989. **74**(5): p. 1836-43.
64. Hadley, T.J., et al., *Falciparum malaria parasites invade erythrocytes that lack glycophorin A and B (MkMk). Strain differences indicate receptor heterogeneity and two pathways for invasion.* J Clin Invest, 1987. **80**(4): p. 1190-3.
65. Pasvol, G., D. Anstee, and M.J. Tanner, *Glycophorin C and the invasion of red cells by Plasmodium falciparum.* Lancet, 1984. **1**(8382): p. 907-8.
66. Pasvol, G., et al., *Glycophorin as a possible receptor for Plasmodium falciparum.* Lancet, 1982. **2**(8305): p. 947-50.
67. Pasvol, G., J.S. Wainscoat, and D.J. Weatherall, *Erythrocytes deficiency in glycophorin resist invasion by the malarial parasite Plasmodium falciparum.* Nature, 1982. **297**(5861): p. 64-6.
68. Berg, J.M., Stryer, Lubert, Tymoczko, John L, *Stryer Biochemie.* Spektrum Verlag, 2010.
69. MacKenzie, K.R., J.H. Prestegard, and D.M. Engelman, *A transmembrane helix dimer: structure and implications.* Science, 1997. **276**(5309): p. 131-3.
70. Adair, B.D. and D.M. Engelman, *Glycophorin A helical transmembrane domains dimerize in phospholipid bilayers: a resonance energy transfer study.* Biochemistry, 1994. **33**(18): p. 5539-44.
71. Anbazhagan, V., F. Cymer, and D. Schneider, *Unfolding a transmembrane helix dimer: A FRET study in mixed micelles.* Arch Biochem Biophys, 2010. **495**(2): p. 159-64.
72. Anbazhagan, V. and D. Schneider, *The membrane environment modulates self-association of the human GpA TM domain--implications for membrane protein folding and transmembrane signaling.* Biochim Biophys Acta, 2010. **1798**(10): p. 1899-907.
73. Fisher, L.E., D.M. Engelman, and J.N. Sturgis, *Detergents modulate dimerization, but not helicity, of the glycophorin A transmembrane domain.* J Mol Biol, 1999. **293**(3): p. 639-51.
74. Fisher, L.E., D.M. Engelman, and J.N. Sturgis, *Effect of detergents on the association of the glycophorin a transmembrane helix.* Biophys J, 2003. **85**(5): p. 3097-105.
75. Russ, W.P. and D.M. Engelman, *The GxxxG motif: a framework for transmembrane helix-helix association.* J Mol Biol, 2000. **296**(3): p. 911-9.
76. Melnyk, R.A., et al., *The affinity of GXXXG motifs in transmembrane helix-helix interactions is modulated by long-range communication.* J Biol Chem, 2004. **279**(16): p. 16591-7.

77. Lawrie, C.M., E.S. Sulistijo, and K.R. MacKenzie, *Intermonomer hydrogen bonds enhance GxxxG-driven dimerization of the BNIP3 transmembrane domain: roles for sequence context in helix-helix association in membranes.* J Mol Biol, 2010. **396**(4): p. 924-36.
78. Bustos, D.M. and J. Velours, *The modification of the conserved GXXXG motif of the membrane-spanning segment of subunit g destabilizes the supramolecular species of yeast ATP synthase.* J Biol Chem, 2005. **280**(32): p. 29004-10.
79. Schneider, D. and D.M. Engelman, *GALLEX, a measurement of heterologous association of transmembrane helices in a biological membrane.* J Biol Chem, 2003. **278**(5): p. 3105-11.
80. Russ, W.P. and D.M. Engelman, *TOXCAT: a measure of transmembrane helix association in a biological membrane.* Proc Natl Acad Sci U S A, 1999. **96**(3): p. 863-8.
81. Langosch, D., et al., *Dimerisation of the glycophorin A transmembrane segment in membranes probed with the ToxR transcription activator.* J Mol Biol, 1996. **263**(4): p. 525-30.
82. Gurezka, R. and D. Langosch, *In vitro selection of membrane-spanning leucine zipper protein-protein interaction motifs using POSSYCCAT.* Journal of Biological Chemistry, 2001. **276**(49): p. 45580-45587.
83. Karimova, G., N. Dautin, and D. Ladant, *Interaction network among Escherichia coli membrane proteins involved in cell division as revealed by bacterial two-hybrid analysis.* J Bacteriol, 2005. **187**(7): p. 2233-43.
84. Tome, L., D. Steindorf, and D. Schneider, *Genetic systems for monitoring interactions of transmembrane domains in bacterial membranes.* Methods Mol Biol, 2013. **1063**: p. 57-91.
85. Cymer, F., C.R. Sanders, and D. Schneider, *Analyzing oligomerization of individual transmembrane helices and of entire membrane proteins in E. coli: A hitchhiker's guide to GALLEX.* Methods Mol Biol, 2013. **932**: p. 259-76.
86. Li, E., M. You, and K. Hristova, *Sodium dodecyl sulfate-polyacrylamide gel electrophoresis and forster resonance energy transfer suggest weak interactions between fibroblast growth factor receptor 3 (FGFR3) transmembrane domains in the absence of extracellular domains and ligands.* Biochemistry, 2005. **44**(1): p. 352-60.
87. Merzlyakov, M. and K. Hristova, *Forster resonance energy transfer measurements of transmembrane helix dimerization energetics.* Methods Enzymol, 2008. **450**: p. 107-27.
88. Hong, H. and J.U. Bowie, *Dramatic destabilization of transmembrane helix interactions by features of natural membrane environments.* J Am Chem Soc, 2011. **133**(29): p. 11389-98.
89. Killian, J.A., *Hydrophobic mismatch between proteins and lipids in membranes.* Biochim Biophys Acta, 1998. **1376**(3): p. 401-15.
90. Weiss, T.M., et al., *Hydrophobic mismatch between helices and lipid bilayers.* Biophys J, 2003. **84**(1): p. 379-85.
91. Duquesne, K. and J.N. Sturgis, *Membrane protein solubilization.* Methods Mol Biol, 2010. **601**: p. 205-17.
92. Schimerlik, M.I., *Overview of membrane protein solubilization.* Curr Protoc Neurosci, 2001. **Chapter 5**: p. Unit 5 9.
93. Orwick-Rydmark, M., et al., *Detergent-free incorporation of a seven-transmembrane receptor protein into nanosized bilayer Lipodisq particles for functional and biophysical studies.* Nano Lett, 2012. **12**(9): p. 4687-92.
94. Long, A.R., et al., *A detergent-free strategy for the reconstitution of active enzyme complexes from native biological membranes into nanoscale discs.* BMC Biotechnol, 2013. **13**: p. 41.
95. Zhang, R., et al., *Characterizing the structure of lipodisq nanoparticles for membrane protein spectroscopic studies.* Biochim Biophys Acta, 2014.
96. Swainsbury, D.J., et al., *Bacterial reaction centers purified with styrene maleic Acid copolymer retain native membrane functional properties and display enhanced stability.* Angew Chem Int Ed Engl, 2014. **53**(44): p. 11803-7.
97. Magalhaes, M.A. and M. Glogauer, *Pivotal Advance: Phospholipids determine net membrane surface charge resulting in differential localization of active Rac1 and Rac2.* J Leukoc Biol, 2010. **87**(4): p. 545-55.
98. McLaughlin, S., *The electrostatic properties of membranes.* Annu Rev Biophys Biophys Chem, 1989. **18**: p. 113-36.

99. Papahadjopoulos, D. and G. Poste, *Calcium-Induced Phase Separation and Fusion in Phospholipid Membranes.* Biophysical Journal, 1975. **15**(9): p. 945-948.
100. Sinn, C.G., M. Antonietti, and R. Dimova, *Binding of calcium to phosphatidylcholine-phosphatidylserine membranes.* Colloids and Surfaces a-Physicochemical and Engineering Aspects, 2006. **282**: p. 410-419.
101. Lee, A.G., *How lipids affect the activities of integral membrane proteins.* Biochim Biophys Acta, 2004. **1666**(1-2): p. 62-87.
102. Orsi, M. and J.W. Essex, *Physical properties of mixed bilayers containing lamellar and nonlamellar lipids: insights from coarse-grain molecular dynamics simulations.* Faraday Discuss, 2013. **161**: p. 249-72; discussion 273-303.
103. Cantor, R.S., *Lipid composition and the lateral pressure profile in bilayers.* Biophys J, 1999. **76**(5): p. 2625-39.
104. Cantor, R.S., *The influence of membrane lateral pressures on simple geometric models of protein conformational equilibria.* Chem Phys Lipids, 1999. **101**(1): p. 45-56.
105. S., O., *Lateral Pressure in Lipid Membranes and Its Role in Function of Membrane Proteins.* Doctoral dissertation Tampere University of Technology, 2010.
106. M., R., *Surfactants and interfacial phenomena.* Wiley Interscience, 2004. **Third Edition**.
107. Tribet, C., R. Audebert, and J.L. Popot, *Amphipols: polymers that keep membrane proteins soluble in aqueous solutions.* Proc Natl Acad Sci U S A, 1996. **93**(26): p. 15047-50.
108. Popot, J.L., et al., *Amphipols: polymeric surfactants for membrane biology research.* Cell Mol Life Sci, 2003. **60**(8): p. 1559-74.
109. Gohon, Y., et al., *Partial specific volume and solvent interactions of amphipol A8-35.* Anal Biochem, 2004. **334**(2): p. 318-34.
110. Popot, J.L., et al., *Amphipols from A to Z.* Annu Rev Biophys, 2011. **40**: p. 379-408.
111. Kleinschmidt, J.H. and J.L. Popot, *Folding and stability of integral membrane proteins in amphipols.* Arch Biochem Biophys, 2014. **564C**: p. 327-343.
112. Champeil, P., et al., *Interaction of amphipols with sarcoplasmic reticulum Ca2+-ATPase.* J Biol Chem, 2000. **275**(25): p. 18623-37.
113. Picard, M., et al., *Protective and inhibitory effects of various types of amphipols on the Ca2+-ATPase from sarcoplasmic reticulum: a comparative study.* Biochemistry, 2006. **45**(6): p. 1861-9.
114. Duncan, R., *The dawning era of polymer therapeutics.* Nat Rev Drug Discov, 2003. **2**(5): p. 347-60.
115. Barz, M., et al., *From defined reactive diblock copolymers to functional HPMA-based self-assembled nanoaggregates.* Biomacromolecules, 2008. **9**(11): p. 3114-8.
116. Hemmelmann, M., et al., *HPMA based amphiphilic copolymers mediate central nervous effects of domperidone.* Macromol Rapid Commun, 2011. **32**(9-10): p. 712-7.
117. Hemmelmann, M., et al., *Aggregation behavior of amphiphilic p(HPMA)-co-p(LMA) copolymers studied by FCS and EPR spectroscopy.* Biomacromolecules, 2012. **13**(12): p. 4065-74.
118. Hemmelmann, M., et al., *Interaction of pHPMA-pLMA Copolymers with Human Blood Serum and Its Components.* Mol Pharm, 2013.
119. Hemmelmann, M., et al., *Amphiphilic HPMA-LMA copolymers increase the transport of Rhodamine 123 across a BBB model without harming its barrier integrity.* J Control Release, 2012. **163**(2): p. 170-7.
120. Allmeroth, M., et al., *HPMA-LMA Copolymer Drug Carriers in Oncology: An in Vivo PET Study to Assess the Tumor Line-Specific Polymer Uptake and Body Distribution.* Biomacromolecules, 2013. **14**(9): p. 3091-101.
121. Franzin, C.M., P. Teriete, and F.M. Marassi, *Structural similarity of a membrane protein in micelles and membranes.* J Am Chem Soc, 2007. **129**(26): p. 8078-9.
122. Melnyk, R.A., A.W. Partridge, and C.M. Deber, *Retention of native-like oligomerization states in transmembrane segment peptides: application to the Escherichia coli aspartate receptor.* Biochemistry, 2001. **40**(37): p. 11106-13.
123. Veerappan, A., et al., *The tetrameric alpha-helical membrane protein GlpF unfolds via a dimeric folding intermediate.* Biochemistry, 2011. **50**(47): p. 10223-30.

124. Grigorieff, N., et al., *Electron-crystallographic refinement of the structure of bacteriorhodopsin.* J Mol Biol, 1996. **259**(3): p. 393-421.
125. Faham, S. and J.U. Bowie, *Bicelle crystallization: a new method for crystallizing membrane proteins yields a monomeric bacteriorhodopsin structure.* J Mol Biol, 2002. **316**(1): p. 1-6.
126. Asaoka, Y., et al., *Potential role of phospholipase A2 in HL-60 cell differentiation to macrophages induced by protein kinase C activation.* Proc Natl Acad Sci U S A, 1993. **90**(11): p. 4917-21.
127. Sasaki, Y., Y. Asaoka, and Y. Nishizuka, *Potentiation of diacylglycerol-induced activation of protein kinase C by lysophospholipids. Subspecies difference.* FEBS Lett, 1993. **320**(1): p. 47-51.
128. Taylor, L.A., et al., *Plasma lyso-phosphatidylcholine concentration is decreased in cancer patients with weight loss and activated inflammatory status.* Lipids Health Dis, 2007. **6**: p. 17.
129. Okita, M., et al., *Elevated levels and altered fatty acid composition of plasma lysophosphatidylcholine(lysoPC) in ovarian cancer patients.* Int J Cancer, 1997. **71**(1): p. 31-4.
130. Sparr, E., et al., *Self-association of transmembrane alpha-helices in model membranes: importance of helix orientation and role of hydrophobic mismatch.* J Biol Chem, 2005. **280**(47): p. 39324-31.
131. Palladino, P., F. Rossi, and R. Ragone, *Effective critical micellar concentration of a zwitterionic detergent: a fluorimetric study on n-dodecyl phosphocholine.* J Fluoresc, 2010. **20**(1): p. 191-6.
132. Harris, F.M., K.B. Best, and J.D. Bell, *Use of laurdan fluorescence intensity and polarization to distinguish between changes in membrane fluidity and phospholipid order.* Biochimica Et Biophysica Acta-Biomembranes, 2002. **1565**(1): p. 123-128.
133. Stangl, M., et al., *A minimal hydrophobicity is needed to employ amphiphilic p(HPMA)-co-p(LMA) random copolymers in membrane research.* Biochemistry, 2014. **53**(9): p. 1410-9.
134. Goldenberg, N.M. and B.E. Steinberg, *Surface charge: a key determinant of protein localization and function.* Cancer Res, 2010. **70**(4): p. 1277-80.
135. Li, L., et al., *Ionic protein-lipid interaction at the plasma membrane: what can the charge do?* Trends Biochem Sci, 2014. **39**(3): p. 130-40.
136. Khuong, T.M., et al., *Synaptic PI(3,4,5)P3 is required for Syntaxin1A clustering and neurotransmitter release.* Neuron, 2013. **77**(6): p. 1097-108.
137. van den Bogaart, G., et al., *Membrane protein sequestering by ionic protein-lipid interactions.* Nature, 2011. **479**(7374): p. 552-5.
138. Shi, X., et al., *Ca2+ regulates T-cell receptor activation by modulating the charge property of lipids.* Nature, 2013. **493**(7430): p. 111-5.
139. Cohen, J.A. and M. Cohen, *Adsorption of monovalent and divalent cations by phospholipid membranes. The monomer-dimer problem.* Biophys J, 1981. **36**(3): p. 623-51.
140. Lau, A., A. McLaughlin, and S. McLaughlin, *The adsorption of divalent cations to phosphatidylglycerol bilayer membranes.* Biochim Biophys Acta, 1981. **645**(2): p. 279-92.
141. Lis, L.J., et al., *Adsorption of divalent cations to a variety of phosphatidylcholine bilayers.* Biochemistry, 1981. **20**(7): p. 1771-7.
142. Lis, L.J., V.A. Parsegian, and R.P. Rand, *Binding of Divalent-Cations to Dipalmitoylphosphatidylcholine Bilayers and Its Effect on Bilayer Interaction.* Biochemistry, 1981. **20**(7): p. 1761-1770.
143. Martin-Molina, A., C. Rodriguez-Beas, and J. Faraudo, *Effect of Calcium and Magnesium on Phosphatidylserine Membranes: Experiments and All-Atomic Simulations.* Biophysical Journal, 2012. **102**(9): p. 2095-2103.
144. McLaughlin, S., et al., *Adsorption of divalent cations to bilayer membranes containing phosphatidylserine.* Journal of General Physiology, 1981. **77**(4): p. 445-73.
145. Eklund, K.K., et al., *Ca2+-induced lateral phase separation in phosphatidic acid/phosphatidylcholine monolayers as revealed by fluorescence microscopy.* Biochemistry, 1988. **27**(9): p. 3433-7.
146. Papahadjopoulos, D., A. Portis, and W. Pangborn, *Calcium-induced lipid phase transitions and membrane fusion.* Ann N Y Acad Sci, 1978. **308**: p. 50-66.

147. D. Papahadjopoulos, G.P., W. J. Vail *Studies on Membrane Fusion with Natural and Model Membranes*, in *Methods in Membrane Biology*, E.D. Korn, Editor. 1979. p. 1-121
148. Stangl, M., et al., *Detergent properties influence the stability of the glycophorin A transmembrane helix dimer in lysophosphatidylcholine micelles.* Biophysical Journal, 2012. **103**(12): p. 2455-64.
149. Stangl, M., et al., *Sequence-specific dimerization of a transmembrane helix in amphipol A8-35.* PLoS One, 2014. **9**(10): p. e110970.
150. Traikia, M., et al., *Formation of unilamellar vesicles by repetitive freeze-thaw cycles: characterization by electron microscopy and 31P-nuclear magnetic resonance.* Eur Biophys J, 2000. **29**(3): p. 184-95.
151. Pedersen, U.R., et al., *The effect of calcium on the properties of charged phospholipid bilayers.* Biochim Biophys Acta, 2006. **1758**(5): p. 573-82.
152. Claessens, M.M., et al., *Opposing effects of cation binding and hydration on the bending rigidity of anionic lipid bilayers.* J Phys Chem B, 2007. **111**(25): p. 7127-32.
153. Anbazhagan, V., et al., *Fluidizing the membrane by a local anesthetic: phenylethanol affects membrane protein oligomerization.* J Mol Biol, 2010. **404**(5): p. 773-7.
154. Fidorra, M., et al., *Absence of fluid-ordered/fluid-disordered phase coexistence in ceramide/POPC mixtures containing cholesterol.* Biophys J, 2006. **90**(12): p. 4437-51.
155. Rossy, J., Y. Ma, and K. Gaus, *The organisation of the cell membrane: do proteins rule lipids?* Curr Opin Chem Biol, 2014. **20**: p. 54-9.
156. Wu, M., X. Wu, and P. De Camilli, *Calcium oscillations-coupled conversion of actin travelling waves to standing oscillations.* Proc Natl Acad Sci U S A, 2013. **110**(4): p. 1339-44.

4. Publikationen

4.1 Detergent Properties Influence the Stability of the Glycophorin A Transmembrane Helix Dimer in Lysophosphatidylcholine Micelles

Michael Stangl, *Anbazhagan Veerappan, Anja Kroeger, Peter Vogel, Dirk Schneider.*

Biophysical Journal, December 2012, Volume 103, Issue 12

Eigener Beitrag: Mitwirkung bei der Planung der Experimente, Mitwirkung bei der Verfassung des Manuskripts und Erstellung der Abbildungen, FRET-Messungen und Auswertung, CMC Messungen und Auswertung, CD-spektroskopische Messungen und Auswertung.

4.2 Sequence-Specific Dimerization of a Transmembrane Helix in Amphipol A8-35

Michael Stangl, *Sebastian Unger, Sandro Keller, Dirk Schneider.*

Plos One, October 2014, Volume 9, Issue 10

Eigener Beitrag: Mitwirkung bei der Planung der Experimente, Mitwirkung bei der Verfassung des Manuskripts und Erstellung der Abbildungen, FRET-Messungen und Auswertung, CD-spektroskopische Messungen und Auswertung.

4.3 A Minimal Hydrophobicity Is Needed To Employ Amphiphilic p(HPMA)-co-p(LMA) Random Copolymers in Membrane Research

Michael Stangl, *Mirjam Hemmelmann, Mareli Allmeroth, Rudolf Zentel, Dirk Schneider.*

Biochemistry, February 2014, Volume 53, Issue 9

Eigener Beitrag: Mitwirkung bei der Planung der Experimente, Mitwirkung bei der Verfassung des Manuskripts und Erstellung der Abbildungen, FRET-Messungen und Auswertung, Peptidfluoreszenz-Messungen und Auswertung, CD-spektroskopische Messungen und Auswertung, Laurdan Messungen und Auswertung, Liposomen-*leakage* Messungen und Auswertung, ANS Messungen und Auswertung.

4.4 Functional Competition within Membranes: Lipid Recognition vs. Transmembrane Helix Oligomerization

Michael Stangl, *Dirk Schneider*

Review, BBA-Biomembranes, Epub ahead of print

Eigener Beitrag: Mitwirkung bei der Verfassung des Manuskripts und Erstellung der Abbildungen

4.5 Weitere Publikationen und Manuskripte

Calcium binding to PG membranes controls transmembrane Helix-Helix-Interactions.

Michael Stangl, *Dirk Schneider*

Manuskript in Bearbeitung

Nicht Teil der vorliegenden Arbeit:

Core-extended terrylene tetracarboxdiimide: synthesis and chiroptical characterization.

Christian Lütke Eversloh, Zhihong Liu, Beate Müller, ***Michael Stangl***, *Chen Li, Klaus Müllen*

Organic Letters, October 2011, Volume 13, Issue 20

Detergent Properties Influence the Stability of the Glycophorin A Transmembrane Helix Dimer in Lysophosphatidylcholine Micelles

Michael Stangl,[†] Anbazhagan Veerappan,[†‡] Anja Kroeger,[§] Peter Vogel,[†] and Dirk Schneider[†*]
[†]Institut für Pharmazie und Biochemie, Johannes Gutenberg-Universität Mainz, Mainz, Germany; [‡]School of Chemical and Biotechnology, SASTRA University, Thanjavur, Tamil Nadu, India; and [§]Max Planck Institute for Polymer Research, Mainz, Germany

ABSTRACT Detergents might affect membrane protein structures by promoting intramolecular interactions that are different from those found in native membrane bilayers, and fine-tuning detergent properties can be crucial for obtaining structural information of intact and functional transmembrane proteins. To systematically investigate the influence of the detergent concentration and acyl-chain length on the stability of a transmembrane protein structure, the stability of the human glycophorin A transmembrane helix dimer has been analyzed in lyso-phosphatidylcholine micelles of different acyl-chain length. While our results indicate that the transmembrane protein is destabilized in detergents with increasing chain-length, the diameter of the hydrophobic micelle core was found to be less crucial. Thus, hydrophobic mismatch appears to be less important in detergent micelles than in lipid bilayers and individual detergent molecules appear to be able to stretch within a micelle to match the hydrophobic thickness of the peptide. However, the stability of the GpA TM helix dimer linearly depends on the aggregation number of the lyso-PC detergents, indicating that not only is the chemistry of the detergent headgroup and acyl-chain region central for classifying a detergent as harsh or mild, but the detergent aggregation number might also be important.

INTRODUCTION

Because they mimic many aspects of cellular membranes, detergents are typically used for membrane protein extraction, purification and structural analyses, and for studies aiming to analyze the energetics of transmembrane (TM) protein folding and stability. Detergents not only provide a hydrophobic environment (thereby stabilizing a protein structure), they also serve as an intimate solvent and impose numerous restrictions on TM protein folding, assembly, and stability. When detergent molecules bind only to the formally lipid-exposed TM protein surface area, but not at sites of protein-protein contacts, the detergent molecules might simply replace bilayer lipids and the structural integrity of a TM protein will be preserved. Indeed, several experiments have shown that secondary and tertiary structure elements may be similar in a micellar environment and in lipid bilayers (1), and even a native protein quaternary structure may be maintained in detergents (2,3). Thus, the overall fold and structure of a TM protein can be preserved in a detergent environment.

However, detergents can also affect TM protein structures by promoting intramolecular interactions different from those found in native membrane bilayers (4,5). For example, bacteriorhodopsin crystallized as a monomer in a bicellar environment, whereas in the lipid cubic phase it crystallized as a trimer (6–8). While it was previously assumed that the *Escherichia coli* diacylglycerol kinase requires lipid cofactors, recent studies have indicated that the protein can sustain its native structure, stability, and activity in a defined lipid-free detergent (9). Thus, selecting proper detergent conditions can be crucial to preserve a correct protein structure and function. However, the ability of some (if not all) detergents to preserve the native structure and function of a TM protein appears to differ on a case-by-case basis. Therefore, determination of the detergent and buffer conditions necessary to maintain the structure and function of a TM protein upon solubilization is still an empirical and frequently time-consuming process.

Interactions of detergents with TM proteins depend on the protein itself, such as the TM amino-acid sequence and the secondary structure propensity, as well as on the actual detergent concentration and on detergent properties, such as the headgroup chemistry, the length of acyl chain, or the micelle structures. Identifying a proper detergent used for TM protein solubilization and analyses may be guided by categorizing detergents into mild or harsh detergents, based on their propensity to preserve or disrupt a TM protein structure (10–12). The characteristics of longer tail length, larger detergent headgroup size, and neutral headgroup charge have been identified, in the main, as preservative of TM protein structures, and would therefore be used to classify a detergent as mild. However, the responses of membrane protein structures to detergent solubilization still cannot be safely predicted. Luckily, the range of detergents available for membrane protein research has increased significantly in recent years, now allowing us to find a proper detergent for gaining deeper insight into structure-function relationship of membrane proteins or in the principle guiding membrane protein folding (11).

Although our understanding of the principles guiding membrane protein folding has significantly improved in recent years, the forces governing protein folding inside lipid bilayers are still poorly understood (13,14). Two

Submitted March 8, 2012, and accepted for publication November 5, 2012.

*Correspondence: dirk.schneider@uni-mainz.de

Editor: William Wimley.

0006-3495/12/12/2455/10 $2.00

http://dx.doi.org/10.1016/j.bpj.2012.11.004

decades ago, the folding of α-helical membrane proteins was simplified as a two-stage process: Stage 1, in which individual helices insert independently into the membrane; and Stage 2, in which these helices subsequently interact to form higher-ordered oligomeric structures (15). While this two-stage model significantly simplifies the problem of α-helical membrane protein folding, it allows an uncomplicated but meaningful analysis of membrane protein folding, because formation of stable α-helices and integration of helices into a membrane are uncoupled from the formation of a three-dimensional membrane protein structure. The human glycophorin A (GpA) TM helix dimer became a paradigm for studying the second stage of this two-stage process, as the TM region of GpA forms a stable, noncovalent helix dimer. The NMR structure of the GpA TM in DPC micelles (16), along with a wealth of information on the sequence-specific dimerization (17–22), have made this system ideal for analyzing the energetics of TM helix-helix interactions in more detail.

The stability of the GpA TM dimer studied in model membrane systems has indicated that interactions between helices are modulated by lipid acyl-chain order, by hydrophobic matching between the peptide and lipid bilayer as well as by the lipid headgroup chemistry (23,24). Thus, the membrane environment significantly influences GpA TM helix dimerization. Furthermore, a micellar environment also significantly influences association and the stability of the GpA helix dimer (25–28). It has been suggested that GpA peptide association is mainly driven by enthalpic forces in micelles, whereas at high detergent concentrations, peptide association is opposed by entropic forces (26).

Increasing detergent concentrations increase the number of available micelles, and thus of the effective solvent of the TM protein, which might result in dilution of the GpA dimer. While the thermodynamics underlying destabilization of the TM helix dimer have been well described for the influence of the headgroup chemistry, the impact of the acyl chain on the thermodynamics of a TM helix structure have been far less elucidated yet (26). The actual concentration of detergent monomers per micelle, the aggregation number, might also affect the stability of a TM helix-helix interaction—an aspect not yet considered. Furthermore, it is still a matter of debate whether the radius of the hydrophobic micelle core affects the stability of a TM structure (i.e., whether hydrophobic match/mismatch determines the stability of a TM structure in a detergent micelle (12,29)).

In this study, we analyzed the stability of the GpA TM helix dimer in detergent micelles. We used lyso-phosphatidylcholine (lyso-PC) micelles of different acyl-chain length to systematically investigate the influence of the detergent concentration and acyl-chain length on the stability of a TM structure, excluding any effects caused by the detergent headgroup chemistry or by introducing mutations into the peptide. Furthermore, we analyzed the influence of the detergent aggregation number as well as that of the micelle's hydrodynamic radius on the stability of a TM structure. Based on our results, dissociation of the GpA TM helix dimer cannot be explained by simple dilution, because, in addition to the detergent concentration, direct protein-detergent interactions or detergent properties (such as the acyl-chain hydrophobicity and the detergent aggregation number) might influence the stability of the α-helical TM protein. Importantly, the GpA TM helix dimer was found to not be most stable when the measured hydrodynamic radius of the micelle matches the hydrophobic region of the TM helix dimer. Consequently, the concept of hydrophobic match/mismatch cannot be easily transferred from membrane systems to detergent environments—at least, not for lyso-PC detergents.

MATERIALS AND METHODS

Materials

Peptides corresponding to residues 69–101 of the human GpA TM domain (SEPEITLIIFGVMAGVIGTILLISYGIRRLIKK) were custom-synthesized and labeled at the N-terminus with the donor and acceptor dyes fluorescein (Fl) and 5-6-carboxyrhodamine (TAMRA), respectively (Peptide Specialty Laboratories, Heidelberg, Germany). The purity of the peptides was confirmed by HPLC and mass spectrometry. Peptides were dissolved in 2,2,2-trifluoroethanol purchased from Sigma-Aldrich (Munich, Germany). Lyso-PC detergents C10–C16 were purchased from Avanti Polar Lipids (Alabaster, AL) and dissolved in chloroform/methanol (2:1).

FRET measurements

For FRET measurements, equal concentrations (1:1 mol ratio) of Fl- and TAMRA-labeled GpA TM domains were used. The concentrations of the peptide stock solutions were determined from absorbance measurements in a Lambda 35 UV/Vis spectrophotometer (PerkinElmer, Boston, MA). In all experiments, we used 0.25 μM for each labeled GpA peptide. Peptides, dissolved in trifluoroethanol and detergent, dissolved in chloroform/methanol (2:1), were mixed and organic solvents were removed in a gentle stream of nitrogen gas. Final traces of the solvents were removed by vacuum desiccation overnight. The dried peptide-detergent film was hydrated in 10 mM HEPES buffer (pH 7.4) containing 150 mM NaCl.

After five freeze-thaw cycles, steady-state fluorescence measurements were performed at 25°C in a Spectronic Bowman series-2 luminescent spectrometer (Thermo Scientific, Waltham, MA) having both the excitation and the emission bandpass filter set at 4 nm. The excitation wavelength was 439 nm and emission spectra were recorded from 480 to 650 nm.

To follow the effect of the detergent environment and increasing detergent concentrations on a defined TM helix-helix interaction, we studied the dissociation of the GpA TM helix dimer following the EmEx-FRET method (30,31), which allows determining the concentration of GpA TM helix dimers in micelles.

Energy transfer E was calculated using the donor fluorescence intensities at 525 nm in the presence and absence of acceptor according to

$$E = 1 - \left(\frac{F_{DA}}{F_D}\right). \tag{1}$$

F_D is the fluorescence intensity of the donor sample and F_{DA} is the fluorescence intensity of the sample containing donor and acceptor GpA TM domain at equal concentrations. The energy transfer of sequence-specific TM helix dimerization, E_D, can be expressed as

$$E_D = f_D P_D E_R, \tag{2}$$

where f_D is the fraction of dimeric TM helices, P_D is the probability for donor quenching when the peptides form a dimer, and E_R is the energy transfer in the dimer.

The probability P_D for donor quenching depends on the molar ratio of the acceptor peptides $\chi_a = [a]/([a]+[d])$, where [a] and [d] are the concentrations of the acceptor and donor peptides, respectively. The distance of the fluorophores in the GpA helix dimer is much smaller than the Förster radius, and thus E_R can be set as 1.

The fraction dimer, f_D, can be written as $f_D = 2[D]/[T]$, where [D] is the concentration of dimeric peptides and [T] the total peptide concentration. Therefore, the dimer concentration [D] can be calculated by

$$[D] = \frac{E_D[T]}{2\chi_a}. \tag{3}$$

The dissociation constant, K_D, and the corresponding standard Gibbs free-energy change of dissociation, ΔG^o, are given by

$$K_D = \frac{[M]^2}{[D]}, \tag{4}$$

$$\Delta G_D^0 = -RT \ln K_D, \tag{5}$$

where the monomer concentration is [M] = [T] – 2[D].

Circular dichroism

Circular dichroism (CD) spectra were recorded on a J-815 spectropolarimeter (JASCO, Easton, MD) at 25°C with a scan speed of 100 nm/min using 0.1-cm-pathlength quartz cells from Hellma (Mühlheim, Germany). The concentration of unlabeled GpA peptide was 18 μM. Data points were collected with a resolution of 1 nm, an integration time of 1 s, and a slit width of 1 nm. Each spectrum shown is the result of at least three averaged consecutive scans, from which buffer scans were subtracted. The measured ellipticity θ (deg) was converted to molar ellipticity by

$$\text{Molar ellipticity} = 100\left(\frac{\theta}{L\,C}\right), \tag{6}$$

where L is the path length and C is the peptide concentration.

The GpA TM domain has been mixed in organic solvent with 20 mM lyso-PCs having acyl-chain lengths ranging from C10 to C16. After removal of the organic solvents by nitrogen and desiccation, samples were hydrated with 50 mM phosphate buffer pH 7.4. Before measuring, samples were treated identically as for the FRET measurements. The secondary structure contents were predicted using the software package DICHROWEB (http://dichroweb.cryst.bbk.ac.uk/html/home.shtml), which contains both soluble and TM proteins as a reference data set (32,33).

Critical micellar concentration and aggregation number N_{agg} determination by fluorescence spectroscopy

The critical micellar concentration (cmc) of each lyso-PC was determined by following 1-anilinonaphtalene-8-sulfonate fluorescence (34). A detergent stock solution (concentration 20- to 40-fold above the expected cmc) was titrated in 10 mM HEPES buffer containing 150 NaCl, 5 μM 1-anilinonaphtalene-8-sulfonate, pH 7.4. After each addition, a fluorescence spectrum was monitored from 450 to 600 nm after excitation at 374 nm. The fluorescence intensity at 490 nm was then plotted as a function of the detergent concentration, and the cmc was evaluated by linear least-squares fitting. Data points before and after the change of the slope were fitted to two straight lines. The cmc values were determined by the intersection of the two straight lines using at least two independent measurements. The R^2 coefficient of determination was always above 0.95 for the fitted straight lines, hence potential errors caused by fitting were neglectable.

The number of molecules forming micelles (aggregation number N_{agg}) was determined by a fluorescence quenching method as described in detail in the literature (35,36). Briefly, 2 μM of pyrene dissolved in 20 mM lyso-PC was quenched with n,n-dibutyl aniline (concentration range varied from 0 to 100 μM) and the fluorescence intensity at 373 nm was measured (excitation at 337 nm). The aggregation number N_{agg} was calculated by

$$N_{agg} = \frac{([D_c] - cmc)}{[M_c]}, \tag{7}$$

where D_c, cmc, and M_c represent the total detergent concentration, the critical micellar concentration, and the actual concentration of micelles, respectively. The unknown parameter, M_c, was determined by

$$\ln\left(\frac{I_0}{I}\right) = \frac{[Q]}{[M_c]}, \tag{8}$$

where I_0 and I are the fluorescence intensity of pyrene before and after addition of n,n-dibutyl aniline, respectively, and $[Q]$ is the quencher concentration. A plot of $\ln(I_0/I)$ versus $[Q]$ was fitted with a straight line with a slope of $1/M_c$. Aggregation numbers N_{agg} can be then calculated using Eq. 7.

Light scattering

Static-light-scattering (SLS) and dynamic-light-scattering (DLS) experiments were performed on an instrument consisting of a goniometer and an ALV-5004 multiple-tau full-digital correlator (320 channels; ALV, Langen/Hessen, Germany), which allows measurements over a time range $10^{-7} \leq t \leq 10^3$ s and an angular range from 30° to 150° corresponding to a scattering vector $q = 6.9 \times 10^{-3} - 2.6 \times 10^{-2}$ nm^{-1}. An He-Ne laser (with a single mode intensity of 25 mW operating at a laser wavelength of $\lambda_0 =$ 632.8 nm; JDS Uniphase, Milpitas, CA) was used as a light source. Dust-free samples for SLS and DLS experiments were obtained by filtration through PTFE membrane filters with a pore-size of 5 μm (LCR syringe filters; Millipore, Billerica, MA) directly into cylindrical silica-glass cuvettes (inner diameter Ø = 20 mm; Hellma) that had been cleaned with acetone in a Thurmont-apparatus. The cuvettes containing the sample solutions were placed into a thermostated refractive index-matching toluene bath held at a constant temperature of $T = 25$°C.

In the SLS experiments, the reduced absolute intensity ratio $R(q)/(Kc)$ at a concentration c was computed from the Rayleigh ratio $R(q)$,

$$R(q) = \frac{I(q)_{so\ \ln} - I(q)_{solv}}{I(q)_t}\left(\frac{n_{solv}}{n_t}\right)^2 R_t, \tag{9}$$

and the optical constant $K = (2\pi \cdot n\, dn/dc)^2/(\lambda_0{}^4 \cdot N_A)$; I_{soln}, I_{solv}, and I_t are the light-scattering intensities of the solution, solvent, and the pure toluene, respectively. Toluene was used as a standard with refractive index n_t and Rayleigh ratio $R_t = 2.2 \cdot 10^{-5}$ cm^{-1}. N_A is the Avogadro number.

The refractive index increment $dn/dc = 0.1359$ mL g^{-1} was determined at $\lambda = 633$ nm using a scanning Michelson interferometer. Further theoretical details of the DLS experiments and specifics of the data evaluation by using the constraint-regularized CONTIN method are given elsewhere (37).

RESULTS

GpA TM helix secondary structure in lyso-PCs

The impact of detergent properties on the stability of the GpA TM helix dimer was systematically analyzed in lyso-PC micelles, having acyl-chain lengths ranging from C10 to C16. To ensure that the secondary structure of the GpA TM helix was preserved in the respective lyso-PC micelles, far-UV CD spectra of the GpA TM peptide were recorded in the various lyso-PCs (Fig. 1). In all tested detergents, the TM domain showed characteristics typical for an α-helical structure with a maximum at ~193 nm and double-minima at 208 nm and 222 nm. Calculation of the secondary structure using the software package DICHROWEB suggested an α-helix content between 78 and 81% for most tested lyso-PCs at a detergent concentration of 20 mM (Table 1). Of note, the α-helix content of the peptides did not depend on the actual lyso-PC concentrations. While the CD data clearly demonstrates that the secondary structure of the GpA TM domain is well preserved in the tested lyso-PCs, it is impossible to determine the fractions of monomeric or dimeric GpA solely by CD, as the peptides have essentially identical CD spectra. Such identical CD spectra of both monomeric and dimeric GpA in detergents have been previously reported (25,27). Therefore, to analyze the stability of the TM helix dimer in lyso-PC micelles, we performed FRET measurements.

The stability of the GpA TM domain dimer depends on the lyso-PC acyl-chain length

To quantitatively analyze the influence of defined lyso-PC properties on a TM helix dimer stability, we monitored GpA TM helix dimerization in lyso-PCs with different acyl-chain lengths by fluorescence spectroscopy. In Fig. S1 in the Supporting Material, we show fluorescence excitation and emission spectra of Fl- and TAMRA-labeled GpA peptides. The Fl emission spectrum overlaps significantly with the TAMRA excitation spectrum. The distance between the amino termini of the GpA TM helices in the dimer, as calculated from the NMR structure, is ~10 Å, which is far below the Förster radius (R_0) of the Fl/TAMRA FRET pair (49–54 Å) (38). Thus, the energy transfer measured as donor emission quenching and/or sensitized acceptor emission (see Fig. S1 *C*) is a direct measure of GpA TM helix dimerization.

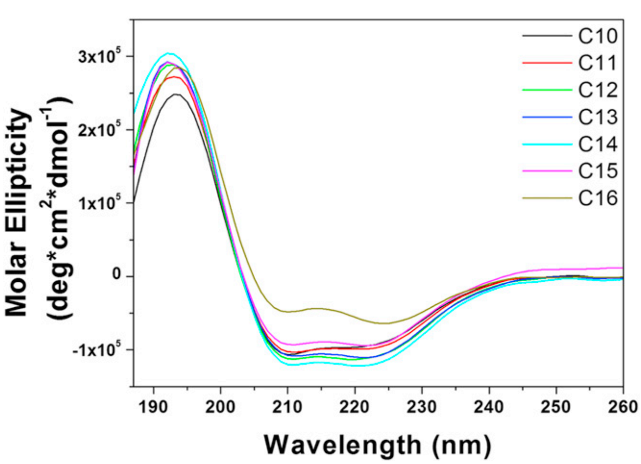

FIGURE 1 Far UV-CD spectra of the GpA TM domain in 20 mM lyso-PCs. C10-lysoPC (*black*), C11-lysoPC (*red*), C12-lysoPC (*green*), C13-lysoPC (*blue*), C14-lysoPC (*cyan*), C15-lysoPC (*magenta*), and C16-lysoPC (*yellow*). The measured ellipticities were converted to molar ellipticity as described in Materials and Methods.

TABLE 1 Helical content of the GpA TM domain in 20 mM lyso-PCs with increasing acyl-chain lengths as determined by the program DICHROWEB

Lyso-PC	α-helical content [%]
10	81
11	81
12	79
13	78
14	78
15	78
16	66

FRET measurements were performed in presence of 20 mM lyso-PCs having increasing acyl-chain length, and the normalized emission spectra of the FRET pair are shown in Fig. 2 *A*. The sensitized emission at 575 nm decreased with increasing acyl-chain length, indicating a decreasing stability of the GpA TM helix dimer. The individual GpA dimer fractions in the various lyso-PCs, as calculated from the donor and FRET pair emission spectra (Fig. 2 *B*), strongly suggest a correlation between the acyl-chain length and the stability of the dimer, with the highest dimer fraction of ~60 % observed in C10 lyso-PC. The stability of the dimer decreases with increasing lyso-PC acyl-chain lengths (Fig. 2), most likely because hydrophobic interactions of the lyso-PCs with the GpA TM helix increase with increasing lyso-PC acyl-chain lengths.

Together, our results suggest that the GpA TM domain forms a stable dimer in all analyzed lyso-PCs and that the lyso-PC acyl-chain length affects the dimerization propensity in micelles.

The stability of the GpA TM domain dimer depends on the lyso-PC concentration

To analyze the influence of the various lyso-PC detergents on the energetics of the TM helix-helix interaction in more detail, we then measured the thermodynamic stability of the GpA TM helix dimer at different lyso-PC concentrations.

Concentration-dependent dimerization of the GpA TM domain in lyso-PC micelles was studied by monitoring resonance energy transfer with fluorescently labeled GpA TM peptides. All experiments were performed at a constant peptide concentration by varying only the lyso-PC

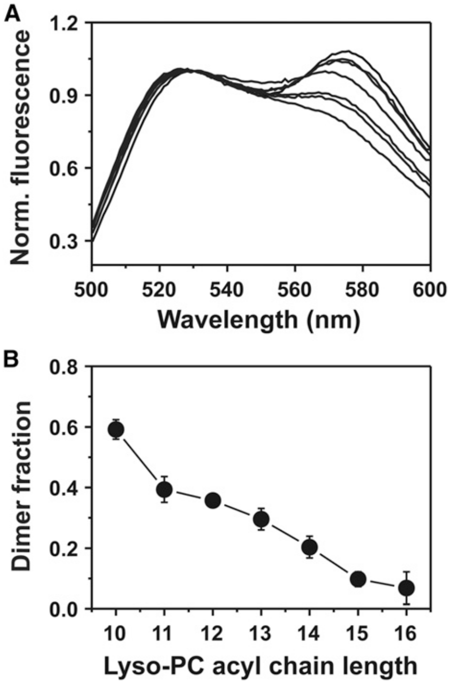

FIGURE 2 Self-association of GpA peptides in 20 mM lyso-PCs. Fluorescence emission was measured in micelles with Fl-labeled peptide alone as well as with the Fl- and TAMRA-labeled peptide pair (1:1 ratio). Energy transfer was calculated from the Fl-fluorescence decrease at 525 nm. (*A*) FRET spectra recorded for Fl- and TAMRA-labeled peptides dissolved in 20 mM C_n lyso-PC detergents. (*Upper spectrum*) This data originates from peptides dissolved in C10-lyso PC micelles and the others were measured in lyso-PCs having increasing acyl-chain lengths (C10–C16), resulting in decreasing energy transfer. (*B*) Fraction dimer plotted against the acyl-chain length of the various lyso-PCs.

concentrations. The inset in Fig. 3 *A* shows representative emission spectra of the FRET pair (1:1 ratio) at increasing lyso-PC concentrations. The relative decrease in the sensitized emission at 575 nm with increasing lyso-PC concentration clearly indicates destabilization of the GpA TM helix dimer. The dimer fractions at increasing detergent concentrations, as calculated from the measurements shown in the inset, are summarized in Fig. 3 *A* for C10 and C16 lyso-PCs. Irrespective of the acyl-chain length, the fraction of dimeric GpA, and thus the stability of the GpA TM helix-helix interaction, decreases nonlinearly with increasing detergent concentrations. Thus, with increasing detergent concentrations, the GpA TM monomer-dimer equilibrium significantly shifts toward the monomer in all analyzed lyso-PCs. Based on measurements as shown in Fig. 3 *A*, the apparent GpA dissociation constants were calculated in the various lyso-PC detergents at increasing concentrations (see Table S1 in the Supporting Material). Fig. 3 *B* shows the apparent K_D values calculated based on the FRET measurements performed in C10 and C16 lyso-PC. All calculated K_D values are summarized in Table S1.

While the stability of the GpA TM helix dimer appears to depend on the lyso-PC acyl-chain length, the observed

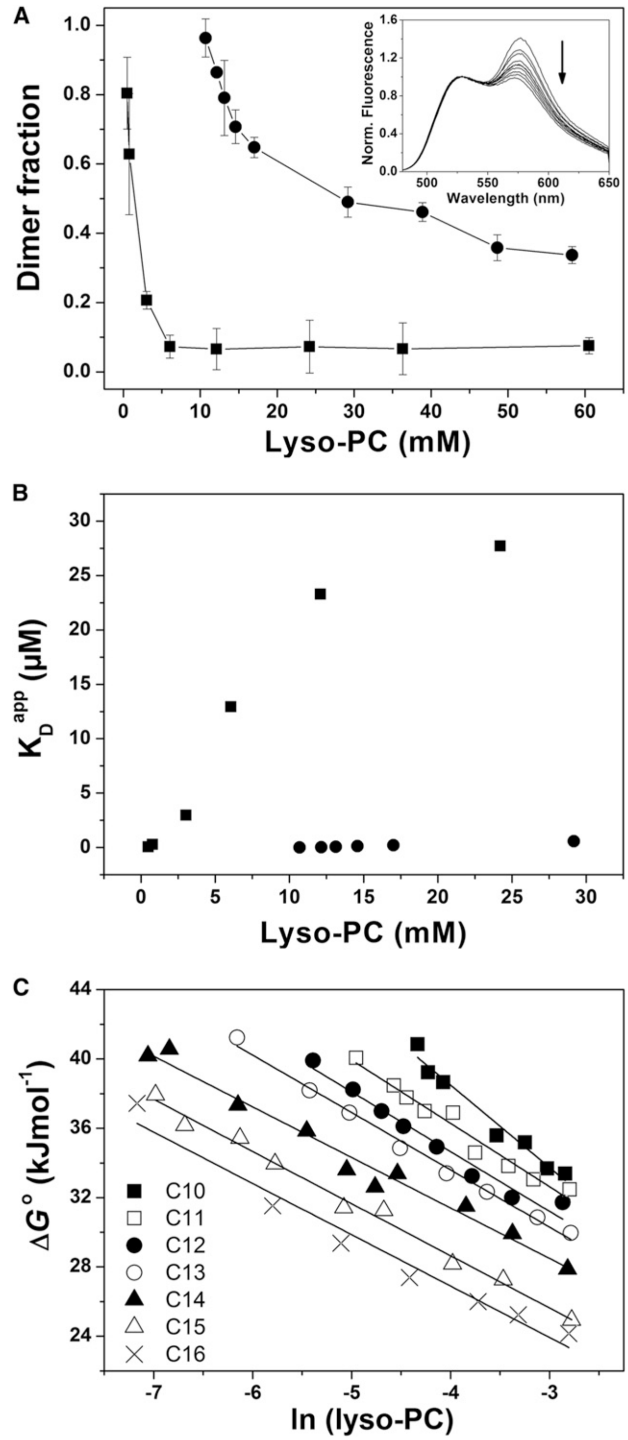

FIGURE 3 Concentration-dependent dimerization of the GpA TM domain. (*A*) GpA TM helix dimer fractions calculated from FRET spectra obtained at various C10 (●) and C16 (■) lyso-PC concentrations. The lyso-PC concentrations are given on the *x* axis. (*Inset*) FRET spectra recorded for Fl- and TAMRA-labeled peptides (1:1 mol ratio) in C10 lyso-PC micelles. All spectra were normalized at 525 nm. (*Arrow*) Spectral shifts at increasing C10 lyso-PC concentrations. (*B*) Apparent GpA TM dissociation constant determined in C10 (●) and C16 (■) lyso-PC micelles at increasing detergent concentrations. (*C*) Apparent dissociation free energy values ($\Delta G°$) calculated from the apparent K_D values shown in panel *A* and summarized in Table S1.

dimerization propensities at a given detergent concentration might not be compared directly, because detergent properties, such as the critical micellar concentration (cmc) or aggregation number of the respective lyso-PCs, vary with increasing acyl-chain length. Thus, we next determined the cmc as well as aggregation numbers of lyso-PC micelles (Table 2). In Fig. S2, the cmc values of the analyzed lyso-PCs are summarized, and the cmc values decrease exponentially with increasing acyl-chain length. The mean aggregation number, N_{agg}, was determined at 20 mM lyso-PC by a pyrene fluorescence-quenching method as described in Materials and Methods (Fig. 4 *A*). To rule out any potential interference from pyrene eximer formation during the fluorescence N_{agg} determination, we additionally measured the pyrene fluorescence from 360 to 500 nm at varying lyso-PC concentrations (see Fig. S3). Because no peak at 480 nm was observed, pyrene eximer formation could be excluded, confirming that the observed fluorescence quenching was only caused by addition of the quencher (*n*,*n*-dibutyl aniline).

The aggregation numbers N_{agg} of lyso PC samples having acyl-chain lengths of C10–C16 were additionally confirmed by light-scattering measurements (Fig. 4 *A*). The apparent weight-average molar masses M_{Wapp} of the resulting supramolecular assemblies (micelles) were obtained from Ornstein-Zernicke plots (Kc/R_{VV} (q) versus q^2), as shown in Fig. 5. The intercept of an extrapolation $q \to 0$ in the linear regime for each sample yields values of $M_{Wapp} = (1.63 \pm 0.2) \times 10^4$ g mol^{-1} for C10 to $M_{Wapp} = (1.03 \pm 0.1)$ 10^5 g mol^{-1} for C16, which results in N_{agg} between 40 and 209, respectively (Table 2). Fig. 4 *A* shows the lyso-PC aggregation numbers as a function of the acyl-chain length determined by fluorescence quenching (*solid circles*), which is supported by the data obtained from light-scattering experiments (*open circles*). While at higher acyl-chain lengths the aggregation numbers determined by the fluorescence method differ from the values obtained by light scattering, the aggregation numbers nearly increase linearly with increasing acyl-chain length of the lyso-PCs (Fig. 4 *A*), as demonstrated by both applied methods.

The N_{agg} values determined by the two techniques vary from 35/47 for C10 lyso-PC to 112 for C16 lyso-PC when determined by the fluorescence technique, or to 209 for C16 lyso-PC when determined by light scattering. As of this writing, there are only a few lyso-PC aggregation numbers available from the literature. For C10 and C12 lyso-PCs, we determined aggregation numbers of 35/40 and 78/82 at a detergent concentration of 20 mM (Table 2), which are in good agreement with values determined by NMR spectroscopy (34 for C10 and 55 for C12 lyso-PC) (39).

Beyond the aggregation numbers of the micelles, the corresponding micelle sizes were determined by DLS experiments and summarized in Table 2 as *z*-average hydrodynamic radii R_h. The R_h values are in the range of 24–37 Å, and increase linearly with increasing lyso-PC acyl-chain length (Fig. 4 *B* and Table 2).

Sequence specificity of GpA TM helix dimerization in lyso PC micelles

To rule out that the results presented in Figs. 2 and 3 and Table S1 are influenced by unspecific aggregation of the TM peptides or by formation of higher-ordered oligomeric structures, formation of a sequence-specific GpA TM helix dimer was analyzed by monitoring energy transfer at constant peptide and detergent concentrations as a function of the donor/acceptor ratio, as reported in the literature (23,40). Fig. 6 shows FRET efficiencies as a function of the acceptor mole ratio in C14 lyso-PC micelles at 1 mM total detergent concentration. As discussed in detail in the literature (25,40), linear dependence of the FRET efficiency on the acceptor mole ratio indicates, exclusively, dimer formation. This control has also been performed in lyso-PCs with increased acyl-chain length at different concentrations (data not shown) and a linear dependence of the FRET efficiency has always been observed.

Thus, we conclude that the observed FRET efficiencies directly measure formation of a dimeric GpA TM helix structure. Nevertheless, the measured FRET signal can have different origins. While on the one hand it originates from so-called real dimer formation, it might also be influenced by simple proximity effects. Because we used very low peptide/detergent molar ratios, ranging from 1:200 to 1:120,000 (see Table S1), proximity effects are very unlikely. However, to exclude proximity effects, we performed

TABLE 2 Characteristics of lyso-PC micelles and the stability of the GpA TM helix dimer in different acyl-chain length lyso-PCs

Lyso-PC	Cmc (mM)	M_{Wapp} (10^4 gmol^{-1})	R_h (Å)	N_{agg} SLS	N_{agg} Fluor.	ΔG°_d (20 mM) (kJmol^{-1})	$d\Delta G^\circ_d/d\ln$(lyso-PC) (kJmol^{-1})
C10	6.06 (6.0–8.0)	1.63	24	40	35	38.12 ± 0.48	−4.75 ± 0.37
C11	1.81 (—)	3.55	26	67	58	34.61 ± 0.26	−3.65 ± 0.25
C12	0.57 (0.4–0.9)	3.62	28	82	78	33.28 ± 0.52	−3.45 ± 0.26
C13	0.15 (—)	4.45	30	98	91	32.34 ± 0.14	−3.31 ± 0.11
C14	0.04 (0.04–0.09)	5.87	33	126	90	31.51 ± 0.11	−2.92 ± 0.15
C15	0.010 (—)	8.80	34	183	100	28.38 ± 1.30	−3.01 ± 0.11
C16	0.004 (0.004–0.008)	10.34	37	209	112	28.15 ± 1.44	−2.96 ± 0.23

Values in parentheses were obtained from a commercial website (Avanti Polar Lipids, Alabaster, AL).

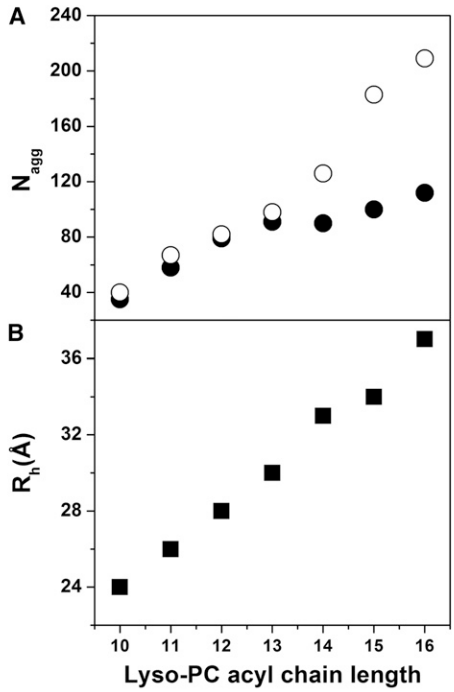

FIGURE 4 Aggregation numbers and hydrodynamic radii of lyso-PC micelles. (*A*) Mean aggregation number N_{agg} as a function of the lyso-PC acyl-chain length at 20 mM detergent concentration determined by fluorescence quenching (●) and SLS (○). (*B*) Hydrodynamic radii R_h of lyso-PC micelles determined by DLS.

FRET measurements upon addition of increasing concentrations of unlabeled GpA peptides, and observed a reduction in the FRET signal (Fig. 7). Upon addition of the unlabeled GpA TM peptides, the FRET signal decreases only if dimerization of the labeled peptides is sequence-specific (25,41).

Thus, the determined FRET efficiencies can be attributed to formation of a sequence-specific GpA TM helix dimer in lyso-PC micelles.

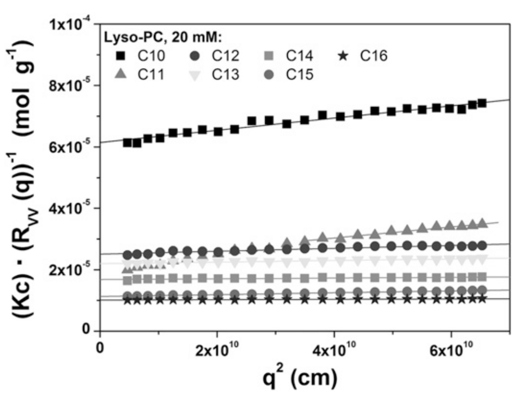

FIGURE 5 Static light-scattering analysis. Absolute light scattering intensity for the various lyso-PC at $c = 20$ mM in an Ornstein-Zernicke presentation for the determination of the molar masses using the intercept of an extrapolation ($q \rightarrow 0$) in the linear regime.

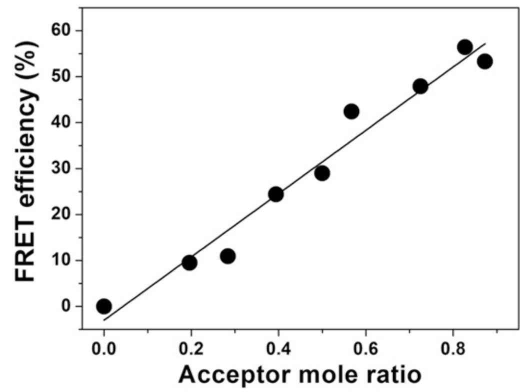

FIGURE 6 Stoichiometry of GpA association. FRET efficiencies as a function of acceptor mole fraction are shown for 1 mM C14 lyso-PC. The total peptide and detergent concentrations were kept constant, whereas the ratio of acceptor and donor peptide varied from 0.2 to 0.85. The linear dependence of the FRET efficiency on the acceptor mole ratio demonstrates exclusive dimer formation.

DISCUSSION

Lysophosphatidylcholines (lyso-PCs) are naturally present in human cells and are released by spontaneous or enzymatic hydrolysis of PC lipids. Lyso-PCs are known to be

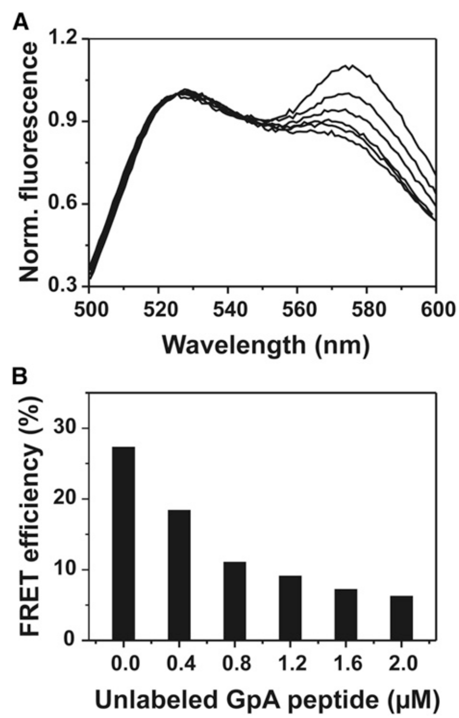

FIGURE 7 FRET competition assay. (*A*) FRET pair emission spectra in 5 mM C12 lyso-PC. Addition of 0.4–2 μM unlabeled GpA TM peptide (compare panel *A* with panel *B*) results in reduced sensitized acceptor emission. Spectra were normalized at 525 nm. (*Upper spectrum*) This data originates from peptides in the absence of unlabeled peptide. Stepwise addition of increasing amounts of unlabeled peptide results in decreased energy transfer, i.e., in decreased fluorescence emission at 575 nm. (*B*) FRET efficiencies calculated from the spectra shown in panel *A*.

involved in T-lymphocyte proliferation and protein kinase C activation (42,43), and the increased plasma lyso-PC concentration found in some cancer patients might be used as a marker for tumor progression (44,45). In vivo, most of the lyso-PC molecules are bound to albumins, which serve as a reservoir to rapidly provide lyso-PCs, if necessary, and eventually preserve membrane lysis (45,46). Because of their detergent properties, lyso-PCs form micellar structures and are membrane-lytic at high concentrations.

In our study, the impact of lyso-PC properties on a sequence-specific TM helix structure has been analyzed. By varying the acyl-chain length only and leaving the detergent headgroup chemistry identical, the influences of just the detergent acyl-chain on the stability of a TM structure have been systematically evaluated.

Thermodynamically, the free energy of helix-helix association in detergent micelles can be written as

$$\Delta G_a = \Delta G_{h-h} + n\Delta G_{d-d} - 2n\Delta G_{h-\mathrm{d}}, \tag{10}$$

where $\Delta G_{h\text{-}h}$, $\Delta G_{d\text{-}d}$, and $\Delta G_{h\text{-}d}$ are the free energies of helix-helix, detergent-detergent, and helix-detergent interactions, respectively. It is assumed that formation of a helix-helix pair displaces $2n$ helix-detergent and results in n gained detergent-detergent interactions. Dimerization of TM helices will be driven by a favorable value of $\Delta G_{h\text{-}h}$, arising, for example, from van der Waals' forces, salt-bridge, or hydrogen-bonding interactions between helices. Furthermore, rather weak interactions of the genetive headgroups with TM helices and poor packing of the acyl chains to the rough surface of TM helices might disfavor helix-detergent interactions and drive helix dimerization. However, interactions between the detergent acyl chains and the hydrophobic TM helix most likely increase with increasing acyl-chain length, which is coupled with increasing acyl-chain hydrophobicity, and consequently the free energies of dimerization decrease in lyso-PC micelles with increasing acyl-chain length (Fig. 3 *C* and Table 2). Notably, this observation contrasts with earlier findings in which it has been concluded that detergents with longer acyl-chain length generally tend to stabilize the structure of TM proteins (11).

However, irrespective of the genitive acyl-chain length, increasing detergent concentrations generally destabilize the GpA helix dimer (Fig. 3), as demonstrated by the increasing dissociation constants (Fig. 3 *B*, and see Table S1). This destabilization has been observed before and might be explained by a simple dilution effect based on entropically driven dissociation (26). In the ideal case, dissociation of helices caused by simple peptide dilution due to increasing detergent concentrations results in a slope of -2.48 kJ mol^{-1} (8.314 J mol^{-1} K^{-1} $\times$ 298 K). However, while the calculated free energies of dissociation linearly depend on the lyso-PC concentration in all tested lyso-PCs (Fig. 3 *C*), the slopes vary from -4.75 to -2.96 kJmol^{-1} (Table 2). Only dimerization in C16 lyso-PC is close to ideality and might be explained by simple dilution. Inconsistency from ideality, as usually observed, suggests a general mechanism driving helix-helix dissociation that is far more complex than simple dilution; and helix-detergent or detergent-detergent interactions, and the corresponding free energies, also eventually influence monomerization. Furthermore, because the properties of detergent micelles (such as the aggregation number or the hydrodynamic micelle radius) change with increasing acyl-chain length, the properties of the most intimate environment of a TM protein (the micelle it resides in) could also influence the stability of the TM helix oligomer. Thus, based on the results presented here, destabilization of a TM helix oligomer by increasing detergent concentration cannot be explained by simple dilution alone; a far more complex model is required.

In the past, several studies have shown that the structure of integral membrane proteins can highly depend on hydrophobic matching conditions, i.e., the thickness of the hydrophobic hydrocarbon core of the lipid bilayer must approximately match the hydrophobic region of the TM protein. Hydrophobic mismatch can result in severe destabilization of TM protein structures (47,48). Preservation of a TM protein structure in a lipid bilayer with changing bilayer thickness will alter lipid packing in the intimate surrounding bilayer, and the bilayer deformation energy is associated with local thickening or thinning of the lipid bilayer to match the hydrophobic region of the TM protein (49). Thus, it appears to be possible that a TM protein structure is most stable whenever the hydrophobic region of a micelle just about matches the hydrophobic region of a TM protein (29). On the other hand, detergent micelles are far more dynamic than lipid bilayers, and a micellar structure might adjust more easily to various TM protein structures (12). GpA dimerized in all tested lyso-PC micelles, and dimerization was most efficient in C10 lyso-PC but decreased with increasing lyso-PC acyl-chain length (Fig. 2 *B*, and see Table S1).

The observed high GpA TM helix dimerization propensity in C10 lyso-PC cannot be explained by simply considering the thickness of the hydrophobic micelle core, as the hydrophobic region of the GpA TM α-helix dimer is ~31.3 $\pm$ 2.2 Å, whereas the diameter of the C10 lyso-PC micelles is only ~24 Å (Table 2). If the thickness of the hydrophobic micelle core were most important for stabilization of the GpA helix dimer (hydrophobic matching), the dimer should have been most stable in C13 or C14 lyso-PCs, having diameters of ~30 and 33 Å, respectively (Table 2). As this has not been observed, it appears to be rather likely that individual detergent molecules stretch within a micelle to match the hydrophobic thickness of the peptide. However, the structural dynamics of the micelle might be impaired when micelles are formed from detergents with longer acyl chains, due to increased detergent-peptide and detergent-detergent interactions. Thus, with increasing acyl-chain length the elastic properties of the acyl chains decrease and eventually become insufficient to compensate a (potential) hydrophobic mismatch, resulting in destabilization of a TM protein structure. Notably, the α-helical structure of the GpA TM domain, as determined by NMR in micelles (16) (PDB ID:1AFO and PDB ID:2KPE) and bicelles (50) (PDB ID:2KPF), was preserved in all analyzed lyso-PCs (Fig. 1).

Closer examination of the lyso-PC micelle properties over the range of the experimentally tested acyl-chain lengths also revealed that the lyso-PC aggregation numbers, N_{agg}, vary considerably for the various lyso-PCs (Fig. 4 *A*). The fraction dimeric GpA measured in 20 mM lyso-PCs with increasing acyl-chain length (Fig. 2) linearly correlates with the aggregation number of the respective detergent (Fig. 8). Because the concentration of detergent monomers per micelle, i.e., the peptide-to-detergent ratio per micelle, eventually influences the stability of a TM protein structure, this might indicate that the aggregation number can also affect the stability of the GpA TM helix dimer in a detergent micelle. With increasing N_{agg}, the number of detergent molecules per micelle (i.e., the concentration of the intimate solvent) is increased and the dimer fraction decreases, based on dilution and the law of mass action.

CONCLUSION

Fine-tuning of detergent properties is crucial for obtaining structural information of intact and functional TM proteins. However, identifying a proper detergent suitable to maintain the structure, integrity, and function of a TM protein upon solubilization is still an empirical and time-consuming process.

Based on several previous studies of detergent properties and their impact on the stability of TM structures, some generalizing rules have emerged, classifying detergents as harsh or mild. However, the presented results indicate that the TM helix oligomer is destabilized in lyso-PCs with increasing chain length, which contrasts with the assumption that longer tails render detergents milder. Thus, the impact of the acyl-chain region on the stability of a TM structure appears to vary and one should be careful about generalizing the impact of an acyl-chain length on the structure and stability of a TM protein. Furthermore, individual detergent molecules appear to be able to stretch within a micelle to match the hydrophobic thickness of the peptide, and the diameter of the hydrophobic micelle core appears to be less important for selecting a proper detergent for structural and/or functional analyses, at least in case of lyso-PCs. Thus, hydrophobic mismatch might be less relevant in detergent micelles than in lipid bilayers.

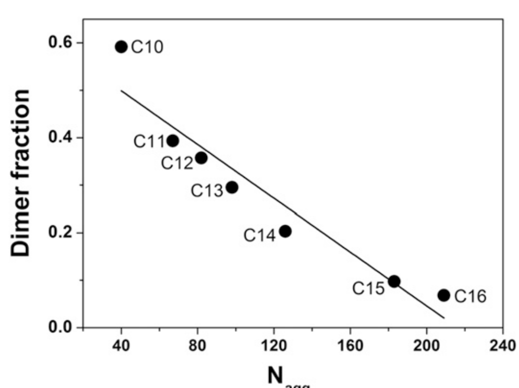

FIGURE 8 GpA stability and lyso-PC aggregation numbers. The fractions of dimeric GpA are plotted as a function of the lyso-PC aggregation number (different acyl-chain length) as determined by light scattering at 20-mM detergent concentration (compare to Fig. 5). The N_{agg} value linearly correlates with the decrease of GpA TM domain dimer fraction with an R^2 of 0.9.

SUPPORTING MATERIAL

One table and three figures are available at http://www.biophysj.org/biophysj/supplemental/S0006-3495(12)01225-8.

We thank H. Pearson for critically reading the manuscript. The authors thank Christine Rosenauer (Max Planck Institute for Polymer Research Mainz) for light-scattering experiments.

This work was supported by grants from the Deutsche Forschungsgemeinschaft, the Research Center for Complex Materials (COMATT), the University of Mainz, and the Max Planck Graduate Center with the University of Mainz.

REFERENCES

1. Franzin, C. M., P. Teriete, and F. M. Marassi. 2007. Structural similarity of a membrane protein in micelles and membranes. *J. Am. Chem. Soc.* 129:8078–8079.
2. Veerappan, A., F. Cymer, …, D. Schneider. 2011. The tetrameric α-helical membrane protein GlpF unfolds via a dimeric folding intermediate. *Biochemistry.* 50:10223–10230.
3. Melnyk, R. A., A. W. Partridge, and C. M. Deber. 2001. Retention of native-like oligomerization states in transmembrane segment peptides: application to the *Escherichia coli* aspartate receptor. *Biochemistry.* 40:11106–11113.
4. Federkeil, S. L., T. L. Winstone, …, R. J. Turner. 2003. Examination of EmrE conformational differences in various membrane mimetic environments. *Biochem. Cell Biol.* 81:61–70.
5. Chou, J. J., J. D. Kaufman, …, A. Bax. 2002. Micelle-induced curvature in a water-insoluble HIV-1 Env peptide revealed by NMR dipolar coupling measurement in stretched polyacrylamide gel. *J. Am. Chem. Soc.* 124:2450–2451.
6. Grigorieff, N., T. A. Ceska, …, R. Henderson. 1996. Electron-crystallographic refinement of the structure of bacteriorhodopsin. *J. Mol. Biol.* 259:393–421.
7. Faham, S., and J. U. Bowie. 2002. Bicelle crystallization: a new method for crystallizing membrane proteins yields a monomeric bacteriorhodopsin structure. *J. Mol. Biol.* 316:1–6.
8. Pebay-Peyroula, E., G. Rummel, …, E. M. Landau. 1997. X-ray structure of bacteriorhodopsin at 2.5 Ångstroms from microcrystals grown in lipidic cubic phases. *Science.* 277:1676–1681.
9. Koehler, J., E. S. Sulistijo, …, C. R. Sanders. 2010. Lysophospholipid micelles sustain the stability and catalytic activity of diacylglycerol kinase in the absence of lipids. *Biochemistry.* 49:7089–7099.

10. le Maire, M., P. Champeil, and J. V. Moller. 2000. Interaction of membrane proteins and lipids with solubilizing detergents. *Biochim. Biophys. Acta.* 1508:86–111.

11. Privé, G. G. 2007. Detergents for the stabilization and crystallization of membrane proteins. *Methods.* 41:388–397.

12. Therien, A. G., and C. M. Deber. 2002. Interhelical packing in detergent micelles. Folding of a cystic fibrosis transmembrane conductance regulator construct. *J. Biol. Chem.* 277:6067–6072.

13. Booth, P. J., and P. Curnow. 2009. Folding scene investigation: membrane proteins. *Curr. Opin. Struct. Biol.* 19:8–13.

14. Bowie, J. U. 2005. Solving the membrane protein folding problem. *Nature.* 438:581–589.

15. Popot, J. L., and D. M. Engelman. 1990. Membrane protein folding and oligomerization: the two-stage model. *Biochemistry.* 29:4031–4037.

16. MacKenzie, K. R., J. H. Prestegard, and D. M. Engelman. 1997. A transmembrane helix dimer: structure and implications. *Science.* 276:131–133.

17. Langosch, D., B. Brosig, …, H. J. Fritz. 1996. Dimerization of the glycophorin A transmembrane segment in membranes probed with the ToxR transcription activator. *J. Mol. Biol.* 263:525–530.

18. Smith, S. O., D. Song, …, S. Aimoto. 2001. Structure of the transmembrane dimer interface of glycophorin A in membrane bilayers. *Biochemistry.* 40:6553–6558.

19. Schneider, D., and D. M. Engelman. 2004. Motifs of two small residues can assist but are not sufficient to mediate transmembrane helix interactions. *J. Mol. Biol.* 343:799–804.

20. Lemmon, M. A., J. M. Flanagan, …, D. M. Engelman. 1992. Sequence specificity in the dimerization of transmembrane α-helices. *Biochemistry.* 31:12719–12725.

21. Doura, A. K., and K. G. Fleming. 2004. Complex interactions at the helix-helix interface stabilize the glycophorin A transmembrane dimer. *J. Mol. Biol.* 343:1487–1497.

22. Finger, C., T. Volkmer, …, D. Schneider. 2006. The stability of transmembrane helix interactions measured in a biological membrane. *J. Mol. Biol.* 358:1221–1228.

23. Anbazhagan, V., and D. Schneider. 2010. The membrane environment modulates self-association of the human GpA TM domain—implications for membrane protein folding and transmembrane signaling. *Biochim. Biophys. Acta.* 1798:1899–1907.

24. Hong, H., and J. U. Bowie. 2011. Dramatic destabilization of transmembrane helix interactions by features of natural membrane environments. *J. Am. Chem. Soc.* 133:11389–11398.

25. Fisher, L. E., D. M. Engelman, and J. N. Sturgis. 1999. Detergents modulate dimerization, but not helicity, of the glycophorin A transmembrane domain. *J. Mol. Biol.* 293:639–651.

26. Fisher, L. E., D. M. Engelman, and J. N. Sturgis. 2003. Effect of detergents on the association of the glycophorin A transmembrane helix. *Biophys. J.* 85:3097–3105.

27. Anbazhagan, V., F. Cymer, and D. Schneider. 2010. Unfolding a transmembrane helix dimer: a FRET study in mixed micelles. *Arch. Biochem. Biophys.* 495:159–164.

28. MacKenzie, K. R., and K. G. Fleming. 2008. Association energetics of membrane spanning α-helices. *Curr. Opin. Struct. Biol.* 18:412–419.

29. Columbus, L., J. Lipfert, …, S. A. Lesley. 2009. Mixing and matching detergents for membrane protein NMR structure determination. *J. Am. Chem. Soc.* 131:7320–7326.

30. Merzlyakov, M., L. Chen, and K. Hristova. 2007. Studies of receptor tyrosine kinase transmembrane domain interactions: the EmEx-FRET method. *J. Membr. Biol.* 215:93–103.

31. Merzlyakov, M., and K. Hristova. 2008. Förster resonance energy transfer measurements of transmembrane helix dimerization energetics. *Methods Enzymol.* 450:107–127.

32. Whitmore, L., and B. A. Wallace. 2004. DICHROWEB, an online server for protein secondary structure analyses from circular dichroism spectroscopic data. *Nucleic Acids Res.* 32(Web Server issue):W668–W673.

33. Whitmore, L., and B. A. Wallace. 2008. Protein secondary structure analyses from circular dichroism spectroscopy: methods and reference databases. *Biopolymers.* 89:392–400.

34. Palladino, P., F. Rossi, and R. Ragone. 2010. Effective critical micellar concentration of a zwitterionic detergent: a fluorimetric study on *n*-dodecyl phosphocholine. *J. Fluoresc.* 20:191–196.

35. Turro, N. J., and A. Yekta. 1978. Luminescent probes for detergent solutions. A simple procedure for determination of the mean aggregation number of micelles. *J. Am. Chem. Soc.* 100:5951–5952.

36. Wolszczak, M., and J. Miller. 2002. Characterization of non-ionic surfactant aggregates by fluorometric techniques. *J. Photochem. Photobiol. Chem.* 147:45–54.

37. Kroeger, A., J. Belack, …, G. Wegner. 2006. Supramolecular structures in aqueous solutions of rigid polyelectrolytes with monovalent and divalent counterions. *Macromolecules.* 39:7098–7106.

38. Wu, P., and L. Brand. 1994. Resonance energy transfer: methods and applications. *Anal. Biochem.* 218:1–13.

39. Vitiello, G., D. Ciccarelli, …, G. D'Errico. 2009. Microstructural characterization of lysophosphatidylcholine micellar aggregates: the structural basis for their use as biomembrane mimics. *J. Colloid Interface Sci.* 336:827–833.

40. Adair, B. D., and D. M. Engelman. 1994. Glycophorin A helical transmembrane domains dimerize in phospholipid bilayers: a resonance energy transfer study. *Biochemistry.* 33:5539–5544.

41. Li, E., M. You, and K. Hristova. 2005. Sodium dodecyl sulfate-polyacrylamide gel electrophoresis and Förster resonance energy transfer suggest weak interactions between fibroblast growth factor receptor 3 (FGFR3) transmembrane domains in the absence of extracellular domains and ligands. *Biochemistry.* 44:352–360.

42. Asaoka, Y., K. Yoshida, …, Y. Nishizuka. 1993. Potential role of phospholipase A2 in HL-60 cell differentiation to macrophages induced by protein kinase C activation. *Proc. Natl. Acad. Sci. USA.* 90:4917–4921.

43. Sasaki, Y., Y. Asaoka, and Y. Nishizuka. 1993. Potentiation of diacylglycerol-induced activation of protein kinase C by lysophospholipids. Subspecies difference. *FEBS Lett.* 320:47–51.

44. Okita, M., D. C. Gaudette, …, B. J. Holub. 1997. Elevated levels and altered fatty acid composition of plasma lysophosphatidylcholine (lysoPC) in ovarian cancer patients. *Int. J. Cancer.* 71:31–34.

45. Taylor, L. A., J. Arends, …, U. Massing. 2007. Plasma lyso-phosphatidylcholine concentration is decreased in cancer patients with weight loss and activated inflammatory status. *Lipids Health Dis.* 6:17.

46. Skipski, V. P., M. Barclay, …, F. M. Archibald. 1967. Lipid composition of human serum lipoproteins. *Biochem. J.* 104:340–352.

47. Lee, A. G. 2003. Lipid-protein interactions in biological membranes: a structural perspective. *Biochim. Biophys. Acta.* 1612:1–40.

48. Nyholm, T. K., S. Ozdirekcan, and J. A. Killian. 2007. How protein transmembrane segments sense the lipid environment. *Biochemistry.* 46:1457–1465.

49. Huang, H. W. 1986. Deformation free energy of bilayer membrane and its effect on gramicidin channel lifetime. *Biophys. J.* 50:1061–1070.

50. Mineev, K. S., E. V. Bocharov, …, A. S. Arseniev. 2011. Dimeric structure of the transmembrane domain of glycophorin a in lipidic and detergent environments. *Acta Naturae.* 3:90–98.

Sequence-Specific Dimerization of a Transmembrane Helix in Amphipol A8-35

Michael Stangl[1], Sebastian Unger[2], Sandro Keller[2], Dirk Schneider[1]*

1 Department of Pharmacy and Biochemistry, Johannes-Gutenberg-University, Mainz, Germany, 2 Molecular Biophysics, University of Kaiserslautern, Kaiserslautern, Germany

Abstract

As traditional detergents might destabilize or even denature membrane proteins, amphiphilic polymers have moved into the focus of membrane-protein research in recent years. Thus far, Amphipols are the best studied amphiphilic copolymers, having a hydrophilic backbone with short hydrophobic chains. However, since stabilizing as well as destabilizing effects of the Amphipol belt on the structure of membrane proteins have been described, we systematically analyze the impact of the most commonly used Amphipol A8-35 on the structure and stability of a well-defined transmembrane protein model, the glycophorin A transmembrane helix dimer. Amphipols are not able to directly extract proteins from their native membranes, and detergents are typically replaced by Amphipols only after protein extraction from membranes. As Amphipols form mixed micelles with detergents, a better understanding of Amphipol-detergent interactions is required. Therefore, we analyze the interaction of A8-35 with the anionic detergent sodium dodecyl sulfate and describe the impact of the mixed-micelle-like system on the stability of a transmembrane helix dimer. As A8-35 may highly stabilize and thereby rigidify a transmembrane protein structure, modest destabilization by controlled addition of detergents and formation of mixed micellar systems might be helpful to preserve the function of a membrane protein in Amphipol environments.

Citation: Stangl M, Unger S, Keller S, Schneider D (2014) Sequence-Specific Dimerization of a Transmembrane Helix in Amphipol A8-35. PLoS ONE 9(10): e110970. doi:10.1371/journal.pone.0110970

Editor: Dariush Hinderberger, Martin-Luther-Universität Halle-Wittenberg, Germany

Received June 27, 2014; **Accepted** September 26, 2014; **Published** October 27, 2014

Data Availability: The authors confirm that all data underlying the findings are fully available without restriction. All relevant data are within the paper and its Supporting Information files.

Funding: The authors have no funding or support to report.

Competing Interests: The authors have declared that no competing interests exist.

* Email: Dirk.Schneider@uni-mainz.de

Introduction

Traditionally, detergents are used to solubilize membrane proteins (MPs) for subsequent purification and *in vitro* analyses. However, as detergents might destabilize or even denature MPs [1], amphiphilic polymers have been introduced as a new class of surfactants suitable for keeping membrane proteins soluble in aqueous solution [2-11]. Amphipols (APols) are such amphiphilic copolymers (terpolymers), possessing a hydrophilic backbone and short hydrophobic chains. The thus far most common and best studied APol A8-35 shows high solubility in water at pH>7.0 and assembles into tetrameric nanoparticles, which together carry 75–80 octyl chains [2,3,5,12]. Similar to detergents, APols do not aggregate until a particular concentration is reached. However, in contrast to most detergents, the critical aggregation concentration (CAC) is in the nanomolar range, allowing APols to form aggregates and stabilize MPs at very low concentrations. However, APols are not able to extract MPs from their native membranes, and thus, MPs are typically still extracted by classical detergents. Only in a subsequent step is the detergent substituted by an APol. Therefore, when working with APols, detergents are still vital. When detergents are added to APols at concentrations below their critical micellar concentration (CMC), APols and detergents form mixed micelles/aggregates [13]. In mixtures of non-ionic detergents with APols, the fraction of detergent molecules in the mixed micelles increases according to a near-ideal mixing behavior as the concentration of free detergent molecules in solution increases [13,14].

Due to their low CAC values and their ability to render MPs soluble in aqueous solutions at very low bulk concentrations, APols are highly attractive for applications in MP research. A low APol-to-protein ratio implies that only few APol molecules are needed to provide a hydrophobic environment for MPs, which reduces the size of the hydrophobic sink when compared to classical detergents [10]. This might explain the less denaturing properties of APols on MPs [3]. Consequently, APols represent a class of membrane-mimetic surfactants that potentially preserve the structure as well as the function of MPs better than many detergents. In fact, more than 30 MPs have already been shown to form water-soluble complexes with APols [6,15]. Bringing the MPs with APols in solution, is one fundamental step but the MPs also have to fold into their native and active conformation. Most MPs seem to still function after being trapped in APol particles [3]. As an example, bacteriorhodopsin correctly folds in A8-35 and accomplishes its entire photocycle, though with slower kinetics compared to detergents [10]. On the other hand, the sarcoplasmic Ca^{2+}-ATPase can be solubilized in A8-35, but it shows very slow hydrolytic activity and Ca^{2+} dissociation [16]. The transmembrane (TM) region of the sarcoplasmic Ca^{2+}-ATPase undergoes large conformational changes during its active process, which seems to be constrained by the tight, multiple A8-35 attachment [17].

As the formation of higher-ordered oligomeric MP structures depends on multiple specific TM helix-helix contacts, analyzing the stability of a sequence-specific TM helix dimer can be helpful in properly elucidating the impact of APols on MP structure and stability.

In recent years, association of TM α-helices has been studied to a great extent using the TM region of the human glycophorin A (GpA) protein, which forms a stable TM helix dimer. Sequence-specific GpA dimerization is mediated by the LIxxGVxxGVxT amino acid motif [18-20]. Especially the GxxxG motif promotes tight packing of two adjacent TM α-helices, resulting in Van der Waals packing interactions and formation of C_α hydrogen bonds [21,22]. In fact, in the last two decades the GpA TM helix dimer became a paradigm for studying sequence-specificity in TM helix dimerization. GpA dimerization has been analyzed in various detergents and lipids [23-28], and the results have indicated that GpA TM helix association is driven by enthalpic and entropic forces [27]. Furthermore, detergent properties, such as head group chemistry, chain length, aggregation number, as well as the concentration of a particular detergent or phospholipid affect the stability of the GpA TM helix dimer [23-28]. Thus, the GpA TM helix can serve as a valuable probe to quantitatively determine the effect of an APol environment on the structure and stability of a sequence-specific TM helix–helix interaction.

Materials and Methods

Materials

Peptides corresponding to residues 69–101 of the human GpA TM domain (SEPEITLIIFGVMAGVIGTILLISYGIRRLIKK) were custom-synthesized and labeled at the N-terminus with either the donor or the acceptor dyes fluorescein (FL) and 5-6-carboxyrhodamine (TAMRA), respectively (Peptide Specialty Laboratories, Heidelberg, Germany). The purity of the labelled peptides was confirmed by high-performance liquid chromatography (HPLC) and mass spectrometry [24]. Based on this, the labeled peptides used in this study were>95% pure. Peptides were dissolved in 2,2,2-trifluoroethanol purchased from Sigma-Aldrich (Munich, Germany). APol A8-35 was purchased from Affymetrix (Santa Clara, USA) and sodium dodecyl sulfate (SDS) from Roth (Karlsruhe, Germany). *N*-dodecyl-β-D-maltopyranoside (DDM) was obtained from Sigma-Aldrich (Munich, Germany).

FRET measurements

For Förster resonance energy transfer (FRET) measurements, equal concentrations of FL- and TAMRA-labeled GpA TM domains were used. Concentrations of the peptide stock solutions were determined from absorbance measurements on a Perkin Elmer Lambda 35 UV/VIS spectrophotometer. In all experiments, we used 0.25 μM for each of the two labeled GpA peptides. Peptides dissolved in TFE and A8-35 dissolved in ethanol were mixed, and organic solvents were removed under a gentle stream of nitrogen gas. Residual solvent traces were removed by vacuum desiccation overnight. The dried peptide/polymer film was then hydrated in 10 mM HEPES buffer (pH 7.4) containing 150 mM NaCl.

After at least 2 h of incubation at 37°C and 10 min of centrifugation at 16,000 *g*, steady-state fluorescence measurements were performed with the supernatant at 25°C on a Horiba Fluoromax 4 system with both excitation and emission slits at 3 nm. The excitation wavelength was set at 439 nm, and emission spectra were recorded from 480 to 650 nm. For FRET measurements with SDS, several concentrations of SDS, both below and above the CMC determined for the given buffer conditions, were used, and hydrated samples were incubated overnight.

Energy transfer E was calculated using the donor fluorescence intensities at 525 nm in presence and absence of acceptor according to

$$E = 1 - (F_{DA}/F_D) \tag{1}$$

F_D is the fluorescence intensity of the donor sample, and F_{DA} is the fluorescence intensity of the sample containing donor and acceptor GpA TM domains at equal concentrations. The energy transfer of sequence-specific TM helix dimerization, E_D, can be expressed as:

$$E_D = f_D P_D E_R \tag{2}$$

where f_D is the fraction of dimeric TM helices, P_D is the probability of donor quenching when the peptides form a dimer, and E_R is the energy transfer in the dimer.

The probability P_D of donor quenching depends on the molar ratio of the acceptor peptides $\chi a = [a]/([a]+[d])$, where [a] and [d] are the concentrations of acceptor and donor peptides, respectively. If the distance of the fluorophores in the dimer is much smaller than the Förster radius, as is the case here, E_R can be taken as unity.

The fraction of dimers can be written as $f_D = 2[D]/[T]$, where [D] is the concentration of dimeric peptides and [T] the total peptide concentration. Hence, the dimer concentration [D] can be calculated as [24,25,29]:

$$[D] = E_D[T]/2\chi a \tag{3}$$

The dissociation constant, K_D, is given by

$$K_D = [M]^2 \Big/ [D] \tag{4}$$

where the monomer concentration is $[M] = [T] - 2[D]$.

Circular dichroism spectroscopy

CD spectra were recorded on a Jasco J-815 spectropolarimeter at 25°C in a step-scan mode using 0.1-cm path length quartz cells from Hellma (Mülheim, Germany). The concentration of unlabeled GpA peptide was 5 μM. Data points were collected at a resolution of 1 nm, an integration time of 1 s, and a bandwidth of 1 nm. Each shown spectrum results from at least three averaged scans from which buffer scans were subtracted. The measured ellipticity θ was converted to molar ellipticity [θ] by:

$$[\theta] = (100\theta M/LC) \tag{5}$$

where M is the molar mass, L the path length, and C the peptide concentration.

The GpA TM domain was reconstituted in 10 mM phosphate buffer (pH 7.4) containing A8-35 as well as in several solvents containing SDS, DDM, or pure TFE, which are known to stabilize α-helical structures. Prior to CD measurements, samples were treated in the same way as described above for FRET measurements. Secondary structure contents were estimated with the DICHROWEB software [30,31] using both soluble and TM proteins as reference datasets (CDSSTR method, reference set 7).

Isothermal titration calorimetry (ITC)

ITC experiments were performed on a VP-ITC (GE Healthcare) at 25°C in 10 mM phosphate buffer (150 mM NaCl, pH 7.4). For demicellization experiments, 5-µL aliquots containing both, SDS at a concentration well above its CMC (10-13 mM) as well as A8-35 at concentrations of 5-140 µM, were injected into the sample cell containing the same amphipol concentration but no SDS. Time spans between injections were chosen long enough to allow for complete re-equilibration. Baseline subtraction and peak integration were accomplished using NITPIC [32], and the resulting isotherms were analyzed by nonlinear least-squares fitting in a spreadsheet program [33].

Results and Discussion

GpA TM helix dimerization in A8-35

First, we determined the secondary structure of GpA TM peptides solubilized in A8-35 by far-UV CD spectroscopy to ensure that the GpA TM peptides were fully solubilized and adopted the expected α-helical structure in the APol environment (Figure 1). As a control, the secondary structure of the GpA TM domain was additionally analyzed in trifluoroethanol (TFE), 5 mM SDS, or 5 mM DDM, since it has been shown that α-helical structures are stabilized in these solvents [24,26,34]. The CD spectra demonstrate that a maximum at 190 nm and double minima at 209 nm and 222 nm are retained in 5 µM A8-35, which are characteristic of α-helical structures. Higher APol concentrations did not significantly affect the peptide's secondary structure. Estimation of the secondary structure contents suggested an α-helix content of 67% in 5 µM A8-35, compared to 62% in TFE, 76% in SDS or 79% in DDM. Thus, the structural hallmarks of the GpA TM helix are largely preserved in A8-35 particles, and therefore the effects of increasing A8-35 concentrations on the stability of the GpA TM helix dimer were studied in subsequent experiments.

To determine the thermodynamic stability of the GpA TM helix dimer, FRET measurements were performed in APol A8-35. To do so, the GpA TM peptides were chemically labeled at the N-terminus with either fluorescein (FL) or carboxytetratmethylrhodamine (TAMRA). Figure S1 shows the emission and excitation spectra of the labelled peptides solubilized in A8-35.

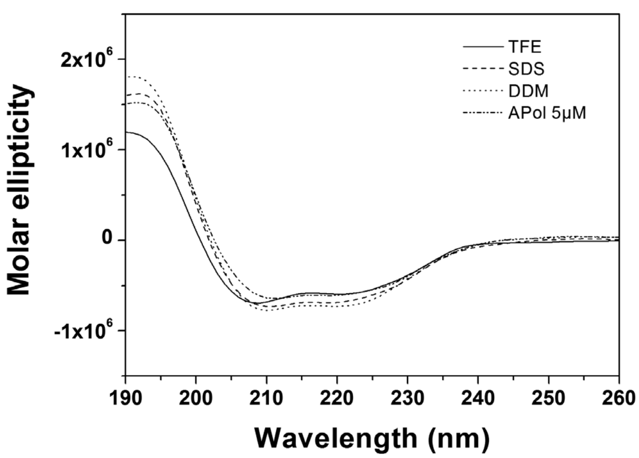

Figure 1. Far-UV CD spectra of the GpA TM domain. GpA TM domain (5 µM) solubilized in 5 µM APol. As controls, GpA TM domain was solubilized in TFE, SDS, or DDM, which are known to support the formation of α-helical structures.
doi:10.1371/journal.pone.0110970.g001

The emission spectrum of the fluorescein-labelled peptide substantially overlaps with the excitation spectrum of the TAMRA-labelled peptide. Therefore, energy transfer is a direct measure of the fraction of dimeric peptide species in the sample [24,25,28,29]. In the first series of experiments, the total peptide concentration of the FRET pair was kept constant at 0.5 µM, while the A8-35 concentration was increased from 5 to 75 µM, which corresponds to APol-to-peptide ratios of 10:1 to 150:1. As can be seen in Figure 2A, the fraction dimeric GpA decreased with increasing A8-35 concentrations. Almost all peptides were dimeric at low A8-35 concentrations, whereas the dimer fraction dropped to a value of about 0.65 at 25 µM A8-35 and thereafter decreased only faintly with increasing polymer concentrations. This indicates that the GpA TM helix dimer is rather stable even at higher A8-35 concentrations and only very high polymer concentrations will dissociate the dimer completely. For comparison, detergent micelles destabilize the GpA dimer to a larger extent, even if the detergent concentration exceeds the CMC only slightly [24,26-28]. However, the extent of GpA dimerization in detergents depends severely on the head group, the chain length and the concentration of the particular detergent. In general, APol A8-35 appears to stabilize the GpA TM domain dimer rather well, as the dissociation constants are below 0.3 µM in the tested A8-35 concentration range (Figure 2B), and even relatively higher A8-35 concentrations do not seem to fully dissociate the GpA dimer, in contrast to detergents. While at low detergent concentrations the dissociation constants of the GpA TM dimer in several tested detergents (SDS, DDMAB, DPC, lyso-PC) are in the same range as in APol (≤0.5 µM), they increase significantly, compared to A8-35, upon further addition of detergent until the dimer is completely dissociated [26-28].

Detergents affect helix association in a rather complex way: In the first place, simple dilution of the peptide in the micellar phase entropically promotes dissociation with increasing detergent concentrations [27]. Additionally, however, opposing enthalpic and entropic effects, which depend on the nature of the detergent and are generally poorly understood, may counteract dilution by enhancing helix association with increasing detergent concentrations. The high stability of the GpA TM helix dimer in A8-35 might be explained by (i) a poor ability of APols to compete with protein/protein interactions, (ii) the reduced size of the hydrophobic sink compared to detergents [35], or (iii) a dampening effect of potential conformational fluctuations due to the viscosity of the polymer backbone [3,36].

To investigate the effect of A8-35 on the GpA dimer stability in greater detail, we next performed kinetic measurements and determined the exchange rates of GpA TM helices between various polymer particles after reconstitution. Upon addition of an excess of a competing surfactant, such as free APols, detergents or phospholipids, MPs can be released from preformed complexes with APols, although at very slow dissociation rates, and *e.g.* integrate into detergent micelles [3,37-39]. To test this, donor- and acceptor-labeled GpA peptides were individually solubilized in 20 µM A8-35 and incubated at 37°C for at least 2 h. Next, A8-35-solubilized donor and acceptor peptides were mixed in a 1:1 ratio, and fluorescence emission spectra were recorded every 10 min for about 17 h (Figure 3A). As a control necessary for calculation of energy transfer, this measurement was also performed with solely the donor sample, for which no changes in fluorescence intensity were observed. Figure 3B shows that 17 h after mixing the two differently labelled GpA TM helices, the energy transfer increased up to ~35%, which corresponds to a dimer fraction of ~0.7, as already observed before in the steady-state measurements (Figure 2A). To compare the exchange rates measured in APols

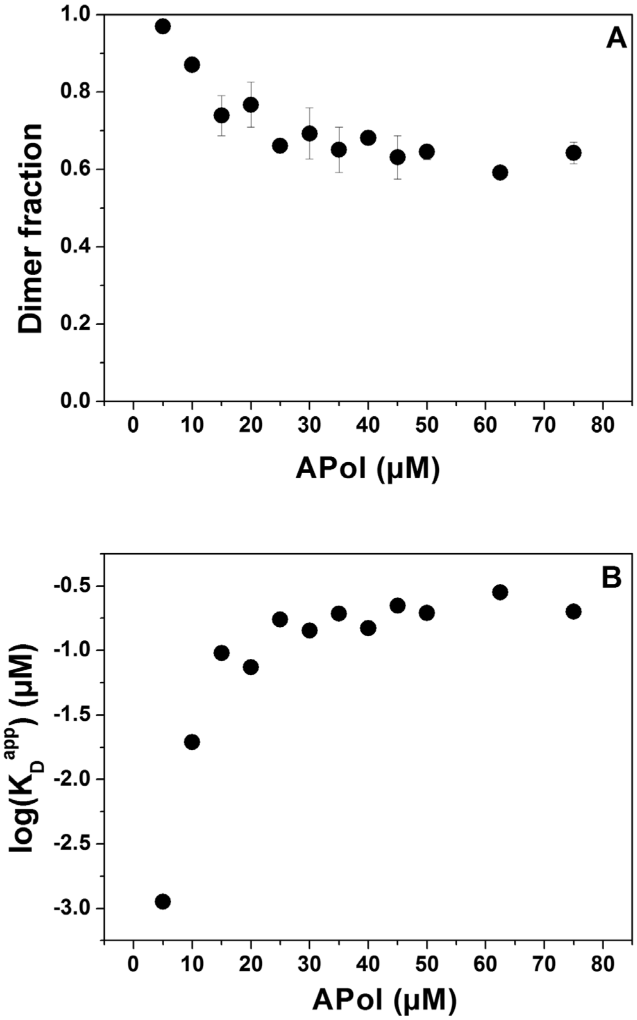

Figure 2. Association of the GpA TM domain in APol. FRET measurements (n = 3) were performed at increasing APol concentrations ranging from 5 to 75 μM, corresponding to APol/peptide ratios of 10:1 to 150:1. (A) Dimer fractions of the GpA TM domain determined by FRET efficiencies of the fluorescence emissions' spectra plotted against APol concentration (see eq. 3). (B) Logarithm of the apparent GpA TM dissociation constants at increasing APol concentration (see eq. 4).
doi:10.1371/journal.pone.0110970.g002

with rates determined in micellar environments, the same experiment was performed in 5 mM DDM micelles (Figure 3C). While the exchange of donor- and acceptor-labeled GpA TM peptides suspended in A8-35 proceeded for several hours, the exchange of labeled peptides between micelles was already complete after several minutes. Proper fits of the measured kinetics were obtained with a double-exponential equation yielding rate constants of 2.2 h^{-1} (amplitude 8.7) and 0.17 h^{-1} (amplitude 12.4) for A8-35, and 41.5 h^{-1} (amplitude 13.3) and 5.8 h^{-1} (amplitude 15.6) for DDM micelles.

Besides formation of GpA dimers, the recorded energy transfer might, in principle, also originate from formation of higher-ordered oligomeric structures, such as trimers or tetramers, or even from unspecific peptide aggregation. Such a possibility can be excluded by measuring energy transfer at different acceptor mole ratios (χ_a) while keeping the total peptide concentration constant. If the energy transfer linearly depends on χ_a, only the formation of dimers will contribute to the energy transfer measured [23]. As

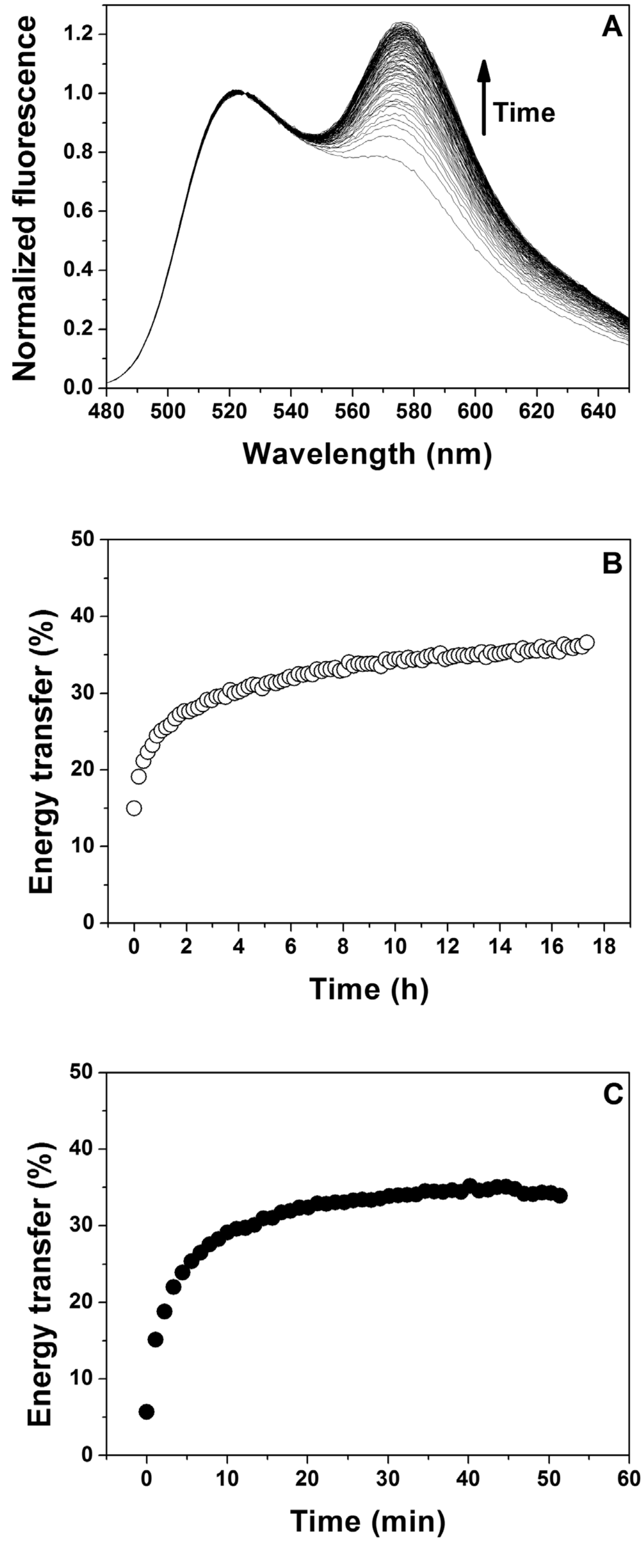

Figure 3. Kinetics of the exchange of GpA TM peptides between APol aggregates. Donor- and acceptor-labelled GpA TM (each 0.25 μM) domains were separately solubilized in 20 μM APol at a final polymer/peptide ratio of 40:1. (A) After incubation at 37°C, donor and acceptor were mixed, and emission spectra (normalized at 525 nm) were recorded every 10 min over a time period of 17 h at 25°C. (B) The energy transfer increased over hours to the level determined by steady-state FRET measurements due to mixing of donor- and acceptor-labelled peptides. (C) Energy transfer change due to peptide exchange in 5 mM DDM micelles was completed after some dozen minutes.
doi:10.1371/journal.pone.0110970.g003

shown in Figure 4, at 5 μM and 50 μM A8-35, the energy transfer linearly depends on χ_a, indicating exclusive formation of GpA dimers in APol A8-35.

GpA TM domain dimerization in mixed APol/SDS micelles

Thermal denaturation of MPs often leads to irreversible aggregation of the MP, and guanidine hydrochloride and urea, which are frequently used in unfolding studies involving soluble proteins, do typically not denature the TM regions of MPs. This is why the thermodynamic stability of integral MPs within membrane-mimetic systems is often assessed by titrating increasing concentrations of the anionic detergent SDS to MPs dissolved in a mild detergent, such as DDM [24,40-44]. SDS is able to form mixed micelles with other detergents typically used for MP solubilization. In SDS-containing mixed micelles, a membrane mimetic environment is maintained and the secondary structure of the MPs TM regions is barely affected by SDS-induced protein unfolding [40]. However, it is worth mentioning that the term "unfolding" in this system in fact describes dissociation of TM helices rather than unfolding of individual TM α-helices [24]. Since mixed DDM/SDS micelles dissociate the GpA TM helix dimer almost completely [24], a similar approach based on the denaturing effect of SDS might be useful for investigating the thermodynamic stability of the GpA TM helix dimer in APol solutions. Furthermore, when amphipols are used *in vitro*, detergents are still needed to extract MPs from their natural membrane, and, therefore intermediate states of MPs in mixed APol/detergent micelles are present during the experimental procedure. Preserving the MPs' structure and activity during this process is fundamental for subsequent experiments. To shed more light on the interactions between A8-35 and the anionic detergent SDS, we performed a series of ITC experiments (Figure 5), in which SDS solutions at concentrations above the CMC (10-13 mM) were diluted into buffer in the presence of increasing A8-35 concentrations. At low APol concentrations, the isotherms thus obtained resembled those measured in SDS demicellization experiments in the absence of APol [45]. However, with increasing A8-35 concentrations, the isotherms became shallower and even changed sign, similarly to what has previously been observed for the interactions of the non-ionic detergent octylglucoside with A8-35 and other amphipols [13]. However, while the latter have been found to follow nearly ideal mixing behavior [13], the interactions of SDS with A8-35 follows a more complex pattern (Figure 5). Although the reaction heats could be fitted on the basis of the regular mixing model at intermediate SDS contents in the mixed aggregates [13], such fits yielded very high nonideality parameters of 3–4 RT, which is incompatible with the near-ideal mixing assumption inherent in this model. At both lower and higher SDS concentrations, the isotherms could not at all be analyzed in terms of simple mixing models, which is most likely due to a charge repulsion between free SDS monomers and mixed APol/SDS aggregates or due to the changes in pH at the surface of the mixed aggregate [46,47]. Thus, care should be taken in interpreting SDS titration data involving anionic APols at a quantitative level, which is why we restrict ourselves to qualitative considerations in the following.

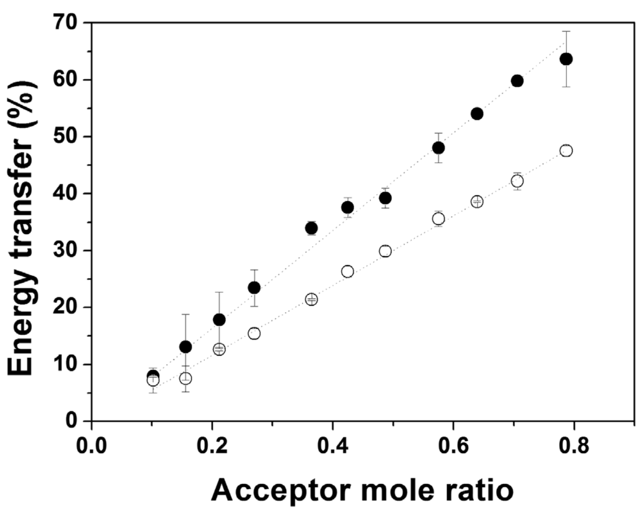

Figure 4. Stoichiometry of GpA TM domain association. Energy transfer efficiency as a function of acceptor mole fraction in 5 μM (●) and 50 μM (○) APol (n = 2). Linear dependence of the energy transfer on the acceptor mole ratio demonstrates exclusive dimer formation of the GpA TM domain in APol.
doi:10.1371/journal.pone.0110970.g004

To address the question of how SDS/APol aggregates/micelles affect TM helix-helix association and hence the stability of α-helical MPs, FRET efficiencies were determined at increasing SDS concentrations, while the concentrations of the GpA TM domain (0.5 μM) and APol A8-35 (20 μM) were kept constant. Under these conditions, the fraction of dimeric GpA decreases from 0.7 in the absence of SDS to about 0.3 at SDS concentrations exceeding 1.5 mM (Figure 6A), corresponding to an increase in the dissociation constant by about one order of magnitude (Figure 6B). This indicates a strong destabilization of the GpA dimer after addition of SDS, resulting in dissociation of GpA TM dimers in mixed A8-35/SDS aggregates. As previously observed in mixed detergent micelles [24], addition of SDS to A8-35-solubilized GpA destabilizes the GpA dimer. However, in contrast to DDM/SDS mixed micelles, in which the GpA dimer is completely unfolded [24], this was not observed in case of APol/SDS mixed micelles, at least not in the analyzed concentration range (Figure 6). Thus, SDS appears to be less denaturing when a MP is solubilized in A8-35 compared to classical detergents. However, a direct comparison of the SDS denaturation data in DDM vs. A8-35 is complicated, as the chemical nature of DDM and A8-35 are very different and usually SDS mole fractions are used for plotting the denaturation process. Using mole fractions is not very helpful in case of APol/SDS, as the high molecular mass polymer carries multiple hydrophobic tails and much lower APol concentrations are needed to solubilize the TM helix compared to DDM. A8-35 aggregates can also not be directly compared with detergent molecules and micellar structures. Furthermore, the mixing behavior of SDS and A8-35 is quite complex, as the ITC data indicate (Figure 5). In addition, the degree of non-ideality in DDM/SDS mixing is also very complex and varies over experimental conditions. Therefore, heterogeneities in the mixed micelles/aggregates cannot be excluded [48], and the spatial structure of APol/SDS assemblies is likely to be very different from a typical micelle due to the long polymer backbone.

To assess the reversibility of the observed changes in dimer stability, FRET was measured at 2 mM SDS and 20 μM APol, both prior to and following dilution of the sample with another sample, containing no SDS but the same concentrations of peptide and APol (Figure 7). Thereby, the SDS concentration was diluted below its CMC (to 0.4 mM), while the concentrations of peptide and APol were kept constant. The fraction of dimeric GpA observed after dilution agrees with the value determined at 0.4 mM SDS (Figure 7) and the titration experiments (Figure 6A), indicating that dissociation and association of the GpA TM helix in APol A8-35, caused by SDS addition and removal, respectively,

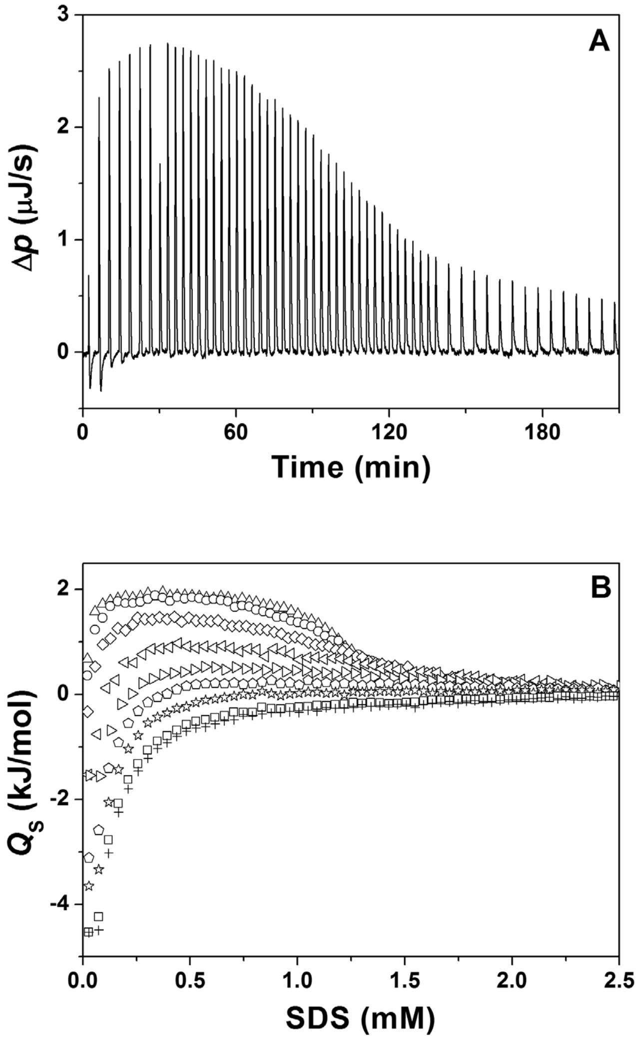

Figure 5. Interactions of SDS with A8-35 monitored by isothermal titration calorimetry. Demicellization of SDS in the presence of various A8-35 concentrations: (A) Differential heating power, Δp, versus time, monitored during the titration of 10 mM SDS and 20 μM A8-35 into 20 μM A8-35. (B) Normalized heats of reaction, Q_S, versus SDS concentration in the cell, [SDS], resulting from the dilution of micellar SDS solutions (10-13 mM) in the presence of A8-35 at A8-35 concentrations of 5 μM (△), 10 μM (O), 20 μM (◇), 40 μM (◁), 60 μM (▷), 80 μM (⌂), 100 μM (☆), 120 μM (□), and 140 μM (+).
doi:10.1371/journal.pone.0110970.g005

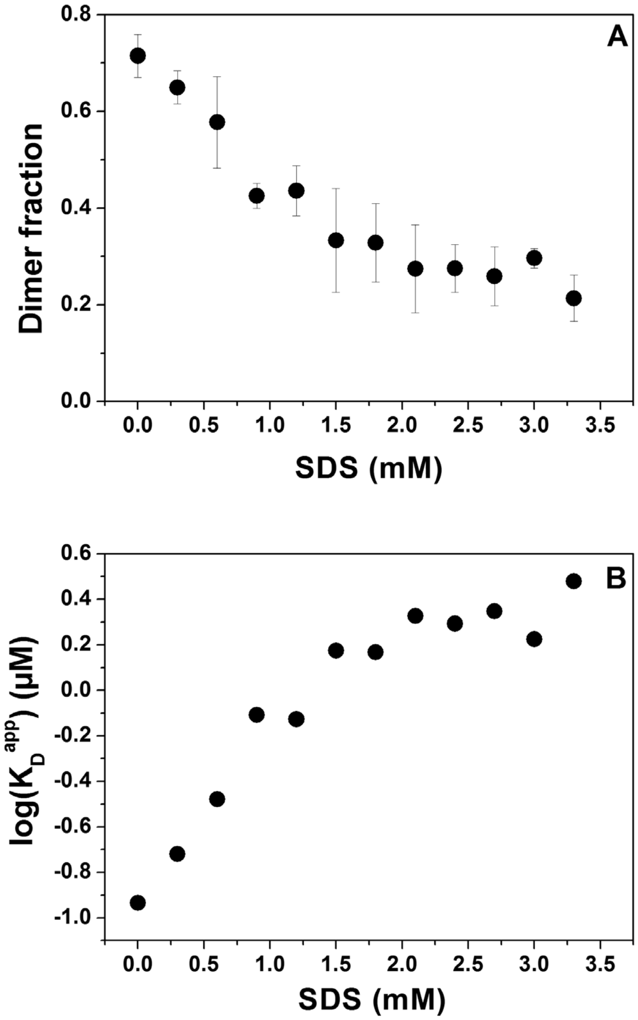

Figure 6. Dissociation of the GpA TM domain in APol upon addition of SDS. Steady-state FRET measurements (n = 3) were performed at a fixed polymer (20 μM) to peptide (0.5 μM) ratio (40:1). SDS was added to preformed APol/GpA complexes, and emission spectra were recorded at 25°C after incubation at 37°C. (A) Dimer fractions of the GpA TM domain determined by FRET efficiencies of the fluorescence emissions spectra plotted against SDS concentration (see eq. 3). (B) Logarithm of the apparent GpA TM dissociation constants at increasing SDS concentration (see eq. 4).
doi:10.1371/journal.pone.0110970.g006

are fully reversible. Thus, addition of SDS to APol-reconstituted GpA TM peptides below the CMC of SDS appears to dramatically destabilize the GpA dimer, which might be caused by the altered structure of the APol aggregate, and thus the altered local environment of the GpA TM helix dimer. Furthermore, addition of extra negative charges might result in increased electrostatic interactions of a stretch of positive charges in the GpA juxtamembrane region, which could destabilize the helix dimer [49], or in an more acidic local pH at the surface of the mixed aggregate [46]. Nevertheless, since mixing of APol and SDS is strongly non-ideal, further analyses are needed for a more detailed, quantitative treatment.

Conclusions

In recent studies, the impact of A8-35 on the stability and activity of selected TM proteins has already been addressed. However, in the preceding studies, polytopic TM proteins have been analyzed, where multiple short- and long-range interactions might stabilize the TM protein structure. Here we showed that trapping a MP in APol A8-35 aggregates does not prevent the sequence-specific interaction of a single TM helix. Refolding and oligomerization of the GpA TM helix dimer in APol A8-35 are possible, avoiding the use of large amounts of detergent. Addition of SDS to APol-trapped GpA weakens the dimerization of the GpA TM helix, as observed in DDM/SDS mixed micelles before, although the effect appears to be less denaturating and low SDS concentrations are tolerated with respect to the formation of tertiary contacts between the helices. The use of APols therefore facilitates the use of very low surfactant concentrations to analyze

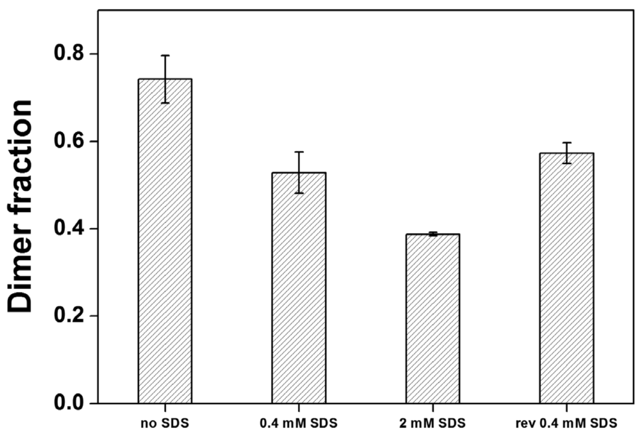

Figure 7. Reversibility of GpA dimer dissociation by SDS addition to APol/GpA complexes. Dimer fractions shown without SDS and with 0.4 mM and 2 mM SDS added. The 2 mM SDS sample was then diluted to 0.4 mM SDS to demonstrate the reversibility of SDS-mediated dimer dissociation. The fraction dimer at 0.4 mM SDS after dilution from higher SDS concentrations is comparable to that observed at 0.4 mM SDS (n = 3).
doi:10.1371/journal.pone.0110970.g007

the folding of a MP under milder conditions. APol/SDS mixed micelles might be useful as a tool for structure-function analyses, since the oligomeric state and the activity of a MP can be tuned judiciously. This can turn out to be important when structural dynamics is needed for protein activity, as the stabilizing environment of APols might inhibit MP function. Thus, addition of detergents could loosen up the surrounding polymer belt, allowing structural dynamics and functionality of an APol-solubilized MP.

Supporting Information

Figure S1 Excitation (solid lines) and emission spectra (dashed lines) of Fl (donor)- and TAMRA (acceptor)-labeled GpA peptides. (A) Fl-GpA, excitation 439 nm, emission 530 nm. (B) TAMRA-GpA, excitation 530 nm, emission 590 nm. Spectra are normalized. (C) Fluorescence emission spectra of donor- and acceptor-labeled peptides (dashed line) as well as control samples containing only donor-labeled peptides (solid line) and only acceptor-labeled peptides (dotted line) upon excitation at 439 nm. Spectra were recorded in 10 mM HEPES buffer containing 150 mM NaCl and 20 µM APol at pH 7.4. Exitation spectra were measured with both slits set at 2 nm. Emission spectra were measured with both slits set at 3 nm.
(TIF)

Author Contributions

Conceived and designed the experiments: MS SK DS. Performed the experiments: MS SU. Analyzed the data: MS SU SK DS. Wrote the paper: MS SU SK DS.

References

1. Bordag N, Keller S (2010) Alpha-helical transmembrane peptides: a "divide and conquer" approach to membrane proteins. Chemistry and Physics of Lipids 163: 1-26.
2. Tribet C, Audebert R, Popot JL (1996) Amphipols: polymers that keep membrane proteins soluble in aqueous solutions. Proc Natl Acad Sci U S A 93: 15047-15050.
3. Popot JL, Althoff T, Bagnard D, Baneres JL, Bazzacco P, et al. (2011) Amphipols from A to Z. Annu Rev Biophys 40: 379-408.
4. Stangl M, Hemmelmann M, Allmeroth M, Zentel R, Schneider D (2014) A Minimal Hydrophobicity Is Needed To Employ Amphiphilic p(HPMA)-co-p(LMA) Random Copolymers in Membrane Research. Biochemistry 53: 1410-1419.
5. Popot JL, Berry EA, Charvolin D, Creuzenet C, Ebel C, et al. (2003) Amphipols: polymeric surfactants for membrane biology research. Cell Mol Life Sci 60: 1559-1574.
6. Pocanschi CL, Dahmane T, Gohon Y, Rappaport F, Apell HJ, et al. (2006) Amphipathic polymers: Tools to fold integral membrane proteins to their active form. Biochemistry 45: 13954-13961.
7. Planchard N, Point E, Dahmane T, Giusti F, Renault M, et al. (2014) The Use of Amphipols for Solution NMR Studies of Membrane Proteins: Advantages and Constraints as Compared to Other Solubilizing Media. J Membr Biol.
8. Etzkorn M, Zoonens M, Catoire LJ, Popot JL, Hiller S (2014) How Amphipols Embed Membrane Proteins: Global Solvent Accessibility and Interaction with a Flexible Protein Terminus. J Membr Biol.
9. Zoonens M, Comer J, Masscheleyn S, Pebay-Peyroula E, Chipot C, et al. (2013) Dangerous liaisons between detergents and membrane proteins. The case of mitochondrial uncoupling protein 2. J Am Chem Soc 135: 15174-15182.
10. Gohon Y, Dahmane T, Ruigrok RWH, Schuck P, Charvolin D, et al. (2008) Bacteriorhodopsin/amphipol complexes: Structural and functional properties. Biophysical Journal 94: 3523-3537.
11. Duarte AMS, Wolfs CJAM, Koehorst RBM, Popot JL, Hemminga MA (2008) Solubilization of V-ATPase transmembrane peptides by amphipol A8-35. Journal of Peptide Science 14: 389-393.
12. Gohon Y, Giusti F, Prata C, Charvolin D, Timmins P, et al. (2006) Well-defined nanoparticles formed by hydrophobic assembly of a short and polydisperse random terpolymer, amphipol A8-35. Langmuir 22: 1281-1290.
13. Diab C, Winnik FM, Tribet C (2007) Enthalpy of interaction and binding isotherms of non-ionic surfactants onto micellar amphiphilic polymers (amphipols). Langmuir 23: 3025-3035.
14. Diab C, Tribet C, Gohon Y, Popot JL, Winnik FM (2007) Complexation of integral membrane proteins by phosphorylcholine-based amphipols. Biochim Biophys Acta 1768: 2737-2747.
15. Popot JL (2010) Amphipols, nanodiscs, and fluorinated surfactants: three nonconventional approaches to studying membrane proteins in aqueous solutions. Annu Rev Biochem 79: 737-775.
16. Picard M, Dahmane T, Garrigos M, Gauron C, Giusti F, et al. (2006) Protective and inhibitory effects of various types of amphipols on the Ca2+-ATPase from sarcoplasmic reticulum: a comparative study. Biochemistry 45: 1861-1869.
17. Toyoshima C, Nomura H (2002) Structural changes in the calcium pump accompanying the dissociation of calcium. Nature 418: 605-611.
18. Lemmon MA, Flanagan JM, Hunt JF, Adair BD, Bormann BJ, et al. (1992) Glycophorin A dimerization is driven by specific interactions between transmembrane alpha-helices. J Biol Chem 267: 7683-7689.
19. Lemmon MA, Flanagan JM, Treutlein HR, Zhang J, Engelman DM (1992) Sequence specificity in the dimerization of transmembrane alpha-helices. Biochemistry 31: 12719-12725.
20. Lemmon MA, Treutlein HR, Adams PD, Brunger AT, Engelman DM (1994) A dimerization motif for transmembrane alpha-helices. Nat Struct Biol 1: 157-163.
21. Mackenzie KR (2006) Folding and stability of alpha-helical integral membrane proteins. Chem Rev 106: 1931-1977.
22. Senes A, Ubarretxena-Belandia I, Engelman DM (2001) The Calpha ---H…O hydrogen bond: a determinant of stability and specificity in transmembrane helix interactions. Proc Natl Acad Sci U S A 98: 9056-9061.
23. Adair BD, Engelman DM (1994) Glycophorin A helical transmembrane domains dimerize in phospholipid bilayers: a resonance energy transfer study. Biochemistry 33: 5539-5544.
24. Anbazhagan V, Cymer F, Schneider D (2010) Unfolding a transmembrane helix dimer: A FRET study in mixed micelles. Arch Biochem Biophys 495: 159-164.
25. Anbazhagan V, Schneider D (2010) The membrane environment modulates self-association of the human GpA TM domain—implications for membrane protein folding and transmembrane signaling. Biochim Biophys Acta 1798: 1899-1907.
26. Fisher LE, Engelman DM, Sturgis JN (1999) Detergents modulate dimerization, but not helicity, of the glycophorin A transmembrane domain. J Mol Biol 293: 639-651.
27. Fisher LE, Engelman DM, Sturgis JN (2003) Effect of detergents on the association of the glycophorin a transmembrane helix. Biophys J 85: 3097-3105.
28. Stangl M, Veerappan A, Kroeger A, Vogel P, Schneider D (2012) Detergent properties influence the stability of the glycophorin a transmembrane helix dimer in lysophosphatidylcholine micelles. Biophys J 103: 2455-2464.
29. Merzlyakov M, Hristova K (2008) Forster resonance energy transfer measurements of transmembrane helix dimerization energetics. Methods Enzymol 450: 107-127.
30. Whitmore L, Wallace BA (2004) DICHROWEB, an online server for protein secondary structure analyses from circular dichroism spectroscopic data. Nucleic Acids Res 32: W668-673.

31. Whitmore L, Wallace BA (2008) Protein secondary structure analyses from circular dichroism spectroscopy: methods and reference databases. Biopolymers 89: 392-400.
32. Keller S, Vargas C, Zhao H, Piszczek G, Brautigam CA, et al. (2012) High-precision isothermal titration calorimetry with automated peak-shape analysis. Anal Chem 84: 5066-5073.
33. Kemmer G, Keller S (2010) Nonlinear least-squares data fitting in Excel spreadsheets. Nat Protoc 5: 267-281.
34. Shiraki K, Nishikawa K, Goto Y (1995) Trifluoroethanol-induced stabilization of the alpha-helical structure of beta-lactoglobulin: implication for non-hierarchical protein folding. J Mol Biol 245: 180-194.
35. Giusti F, Popot JL, Tribet C (2012) Well-defined critical association concentration and rapid adsorption at the air/water interface of a short amphiphilic polymer, amphipol A8-35: a study by Forster resonance energy transfer and dynamic surface tension measurements. Langmuir 28: 10372-10380.
36. Pocanschi CL, Popot JL, Kleinschmidt JH (2013) Folding and stability of outer membrane protein A (OmpA) from Escherichia coli in an amphipathic polymer, amphipol A8-35. Eur Biophys J.
37. Tribet C, Audebert R, Popot JL (1997) Stabilization of hydrophobic colloidal dispersions in water with amphiphilic polymers: Application to integral membrane proteins. Langmuir 13: 5570-5576.
38. Tribet C, Diab C, Dahmane T, Zoonens M, Popot JL, et al. (2009) Thermodynamic characterization of the exchange of detergents and amphipols at the surfaces of integral membrane proteins. Langmuir 25: 12623-12634.
39. Zoonens M, Giusti F, Zito F, Popot JL (2007) Dynamics of membrane Protein/Amphipol association studied by forster resonance energy transfer: Implications for in vitro studies of amphipol-stabilized membrane proteins. Biochemistry 46: 10392-10404.
40. Lau FW, Bowie JU (1997) A method for assessing the stability of a membrane protein. Biochemistry 36: 5884-5892.
41. Faham S, Yang D, Bare E, Yohannan S, Whitelegge JP, et al. (2004) Side-chain contributions to membrane protein structure and stability. J Mol Biol 335: 297-305.
42. Otzen DE (2003) Folding of DsbB in mixed micelles: a kinetic analysis of the stability of a bacterial membrane protein. J Mol Biol 330: 641-649.
43. Sehgal P, Otzen DE (2006) Thermodynamics of unfolding of an integral membrane protein in mixed micelles. Protein Sci 15: 890-899.
44. Yohannan S, Yang D, Faham S, Boulting G, Whitelegge J, et al. (2004) Proline substitutions are not easily accommodated in a membrane protein. J Mol Biol 341: 1-6.
45. Keller S, Heerklotz H, Jahnke N, Blume A (2006) Thermodynamics of lipid membrane solubilization by sodium dodecyl sulfate. Biophys J 90: 4509-4521.
46. Weber M, Prodohl A, Dreher C, Becker C, Underhaug J, et al. (2011) SDS-Facilitated In vitro Formation of a Transmembrane B-Type Cytochrome Is Mediated by Changes in Local pH. Journal of Molecular Biology 407: 594-606.
47. Keller S, Heerklotz H, Blume A (2006) Monitoring lipid membrane translocation of sodium dodecyl sulfate by isothermal titration calorimetry. J Am Chem Soc 128: 1279-1286.
48. Otzen DE (2003) Folding of DsbB in mixed micelles: A kinetic analysis of the stability of a bacterial membrane protein. Journal of Molecular Biology 330: 641-649.
49. Hong H, Bowie JU (2011) Dramatic destabilization of transmembrane helix interactions by features of natural membrane environments. J Am Chem Soc 133: 11389-11398.

BIOCHEMISTRY
including biophysical chemistry & molecular biology

Article

pubs.acs.org/biochemistry

A Minimal Hydrophobicity Is Needed To Employ Amphiphilic p(HPMA)-co-p(LMA) Random Copolymers in Membrane Research

Michael Stangl,[†] Mirjam Hemmelmann,[‡] Mareli Allmeroth,[‡] Rudolf Zentel,[‡] and Dirk Schneider*[,†]

[†]Institut für Pharmazie und Biochemie, Johannes Gutenberg-Universität Mainz, Johann-Joachim-Becher-Weg 30, 55128 Mainz, Germany

[‡]Institut für Organische Chemie, Johannes Gutenberg-Universität Mainz, Duesbergweg 10-14, 55128 Mainz, Germany

S *Supporting Information*

ABSTRACT: Because a polymer environment might be milder than a detergent micelle, amphiphilic polymers have attracted attention as alternatives to detergents in membrane biochemistry. The polymer poly[*N*-(2-hydroxypropyl)-methacrylamid] [p(HPMA)] has recently been modified with hydrophobic lauryl methacrylate (LMA) moieties, resulting in the synthesis of amphiphilic p(HPMA)-co-p(LMA) polymers. p(HPMA)-co-p(LMA) polymers with a LMA content of 5 or 15% have unstable hydrophobic cores. This, on one hand, promotes interactions of the hydrophobic LMA moieties with membranes, resulting in membrane rupture, but at the same time prevents formation of a hydrophobic, membrane mimetic environment that is sufficiently stable for the incorporation of transmembrane proteins. On the other hand, the p(HPMA)-co-p(LMA) polymer with a LMA content of 25% forms a stable hydrophobic core structure, which prevents hydrophobic interactions with membrane lipids but allows stable incorporation of membrane proteins. On the basis of our data, it becomes obvious that amphiphilic polymers have to have threshold hydrophobicities should an application in membrane protein research be anticipated.

To analyze the structure and function of highly hydrophobic membrane proteins *in vitro*, detergents or lipids are traditionally used in membrane biochemistry. However, amphiphilic polymers have attracted attention as an alternative to detergents and lipids, and amphiphilic polymers, the best characterized class of Amphipols, have already been used successfully as stabilizing and nondenaturing solvents in membrane protein research.[1−11] The polymer poly[*N*-(2-hydroxypropyl)-methacrylamid] [p(HPMA)] is a water-soluble, nontoxic, and nonimmunogenic polymer,[12] dating back to the invention of pharmacological active polymers by H. Ringsdorf in the 1970s.[12−16] Recently, p(HPMA) polymers with a narrow size distribution became available[16] and have been modified with hydrophobic lauryl methacrylate (LMA) moieties, resulting in the synthesis of amphiphilic copolymers.[17] p(HPMA)-co-p(LMA) copolymers (Figure 1) self-assemble spontaneously in aqueous solutions into micelle-like aggregates, which allow encapsulation of hydrophobic compounds.[18−21] The formation of p(HPMA)-co-p(LMA) aggregates, as well as its properties, e.g., the size of the aggregates or the composition of the hydrophobic core, might be controlled by the content of the hydrophobic LMA block within the polymer, which is statistically spread across the hydrophilic backbone. Initial studies have indicated that p(HPMA)-co-p(LMA) polymers form aggregates with a micellar substructure, when the polymer contains at least 5 mol % of the hydrophobic LMA side chains.[20] Thus, p(HPMA)-co-p(LMA) polymers might make up a new class of surfactants used for membrane protein solubilization and characterization or the transport of pharmaceutically active, hydrophobic peptides to specific cellular targets. While in the case of a polymer with 5% LMA, the amount of aggregates is very small and the aggregates are rather unstable, incorporation of hydrophobic compounds eventually results in formation of a more stable hydrophobic core.[20] In contrast, polymers containing 10% LMA form stable hydrophobic core structures by themselves.[20] Although the exact structures of these aggregates are still enigmatic, the polymers comply with the conditions that are essential for membrane protein research, as they form a hydrophobic environment in aqueous solutions and thereby mimic a membrane environment, similar to classical detergent micelles. However, detergents typically have high aggregation numbers and critical micelle concentrations (CMCs), and thus, high detergent-to-protein ratios are typically needed to solubilize membrane proteins. This results in an environment of strong entropic forces, which may destabilize or even denature membrane proteins.[22] In contrast, a copolymer environment might be milder than a detergent micelle and thus may destabilize membrane proteins to a lesser extent.

In this study, we have analyzed the properties of p(HPMA)-co-p(LMA) polymers with LMA contents of approximately 5, 15, and 25% (**C5**, **C15**, and **C25**, respectively) for applications

Received: December 3, 2013
Revised: February 14, 2014
Published: February 17, 2014

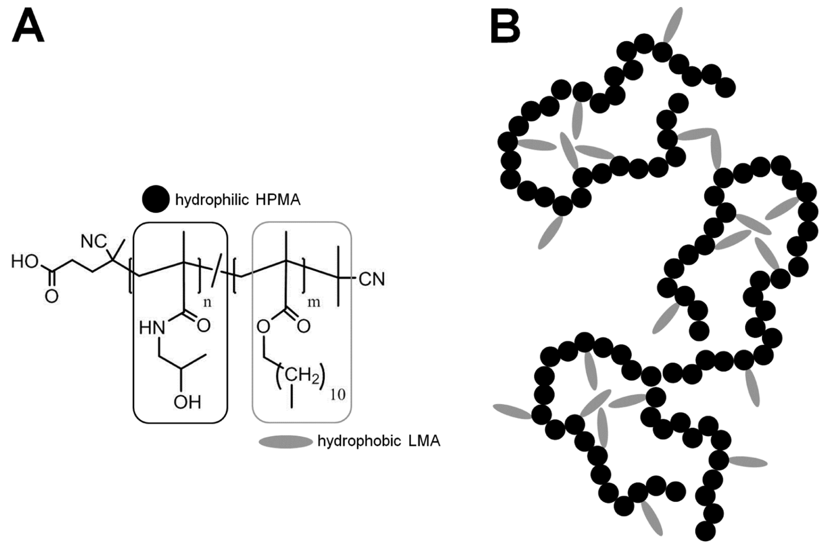

Figure 1. Chemical structure of the p(HPMA)-co-p(LMA) polymer and its aggregate in aqueous solution. (A) Chemical structure of the p(HPMA)-co-p(LMA) random copolymer with its hydrophobic LMA and its hydrophilic HPMA monomers. n represents the mole percent of HPMA and m the mole percent of LMA (5, 15, and 25% in this study). (B) Scheme of a p(HPMA)-co-p(LMA) aggregate composed of three individual copolymer chains in aqueous solution.

in membrane protein research. The **C5** polymer interacted with a phosphatidylcholine (PC) model membrane, and the interaction resulted in membrane rupture. While the **C15** polymer had a similar effect on membranes, in the case of the **C25** polymer no influence on the structure of the analyzed model membrane system has been determined. Furthermore, while in **C5** and **C15** polymers formation of a transmembrane (TM) helix dimer structure was not well-supported, the secondary as well as the quaternary structure of this protein was well-preserved in **C25** polymer solutions. Together, our data show that the two p(HPMA)-co-p(LMA) polymers with LMA contents of 5 and 15% have unstable hydrophobic cores, which on one hand promotes interactions of the hydrophobic LMA moieties with membranes but at the same time prevents formation of a membrane mimetic environment that is sufficiently stable for the incorporation of TM proteins. On the other hand, the **C25** p(HPMA)-co-p(LMA) polymer forms a stable hydrophobic core, which prevents hydrophobic interactions with membrane lipids but allows the stable incorporation of membrane proteins. Thus, the **C25** polymer is introduced as a new potential tool in membrane protein research. Furthermore, on the basis of our data for copolymers with increasing LMA contents, it becomes obvious that newly designed polymers must exceed threshold hydrophobicities should an application in membrane protein research be anticipated.

■ MATERIALS AND METHODS

Materials for Fluorescence and Circular Dichroism Measurements. Peptides corresponding to residues 69−101 of the human glycophorin A (GpA) TM domain (SEPEITLIIFGVMAGVIGTILLISYGIRRLIKK) were custom-synthesized and labeled at the N-terminus with either the donor and acceptor dyes fluorescein (FL) and 5-6-carboxyrhodamine (TAMRA), respectively (Peptide Specialty Laboratories, Heidelberg, Germany).[23] Peptides were dissolved in 2,2,2-trifluoroethanol (TFE) purchased from Sigma-Aldrich (Munich, Germany). 1,2-Dieicosenoyl-*sn*-glycero-3-phosphocholine (20:1 PC), 1,2-dioleoyl-*sn*-glycero-3-phosphocholine (DOPC), and 1,2-dioleoyl-*sn*-glycero-3-phosphoethanolamine-*N*-(lissamine rhodamine B sulfonyl) (ammonium salt) (Liss Rhod PE) were purchased from Avanti Polar Lipids (Alabaster, AL). Laurdan (6-dodecanoyl-*N*,*N*-dimethyl-2-naphthylamine), *n*-dodecyl *β*-D-maltopyranoside (DDM), and 8-anilino-1-naphthalenesulfonic acid ammonium salt (ANS) were purchased from Sigma-Aldrich. Amphipol A8-35 was purchased from Affymetrix (Santa Clara, CA). PD10 columns were purchased from GE Healthcare (Buckinghamshire, Great Britain). 8-Aminonaphthalene-1,3,6-trisulfonic acid, disodium salt (ANTS), and *p*-xylene-bis-pyridinium bromide (DPX) were purchased from Invitrogen Life Technologies (Carlsbad, CA).

Polymer Synthesis. Polymers **C5**, **C15**, and **C25** were synthesized following previously published procedures[17,24] with some alterations.[20,21]

4-Cyano-4-[(thiobenzoyl)sulfanyl]pentanoic acid, synthesized according to published procedures,[25] was used as a CTA (chain transfer agent).

Pentafluorophenyl methacrylate (PFPMA) was prepared following described procedures.[26,27]

In a typical reaction, 3 g (12 mmol) of PFPMA, 41 mg (0.16 mmol) of CTP with AIBN as an initiator (1:8 AIBN:CTP molar ratio), and the respective amounts of lauryl methacrylate (LMA) (5 mol % for **C5**, 15 mol % for **C15**, and 25 mol % for **C25**) were dissolved in 5 mL of dry dioxane in a Schlenk tube. After three freeze−vacuum−thaw cycles, the reaction mixture was stirred at 65 °C overnight. The p(PFPMA)-co-p(LMA) polymer was precipitated three times in hexane, isolated by centrifugation, and dried for 12 h at 40 °C under vacuum. A pink powder was obtained with 60% yield: ^{1}H NMR (300 MHz, $CDCl_3$) δ 0.86 (br t), 1.20−1.75 (br), 2.00−2.75 (br s); ^{19}F NMR (400 MHz, $CDCl_3$) δ −162 (br), −157 (br), −152 to −150 (br).

Postpolymerization Modification to p(HPMA)-co-p-(LMA) Random Copolymers. **C5** is used as an example to describe the reaction procedure: 280 mg of the precursor polymer (M_n = 23000 g/mol) was dissolved in absolute dioxane, and 48 mg (0.9 mmol) of 2-hydroxypropanamine and 183 mg (1.8 mmol) of triethylamine were added to the reaction mixture. The reaction continued overnight at 60 °C. To ensure complete removal of reactive ester groups, an excess of 48 mg of 2-hydroxypropanamine and 183 mg of triethylamine were added again to the reaction mixture. Completion of the reaction was assessed using ^{19}F NMR. The final polymer was precipitated three times in diethyl ether, dissolved in 1 mL of DMSO, and dialyzed against deionized water. A colorless fluffy powder was obtained in 76% yield after lyophilization: ^{1}H NMR (400 MHz, DMSO-*d*) δ 0.85 (br t), 0.90−1.40 (br), 1.6−2.20 (br), 2.75−3.10 (br), 3.50−3.80 (br), 4.60−4.80 (br).

The polymers contain ∼5, ∼15, or ∼25 mol % hydrophobic LMA as verified by NMR. Polymer characteristics are summarized in Table 1. Their molecular weights were determined by gel permeation chromatography in THF.

Table 1. Overview of the C5, C15, and C25 Random Copolymers[a]

polymer	HPMA:LMA ratio	M_n (g/mol)	PDI	ref
C5	95:5	13500	1.20	20, 21
C15	85:15	14000	1.17	21
C25	75:25	17000	1.23	48

[a]Molecular weights (M_n) and the polydispersity index (PDI) were determined by gel permeation chromatography. For the sake of comparison, please note that **C5** and **C15** are identical to **C5** and **C15**, respectively, in refs 20 and 21 and **C25** is comparable to **P2*** in ref 48, which has, however, a higher molecular weight.

Pyrene Fluorescence Spectroscopy. Critical aggregate concentrations of the polymers, i.e., the equivalent of CMC values characterizing detergent micelle formation, were determined as described in detail recently.[28] Briefly, a stock solution of the **C15** and **C25** copolymers was prepared at a concentration of 0.1 g/L by dissolving the polymers in DMSO. The polymer stock solution was subsequently diluted to 10 different concentrations down to 1×10^{-6} g/L using an aqueous NaCl solution. We then prepared each sample by dropping carefully 40 μL of a pyrene solution (2.5×10^{-5} mol/L in acetone) into an empty vial, evaporating the acetone by gently heating at 50−60 °C, adding 2 mL of one of the polymer solutions, and stirring the closed and light-protected vials for 48−72 h at 50−60 °C. The final concentration of pyrene in water thus reached 5.0×10^{-7} mol/L, which is slightly below the pyrene saturation concentration in water at 22 °C. Steady-state fluorescence spectra of the air-equilibrated samples were recorded using an LS 50 B Perkin-Elmer luminescence spectrometer (right angle geometry, 1 cm × 1 cm quartz cell) using the following conditions: excitation at 333 nm and slit widths of 10 nm for excitation and 2.5 nm for emission. The intensities of the fluorescence emission at 372 and 383 nm were then evaluated. The decrease for 372 and 383 nm versus the logarithmically plotted polymer concentration was used to determine the critical aggregation concentration.

Circular Dichroism (CD) Spectroscopy. CD spectra were recorded on a Jasco J-815 spectropolarimeter at 25 °C in a step-scan mode using 0.1 cm path length quartz cells from Hellma (Müllheim, Germany). The concentration of the unlabeled GpA peptide was 5 μM. Data points were collected at a resolution of 1 nm, an integration time of 1 s, and a bandpass of 1 nm. Each spectrum shown resulted from at least three averaged scans from which buffer scans were subtracted. To measure how well the respective polymers dissolve the GpA TM helix, the peptides were mixed together with the polymers in organic solvent and dried in a gentle stream of nitrogen with subsequent desiccation overnight. The GpA TM domain was reconstituted in 10 mM phosphate buffer (pH 7.4). As a positive control, the peptides were reconstituted in a 5 mM DDM detergent solution, which is known to stabilize α-helical structures and to solubilize the GpA TM domain very well. Prior to CD measurements, samples were incubated for 2 h at 37 °C followed by sonication for 10 min and centrifugation at 16100*g* for 10 min. Secondary structure contents were predicted with DICHROWEB using both soluble and TM proteins as a reference data set (CDSSTR method, reference set 7).[29,30]

Fluorescence and Förster Resonance Energy Transfer Measurements. Steady-state fluorescence measurements were performed using the FL-labeled GpA TM helix (0.25 μM) mixed with the respective polymer (5−50 μM). For Förster resonance energy transfer (FRET) measurements, equal concentrations of FL- and TAMRA-labeled GpA TM domains were used. Concentrations of the peptide stock solutions were determined from absorbance measurements in a Perkin-Elmer Lambda 35 UV−vis spectrophotometer. In all experiments, we used a concentration of 0.25 μM for each of the two labeled GpA peptides. Peptides dissolved in TFE and the p(HPMA)-co-p(LMA) polymer dissolved in ethanol were mixed, and organic solvents were removed in a gentle stream of nitrogen gas. Residual solvent traces were removed by vacuum desiccation overnight. The dried peptide−polymer film was then hydrated in 10 mM HEPES buffer (pH 7.4) containing 150 mM NaCl. After incubation at 37 °C for at least 2 h, sonication for 10 min, and centrifugation at 16100*g* for 10 min, steady-state fluorescence measurements were performed at 25 °C on a Horiba Fluoromax 4 system with both excitation and emission slits set to 2 nm. The excitation wavelength was 439 nm, and emission spectra were recorded from 480 to 650 nm.

The sensitized donor emission was calculated using the FRET pair fluorescence intensities at 520 and 575 nm according to

$$E_{sens} = F_{575\,nm}/F_{520\,nm} \quad (1)$$

Increasing E_{sens} ratios indicate an increase in the extent of GpA dimerization. The FL spectrum yields an E_{sens} ratio of only ∼0.3, defining the lowest possible ratio at which no dimer is present.

Generalized Polarization. Large unilamellar vesicles (LUVs, 1 mM) of 1,2-dieicosenoyl-*sn*-glycero-3-phosphocholine (20:1 PC) containing the fluorescent lipid probe Laurdan (2 μM) were prepared by hydration of the dried lipid film in 10 mM HEPES buffer (pH 7.4) containing 150 mM NaCl, followed by eight freeze−thaw cycles. The polymers were prepared as described above, yielding a polymer concentration of 100 μM, and titrated into the LUV-containing solutions. Steady-state fluorescence measurements were performed after polymer addition, mixing, and incubation at 25 °C. The excitation wavelength was set to 350 nm, and Laurdan emission spectra were recorded from 400 to 550 nm at a slit width of 1 nm for both excitation and emission slits. GP values were calculated using the following equation:

$$GP = (F_{435\,nm} - F_{490\,nm})/(F_{435\,nm} + F_{490\,nm}) \quad (2)$$

Low GP values indicate a low level of membrane lipid order, whereas increasing GP values imply the membrane is becoming more rigid because of the attachment of copolymers.

Liposome Content Release. DOPC and Liss Rhod PE (1:1000) were mixed in organic solvent, dried under a nitrogen stream, and desiccated overnight. The lipid film was then hydrated with 10 mM HEPES buffer (pH 7.4) containing 150 mM NaCl, the fluorescent dye ANTS (12.5 mM), and the quencher DPX (45 mM). Unilamellar vesicles, having a concentration of 0.5 mM, were prepared by performing eight freeze−thaw cycles. Nonencapsulated dye and quencher molecules were removed from the LUVs on a PD10 gel filtration column (filled with Sephadex G-25 M, GE Healthcare). Elution fractions were collected on 96-well plates, and ANTS and Liss Rhod fluorescence were detected in a Fluostar Omega microplate reader (BMG Labtech) to identify the fractions containing the loaded lipid vesicles. Immediately before the measurement, the vesicles loaded with ANTS and DPX were diluted with buffer [10 mM HEPES buffer (pH 7.4) and 150 mM NaCl] and mixed with a polymer solution (100 μM stock, prepared as described above) to a final lipid concentration of 0.1 mM and polymer concentrations of 5 and 20 μM. Because of the mixing of the compounds prior to the measurement, the dead time of the measurement was approximately 10 s, which is neglected in the final data analysis. Fluorescence measurements were performed at 25 °C on a Horiba Fluoromax 4 spectrofluorimeter. The excitation wavelength was set to 360 nm, and fluorescence emission was recorded at 530 nm, with both slits set to 5 nm. For each measurement, positive (addition of 1% Triton X-100) and negative (liposomes without polymer) controls were performed. Assuming that the amount of leakage L is 0 in negative control N and 1 (100%) in positive control P, the time-dependent leakage, induced by the addition of polymer, can be calculated using fluorescence intensity I at 530 nm of each sample S and the following eq 3 according to ref 31

$$L(t) = [I_S(t) - I_N(t)]/[I_P(t) - I_N(t)] \quad (3)$$

ANS Fluorescence Measurement. ANS is a widely used fluorescent dye, the fluorescence emission of which dramatically increases after binding to hydrophobic regions of molecules and assemblies. It is used as an extrinsic tool in studies regarding protein folding and formation of hydrophobic assemblies, such as micelles.[32−34] Changes in the spectral shape and fluorescence intensity of ANS can be attributed to the formation or collapse of hydrophobic regions in the analyzed molecules, which are the copolymer assemblies in this case. Polymers **C5**, **C15**, and **C25** were dissolved as described above in 10 mM HEPES (pH 7.4), 150 mM NaCl buffer, which additionally contained 5 μM ANS probe. During the measurements, the temperature was increased from 25 to 80 °C in 5 °C steps. For each temperature, ANS emission spectra were recorded from 450 to 600 nm after excitation at 374 nm (both slits set to 4 nm).

RESULTS AND DISCUSSION

Interaction of the p(HPMA)-co-p(LMA) Polymer with Model Membranes. Almost 20 years ago, amphiphilic polymers were introduced for the first time in membrane protein research, and the class of so-called Amphipols is currently the best studied and most widely used. However, as there still is a need to develop new detergents and/or surfactants for membrane protein research, new amphiphilic polymers might enter the field. Recently, it has been concluded that **C5** and **C10** p(HPMA)-co-p(LMA) polymers interact with membranes,[20] and moreover, **C10** interacts with blood serum components, such as VLDL particles.[19] However, a potential application of p(HPMA)-co-p(LMA) polymers in membrane biochemistry has never been elucidated. The three p(HPMA)-co-p(LMA) polymers used in this study differ in the contents of their hydrophobic LMA moieties, which affects the stability of the polymer aggregates in aqueous solution. While the polymer with 5% LMA appears to form aggregates, the amount of aggregates is very small and the aggregates are rather unstable,[20] whereas polymers containing >10% LMA form a stable hydrophobic core.[20] As described in Materials and Methods, by monitoring changes in pyrene fluorescence emission, we determined the critical aggregation concentrations of the **C15** and **C25** polymers to be 59 and 10 nM, respectively. These concentrations are far below the polymer concentrations used in our measurements, and hence, these polymers form stable aggregates under our experimental conditions. p(HPMA)-co-p(LMA) polymers with 10 and 15% LMA are believed to interact with membranes of living cells.[21] However, the exact mode of interaction remains elusive, and it is currently unclear whether the polymers interact directly with membrane lipids or whether membrane association and/or integration is mediated by membrane-associated proteins. To elucidate a direct interaction of the polymers with membrane lipids, we measured interactions of selected p(HPMA)-co-p(LMA) polymers with LUVs by monitoring the fluorescence emission of the dye Laurdan, a fluorescent membrane probe, which detects changes in lipid packing and membrane fluidity. As shown in Figure 2, upon addition of both polymers **C5** and **C15** to LUVs, the Laurdan GP value increased strongly, and thus, both polymers interact significantly with the membrane lipids. It is noteworthy that after addition of the polymers to the LUV-containing solution, the GP values changed immediately, and no additional changes were observed when the fluorescence was followed for

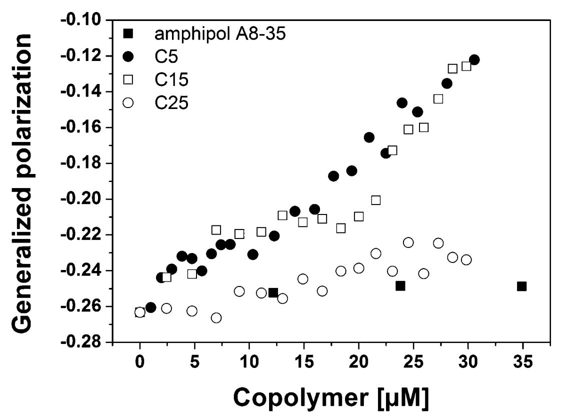

Figure 2. Interactions of the polymer with model membranes monitored by Laurdan generalized polarization. Generalized polarization (GP) was determined using the Laurdan fluorescent probe (2 μM) embedded in 1 mM 20:1 PC LUVs upon addition of the p(HPMA)-co-p(LMA) polymers at 25 °C. Polymers were titrated into the LUV solution, and the Laurdan probe was excited at 350 nm. Fluorescence emission was recorded from 400 to 550 nm. An increase in the GP value reflects a decrease in membrane fluidity and thus an increased level of bilayer lipid order. The large increase in GP in the case of polymers **C5** and **C15** indicates a significant interaction of the polymers with the membranes. For the sake of comparison, GP values monitored in the presence of Amphipol A8-35, which is known to stabilize membrane proteins very well and is able to form a stable hydrophilic core, are shown. Both, Amphipol A8-35 and the **C25** polymer hardly influence the GP value and thus only marginally influence the membrane structure.

dx.doi.org/10.1021/bi401611f | *Biochemistry* 2014, 53, 1410−1419

an additional 60 min (data not shown). In contrast to the **C5** and **C15** polymers, **C25** and Amphipol A8-35, which was used as a control, appear to hardly interact with the model membrane, as the determined GP values increased only slightly upon addition of increasing amounts of the **C25** polymer to the liposomes (Figure 2). It is notable that also in LUVs composed of a PC lipid with a shorter acyl chain length (DOPC), as well as LUVs composed of the negatively charged lipid DOPG, significant interaction of **C5** and **C15**, but not of **C25** or Amphipol A8-35, with the membrane was observed (Figure S1 of the Supporting Information), indicating that membrane interaction does not strictly depend on the lipid species. To elucidate whether membrane interaction of the polymers interferes with membrane stability, e.g., resulting in leakage of encapsulated vesicle content, we next monitored the release of soluble liposome content upon polymer addition (Figure 3).

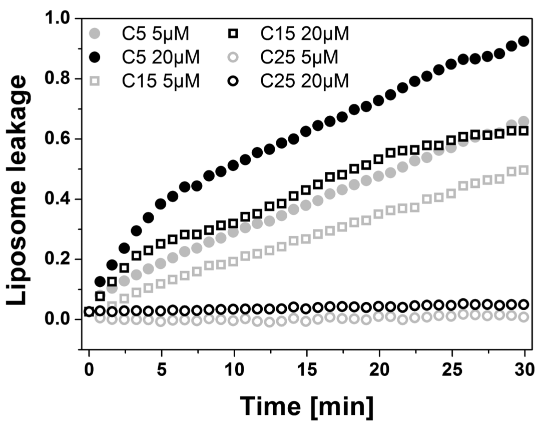

Figure 3. Release of soluble content encapsulated in LUVs after the addition of **C5**, **C15**, and **C25** copolymers. DOPC (0.1 mM lipid) liposomes loaded with the fluorescent dye ANTS (12.5 mM) and the quencher DPX (45 mM) were treated with 5 or 20 μM copolymers (**C5**, **C15**, or **C25**). The fluorescence of the ANTS dye increased upon leakage of the DOPC liposomes. As a positive control representing 100% leakage, 1% Triton X-100 was added to the liposomes. As a negative control, the fluorescence of the pure liposomes was monitored over the same period of time. Liposome leakage was calculated using the fluorescence intensities at 530 nm and eq 3. Polymer **C25** induces no leakage at either tested polymer concentration, whereas **C15** and even more significantly **C5** induce leakage in a concentration-dependent manner, indicating interactions of the **C5** and **C15** polymers with the membranes.

Addition of **C25** to LUVs loaded with a fluorophore and quencher did not show any increase in fluorescence emission, further supporting the idea that **C25** does not significantly interact with membranes and demonstrating that **C25** does not affect liposome stability. In contrast, when the **C5** polymer was added, a large increase in fluorescence emission was observed because of the destabilization of the LUV structure and the release of liposome content. Also, addition of **C15** resulted in the release of liposome content, and thus, this polymer also affects liposome stability and membrane integrity, although to a lesser extent than the **C5** polymer. We can therefore conclude that **C5** and **C15**, but not **C25**, interact with membranes and destabilize the vesicular membrane structure.

Potentially, because of the increased hydrophobicity of the **C25** polymer, this polymer forms aggregates with a more stable hydrophobic core. To test this assumption, we incorporated the hydrophobic fluorescent probe ANS into the polymer aggregates and measured ANS fluorescence emission at increasing temperatures. Melting of the hydrophobic aggregate core structure, into which ANS is incorporated, will result in a decrease in fluorescence emission, due to ANS release. As shown in Figure 4, increasing the temperature of a **C25**

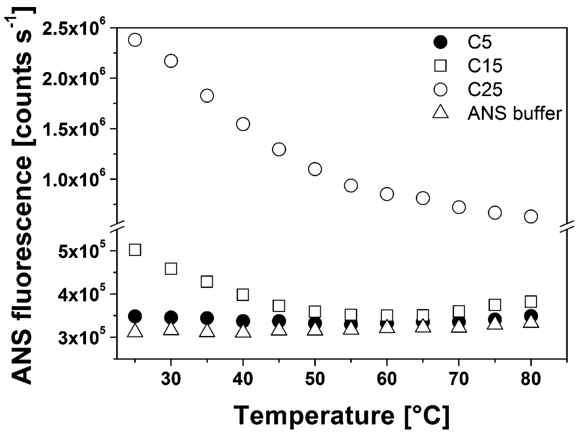

Figure 4. Temperature-dependent fluorescence changes of the hydrophobicity-sensitive dye ANS in copolymer solutions. Copolymers **C5**, **C15**, and **C25** (20 μM) were dissolved in 10 mM HEPES (pH 7.4), 150 mM NaCl buffer containing 5 μM ANS. The fluorescence emission of the ANS dye is sensitive to changes in the hydrophobicity of its environment. The stability of the polymers' hydrophobic core was tested by thermally unfolding the polymer assemblies. ANS was excited at 374 nm, and the fluorescence intensities measured at 490 nm are plotted vs temperature. Polymer **C25** shows the highest fluorescence at room temperature, indicating the formation of a hydrophobic core, which is more stable than in the case of the **C15** and **C5** polymer solutions, where only little fluorescence emission was observed. Higher temperatures lead to a decreased fluorescence emission due to destabilization of the hydrophobic polymer assembly cores. **C25** preserves a hydrophobic environment much better than the other polymers, even at 80 °C.

polymer solution resulted in a decreased ANS fluorescence. While melting of **C15** polymer aggregates was similar to that of **C25**, in the case of **C5** the ANS fluorescence essentially does not change. However, while the initial ANS fluorescence was high in the case of **C25**, indicating stable incorporation of the probe into a hydrophobic core structure, the ANS fluorescence was significantly lower in the case of the **C15** polymer, and no increased ANS fluorescence was observed in the **C5** polymer solution. Thus, this polymer does not form a hydrophobic core structure that is sufficiently stable to incorporate the hydrophobic ANS probe, which is in line with recent observations.[20]

Together, these data show that the **C25** polymer forms the most stable hydrophobic core structure, which is significantly more stable than that observed in the case of the two remaining polymers. While the **C15** polymer also appears to form a (marginally stable) hydrophobic core, in the case of the **C5** polymer, the results indicate that the polymer aggregates are not stable. The **C25** polymer aggregates do not expose hydrophobic structures and remain stable even in the presence of lipids. Consequently, while these data indicate that **C25** cannot be used to efficiently extract lipids or proteins from biological membranes, the stability of the **C25** hydrophobic core might be beneficial for incorporating and stabilizing membrane proteins.

Solubilization of the GpA TM Peptide and Secondary Structure Formation. As at least the **C15** and **C25** polymers appear to form hydrophobic cores, we next studied how the individual polymers solubilize a TM protein. Therefore, we first monitored solubilization of the 33-amino acid hydrophobic human erythrocyte GpA TM peptide by following the fluorescence signal of a fluorescein (FL)-labeled GpA TM helix in solution after addition of increasing polymer concentrations. The labeled peptide (0.25 μM) was dissolved in different concentrations of **C5**, **C15**, and **C25** p(HPMA)-co-p(LMA), reaching a final polymer concentration of 50 μM. In all three polymer solutions, the intensity of the fluorescence signal increased nonlinearly with an increasing polymer concentration, and a maximal fluorescence yield was reached at polymer concentrations exceeding 20−25 μM (Figure 5).

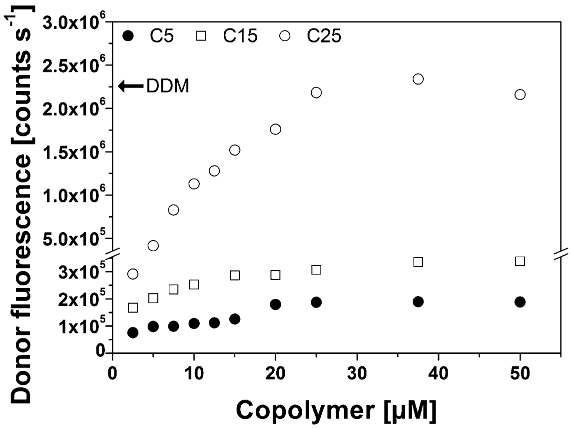

Figure 5. Fluorescence emission of the donor-labeled GpA TM peptide solubilized in a **C5**, **C15**, or **C25** polymer solution. Fluorescein-labeled GpA peptides (0.25 μM) were solubilized in the **C5**, **C15**, or **C25** p(HPMA)-co-p(LMA) polymer, as described in Materials and Methods. The peptide fluorescence intensities at 520 nm increase with increasing polymer concentrations to a value monitored after dissolving the fluorescein-labeled GpA peptides in 5 mM DDM (marked by the arrow). The maximal fluorescence emission is ~7-fold higher in the **C25** polymer solution than in the **C5** and **C15** solutions, indicating that the **C5** and **C15** polymers solubilize the GpA TM peptide less well than **C25**.

While the intensity of the fluorescence signal measured in the **C15** solution was ~2 times higher than determined in **C5**, the measured fluorescence intensities of the FL-GpA peptide in the presence of both **C5** and **C15** were at least 7-fold lower than for the **C25** solution. Here, at a **C25** polymer concentration of ~25 μM, the signal intensity reached a value comparable to the value obtained in DDM solutions. This analysis clearly indicates that the **C25** polymer is most efficient in solubilizing a simple TM protein. However, the results do not allow us to draw any conclusions about the structure and stability of TM proteins solubilized in the individual polymers. Thus, the question of how stable a given TM protein structure will be in the individual polymer solutions arose. Therefore, we next monitored by CD spectroscopy whether the p(HPMA)-co-p(LMA) polymers promote formation of the GpA TM helix secondary structure, compared to the mild and widely used detergent DDM. As shown in Figure 6A, in all three tested p(HPMA)-co-p(LMA) polymers, 5 μM GpA TM domain might be solubilized and the expected α-helical structure forms in all tested polymer solutions. The α-helix contents, calculated from the CD spectra, were comparable to the value obtained after solubilizing the GpA TM helix in 5 mM DDM. However, different polymer concentrations were needed to achieve

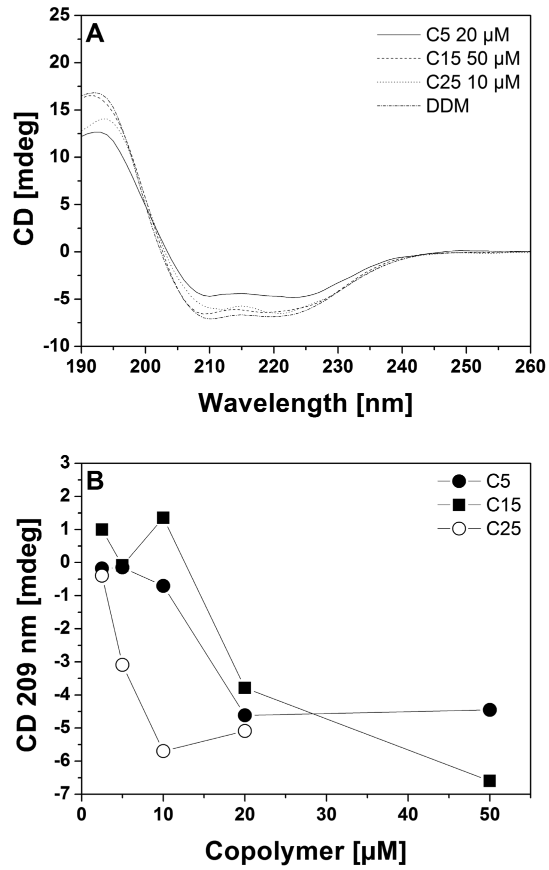

Figure 6. Far-UV CD spectra of the GpA TM domain solubilized in **C5**, **C15**, and **C25** p(HPMA)-co-p(LMA) polymer solutions. (A) The GpA TM domain (5 μM) was solubilized in **C5**, **C15**, and **C25** p(HPMA)-co-p(LMA) polymers at different concentrations. Spectra were recorded at 25 °C in phosphate buffer (pH 7.4). As a positive control, the GpA TM domain has been solubilized in 5 mM DDM detergent, which is known to support the formation of α-helices. (B) CD signal intensity at 209 nm, a characteristic minimum for α-helical protein structures, plotted vs polymer concentration. The corresponding value of the GpA TM helix solubilized in DDM is ~7 mdeg. The CD spectrum of GpA in 50 μM **C25** could not be measured, because of the high background absorption at low UV wavelengths. The CD spectra demonstrate the good solubility of the GpA TM helix in **C25**, even at low polymer concentrations. In the case of **C5** and **C15**, higher concentrations are needed to solubilize the GpA TM domain at the same level as the DDM detergent. The helical content of the GpA TM domain (5 μM) was 87% in 20 μM **C5** and 50 μM **C15** and 92% in 10 μM **C25** and 5 mM DDM, as determined using the DICHROWEB algorithm (CDSSTR).

proper CD spectra and thus to properly stabilize the α-helical structure of the peptides. In polymer **C5**, the best CD signal has been monitored at a polymer concentration of 20 μM, whereupon the CD signal did not improve further. However, at no concentration did the signal intensity at 209 nm reach the value obtained after solubilization of the GpA TM peptides in DDM. In the case of 50 μM **C15**, the CD spectrum was comparable to that monitored in a DDM solution or in 10 μM **C25**, indicating the proper formation of the peptides' secondary structure. However, at **C5** and **C15** polymer concentrations of <20 μM, essentially no CD signal was detected (Figure 6B), once again demonstrating the inability of these polymers to dissolve the peptides at such low concentrations (compare above). In contrast, the **C25** polymer efficiently solubilized the

dx.doi.org/10.1021/bi401611f | *Biochemistry* 2014, 53, 1410−1419

GpA TM domain at a concentration as low as ~10 μM, and the GpA TM domain was fully solubilized and correctly folded, as indicated by the predicted α-helix content of 92%. Higher concentrations of the **C25** polymer did not improve the CD signal further.

Together, these results indicate that the **C25** polymer aggregates have a stable hydrophobic core, which allows solubilization of TM proteins already at low polymer concentrations, whereby the protein's secondary structure remains fully preserved.

Stability of the GpA Quaternary Structure in Polymer Solutions. These results allow the classification of the propensity of the three analyzed p(HPMA)-co-p(LMA) polymers to solubilize a TM protein, as well as their abilities to support and/or preserve the secondary structure of TM helices. However, defined interactions of various individual TM helices are typically involved in the formation of a final TM protein structure. As formation of larger TM helix bundles is mostly mediated by defined TM helix–helix interactions, the GpA TM helix dimer can serve as an excellent probe for studying the impact of a lipid, detergent, or polymer environment on the formation of sequence-specific TM helix oligomers. To study GpA TM helix dimerization, the donor-labeled FL-GpA and the acceptor-labeled TAMRA-GpA were used in FRET measurements. The distance of the N-termini in the GpA TM helix dimer is approximately 10 Å, which is far below the Förster radius of the FRET pair dyes (49–54 Å).[35] Therefore, upon formation of the GpA TM helix dimer, the acceptor fluorescence emission at 575 nm is sensitized because of the resonance energy transfer from the donor to the acceptor. This FRET-based assay has already been used in several detergents and artificial membranes to study the impact of different environmental factors on the stability of an oligomeric TM protein.[22,23,36−40] In Figure 7, we compare the energy transfer (sensitized emission) at increasing polymer concentrations, which reflects the dimerization propensity of the GpA TM helix in the different polymer environments. The ratio of the FRET pair fluorescence intensities at 575 and 520 nm has a theoretical minimum, which is defined by the ratio of these wavelengths in the pure FL-GpA spectrum, because the FL fluorescence emission at 575 nm is not zero in absence of the acceptor dye. This minimal ratio is on the order of ~0.3, whereas higher ratios indicate formation of GpA dimers or higher-order oligomers. Figure 7A shows normalized FRET pair emission spectra in the three polymers, at polymer concentrations of 2.5–50 μM. With increasing polymer concentrations, the sensitized acceptor emission increases in the **C15** and **C25** polymers to a particular concentration (~15 μM **C15** and ~10 μM **C25**). A further increase of the polymer concentration did not further change the sensitized acceptor emission significantly. In the **C5** polymer, formation of GpA oligomers was essentially not observed, and with increasing polymer concentrations, the FRET pair ratio increased only modestly (from 0.3 to 0.45). In the **C15** polymer, oligomerization of the GpA TM domain was slightly enhanced compared to that with the **C5** polymer, resulting in an ultimately reached FRET pair ratio of 0.5 (Figure 7B). However, in both **C5** and **C15** polymer solutions, the maximal FRET pair ratios were rather low, compared to values obtained in DDM micelles (~1.3) or in **C25** polymer solutions. Thus, the GpA TM helix dimer is dramatically more stable in **C25** than in the polymers with lower LMA contents. Up to a **C25** polymer concentration of ~10 μM, the FRET pair ratio

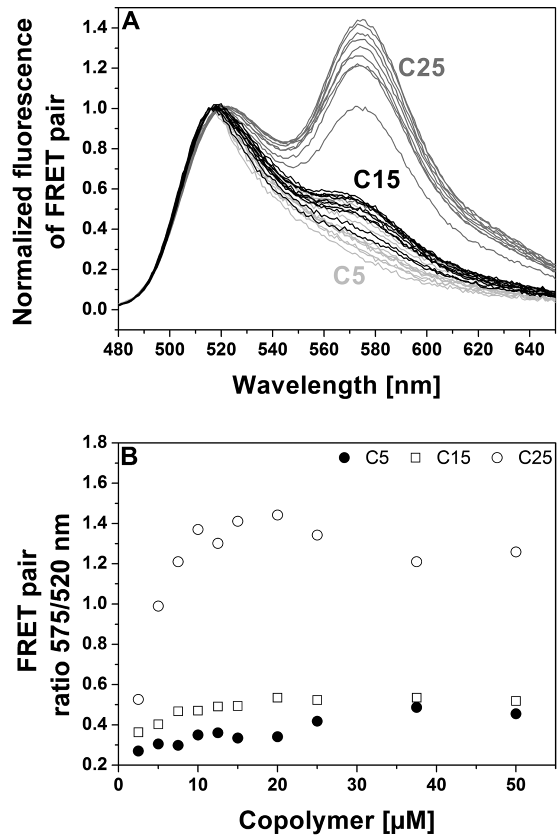

Figure 7. Dimerization of the GpA TM helix in **C5**, **C15**, and **C25** p(HPMA)-co-p(LMA) polymer solutions. (A) Donor- and acceptor-labeled peptides (0.25 μM each) were mixed at a 1:1 ratio and solubilized in the **C5**, **C15**, and **C25** polymers. At increasing polymer concentrations (2.5–50 μM), FRET pair emission spectra were recorded at 25 °C after excitation at 439 nm, and spectra were normalized at 520 nm. The increasing acceptor emission at 575 nm indicates an increased level of dimerization of the GpA TM domain. (B) Ratio of the fluorescence emission measured at 575 and 520 nm as a function of polymer concentration. While the **C5** and **C15** polymers essentially do not promote dimerization, the **C25** polymer facilitates dimerization well, even at very low concentrations. The dimerization propensity of the GpA TM helix in polymer **C25** is equal to the dimerization propensity in 5 mM DDM.

increased significantly from 0.5 to 1.4 and did not increase further afterward. However, at **C25** polymer concentrations exceeding 25 μM, the FRET pair ratio marginally decreased, which might indicate destabilization of the GpA TM helix dimer at higher polymer concentrations. This has been observed before at increasing concentrations of various detergents.[22,23,37,40] To exclude the possibility that the energy transfer arose because of unspecific aggregation of the labeled peptides, we measured energy transfer in polymer aggregates at changing acceptor mole ratios. As shown in Figure S2 of the Supporting Information, the FRET pair ratio, i.e., the energy transfer efficiency, linearly depends on the acceptor mole fraction, and this is only the case when the formed oligomer is a dimer, as derived in detail in, e.g., refs. 37 and 41.

Consequently, the **C25** polymer with a hydrophobic LMA content of 25% appears to be well suited to solubilize the GpA TM helix as well as to stabilize tertiary and quaternary contacts of TM proteins.

p(HPMA)-co-p(LMA) C25 Keeps TM Proteins in Solution and Preserves Quaternary Contacts. The C5 polymer has the smallest amount of hydrophobic LMA side chains, and the hydrophobic nature of the three analyzed compounds increases with an increasing LMA content. As determined in this study, only the **C5** and **C15** polymers interact with lipid bilayers and disturb the membrane structure. In contrast, addition of the **C25** polymer to model membranes did not alter the spectroscopic properties of the membrane probe or disrupt the membrane, and thus, the polymer does not appear to interact with the membranes. Most likely, the **C5** and **C15** polymers interact with the bilayer via their hydrophobic moieties, i.e., via their LMA side chains. The stronger the hydrophobic core of the polymer, and thus the more the hydrophobic side chains are shielded from the surrounding medium, the less they interact with the model membranes. As seen in the ANS measurements, the **C5** and **C15** polymer aggregates do not form highly stable hydrophobic core structures, which shield the hydrophobic portions of the molecules from the surrounding medium, but certain hydrophobic regions appear to be free to interact with membrane lipids. In contrast, the hydrophobic moieties of the **C25** polymer do not interact with the membrane, as the increased LMA content results in the formation of a rather stable hydrophobic core, which shields the hydrophobic structures and disables hydrophobic membrane contacts. However, the propensity of the individual polymers to interact with membranes is inversely proportional to their propensity to solubilize and stabilize TM proteins. Polymer **C5** solubilizes the GpA membrane protein less effectively than the remaining polymers, and the **C15** polymer was only slightly effective. Only the **C25** polymer rendered the GpA TM helix soluble and preserved the structure of the TM helix dimer. It is noteworthy that the **C25** polymer was approximately as efficient as Amphipol A8-35, which is known to solubilize and stabilize membrane protein oligomers well.[2,4,5,8−11,42−47]

Together, these results indicate that **C25** forms a stable hydrophobic core, and formation of such stable core structures appears to be a fundamental prerequisite for successfully solubilizing and stabilizing membrane proteins in aqueous solutions.

■ CONCLUSION AND PERSPECTIVE

In this analysis, we have tested three amphiphilic copolymers, having increasing hydrophobicities. These results indicate that only at a LMA concentration of 25% is the p(HPMA) copolymer able to form a stable hydrophobic core, into which hydrophobic TM proteins might be incorporated. Thus, there appears to be a threshold in the molecular hydrophobicity of polymers for their application in membrane protein research. At lower hydrophobicities, the polymers were not able to properly solubilize the TM protein and the structure of the TM proteins was not well preserved. Thus, an LMA content of >15% is needed to properly incorporate a TM protein. However, while these polymers allow the analysis of TM proteins in solution, such polymers do not significantly interact with membrane lipids (compare Figures 2 and 3) and thus do not alter the structure of biological membranes or extract lipids and proteins from membranes. Thus, using **C25** polymers together with living cells eventually will allow researchers to monitor interactions of soluble domains of TM proteins (solubilized in **C25**) with proteins at a eukaryotic plasma membrane, without interacting with and influencing the structure or stability of the cell membrane. When a TM protein is solubilized in conventional detergents, (i) the detergents will be diluted below their CMC and thus the micellar structures will collapse and/or (ii) the detergent molecules will affect the molecular structure of the biological membrane system. As the amphiphilic **C25** polymer prevents such devastating effects, this detergent substitute might allow future *in vitro* studies with membrane proteins, which were not feasible before.

■ ASSOCIATED CONTENT

Supporting Information

Interaction of polymers with DOPC and DOPG membranes monitored by Laurdan generalized polarization (Figure S1) and stoichiometry of GpA association (Figure S2). This material is available free of charge via the Internet at http://pubs.acs.org.

■ AUTHOR INFORMATION

Corresponding Author

*Department of Pharmacy and Biochemistry, Johannes Gutenberg-University Mainz, Johann-Joachim-Becher-Weg 30, 55128 Mainz, Germany. Phone: +49 6131 39-25833. Fax: +49 6131 39-25348. E-mail: dirk.schneider@uni-mainz.de.

Author Contributions

M.S., D.S., and R.Z. designed the research. M.H. and M.A. synthesized polymers and determined CMC and CAG values. M.S. performed all other described experiments. M.S. and D.S. analyzed data. M.S., D.S., and R.Z. wrote the manuscript.

Funding

This work was supported by a grant from the center of complex matter (COMATT) at the University of Mainz.

Notes

The authors declare no competing financial interest.

■ ABBREVATIONS

CAG, critical aggregation concentration; DOPG, 1,2-Dioleoyl-sn-glycero-3-phosphtidylglycerol; p(HPMA), poly[*N*-(2-hydroxypropyl)-methacrylamid]; LMA, lauryl methacrylate; CMC, critical micelle concentration; PC, phosphatidylcholine; **C5**, p(HPMA)-co-p(LMA) copolymer with 5% LMA; **C10**, p(HPMA)-co-p(LMA) copolymer with 10% LMA; **C15**, p(HPMA)-co-p(LMA) copolymer with 15% LMA; **C25**, p(HPMA)-co-p(LMA) copolymer with 25% LMA; TM, transmembrane; GpA, human glycophorin A; FL, fluorescein; TAMRA, 5-6-carboxyrhodamine; TFE, 2,2,2-trifluoroethanol; Laurdan, 6-dodecanoyl-*N*,*N*-dimethyl-2-naphthylamine; 20:1 PC, 1,2-dieicosenoyl-*sn*-glycero-3-phosphocholine; DOPC, 1,2-dioleoyl-*sn*-glycero-3-phosphocholine; Liss Rhod PE, 1,2-dioleoyl-*sn*-glycero-3-phosphoethanolamine-*N*-(lissamine rhodamine B sulfonyl) (ammonium salt); ANTS, 8-aminonaphthalene-1,3,6-trisulfonic acid, disodium salt; DPX, *p*-xylene-bis-pyridinium bromide; DDM, *n*-dodecyl β-D-maltopyranoside; CTA, chain transfer agent; PFPMA, pentafluorophenyl methacrylate; CTP, chain transfer polymer; AIBN, 2,2′-azobis(2-methylpropionitrile); DMSO, dimethyl sulfoxide; PDI, polydispersity index; CD, circular dichroism; FRET, Förster resonance energy transfer; HEPES, 4-(2-hydroxyethyl)-1-piperazineethanesulfonic acid; GP, generalized polarization; LUV, large unilamellar vesicle; ANS, 8-anilino-1-naphthalene-sulfonic acid ammonium salt; NMR, nuclear magnetic resonance.

REFERENCES

(1) Tribet, C., Audebert, R., and Popot, J. L. (1996) Amphipols: Polymers that keep membrane proteins soluble in aqueous solutions. *Proc. Natl. Acad. Sci. U.S.A. 93*, 15047−15050.

(2) Tifrea, D. F., Sun, G., Pal, S., Zardeneta, G., Cocco, M. J., Popot, J. L., and de la Maza, L. M. (2011) Amphipols stabilize the *Chlamydia major* outer membrane protein and enhance its protective ability as a vaccine. *Vaccine 29*, 4623−4631.

(3) Diab, C., Tribet, C., Gohon, Y., Popot, J. L., and Winnik, F. M. (2007) Complexation of integral membrane proteins by phosphorylcholine-based amphipols. *Biochim. Biophys. Acta 1768*, 2737−2747.

(4) Duarte, A. M. S., Wolfs, C. J. A. M., Koehorst, R. B. M., Popot, J. L., and Hemminga, M. A. (2008) Solubilization of V-ATPase transmembrane peptides by amphipol A8-35. *J. Pept. Sci. 14*, 389−393.

(5) Gorzelle, B. M., Hoffman, A. K., Keyes, M. H., Gray, D. N., Ray, D. G., and Sanders, C. R. (2002) Amphipols can support the activity of a membrane enzyme. *J. Am. Chem. Soc. 124*, 11594−11595.

(6) Kyrychenko, A., Rodnin, M. V., Vargas-Uribe, M., Sharma, S. K., Durand, G., Pucci, B., Popot, J. L., and Ladokhin, A. S. (2012) Folding of diphtheria toxin T-domain in the presence of amphipols and fluorinated surfactants: Toward thermodynamic measurements of membrane protein folding. *Biochim. Biophys. Acta 1818*, 1006−1012.

(7) Nagy, J. K., Hoffmann, A. K., Keyes, M. H., Gray, D. N., Oxenoid, K., and Sanders, C. R. (2001) Use of amphipathic polymers to deliver a membrane protein to lipid bilayers. *FEBS Lett. 501*, 115−120.

(8) Pocanschi, C. L., Dahmane, T., Gohon, Y., Rappaport, F., Apell, H. J., Kleinschmidt, J. H., and Popot, J. L. (2006) Amphipathic polymers: Tools to fold integral membrane proteins to their active form. *Biochemistry 45*, 13954−13961.

(9) Pocanschi, C. L., Popot, J. L., and Kleinschmidt, J. H. (2013) Folding and stability of outer membrane protein A (OmpA) from *Escherichia coli* in an amphipathic polymer, amphipol A8-35. *Eur. Biophys. J. 42*, 103−118.

(10) Popot, J. L., Althoff, T., Bagnard, D., Baneres, J. L., Bazzacco, P., Billon-Denis, E., Catoire, L. J., Champeil, P., Charvolin, D., Cocco, M. J., Cremel, G., Dahmane, T., de la Maza, L. M., Ebel, C., Gabel, F., Giusti, F., Gohon, Y., Goormaghtigh, E., Guittet, E., Kleinschmidt, J. H., Kuhlbrandt, W., Le Bon, C., Martinez, K. L., Picard, M., Pucci, B., Sachs, J. N., Tribet, C., van Heijenoort, C., Wien, F., Zito, F., and Zoonens, M. (2011) Amphipols from A to Z. *Annu. Rev. Biophys. 40*, 379−408.

(11) Popot, J. L., Berry, E. A., Charvolin, D., Creuzenet, C., Ebel, C., Engelman, D. M., Flotenmeyer, M., Giusti, F., Gohon, Y., Hong, Q., Lakey, J. H., Leonard, K., Shuman, H. A., Timmins, P., Warschawski, D. E., Zito, F., Zoonens, M., Pucci, B., and Tribet, C. (2003) Amphipols: Polymeric surfactants for membrane biology research. *Cell. Mol. Life Sci. 60*, 1559−1574.

(12) Kopecek, J., Kopeckova, P., Minko, T., and Lu, Z. (2000) HPMA copolymer-anticancer drug conjugates: Design, activity, and mechanism of action. *Eur. J. Pharm. Biopharm. 50*, 61−81.

(13) Ringsdorf, H. (1975) Structure and Properties of Pharmacologically Active Polymers. *J. Polym. Sci., Part C: Polym. Symp.*, 135−153.

(14) Duncan, R. (2006) Polymer conjugates as anticancer nanomedicines. *Nat. Rev. Cancer 6*, 688−701.

(15) Thanou, M., and Duncan, R. (2003) Polymer-protein and polymer-drug conjugates in cancer therapy. *Curr. Opin. Invest. Drugs 4*, 701−709.

(16) Duncan, R. (2003) The dawning era of polymer therapeutics. *Nat. Rev. Drug Discovery 2*, 347−360.

(17) Barz, M., Tarantola, M., Fischer, K., Schmidt, M., Luxenhofer, R., Janshoff, A., Theato, P., and Zentel, R. (2008) From defined reactive diblock copolymers to functional HPMA-based self-assembled nanoaggregates. *Biomacromolecules 9*, 3114−3118.

(18) Hemmelmann, M., Knoth, C., Schmitt, U., Allmeroth, M., Moderegger, D., Barz, M., Koynov, K., Hiemke, C., Rosch, F., and Zentel, R. (2011) HPMA based amphiphilic copolymers mediate central nervous effects of domperidone. *Macromol. Rapid Commun. 32*, 712−717.

(19) Hemmelmann, M., Mohr, K., Fischer, K., Zentel, R., and Schmidt, M. (2013) Interaction of pHPMA-pLMA Copolymers with Human Blood Serum and Its Components. *Mol Pharmaceutics 10*, 3769−3775.

(20) Hemmelmann, M., Kurzbach, D., Koynov, K., Hinderberger, D., and Zentel, R. (2012) Aggregation behavior of amphiphilic p(HPMA)-co-p(LMA) copolymers studied by FCS and EPR spectroscopy. *Biomacromolecules 13*, 4065−4074.

(21) Hemmelmann, M., Metz, V. V., Koynov, K., Blank, K., Postina, R., and Zentel, R. (2012) Amphiphilic HPMA-LMA copolymers increase the transport of Rhodamine 123 across a BBB model without harming its barrier integrity. *J. Controlled Release 163*, 170−177.

(22) Fisher, L. E., Engelman, D. M., and Sturgis, J. N. (2003) Effect of detergents on the association of the glycophorin a transmembrane helix. *Biophys. J. 85*, 3097−3105.

(23) Anbazhagan, V., Cymer, F., and Schneider, D. (2010) Unfolding a transmembrane helix dimer: A FRET study in mixed micelles. *Arch. Biochem. Biophys. 495*, 159−164.

(24) Chytil, P., Etrych, T., Konak, C., Sirova, M., Mrkvan, T., Boucek, J., Rihova, B., and Ulbrich, K. (2008) New HPMA copolymer-based drug carriers with covalently bound hydrophobic substituents for solid tumour targeting. *J. Controlled Release 127*, 121−130.

(25) Moad, G., Rizzardo, E., and Thang, S. H. (2005) Living radical polymerization by the RAFT process. *Aust. J. Chem. 58*, 379−410.

(26) Eberhardt, M., Mruk, R., Zentel, R., and Theato, P. (2005) Synthesis of pentafluorophenyl(meth)acrylate polymers: New precursor polymers for the synthesis of multifunctional materials. *Eur. Polym. J. 41*, 1569−1575.

(27) Eberhardt, M., and Theato, P. (2005) RAFT polymerization of pentafluorophenyl methacrylate: Preparation of reactive linear diblock copolymer. *Macromol. Rapid Commun. 26*, 1488−1493.

(28) Barz, M., Luxenhofer, R., Zentel, R., and Kabanov, A. V. (2009) The uptake of N-(2-hydroxypropyl)-methacrylamide based homo, random and block copolymers by human multi-drug resistant breast adenocarcinoma cells. *Biomaterials 30*, 5682−5690.

(29) Whitmore, L., and Wallace, B. A. (2004) DICHROWEB, an online server for protein secondary structure analyses from circular dichroism spectroscopic data. *Nucleic Acids Res. 32*, W668−W673.

(30) Whitmore, L., and Wallace, B. A. (2008) Protein secondary structure analyses from circular dichroism spectroscopy: Methods and reference databases. *Biopolymers 89*, 392−400.

(31) Zschornig, O., Paasche, G., Thieme, C., Korb, N., and Arnold, K. (2005) Modulation of lysozyme charge influences interaction with phospholipid vesicles. *Colloids Surf., B 42*, 69−78.

(32) Hawe, A., Sutter, M., and Jiskoot, W. (2008) Extrinsic fluorescent dyes as tools for protein characterization. *Pharm. Res. 25*, 1487−1499.

(33) Palladino, P., Rossi, F., and Ragone, R. (2009) Effective critical micellar concentration of a zwitterionic detergent: A fluorimetric study on n-dodecyl phosphocholine. *J. Fluoresc. 20*, 191−196.

(34) Schonbrunn, E., Eschenburg, S., Luger, K., Kabsch, W., and Amrhein, N. (2000) Structural basis for the interaction of the fluorescence probe 8-anilino-1-naphthalene sulfonate (ANS) with the antibiotic target MurA. *Proc. Natl. Acad. Sci. U.S.A. 97*, 6345−6349.

(35) Wu, P., and Brand, L. (1994) Resonance energy transfer: Methods and applications. *Anal. Biochem. 218*, 1−13.

(36) Anbazhagan, V., and Schneider, D. (2010) The membrane environment modulates self-association of the human GpA TM domain: Implications for membrane protein folding and transmembrane signaling. *Biochim. Biophys. Acta 1798*, 1899−1907.

(37) Fisher, L. E., Engelman, D. M., and Sturgis, J. N. (1999) Detergents modulate dimerization, but not helicity, of the glycophorin A transmembrane domain. *J. Mol. Biol. 293*, 639−651.

(38) Lemmon, M. A., Flanagan, J. M., Hunt, J. F., Adair, B. D., Bormann, B. J., Dempsey, C. E., and Engelman, D. M. (1992) Glycophorin A dimerization is driven by specific interactions between transmembrane α-helices. *J. Biol. Chem. 267*, 7683−7689.

(39) Song, J., Carson, J. H., Barbarese, E., Li, F. Y., and Duncan, I. D. (2003) RNA transport in oligodendrocytes from the taiep mutant rat. *Mol. Cell. Neurosci. 24*, 926−938.

(40) Stangl, M., Veerappan, A., Kroeger, A., Vogel, P., and Schneider, D. (2012) Detergent properties influence the stability of the glycophorin a transmembrane helix dimer in lysophosphatidylcholine micelles. *Biophys. J. 103*, 2455−2464.

(41) Adair, B. D., and Engelman, D. M. (1994) Glycophorin A helical transmembrane domains dimerize in phospholipid bilayers: A resonance energy transfer study. *Biochemistry 33*, 5539−5544.

(42) Bazzacco, P., Billon-Denis, E., Sharma, K. S., Catoire, L. J., Mary, S., Le Bon, C., Point, E., Baneres, J. L., Durand, G., Zito, F., Pucci, B., and Popot, J. L. (2012) Nonionic homopolymeric amphipols: Application to membrane protein folding, cell-free synthesis, and solution nuclear magnetic resonance. *Biochemistry 51*, 1416−1430.

(43) Popot, J. L. (2010) Amphipols, nanodiscs, and fluorinated surfactants: Three nonconventional approaches to studying membrane proteins in aqueous solutions. *Annu. Rev. Biochem. 79*, 737−775.

(44) Breyton, C., Pucci, B., and Popot, J. L. (2010) Amphipols and fluorinated surfactants: Two alternatives to detergents for studying membrane proteins in vitro. *Methods Mol. Biol. 601*, 219−245.

(45) Picard, M., Dahmane, T., Garrigos, M., Gauron, C., Giusti, F., le Maire, M., Popot, J. L., and Champeil, P. (2006) Protective and inhibitory effects of various types of amphipols on the Ca^{2+}-ATPase from sarcoplasmic reticulum: A comparative study. *Biochemistry 45*, 1861−1869.

(46) Champeil, P., Menguy, T., Tribet, C., Popot, J. L., and le Maire, M. (2000) Interaction of amphipols with sarcoplasmic reticulum Ca^{2+}-ATPase. *J. Biol. Chem. 275*, 18623−18637.

(47) Tribet, C., Audebert, R., and Popot, J. L. (1997) Stabilization of hydrophobic colloidal dispersions in water with amphiphilic polymers: Application to integral membrane proteins. *Langmuir 13*, 5570−5576.

(48) Allmeroth, M., Moderegger, D., Gundel, D., Koynov, K., Buchholz, H. G., Mohr, K., Rosch, F., Zentel, R., and Thews, O. (2013) HPMA-LMA Copolymer Drug Carriers in Oncology: An in Vivo PET Study to Assess the Tumor Line-Specific Polymer Uptake and Body Distribution. *Biomacromolecules 14*, 3091−3101.

Biochimica et Biophysica Acta xxx (2015) xxx–xxx

Contents lists available at ScienceDirect

Biochimica et Biophysica Acta

journal homepage: www.elsevier.com/locate/bbamem

Review

Functional competition within a membrane: Lipid recognition *vs.* transmembrane helix oligomerization ☆

Michael Stangl, Dirk Schneider *

Department of Pharmacy and Biochemistry, Johannes-Gutenberg-University Mainz, Johann-Joachim-Becher-Weg 30, 55128 Mainz, Germany

ARTICLE INFO

Article history:
Received 7 January 2015
Received in revised form 9 March 2015
Accepted 9 March 2015
Available online xxxx

Keywords:
Membrane protein
Lipid binding
Oligomerization
p24
C99
Syntaxin 1A

ABSTRACT

Binding of specific lipids to large, polytopic membrane proteins is well described, and it is clear that such lipids are crucial for protein stability and activity. In contrast, binding of defined lipid species to individual transmembrane helices and regulation of transmembrane helix monomer–oligomer equilibria by binding of distinct lipids is a concept, which has emerged only lately. Lipids bind to single-span membrane proteins, both in the juxta-membrane region as well as in the hydrophobic membrane core. While some interactions counteract transmembrane helix oligomerization, in other cases lipid binding appears to enhance oligomerization. As reversible oligomerization is involved in activation of many membrane proteins, binding of defined lipids to single-span transmembrane proteins might be a mechanism to regulate and/or fine-tune the protein activity. But how could lipid binding trigger the activity of a protein? How can binding of a single lipid molecule to a transmembrane helix affect the structure of a transmembrane helix oligomer, and consequently its signaling state? These questions are discussed in the present article based on recent results obtained with simple, single-span transmembrane proteins. This article is part of a Special Issue entitled: Lipid–protein interactions.

Contents

1. Dimerization of TM helices regulates cellular functions

Folding of large, polytopic transmembrane (TM) proteins involves interactions of multiple TM helices, and thus individual TM helix–helix interactions can affect or even dictate the assembly of large protein complexes [1–4]. In fact, altered interaction propensities of individual TM helices might be linked to various diseases, due to destabilization or misfolding of polytopic TM proteins [4–6]. However, almost half of the whole human TM proteome consists of single-span TM proteins [7,8]. Single-spanning membrane proteins (MPs) mediate a wide range of cellular processes, including cell–cell adhesion (integrins) [9,10], immune recognition (major histocompatibility complex, MHC) [11] and signal transduction (*e.g.*, receptor

Abbreviations: TM, transmembrane; MP, membrane protein; GpA, glycophorin A; PIP, phosphatidylinositol phosphate; PI, phosphatidylinositide; RTK, receptor tyrosine kinase; MHC, major histocompatibility complex; PG, phosphatidyl glycerol; PS, phosphatidyl serine; PLC, phospholipase C; PH, pleckstrin homology; NMR, nuclear magnetic resonance; COP, coat protein complex; APP, amyloid precursor protein; ErbB, epidermal growth factor receptor; CRAC, cholesterol recognition amino acid consensus; CARC, inversed cholesterol recognition amino acid consensus; Kir, inwardly rectifying potassium channel; ER, endoplasmic reticulum; GOLD, Golgi dynamic; HIV, human immunodeficiency virus; SBD, sphingolipid-binding domain; SM, sphingomyelin; GPCR, G-protein coupled receptor; SNARE, soluble *N-ethylmaleimide sensitive factor* attachment protein receptor; CCM, cholesterol consensus motif

☆ This article is part of a Special Issue entitled: Lipid–protein interactions.

* Corresponding author. Tel.: +49 6131 39 25833; fax: +49 6131 39 25348.
E-mail address: Dirk.Schneider@uni-mainz.de (D. Schneider).

http://dx.doi.org/10.1016/j.bbamem.2015.03.011
0005-2736/© 2015 Published by Elsevier B.V.

tyrosine kinases, RTKs) [12], and contacts between individual bitopic MPs are common [13,14]. Importantly, the TM helices that anchor MPs in the membrane are often critically involved in oligomerization of the full-length MPs. While strongly associating single-span TM helices are thought to form stable membrane-inserted protein–protein complexes, modestly strong interacting TM helices exist in a dynamic equilibrium of the free monomers and the associated oligomers. Reversible oligomerization of individual TM helices can trigger and regulate signaling processes at and across cellular membranes. *E.g.,* while dimerization of the various integrin α- and β-subunits is not completely understood, the respective TM domains are most likely crucially involved in integrin dimerization, and it has been shown that integrin TM domain interactions trigger integrin functions [15–19]. The immune active MHC class II complex is formed by an α/β-heterodimer and invariant chain proteins. Recent results also indicate that here TM helix–helix contacts are crucial for formation of the MHC II complex [20]. RTKs form dimers or even higher-ordered multimeric complexes, and a plethora of data has demonstrated in recent years that dimerization and activation of RTK-family members are mediated by the single TM helix [21–26]. In line with this, the isolated single-span TM domains of all human RTKs have been shown to have an intrinsic propensity to interact, and thus oligomerization of RTK TM helices appears to be common [27]. In the case of ErbB (HER) proteins, probably the best characterized RTK family members, defined adjustments of the TM helix dimer structure appear to be involved in signaling [21,28]. A recent analysis of the human single-span TM proteome has revealed that the isolated TM helices of many single-span TM proteins have an intrinsic propensity to form higher ordered oligomeric structures [14], and thus oligomerization of single-span TM proteins appears to be the rule rather than the exception.

Molecular forces driving interactions of single- and multi-span TM proteins within the membrane include Van der Waals interactions, resulting from close packing of interacting helices, hydrogen bonding, as well as ionic and aromatic interactions [5,29–31]. That formation of tightly packed, homo-oligomeric helix bundles driven by sequence-specific interaction of TM helices was demonstrated more than 25 years ago for the TM domain of the human glycophorin A (GpA) protein [32], a membrane integral protein located in the red blood cell plasma membrane. Later, seven amino acids of the LIxxGVxxGVxxT-motif were identified in a mutational study to be involved in dimerization [33–35]. The GxxxG-core of the GpA interaction motif turned out to be highly overrepresented in TM proteins and still represents the most significant motif in interacting TM helices identified thus far [36,37]. Besides this, several motifs mediating oligomerization of TM domains have been identified, including Ser and/or Thr-containing motifs [38,39], motifs containing aromatic residues [40,41] or residues with carboxamide side chains [42–47], as well as the QxxS-motif [48,49]. More than one dozen high-resolution structures of simple TM helix oligomers have been published in recent years, revealing defined helix–helix contact interfaces. However, often no defined interaction motifs have been identified, and two TM helices interact by forming complementary surfaces, which allow close helix packing, as summarized recently in Cymer et al. [30]. However, since reversible interactions of TM helices might be involved in inhibition or activation of the full-length proteins, TM helix oligomerization has to be regulated to avoid constitutive activation or inhibition of the proteins. Formation and stability of TM helix bundles are not only defined by the specific amino acid context, but also by the composition of the intimate lipid environment, as well as by the overall physico-chemical properties of the membrane. MPs communicate with the lipid environment and thereby the association and activity of MPs might be manipulated and/or triggered.

2. Lipids interact with membrane proteins

Eukaryotic membranes are composed of diverse phospholipids with different head groups and acyl chain lengths as well as cholesterol [50]. It is not finally resolved yet why membrane lipids have different acyl chain lengths. Possibly, it is important for grouping proteins and lipids with similar hydrophobic thicknesses, as hydrophobic regions of TM domains also differ in their length in membrane proteins. In fact, based on the OMP database [51], the hydrophobic thickness of dimeric single-span human TM proteins found in the human plasma membrane varies between 30 and 36 Å, which strongly indicates that the thickness of the lipid bilayer locally adjusts to completely mask the hydrophobic region. Hydrophobic mismatch conditions can result in protein aggregation within lipid bilayer environments [52–56].

Besides the hydrophobic thickness of the membrane, the lateral pressure profile within the acyl chain region as well as the distribution of lipid head group charges at a protein–lipid interface control interactions of MPs with lipids [30,57–59]. In general, lipid binding to a MP can be stabilized by electrostatic and hydrophobic interactions between the lipid head groups and amino acid residues and additionally by a large number of hydrophobic interactions between the hydrophobic lipid tails and TM moieties of the protein (Fig. 1).

Based on the residence time of a particular lipid at the lipid–MP interface, three types of interactions of lipids with MPs might be distinguished (Fig. 2) [60]. Lipids, which diffuse rapidly within the bilayer plane and show a low residence time at the protein–lipid interface, so-called bulk lipids, do not directly affect the structure and/or function of MPs. The bulk lipid phase represents the total lipid volume of the membrane and determines its global characteristics, such as the membrane fluidity, the lateral pressure, the bilayer thickness or the membrane surface charge. When the polar lipid head group interacts with a MP or when hydrophobic matching between the lipids and the TM domain of the MP is crucial, the residence time of the lipids might significantly increase and a shell of annular lipids is formed around the MP. The composition of this annular lipid shell is determined by the local architecture of the protein. In the annular lipid shell, which is composed of around 50–100 lipids and which is not necessarily homogeneous [61], the specific characteristics of the lipids can strongly affect the structure and function of a MP [62,63].

If the interaction of lipids and MPs is even stronger, the so-called non-annular surface lipids will bind specifically and tightly to MPs, typically in cavities and clefts of hydrophobic binding pockets [64]. Non-annular lipids often remain bound to MPs, even if the MPs were purified and crystallized in detergent [65,66]. Especially in larger protein complexes, non-annular lipids fill the crevices between adjacent monomers or subunits and thereby mediate protein complex formation. These lipids seem to play an important role in the structural stability of MPs, and tightly bound lipids can be essential for the activity of MPs [67].

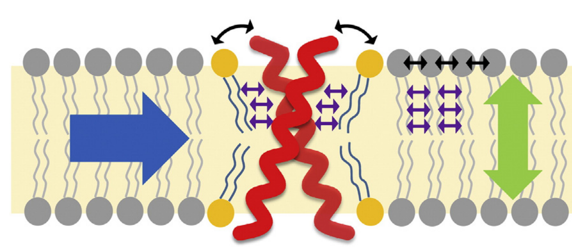

Fig. 1. How the lipid environment can affect transmembrane protein structures. Non-annular lipids (orange) bind specifically at the surface of TM proteins *via* salt bridges between charged lipid head groups and charged residues at the membrane water interface (black arrows). Hydrophobic, Van der Waals and weak dipolar interactions might additionally be involved in lipid binding. Van der Waals interactions between the acyl chain and hydrophobic amino acids further contribute to tight lipid binding (purple arrows). Annular lipids define the global membrane environment of TM proteins and affect membrane protein folding *via* membrane properties, such as the hydrophobic thickness (green arrow) and the lateral membrane pressure profile (blue arrow). The geometry of the lipids (bilayer-forming *vs.* non-bilayer-forming) as well as electrostatic interactions between the lipid head groups (black arrows) and packing of the lipid acyl chains determine the global membrane properties.

Please cite this article as: M. Stangl, D. Schneider, Functional competition within a membrane: Lipid recognition *vs.* transmembrane helix oligomerization, Biochim. Biophys. Acta (2015), http://dx.doi.org/10.1016/j.bbamem.2015.03.011

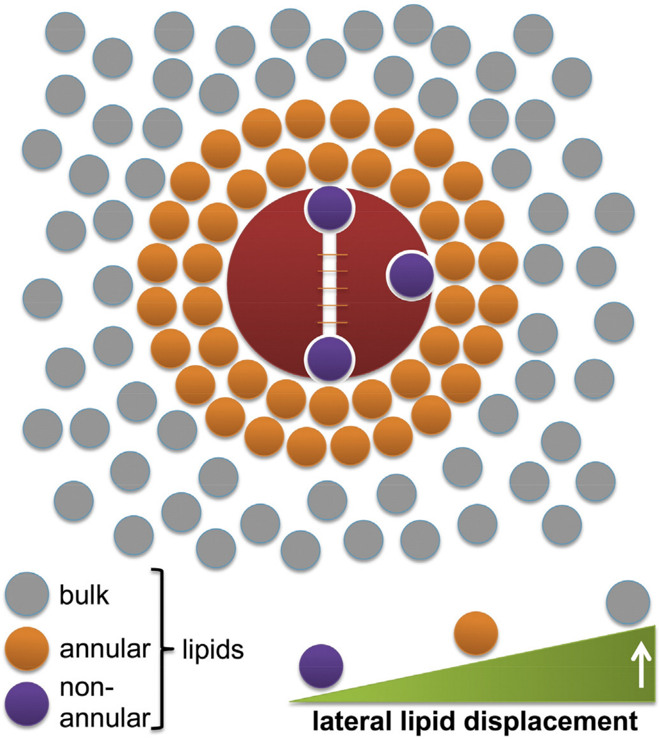

Fig. 2. Intramembrane protein–lipid interactions — a top view on the membrane. A membrane protein dimer stabilized by tightly bound non-annular lipids. Non-annular lipids fit into cavities at the protein surface, and these lipids are often found to be still bound in isolated proteins. A belt of annular lipids define the intimate environment of a membrane protein. While the structure and size of this lipid belt varies, it was suggested that a protein is typically surrounded by 50–100 annular lipids [61]. Annular lipids have higher exchange rates at the membrane protein than non-annular lipids, but the diffusion rate of the annular lipids is significantly reduced compared to the bulk lipid phase. Lipids with low degree of interaction with the TM protein are considered to be "bulk" lipids, which have high lateral displacement and diffusion rates.

This is *e.g.*, observed in the case of the KscA potassium channel, which is only active when negatively charged lipids are bound [68–70], and ADP/ATP carriers require binding of cardiolipins (compare Fig. 3) for activity [71,72]. More examples and detailed information on how non-annular lipids affect MPs' activities can be found in Lee et al. [62].

Cholesterol binding to MPs has been studied to a great extent in recent years. A cholesterol-binding motif was initially identified in the peripheral-type benzodiazepine receptor [73] (Table 1). The CRAC (*C*holesterol *R*ecognition *A*mino acid *C*onsensus) motif (L/V-$(x)_{1-5}$-Y-
Q5 Q4 $(x)_{1-5}$-R/K), where x represents an arbitrary amino acid, consists of hydrophobic, aromatic and positively charged amino acids. Later, the reversed motif (CARC-motif, K/R-$(x)_{1-5}$-Y-$(x)_{1-5}$-(L/V)) (Table 1) was postulated to be important for cholesterol binding [74]. In general, binding of cholesterol appears to require the presence of a polar amino acid that is able to hydrogen bond to the 3β-OH group of cholesterol (compare Fig. 3), as well as small hydrophobic as well as aromatic amino acids that are involved in hydrophobic and π–π stacking interactions at the lipid–protein interface [75]. However, the interaction of CRAC and CARC motifs with cholesterol remains unclear, and the currently available MP X-ray structures do not indicate that any distinct amino acid motif mediates cholesterol binding to MPs [67]. Furthermore, the CRAC motif has been identified more than 5000 times in the proteome (2100 proteins) of a cholesterol-free bacterium [76], and thus the prediction value of cholesterol-binding sites, using these motifs, appears to be very low. Furthermore, cholesterol, one of the best studied lipids in biochemical and medical research, has a dramatically different structure than typical bilayer-forming di-acyl phospholipids (Fig. 3). Thus, cholesterol binding might be rather specific.

2.1. Binding to negatively charged lipid head groups can control TM peptide oligomerization and clustering

The impact of global bilayer properties on the oligomerization of TM helices has already been analyzed to some extent, and single-span TM helices frequently serve as manageable models to reveal the impact of the lipid bilayer on a MP structure. While binding of specific non-annular lipids to polytopic TM proteins has been identified and analyzed to some degree in the past, recent work has also identified lipid-recognition by single-span TM helices, and lipid binding appears to severely affect protein folding as well as the cellular functions of the proteins (as further discussed below).

The GpA TM helix dimer has for a long time served as a paradigm in studies, aiming at identifying sequence determinants in a TM helix–helix interaction. Several recent *in vitro* studies have shown that the detergent environment can severely affect TM helix dimerization propensities of GpA and other dimerizing TM helices [77–85]. Global lipid bilayer properties, such as the order of the lipid acyl chains or the membrane thickness, also affect the structure of the GpA TM helix in membranes [86–88]. Furthermore, in model membrane systems, the anionic lipids phosphatidylglycerol (PG) and phosphatidylserine (PS) (compare Fig. 3) severely destabilize the GpA TM helix dimer [89]. The negatively charged lipid head groups appear to specifically bind at the juxtamembrane region to a stretch of basic amino acids, which follow the C-terminus of the GpA TM helix [89]. Binding of the negatively charged lipids destabilized the GpA helix dimer, although it is currently unclear how the TM helix dimer structure is weakened. How is the signal "bound lipid" transferred from the juxtamembrane region to the TM helix–helix interface, resulting in TM helix dimer destabilization? Is this deleterious effect merely based on the negative net charges of the lipids but not on the acyl chains? And if solely the negative charge matters, how do even more negatively charged lipids, such as phosphatidylinositol phosphates, affect the structure of oligomeric single-span MPs after binding?

Phosphatidylinositol 4,5-bisphosphate (PIP_2) is the most abundant PI in mammalian plasma membranes, with about 1% of the total lipid located in the inner leaflet of the membrane [90,91]. PIPs are lipids with an inositol head group conjugated with three phosphate groups (Fig. 3). The phosphate at the first carbon atom is esterified with glycerol that carries two fatty acid residues. PIP_2 with its two phosphate groups at carbon atoms four and five is *e.g.*, a substrate of phospholipase C (PLC), controlling downstream signaling cascades [92,93]. Furthermore, PIP_2, as well as its phosphorylated form PIP_3, can also directly act as a docking lipid for enzymes, thereby recruiting proteins to the plasma membrane [91,94]. PIP_2 electrostatically interacts *via* its negatively charged phosphate groups with non-contiguous basic residue-rich clusters at proteins [91,95]. PIP phosphates at positions four and five form several hydrogen bonds with residues in the PLC pleckstrin homology (PH) domain, and especially electrostatic interactions with two lysine residues fasten the protein at the membrane surface [96,97]. However, >250 other identified PH domains only weakly interact with inositides, rendering lipid binding exclusively to the PLC PH domain unlikely. Besides the PH domain, other PIP_2 binding domains exist in soluble proteins, as discussed in greater detail in recent reviews [91,95,98]. However, are PIP_2 binding domains also present in integral MPs? In fact, the K^+ channel Kir2.1 requires binding of multiple PIP_2-molecules for channel activity. Here, PIP_2 electrostatically interacts with three independent sites at the channels' C-terminus, thereby stabilizing an active channel conformation [99]. While the TM domain appears to bind any diacylglycerol with a 1′ phosphate, the juxtamembrane region specifically interacts only with the PIP_2 head group and thereby defines the lipid-binding specificity. Importantly, while PIP_2-binding does not change the tetrameric assembly of the related Kir2.2 channel, lipid binding induces a conformational change in a flexible linker region, which results in reorganization of the entire channel structure and finally in channel activation [100].

Please cite this article as: M. Stangl, D. Schneider, Functional competition within a membrane: Lipid recognition *vs.* transmembrane helix oligomerization, Biochim. Biophys. Acta (2015), http://dx.doi.org/10.1016/j.bbamem.2015.03.011

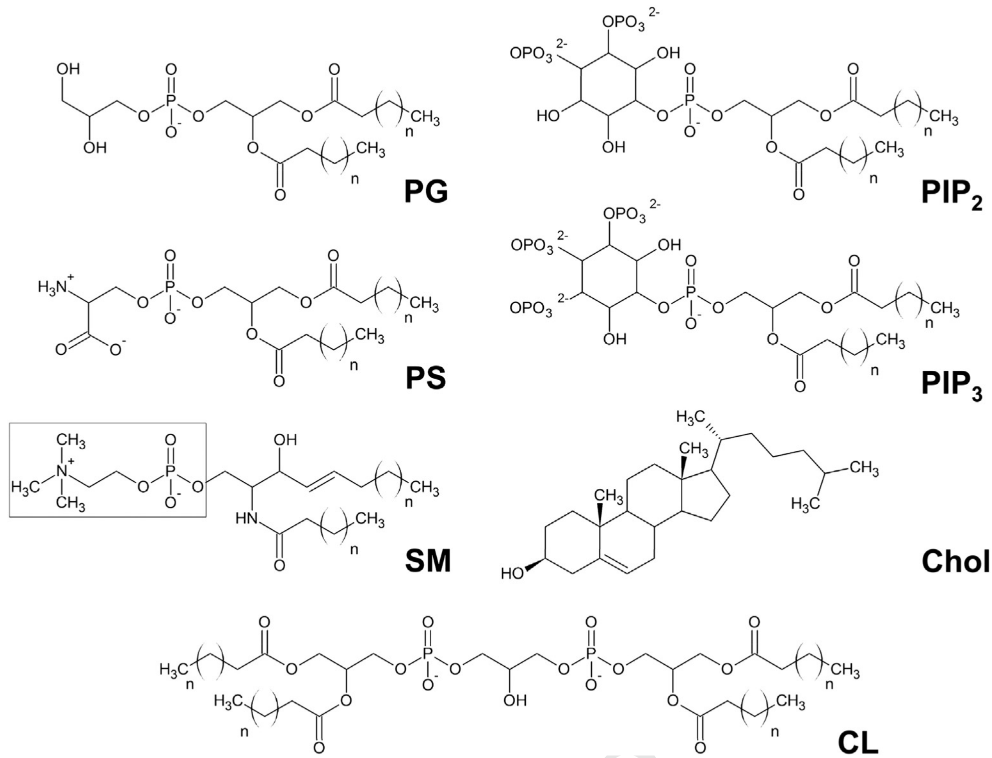

Fig. 3. Chemical structures of lipids. Depicted are the lipid species discussed in this article. PG: phosphatidylglycerol, PS: phosphatidylserine, SM: sphingomyelin, PIP$_2$: phosphatidylinositol-4,5-bisphosphate, PIP$_3$: phosphatidylinositol-3,4,5-trisphosphate, Chol: cholesterol, CL: cardiolipin. Typical n-values of the discussed phospholipids vary between 12 and 18. In the case of the SM C18:0 sphingomyelin species discussed in the text, the fatty acid chain carries 18 carbon atoms. Not shown is ceramide, which is SM without the phosphocholine head group (boxed).

PIP$_2$ might form clusters in eukaryotic plasma membranes, and several studies showed a co-localization of syntaxin 1A with such PIP$_2$ clusters, indicating that PIP$_2$ is required for syntaxin clustering [101–103]. The membrane target SNARE (tSNARE) syntaxin 1A is composed of an N-terminal three-helix bundle H$_{abc}$, an amphipathic helix H$_3$ that interacts with other SNARE proteins to form a fusion complex (or the H$_{abc}$ domain), and a C-terminal TM domain [104–107]. Interaction of PIP$_2$ with the single TM helix of syntaxin 1A leads to sequestration of the protein and the lipid [102]. Even though it is much less abundant than PIP$_2$ in cellular membranes, PIP$_3$ is also important for syntaxin 1A clustering and the function of the SNAP–SNARE complex [94]. The interaction of syntaxin 1A with PIP lipids is mediated by a stretch of basic amino acids. The critical residues are directly adjacent to the TM helix and are in contact with the lipid head groups [108, 109]. The positive residues of the ^{260}KARRKK^{265} amino acid motif interact with PIP$_2$ (Fig. 4), and a strong reduction of the lipid–protein interaction was observed when Lys^{264} and/or Lys^{265} were mutated to Ala [102]. Mutation of the wt syntaxin 1A sequence also led to reduced vesicle fusion in cells, which additionally demonstrates the *in vivo* importance of the basic amino acids and of PIP binding [110]. PIP$_3$ binds even more efficiently to syntaxin 1A and can replace PIP$_2$ at the interaction site, also mediated by electrostatic interactions with the above-mentioned stretch of positively charged amino acids [94]. Recently, PIP$_3$ has been identified as an inducer of syntaxin 1A clustering in cellular membranes [94], and the concomitant mutation of Lys^{264} and Lys^{265} abolished PIP$_3$-syntaxin 1A clustering. These data indicate that mainly electrostatic interactions stabilize the binding of PIPs to syntaxin 1A, due to the strong negative net charge of the lipid head groups. As also observed in the case of the Kir2 K$^+$ channels, no further structural prerequisites for PIP binding to syntaxin 1A are described yet. Additionally, as PS, with its one net negative charge, does not induce syntaxin 1A clustering, even in the presence of 20% PS [94], not only the negative head group charge but also the chemistry of the lipid head group might matter. Furthermore, the entropy cost for binding two or three lipids *via* electrostatic interactions is much higher than binding a single lipid with multiple charges, so that binding of PIP$_3$, with its four negative charges, might be preferred over PIP$_2$ or PS. PIPs mediate syntaxin 1A clustering, and additionally

Table 1
Lipid binding motifs identified in membrane integrated proteins.

Motif	Bound lipid	aa sequence	First identified	Ref.
CRAC	Cholesterol	L/V-x$_{1-5}$-Y-x$_{1-5}$-K/R	P-type benzodiazepine receptor	[73,185]
CARC	Cholesterol	K/R-x$_{1-5}$-Y/F-x$_{1-5}$-L/V	Nicotinic acetylcholine receptor	[74,185]
CCM	Cholesterol	Formed by helices 1–4[a] [4.39–4.43 (R,K)]–[4.50 (W,Y)]–[4.46 (I,V,L)]–[2.41 (F,Y)]	β_2-adrenergic receptor	[185,186]
Tilted peptides	Cholesterol	ExxxxNxGxxxGxxxGG	C99	[146,185,187]
SBD	Glycosphingolipid	Loop: aromatic AAs + basic AA in proximity	HIV gp120, APP	[128,188]
	Sphingomyelin C18:0	VxxTLxxIY	p24	[123,130]
PIP binding motif	Phosphatidylinositol-phosphates	KARRKK	Syntaxin 1A	[94,102,189]

For further information and examples see reviews [64,190].
[a] Numbering based on the Ballesteros–Weinstein. x = apolar aa-residue.

Please cite this article as: M. Stangl, D. Schneider, Functional competition within a membrane: Lipid recognition *vs.* transmembrane helix oligomerization, Biochim. Biophys. Acta (2015), http://dx.doi.org/10.1016/j.bbamem.2015.03.011

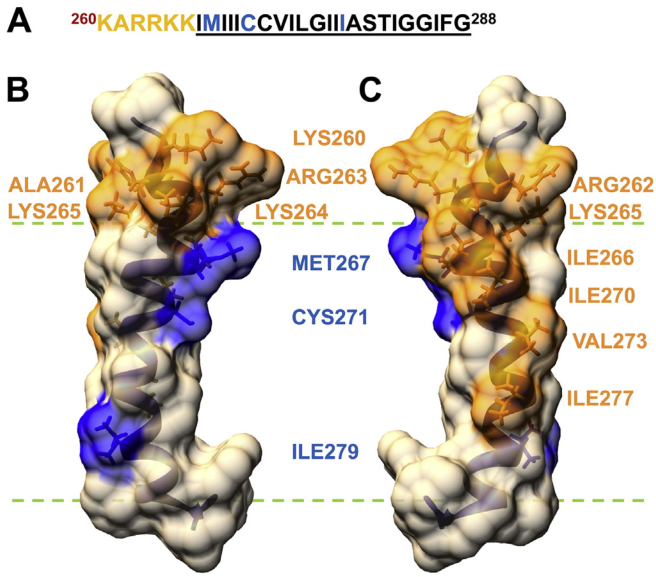

Fig. 4. The syntaxin 1A transmembrane helix. (A) Amino acid sequence of the syntaxin 1A transmembrane region. The TM domain is underlined. (B) Surface structure of the syntaxin 1A transmembrane helix. (C) Rotated syntaxin structure (~180°). (B, C): PDB ID: 2M8R. Residues involved in lipid (PIP) binding are highlighted in orange, whereas residues triggering dimerization of the TM helices are depicted in blue.

the syntaxin TM domain homodimerizes [111,112]. Critical residues mediating homodimerization of syntaxin and heterodimerization with its natural interaction partner synaptobrevin II are Met^{267}, Cys^{271} and Ile^{279} [112] (Fig. 4). Looking at the NMR structure of syntaxin 1A, the β-branched Ile residues 266, 270, 277 (possibly also Val^{273}) form a smooth and very hydrophobic surface at one side of the syntaxin 1A TM helix (Fig. 4). These residues are most likely not involved in dimerization of syntaxin 1A, and thus they might additionally stabilize PIP_2 binding *via* hydrophobic interactions between the lipid acyl chains and the hydrophobic TM surface. However, such an assumption has to be tested in future experiments.

2.2. Sphingomyelin binding to the transmembrane helix triggers oligomerization of the COP I machinery protein p24

Formation of COP I and COP II complexes is a crucial step in the transport of proteins between the endoplasmic reticulum (ER) and the Golgi apparatus in eukaryotic cells. COP I is involved in the anterograde vesicle transport from the ER to the Golgi, whereas COP II vesicles are involved in the retrograde transport from the Golgi to the ER [113,114]. For traveling between these compartments, both pathways depend on immobilization of coat complexes at the vesicular surface. Coat complex formation at the vesicle surface is mastered by a type-I TM protein with a mass of ~24 kDa, hence the name p24. Potential roles for p24 proteins in cargo reception and coat recruitment are discussed in Strating et al. [115]. The p24 protein family can be subdivided into four subfamilies (α, β, γ, δ) [116]. However, the bewildering variety of names of several members of the p24 family makes it difficult to identify the protein of interest [115]. The p24 protein we discuss here is the protein $p24\beta_1$, or TMED2, or p24 or p24a and will further just be called p24.

All p24 proteins share a similar structural arrangement. A large globular N-terminal GOLD (Golgi dynamic) domain [117] is located at the luminal side of the membrane. The exact function of this domain is enigmatic but it co-occurs with lipid-, sterol- or fatty acid-binding domains, such as PH, Sec14p, FYVE and RUN [117]. The GOLD domain is followed by an undefined coiled-coil region, a TM α-helix and a short C-terminal cytoplasmic tail, which is involved in COP I and COP II coat complex binding [115,118]. p24 proteins are known to form homo- and heterodimers, depending on their localization [119]. An involvement of the coiled-coil [120] and the cytoplasmic region in p24 dimerization is discussed [121,122], albeit recent results suggest that TM helix–helix interactions mediate dimerization of p24, triggered by binding of a sphingolipid [123].

Sphingolipid-binding motifs were initially identified in HIV-1 virus and amyloid proteins (Table 1) [124–127]. The identified motif is part of a hairpin structure of the gp120 protein at the surface of HIV-1 and Alzheimer-β-amyloid peptides. The aromatic residues Tyr, Trp and Phe are part of the sphingolipid-binding domain (SBD) and the glycosphingolipids are mainly bound *via* π-stacking and electrostatic interactions with the sugar head groups. These interactions are accompanied by structural rearrangements of both binding partners [128]. The interaction motif, which has also been identified in the serotonin receptor family and can be predicted in several other MPs [128,129], binds glycosylated sphingolipid species restrictively.

p24 selectively binds a single sphingomyelin (SM) species, SM C18:0, but not ceramide (lacking choline head group) or phosphocholine analogs (Fig. 3) [123]. Further analyses revealed a remarkable preference of p24 to bind C18:0 SM, and shorter and longer chain length SMs appear to not interact with the p24 TM domain [123]. Thus, p24 preferentially binds sphingomyelins and both the head group, as well as the hydrophobic acyl chain regions of the lipids are important. As the head group of phosphatidylcholine and SM is identical, the hydrophobic acyl chain region is supposed to determine the specific binding of SM derivatives to the p24 TM helix. To identify amino acids involved in lipid binding, each residue of the p24 TM domain was mutated to Ala and SM binding was analyzed. Based on this analysis, a VxxTLxxIY amino acid motif in the TM helix determines SM binding to p24 (Table 1). Molecular modeling has indicated that SM C18:0 fits perfectly into a cavity formed by the residues Val^{13}, Thr^{16} and Leu^{17} (Fig. 5) [123]. Mutation of a single residue in this cavity to an amino acid with a bulky side chain in fact completely abolished SM binding [123]. However, it was suggested that the lipid head group too is important for binding since the structurally similar ceramide did not interact with p24. Unfortunately, the described binding motif only covers the TM helix. It is very likely that electrostatic interactions between the protein and the sphingolipid head group also play a role in lipid binding, as *e.g.*, described above concerning syntaxin 1A. In the case of p24, only a few amino acids are available for interactions, as the C-terminus, attached to the sphingolipid-binding site, is very short

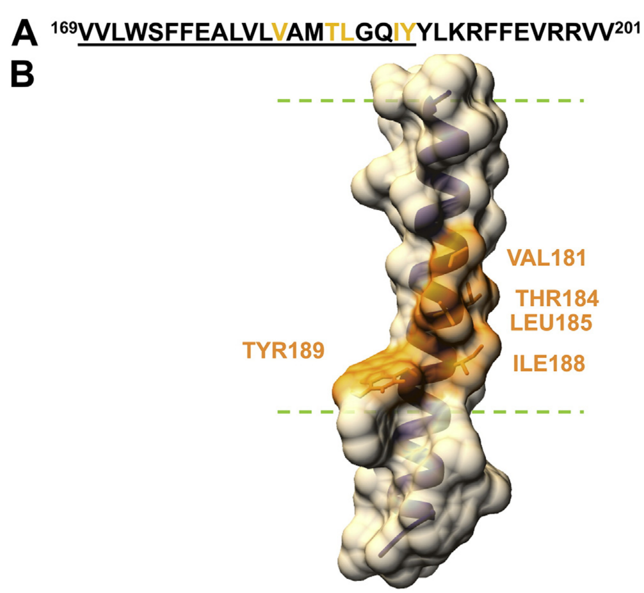

Fig. 5. The p24 transmembrane helix. (A) Amino acid sequence of the p24 transmembrane region. The TM domain is underlined. (B) Structure of the p24 transmembrane helix. The structure was modeled using the PEP-FOLD Peptide Structure Prediction Server [191–193]. Residues involved in lipid (SM18:0) binding are highlighted in orange.

Please cite this article as: M. Stangl, D. Schneider, Functional competition within a membrane: Lipid recognition *vs.* transmembrane helix oligomerization, Biochim. Biophys. Acta (2015), http://dx.doi.org/10.1016/j.bbamem.2015.03.011

and also involved in COP vesicle contacts. It is worth mentioning that sphingolipids also bind to G-protein-coupled receptors (GPCRs), mediated by an amino acid motif, similar to the p24 sphingolipid-binding motif, and sphingolipid binding to a single TM helix of the receptor might stabilize different GPCR conformations [130].

As mentioned, p24 is able to form homo- or hetero-dimers with other proteins of the p24 family, which is a crucial step in COP vesicle formation. However, dimerization of p24 appears to be linked to sphingolipid binding. In SM C18:0 containing liposomes, p24 homodimerization is significantly increased, whereas a SM-binding deficient mutant has a decreased dimerization propensity, even in the presence of SM C18:0. Unfortunately, the dimerization interface in the p24 TM helix is not described yet, although a molecular dynamics simulation study suggests a rather polar dimerization interface, which does not overlap with the sphingomyelin binding site [123].

It is suggested that the dimeric p24 family proteins immobilize the COP complex at the membrane surface. However, the SM concentrations, which could severely modulate dimerization of p24, significantly differ from the ER to the Golgi and the plasma membrane. Thus, the sphingolipid concentration within a given organelle membrane might directly influence the secretory pathway by triggering the oligomeric state of p24. However, the heterogeneous distribution of SM within a single membrane further complicates such an interpretation, as sphingolipids and cholesterol can form specific lipid microdomains in cellular membranes [131–137].

2.3. C99, the β-secretase cleavage product of the amyloid precursor protein APP specifically binds cholesterol

The TM protein C99, also known as β-CTF, is a key protein in the amyloidogenic pathway. It is associated with the release of amyloid β-peptides and therefore represents a key protein in the development of Alzheimer's disease [138–141]. C99 is produced by the amyloidogenic cleavage of the full-length amyloid precursor protein APP, catalyzed by the β-secretase [141]. This cleavage generates the 99-amino-acid-long single-spanning TM protein C99, which is then cleaved inside the membrane by the γ-secretase to release amyloid-β peptides [142,143]. The structure of the monomeric as well as of the dimeric C99 has been determined by NMR in micellar solutions [144–146] (Fig. 6). An extracellular N-terminus is followed by a surface-attached helix (N-helix) (residues 688–694) and a flexible loop (N-loop) (residues 695–699). The highly curved TM helix (residues 700–723) is kinked close to the center of the micelle, near Gly^{708} and Gly^{709}. This might be related to the processive cleavage by the γ-secretase, as flexibility allows the helix to adopt to the sluice-like active site of the protease [146–149]. Importantly, the proteolytic efficiency is enhanced 2–4 fold in the presence of cholesterol [150].

In recent studies a cholesterol-binding site and a homodimerization interface at C99 were defined [146,151–153]. Homodimerization and cholesterol binding were found to compete, as both involve the glycine zipper motif $G^{700}xxxG^{704}xxxG^{708}G^{709}$ [151] (Fig. 6A). Especially the GxxxG-motifs were expected to promote tight packing of two adjacent C99 TM α-helices, resulting in Van der Waals packing interactions and potentially in formation of C_α hydrogen bonds, as demonstrated for other TM proteins [3,103,154,155]. Indeed, both APP as well as the C99 fragment were found to dimerize, and dimerization is mediated by the GxxxG-motif [110,144,145,156–159]. The isolated C99 TM helix was found to oligomerize strongly in a bacterial membrane when measured with the ToxR-system, and oligomerization was impaired when critical Gly residues of a GxxxG-motif were replaced [110]. Based on the current available data, the β-secretase cleavage product of APP, C99, forms a stable dimer, stabilized by the glycine zipper motif located in the TM domain.

However, the physiological relevance of C99 dimerization is still a matter of debate [151]. In fact, the equilibrium dissociation constant for the dimer was determined to be in the range of 0.5 mol%, indicating

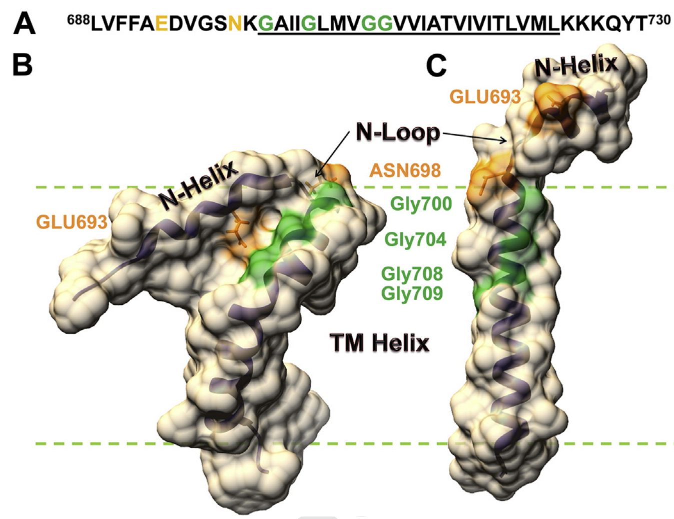

Fig. 6. The transmembrane protein C99. (A) Amino acid sequence of the C99 protein. The TM domain is underlined. (B) C99 structure determined in lyso-myristoylphosphatidylglycerol detergent micelles by nuclear magnetic resonance (NMR) spectroscopy at pH 6.5 (PDB ID: 2LP1). (C). C99 structure determined in dodecylphosphocholine detergent micelles by NMR spectroscopy at pH 4.3–5.3 (PDB ID: 2LLM). In both structures the N-helix and N-loop are labeled, which can rotate freely as their relative position to the TM helix is random in different calculated conformers. The TM helix appears to be more kinked in the 2LP1 structure (B). Residues involved in lipid (cholesterol) binding are highlighted in orange. Amino acids involved in both lipid binding and TM helix dimerization are depicted in green.

that the protein appears to be mainly monomeric at a C99/lipid ratio of 1:200. While the exact C99 concentration has not been quantified in eukaryotic cells, the concentration of the amyloid precursor protein APP in neuronal membranes is in the range of 10^{-3}–10^{-4} mol% [159]. Therefore, C99 might be mostly monomeric under physiological conditions, while it cannot be ruled out that C99 exceeds the concentration of 0.5 mol% in heterogenic membranes and defined lipid domains, where it possibly forms dimers. Recently, the protein and lipid composition of a synaptic vesicle has been determined [160], and here on average about 600 TM domains together with ~7000 phospholipids and ~5000 cholesterol molecules form the vesicle membrane. About one quarter of the membrane volume is represented by the TM domains, and as annular lipids bind more tightly to the TM domains, only a minor fraction of the lipids is expected to be free. At a TM helix-to-lipid ratio of ~1:20, as determined in this study, a significant fraction of the C99 TM domain might be dimeric.

Cholesterol, which is crucial for the formation of lipid domains [161], is suspected to be involved in the development of Alzheimer's disease, as neuronal cholesterol levels increase the production of amyloid-β peptides. Both APP as well as solely the C99 fragment can specifically bind cholesterol, and consequently the C99 TM region is responsible for cholesterol attraction, while the N-terminal C99 extramembrane domain contributes to formation of the lipid-binding site [146,151,156]. The determined equilibrium dissociation constant for cholesterol binding (~3 mol%) is on the low end of the physiological cholesterol concentration in mammalian cells [50,151]. The level of cholesterol in membranes of animal cells can make up to 50 mol% of the membrane lipid content but varies between membrane systems and tissues. The ER and nuclear membrane usually contain 1 to 10 mol% cholesterol, which increases to about 10 to 25 mol% in Golgi stacks and 30–40% in the plasma membrane [50,162–169]. Thus, cholesterol is most likely tightly bound to C99 under physiological conditions. But where and how does cholesterol bind to the short C99 peptide? Previous studies suggested a possible lipid-binding site around the N-helix/N-loop/TM domain element [145,170]. Due to the *trans* ring junctions, cholesterol is a flat molecule (Fig. 3), and binding of the rigid cholesterol to the TM helix is generally expected to be entropically favored over an association of the helix with more flexible diacyl phospholipids. One face of

Please cite this article as: M. Stangl, D. Schneider, Functional competition within a membrane: Lipid recognition *vs.* transmembrane helix oligomerization, Biochim. Biophys. Acta (2015), http://dx.doi.org/10.1016/j.bbamem.2015.03.011

cholesterol, the α-face, is smooth. The opposed β-face carries two methyl groups (C18, C19), resulting in a rough side. Interestingly, residues Gly[700], Gly[704] and Gly[708] of the TM domain, which have been shown to play a crucial role in C99 homooligomerization, appear to be involved in formation of the cholesterol-binding site (Table 1 and Fig. 6), suggesting a competition of homodimerization and cholesterol binding at the glycine zipper motif [151]. The tandem GxxxG motif (+GxxxA) on the C99 TM helix provides a large flat surface spanning over about three helix turns near the extracellular space, which is well-suited to interact with the cholesterol molecule, allowing Van der Waals interactions between the lipid ring system and the TM helix. Cholesterol binds with its relatively rough β-face to the TM domain, whereas the smooth α-face is oriented towards the surrounding lipids. The two methyl groups of the β-face might intrude in protein cavities, resulting in tighter binding [162]. Binding of cholesterol might be further enhanced by hydrogen bond formation between Glu[693] and Asn[698] of the N-loop and the N-helix, respectively, with the 3β OH-group of cholesterol. To optimize the interaction of cholesterol with the soluble regions of C99, a certain flexibility of the N-Loop is given, which allows the N-helix to rotate and to adapt a suitable position to interact with the cholesterol molecule in an induced-fit clamp-like manner [146]. Noteworthy, residues involved in cholesterol binding to C99 are different from postulated cholesterol-binding motifs found in other proteins (CRAC, CARC, CCM) [75,162]. Together, these results indicate that cholesterol binding of C99 depends on (i) the tandem GxxxG motif near the membrane surface, providing a flat attachment surface, (ii) a flexible loop at the membrane water interface and (iii) hydrogen bond formation between amino acids in the soluble region of the MP and the 3β OH-group of cholesterol. In the presence of cholesterol, C99 preferentially interacts with cholesterol rather than with a second monomer to form a homodimer [151]. As the dimerization propensity of C99 is supposed to be low under physiological conditions, and as the interfaces for cholesterol binding and homodimerization highly overlap, cholesterol binding directly competes with TM helix dimerization [151].

However, does cholesterol binding to C99 have an effect on the proteolytic cleavage by the γ-secretase? Numerous reports associate β- and γ-secretase with cholesterol-rich lipid phases in membranes, where the amyloidogenic pathway is active [171–178]. The α-secretase, which is responsible for the non-amyloidogenic pathway, resides in the bulk membrane phase, indicating a specific cholesterol dependence of the amyloidogenic pathway [68,179]. Proteolytic cleavage of C99 by the γ-secretase is dramatically enhanced in cholesterol-containing membranes [150]. Whether cholesterol is bound to C99 during the cleavage process remains an open question. This may be the case, since C99 is cleaved directly below the residues involved in cholesterol binding. Therefore, cholesterol binding might preserve the C99 structure necessary for cleavage by the γ-secretase or acts as a molecular "glue" between C99 and γ-secretase. The γ-secretase appears to cleave both dimeric and monomeric C99 substrates, while the cleavage of monomeric proteins alters the distribution of different amyloid β peptides that are generated [110,158,180,181]. While dimerization of C99 does not conflict with the observations made and also does not affect γ-secretase cleavage [180,181], cholesterol binding to C99 might directly activate γ-secretase cleavage [150] and at the same time directly inhibits α-secretase cleavage [182].

3. Summary: how could lipids control oligomerization of TM helices?

Tight binding of specific lipids to large, polytopic MPs is well described and it is clear that such lipids are intrinsic and essential parts of the MP structure, crucial for the stability and activity of the MP. Effects of global lipid properties, such as the hydrophobic thickness, the lipid head group chemistry, lipid asymmetry or the lateral pressure profile on the interaction of simple, single-span TM proteins have also been analyzed to some extent in the past decade. In contrast, binding of defined lipid species to individual TM helices has moved into the research focus only recently, and regulation of TM helix monomer–oligomer equilibria by binding of defined lipids is a concept, which has emerged only lately.

Lipids bind to single-span MPs, both in the juxta-membrane region as well as in the hydrophobic membrane core. The lipid head groups typically bind *via* electrostatic interactions and hydrogen bond formation at the membrane surface to the protein. Especially, negatively charged lipid head groups appear to be recognized and bound by the extra-membrane regions following individual TM helices. However, in several cases – potentially in all cases – also the acyl chains of a given lipid bind to cavities at the surface of a TM helix *via* Van der Waals interactions. On the surface of the p24 and the C99 protein, regions have been identified, which allow defined packing of the hydrophobic lipid moieties. Nevertheless, an acyl chain region can hardly determine specificity in binding of a diacyl membrane lipid. Only the acyl chain length and/or the degree of saturation are possible determinants for specificity. Thus, it appears to be likely that many different lipids with identical acyl chains can transiently bind to a given TM helix but only lipids with both the correct acyl chain and head group bind more tightly and reside at a TM helix surface for a longer time span. In the case of cholesterol, binding of the hydrophobic region might already be highly specific and defined interactions in the hydrophilic region potentially stabilize the bound lipid.

As summarized here, lipid binding to single-span TM helices can affect the equilibrium between TM helix monomers and higher ordered oligomers. Some interactions counteract oligomerization and in other cases, lipid binding appears to enhance oligomerization. As reversible oligomerization is involved in activation of many MPs, binding of defined lipids to single-span TM proteins might be a mechanism to regulate and/or fine-tune the protein activity. But how could lipid binding trigger the activity of a protein? How can binding of a single lipid molecule to a TM helix affect the structure of a TM helix oligomer, and consequently its signaling state?

The thus far analyzed and here discussed examples of lipid-binding single-span TM proteins highlight some common grounds to be considered in further studies as well as in the design of novel lipid-binding TM sequences (Fig. 7).

1. It still is completely unclear, at which stage TM helix oligomerization and lipid binding eventually compete. Lipids could either bind to a preformed oligomer and thereby stabilize or weaken a TM helix–helix interaction. Alternatively, lipids bind to monomeric proteins and thereby either stabilize the monomeric state or generate an oligomerization-competent monomer. Cholesterol more likely binds to the monomeric C99 protein and thereby hinders formation of TM helix–helix contacts.
2. Binding of negatively charged lipid head groups to stretches of basic amino acids could simply shield clusters of positive charges, decreasing repulsion of positively charged protein regions. Thereby, the positive free energy term caused by the repulsion is diminished, resulting in increased stability of a TM helix oligomer.
3. If binding of a lipid head group is mediated by amino acids located on two different proteins, *i.e.*, if the lipid-binding domain is formed by two different proteins, binding of a lipid would result in formation of a dimeric structure. *E.g.*, in the case of the bacterial light-harvesting proteins, where two individual TM helices interact with pigments, individual pigments intercalate between the two individual TM helices and thereby stabilize the dimeric structure [183, 184]. Similarly, a bound lipid could act as molecular "glue". This might occur in the soluble domains, but promoting and stabilizing TM helix–helix interactions in the hydrophobic TM region are also possible. Intercalation of individual lipids between different proteins is well described in case of large, polytopic TM protein complexes [67].
4. As shown in the case of the Kir2 K^+ channels, binding of a lipid head group to an extra-membrane domain of a protein can induce a conformational change in the extra-membranous regions, which results in

Please cite this article as: M. Stangl, D. Schneider, Functional competition within a membrane: Lipid recognition *vs.* transmembrane helix oligomerization, Biochim. Biophys. Acta (2015), http://dx.doi.org/10.1016/j.bbamem.2015.03.011

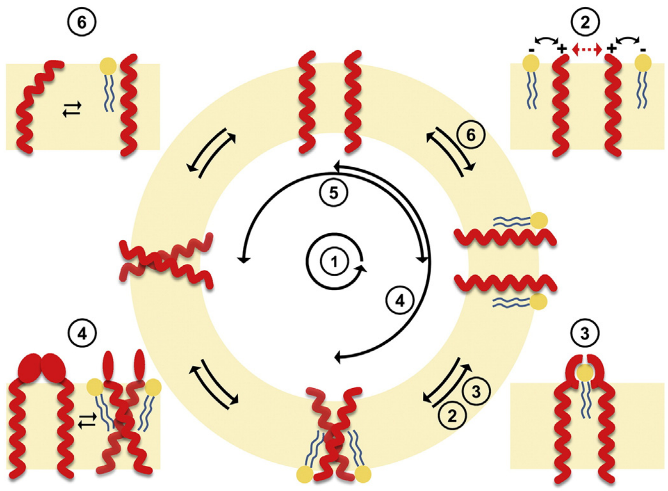

Fig. 7. Lipid binding influences transmembrane helix oligomerization. The monomer–oligomer equilibrium of TM helices might be affected by lipid binding in different ways. (1) Lipids could bind to the monomeric or the oligomeric MPs, and lipid binding could promote or prevent oligomerization. (2) Lipid binding to positively charged amino acids could shield clusters of positive charges and could be involved in the proper positioning of a TM helix within the membrane plane. (3) A lipid-binding cavity might be formed in between two separate proteins, and thus the lipid could act as a molecular "glue". (4) Interaction of protein domains with a lipid can induce structural re-arrangements, preventing or promoting TM helix–helix interactions. (5) When a lipid-binding site overlaps with a dimerization motif, helix–helix interactions directly compete with helix–lipid interactions. (6) Lipid binding to a TM helix can influence the structural dynamics of a TM helix, which impacts TM helix–helix interactions. For further details see the text. The numbers refer to the respective categorization discussed in Section 3.

reorganization of soluble domain interactions, altered steric constraints and finally in altered TM helix–helix interactions. This can then lead to the formation of a TM helix oligomer with an altered structure, favor formation of a TM helix oligomer or drive monomerization of an oligomer.

5. If a lipid binds in a TM region, which is also involved in TM helix oligomerization, as *e.g.*, observed in the case of the C99 TM helix dimer, lipid binding directly competes with TM helix oligomerization and thus, the local concentration of a lipid triggers the oligomeric state.
6. Lipid binding to a surface of a TM helix, which is not involved in formation of TM helix–helix contacts, might induce structural alterations in the TM helix, resulting in increased or diminished interaction propensities. Lipid binding could alter the helix flexibility, which might be required for stable TM helix–helix contacts. Alternatively, lipid binding could affect bending of a helix, which eventually also affects interaction propensities.

Transparency document

The Transparency document associated with this article can be found, in the online version.

Acknowledgments

We would like to thank the Deutsche Forschungsgemeinschaft and the "Stiftung Rheinland-Pfalz für Innovation" for generously supporting our research.

References

[1] W.F. DeGrado, H. Gratkowski, J.D. Lear, How do helix–helix interactions help determine the folds of membrane proteins? Perspectives from the study of homo-oligomeric helical bundles, Protein Sci. 12 (2003) 647–665.
[2] D. Schneider, Rendezvous in a membrane: close packing, hydrogen bonding, and the formation of transmembrane helix oligomers, FEBS Lett. 577 (2004) 5–8.
[3] K.R. Mackenzie, Folding and stability of alpha-helical integral membrane proteins, Chem. Rev. 106 (2006) 1931–1977.
[4] D.P. Ng, B.E. Poulsen, C.M. Deber, Membrane protein misassembly in disease, Biochim. Biophys. Acta 1818 (2012) 1115–1122.
[5] E. Li, W.C. Wimley, K. Hristova, Transmembrane helix dimerization: beyond the search for sequence motifs, Biochim. Biophys. Acta 1818 (2012) 183–193.
[6] C.R. Sanders, J.K. Nagy, Misfolding of membrane proteins in health and disease: the lady or the tiger? Curr. Opin. Struct. Biol. 10 (2000) 438–442.
[7] R. Worch, C. Bokel, S. Hofinger, P. Schwille, T. Weidemann, Focus on composition and interaction potential of single-pass transmembrane domains, Proteomics 10 (2010) 4196–4208.
[8] G. Kemp, F. Cymer, Small membrane proteins — elucidating the function of the needle in the haystack, Biol. Chem. 395 (2014) 1365–1377.
[9] I.D. Campbell, M.J. Humphries, Integrin structure, activation, and interactions, Cold Spring Harb. Perspect. Biol. 3 (2011).
[10] D.S. Harburger, D.A. Calderwood, Integrin signalling at a glance, J. Cell Sci. 122 (2009) 159–163.
[11] H.O. McDevitt, Discovering the role of the major histocompatibility complex in the immune response, Annu. Rev. Immunol. 18 (2000) 1–17.
[12] M.A. Lemmon, J. Schlessinger, Cell signaling by receptor tyrosine kinases, Cell 141 (2010) 1117–1134.
[13] M. Zviling, U. Kochva, I.T. Arkin, How important are transmembrane helices of bitopic membrane proteins? Biochim. Biophys. Acta Biomembr. 1768 (2007) 387–392.
[14] J. Kirrbach, M. Krugliak, C.L. Ried, P. Pagel, I.T. Arkin, D. Langosch, Self-interaction of transmembrane helices representing pre-clusters from the human single-span membrane proteins, Bioinformatics 29 (2013) 1623–1630.
[15] K.E. Gottschalk, P.D. Adams, A.T. Brunger, H. Kessler, Transmembrane signal transduction of the alpha(IIb)beta(3) integrin, Protein Sci. 11 (2002) 1800–1812.
[16] R. Li, R. Gorelik, V. Nanda, P.B. Law, J.D. Lear, W.F. DeGrado, J.S. Bennett, Dimerization of the transmembrane domain of Integrin alphaIIb subunit in cell membranes, J. Biol. Chem. 279 (2004) 26666–26673.
[17] M. Kim, C.V. Carman, T.A. Springer, Bidirectional transmembrane signaling by cytoplasmic domain separation in integrins, Science 301 (2003) 1720–1725.
[18] C. Lu, J. Takagi, T.A. Springer, Association of the membrane proximal regions of the alpha and beta subunit cytoplasmic domains constrains an integrin in the inactive state, J. Biol. Chem. 276 (2001) 14642–14648.
[19] D. Schneider, D.M. Engelman, Involvement of transmembrane domain interactions in signal transduction by alpha/beta integrins, J. Biol. Chem. 279 (2004) 9840–9846.
[20] G. King, A.M. Dixon, Evidence for role of transmembrane helix–helix interactions in the assembly of the Class II major histocompatibility complex, Mol. BioSyst. 6 (2010) 1650–1661.
[21] F. Cymer, D. Schneider, Transmembrane helix–helix interactions involved in ErbB receptor signaling, Cell Adhes. Migr. 4 (2010) 299–312.
[22] E.V. Bocharov, K.S. Mineev, P.E. Volynsky, Y.S. Ermolyuk, E.N. Tkach, A.G. Sobol, V.V. Chupin, M.P. Kirpichnikov, R.G. Efremov, A.S. Arseniev, Spatial structure of the dimeric transmembrane domain of the growth factor receptor ErbB2 presumably corresponding to the receptor active state, J. Biol. Chem. 283 (2008) 6950–6956.
[23] E. Li, K. Hristova, Receptor tyrosine kinase transmembrane domains: function, dimer structure and dimerization energetics, Cell Adhes. Migr. 4 (2010) 249–254.
[24] P.E. Volynsky, A.A. Polyansky, G.N. Fakhrutdinova, E.V. Bocharov, R.G. Efremov, Role of dimerization efficiency of transmembrane domains in activation of fibroblast growth factor receptor 3, J. Am. Chem. Soc. 135 (2013) 8105–8108.
[25] E. Li, K. Hristova, Role of receptor tyrosine kinase transmembrane domains in cell signaling and human pathologies, Biochemistry 45 (2006) 6241–6251.
[26] W.C. Peng, X. Lin, J. Torres, The strong dimerization of the transmembrane domain of the fibroblast growth factor receptor (FGFR) is modulated by C-terminal juxtamembrane residues, Protein Sci. 18 (2009) 450–459.
[27] C. Finger, C. Escher, D. Schneider, The single transmembrane domains of human receptor tyrosine kinases encode self-interactions, Sci. Signal. 2 (2009) ra56.
[28] S.J. Fleishman, J. Schlessinger, N. Ben-Tal, A putative molecular-activation switch in the transmembrane domain of erbB2, Proc. Natl. Acad. Sci. U. S. A. 99 (2002) 15937–15940.
[29] S.E. Harrington, N. Ben-Tal, Structural determinants of transmembrane helical proteins, Structure 17 (2009) 1092–1103.
[30] F. Cymer, A. Veerappan, D. Schneider, Transmembrane helix–helix interactions are modulated by the sequence context and by lipid bilayer properties, Biochim. Biophys. Acta 1818 (2012) 963–973.
[31] H. Hong, Toward understanding driving forces in membrane protein folding, Arch. Biochem. Biophys. 564C (2014) 297–313.
[32] B.J. Bormann, W.J. Knowles, V.T. Marchesi, Synthetic peptides mimic the assembly of transmembrane glycoproteins, J. Biol. Chem. 264 (1989) 4033–4037.
[33] M.A. Lemmon, J.M. Flanagan, J.F. Hunt, B.D. Adair, B.J. Bormann, C.E. Dempsey, D.M. Engelman, Glycophorin A dimerization is driven by specific interactions between transmembrane alpha-helices, J. Biol. Chem. 267 (1992) 7683–7689.
[34] M.A. Lemmon, J.M. Flanagan, H.R. Treutlein, J. Zhang, D.M. Engelman, Sequence specificity in the dimerization of transmembrane alpha-helices, Biochemistry 31 (1992) 12719–12725.
[35] B. Brosig, D. Langosch, The dimerization motif of the glycophorin A transmembrane segment in membranes: importance of glycine residues, Protein Sci. 7 (1998) 1052–1056.
[36] A. Senes, M. Gerstein, D.M. Engelman, Statistical analysis of amino acid patterns in transmembrane helices: the GxxxG motif occurs frequently and in association with beta-branched residues at neighboring positions, J. Mol. Biol. 296 (2000) 921–936.

[37] A.R. Curran, D.M. Engelman, Sequence motifs, polar interactions and conformational changes in helical membrane proteins, Curr. Opin. Struct. Biol. 13 (2003) 412–417.
[38] J.P. Dawson, J.S. Weinger, D.M. Engelman, Motifs of serine and threonine can drive association of transmembrane helices, J. Mol. Biol. 316 (2002) 799–805.
[39] J.P. Dawson, J. Weinger, D.M. Engelman, Hydrogen bonding between serines and threonines drives association of transmembrane helices, Biophys. J. 82 (2002) 533a–534a.
[40] R.M. Johnson, K. Hecht, C.M. Deber, Aromatic and cation–pi interactions enhance helix–helix association in a membrane environment, Biochemistry 46 (2007) 9208–9214.
[41] A. Ridder, P. Skupjen, S. Unterreitmeier, D. Langosch, Tryptophan supports interaction of transmembrane helices, J. Mol. Biol. 354 (2005) 894–902.
[42] R. Laage, D. Langosch, Dimerization of the synaptic vesicle protein synaptobrevin (vesicle-associated membrane protein) II depends on specific residues within the transmembrane segment, Eur. J. Biochem. 249 (1997) 540–546.
[43] H. Gratkowski, J.D. Lear, W.F. DeGrado, Polar side chains drive the association of model transmembrane peptides, Proc. Natl. Acad. Sci. U. S. A. 98 (2001) 880–885.
[44] C. Choma, H. Gratkowski, J.D. Lear, W.F. DeGrado, Asparagine-mediated self-association of a model transmembrane helix, Nat. Struct. Biol. 7 (2000) 161–166.
[45] F.X. Zhou, M.J. Cocco, W.P. Russ, A.T. Brunger, D.M. Engelman, Interhelical hydrogen bonding drives strong interactions in membrane proteins, Nat. Struct. Biol. 7 (2000) 154–160.
[46] F.X. Zhou, H.J. Merianos, A.T. Brunger, D.M. Engelman, Polar residues drive association of polyleucine transmembrane helices, Proc. Natl. Acad. Sci. U. S. A. 98 (2001) 2250–2255.
[47] T. Stockner, W.L. Ash, J.L. MacCallum, D.P. Tieleman, Direct simulation of transmembrane helix association: role of asparagines, Biophys. J. 87 (2004) 1650–1656.
[48] N. Sal-Man, D. Gerber, Y. Shai, The composition rather than position of polar residues (QxxS) drives aspartate receptor transmembrane domain dimerization in vivo, Biochemistry 43 (2004) 2309–2313.
[49] N. Sal-Man, D. Gerber, Y. Shai, The identification of a minimal dimerization motif QXXS that enables homo- and hetero-association of transmembrane helices in vivo, J. Biol. Chem. 280 (2005) 27449–27457.
[50] G. van Meer, D.R. Voelker, G.W. Feigenson, Membrane lipids: where they are and how they behave, Nat. Rev. Mol. Cell Biol. 9 (2008) 112–124.
[51] M.A. Lomize, A.L. Lomize, I.D. Pogozheva, H.I. Mosberg, OPM: orientations of proteins in membranes database, Bioinformatics 22 (2006) 623–625.
[52] D.L. Parton, J.W. Klingelhoefer, M.S. Sansom, Aggregation of model membrane proteins, modulated by hydrophobic mismatch, membrane curvature, and protein class, Biophys. J. 101 (2011) 691–699.
[53] J.A. Killian, Hydrophobic mismatch between proteins and lipids in membranes, Biochim. Biophys. Acta 1376 (1998) 401–415.
[54] T.M. Weiss, P.C. van der Wel, J.A. Killian, R.E. Koeppe 2nd, H.W. Huang, Hydrophobic mismatch between helices and lipid bilayers, Biophys. J. 84 (2003) 379–385.
[55] T. Kim, W. Im, Revisiting hydrophobic mismatch with free energy simulation studies of transmembrane helix tilt and rotation, Biophys. J. 99 (2010) 175–183.
[56] I. Basu, A. Chattopadhyay, C. Mukhopadhyay, Ion channel stability of Gramicidin A in lipid bilayers: effect of hydrophobic mismatch, Biochim. Biophys. Acta 1838 (2014) 328–338.
[57] D.C. Mitchell, Progress in understanding the role of lipids in membrane protein folding, Biochim. Biophys. Acta 1818 (2012) 951–956.
[58] D. Marsh, Lateral pressure profile, spontaneous curvature frustration, and the incorporation and conformation of proteins in membranes, Biophys. J. 93 (2007) 3884–3899.
[59] D. Marsh, Lateral pressure in membranes, Biochim. Biophys. Acta 1286 (1996) 183–223.
[60] A.G. Lee, Lipid–protein interactions in biological membranes: a structural perspective, Biochim. Biophys. Acta Biomembr. 1612 (2003) 1–40.
[61] P.S. Niemela, M.S. Miettinen, L. Monticelli, H. Hammaren, P. Bjelkmar, T. Murtola, E. Lindahl, I. Vattulainen, Membrane proteins diffuse as dynamic complexes with lipids, J. Am. Chem. Soc. 132 (2010) 7574–7575.
[62] A.G. Lee, How lipids affect the activities of integral membrane proteins, Biochim. Biophys. Acta Biomembr. 1666 (2004) 62–87.
[63] A.G. Lee, Lipid–protein interactions, Biochem. Soc. Trans. 39 (2011) 761–766.
[64] F.X. Contreras, A.M. Ernst, F. Wieland, B. Brugger, Specificity of intramembrane protein–lipid interactions, Cold Spring Harb. Perspect. Biol. 3 (2011).
[65] A.M. Ernst, F.X. Contreras, B. Brugger, F. Wieland, Determinants of specificity at the protein–lipid interface in membranes, FEBS Lett. 584 (2010) 1713–1720.
[66] C. Hunte, S. Richers, Lipids and membrane protein structures, Curr. Opin. Struct. Biol. 18 (2008) 406–411.
[67] P.L. Yeagle, Non-covalent binding of membrane lipids to membrane proteins, Biochim. Biophys. Acta 1838 (2014) 1548–1559.
[68] L. Heginbotham, L. Kolmakova-Partensky, C. Miller, Functional reconstitution of a prokaryotic K+ channel, J. Gen. Physiol. 111 (1998) 741–749.
[69] P. Marius, S.J. Alvis, J.M. East, A.G. Lee, The interfacial lipid binding site on the potassium channel KcsA is specific for anionic phospholipids, Biophys. J. 89 (2005) 4081–4089.
[70] F.I. Valiyaveetil, Y. Zhou, R. MacKinnon, Lipids in the structure, folding, and function of the KcsA K+ channel, Biochemistry 41 (2002) 10771–10777.
[71] B. Hoffmann, A. Stockl, M. Schlame, K. Beyer, M. Klingenberg, The reconstituted ADP/ATP carrier activity has an absolute requirement for cardiolipin as shown in cysteine mutants, J. Biol. Chem. 269 (1994) 1940–1944.
[72] E. Pebay-Peyroula, C. Dahout-Gonzalez, R. Kahn, V. Trezeguet, G.J. Lauquin, G. Brandolin, Structure of mitochondrial ADP/ATP carrier in complex with carboxyatractyloside, Nature 426 (2003) 39–44.
[73] H. Li, V. Papadopoulos, Peripheral-type benzodiazepine receptor function in cholesterol transport. Identification of a putative cholesterol recognition/interaction amino acid sequence and consensus pattern, Endocrinology 139 (1998) 4991–4997.
[74] C.J. Baier, J. Fantini, F.J. Barrantes, Disclosure of cholesterol recognition motifs in transmembrane domains of the human nicotinic acetylcholine receptor, Sci. Rep. 1 (2011) 69.
[75] Y.L. Song, A.K. Kenworthy, C.R. Sanders, Cholesterol as a co-solvent and a ligand for membrane proteins, Protein Sci. 23 (2014) 1–22.
[76] M. Palmer, Cholesterol and the activity of bacterial toxins, FEMS Microbiol. Lett. 238 (2004) 281–289.
[77] V. Anbazhagan, F. Cymer, D. Schneider, Unfolding a transmembrane helix dimer: A FRET study in mixed micelles, Arch. Biochem. Biophys. 495 (2010) 159–164.
[78] M. Stangl, A. Veerappan, A. Kroeger, P. Vogel, D. Schneider, Detergent properties influence the stability of the glycophorin A transmembrane helix dimer in lysophosphatidylcholine micelles, Biophys. J. 103 (2012) 2455–2464.
[79] L.E. Fisher, D.M. Engelman, J.N. Sturgis, Detergents modulate dimerization, but not helicity, of the glycophorin A transmembrane domain, J. Mol. Biol. 293 (1999) 639–651.
[80] L.E. Fisher, D.M. Engelman, J.N. Sturgis, Effect of detergents on the association of the glycophorin a transmembrane helix, Biophys. J. 85 (2003) 3097–3105.
[81] A.G. Therien, C.M. Deber, Interhelical packing in detergent micelles. Folding of a cystic fibrosis transmembrane conductance regulator construct, J. Biol. Chem. 277 (2002) 6067–6072.
[82] M. Orzaez, D. Lukovic, C. Abad, E. Perez-Paya, I. Mingarro, Influence of hydrophobic matching on association of model transmembrane fragments containing a minimised glycophorin A dimerisation motif, FEBS Lett. 579 (2005) 1633–1638.
[83] M. Stangl, S. Unger, S. Keller, D. Schneider, Sequence-specific dimerization of a transmembrane helix in amphipol A8–35, PLoS One 9 (2014) e110970.
[84] M. Stangl, M. Hemmelmann, M. Allmeroth, R. Zentel, D. Schneider, A minimal hydrophobicity is needed to employ amphiphilic p(HPMA)-co-p(LMA) random copolymers in membrane research, Biochemistry 53 (2014) 1410–1419.
[85] K.G. Fleming, C.C. Ren, A.K. Doura, M.E. Eisley, F.J. Kobus, A.M. Stanley, Thermodynamics of glycophorin A transmembrane helix dimerization in C14 betaine micelles, Biophys. Chem. 108 (2004) 43–49.
[86] B.D. Adair, D.M. Engelman, Glycophorin A helical transmembrane domains dimerize in phospholipid bilayers: a resonance energy transfer study, Biochemistry 33 (1994) 5539–5544.
[87] V. Anbazhagan, D. Schneider, The membrane environment modulates self-association of the human GpA TM domain—implications for membrane protein folding and transmembrane signaling, Biochim. Biophys. Acta 1798 (2010) 1899–1907.
[88] H.I. Petrache, A. Grossfield, K.R. MacKenzie, D.M. Engelman, T.B. Woolf, Modulation of glycophorin A transmembrane helix interactions by lipid bilayers: molecular dynamics calculations, J. Mol. Biol. 302 (2000) 727–746.
[89] H. Hong, J.U. Bowie, Dramatic destabilization of transmembrane helix interactions by features of natural membrane environments, J. Am. Chem. Soc. 133 (2011) 11389–11398.
[90] B.H. Falkenburger, J.B. Jensen, E.J. Dickson, B.C. Suh, B. Hille, Phosphoinositides: lipid regulators of membrane proteins, J. Physiol. 588 (2010) 3179–3185.
[91] S. McLaughlin, J. Wang, A. Gambhir, D. Murray, PIP(2) and proteins: interactions, organization, and information flow, Annu. Rev. Biophys. Biomol. Struct. 31 (2002) 151–175.
[92] L.F. Horowitz, W. Hirdes, B.C. Suh, D.W. Hilgemann, K. Mackie, B. Hille, Phospholipase C in living cells: activation, inhibition, Ca2+ requirement, and regulation of M current, J. Gen. Physiol. 126 (2005) 243–262.
[93] S.B. Lee, S.G. Rhee, Significance of PIP2 hydrolysis and regulation of phospholipase C isozymes, Curr. Opin. Cell Biol. 7 (1995) 183–189.
[94] T.M. Khuong, R.L. Habets, S. Kuenen, A. Witkowska, J. Kasprowicz, J. Swerts, R. Jahn, G. van den Bogaart, P. Verstreken, Synaptic PI(3,4,5)P3 is required for syntaxin1A clustering and neurotransmitter release, Neuron 77 (2013) 1097–1108.
[95] S. McLaughlin, D. Murray, Plasma membrane phosphoinositide organization by protein electrostatics, Nature 438 (2005) 605–611.
[96] G. Riddihough, More meanders and sandwiches, Nat. Struct. Biol. 1 (1994) 755–757.
[97] K.M. Ferguson, M.A. Lemmon, J. Schlessinger, P.B. Sigler, Structure of the high affinity complex of inositol trisphosphate with a phospholipase C pleckstrin homology domain, Cell 83 (1995) 1037–1046.
[98] M.A. Lemmon, Pleckstrin homology (PH) domains and phosphoinositides, Biochem. Soc. Symp. (2007) 81–93.
[99] M. Soom, R. Schonherr, Y. Kubo, C. Kirsch, R. Klinger, S.H. Heinemann, Multiple PIP2 binding sites in Kir2.1 inwardly rectifying potassium channels, FEBS Lett. 490 (2001) 49–53.
[100] S.B. Hansen, X. Tao, R. MacKinnon, Structural basis of PIP2 activation of the classical inward rectifier K+ channel Kir2.2, Nature 477 (2011) 495–498.
[101] K. Aoyagi, T. Sugaya, M. Umeda, S. Yamamoto, S. Terakawa, M. Takahashi, The activation of exocytotic sites by the formation of phosphatidylinositol 4,5-bisphosphate microdomains at syntaxin clusters, J. Biol. Chem. 280 (2005) 17346–17352.
[102] G. van den Bogaart, K. Meyenberg, H.J. Risselada, H. Amin, K.I. Willig, B.E. Hubrich, M. Dier, S.W. Hell, H. Grubmuller, U. Diederichsen, R. Jahn, Membrane protein sequestering by ionic protein–lipid interactions, Nature 479 (2011) 552–555.
[103] A. Senes, I. Ubarretxena-Belandia, D.M. Engelman, The Calpha–H…O hydrogen bond: a determinant of stability and specificity in transmembrane helix interactions, Proc. Natl. Acad. Sci. U. S. A. 98 (2001) 9056–9061.
[104] I. Fernandez, J. Ubach, I. Dulubova, X. Zhang, T.C. Sudhof, J. Rizo, Three-dimensional structure of an evolutionarily conserved N-terminal domain of syntaxin 1A, Cell 94 (1998) 841–849.

[105] J.C. Lerman, J. Robblee, R. Fairman, F.M. Hughson, Structural analysis of the neuronal SNARE protein syntaxin-1A, Biochemistry 39 (2000) 8470–8479.
[106] R.B. Sutton, D. Fasshauer, R. Jahn, A.T. Brunger, Crystal structure of a SNARE complex involved in synaptic exocytosis at 2.4 A resolution, Nature 395 (1998) 347–353.
[107] K.M. Misura, R.H. Scheller, W.I. Weis, Three-dimensional structure of the neuronal-Sec1–syntaxin 1a complex, Nature 404 (2000) 355–362.
[108] D.H. Kweon, C.S. Kim, Y.K. Shin, The membrane-dipped neuronal SNARE complex: a site-directed spin labeling electron paramagnetic resonance study, Biochemistry 41 (2002) 9264–9268.
[109] A.D. Lam, P. Tryoen-Toth, B. Tsai, N. Vitale, E.L. Stuenkel, SNARE-catalyzed fusion events are regulated by syntaxin1A–lipid interactions, Mol. Biol. Cell 19 (2008) 485–497.
[110] L.M. Munter, P. Voigt, A. Harmeier, D. Kaden, K.E. Gottschalk, C. Weise, R. Pipkorn, M. Schaefer, D. Langosch, G. Multhaup, GxxxG motifs within the amyloid precursor protein transmembrane sequence are critical for the etiology of Abeta42, EMBO J. 26 (2007) 1702–1712.
[111] M. Margittai, H. Otto, R. Jahn, A stable interaction between syntaxin 1a and synaptobrevin 2 mediated by their transmembrane domains, FEBS Lett. 446 (1999) 40–44.
[112] R. Laage, J. Rohde, B. Brosig, D. Langosch, A conserved membrane-spanning amino acid motif drives homomeric and supports heteromeric assembly of presynaptic SNARE proteins, J. Biol. Chem. 275 (2000) 17481–17487.
[113] J.S. Bonifacino, J. Lippincott-Schwartz, Coat proteins: shaping membrane transport, Nat. Rev. Mol. Cell Biol. 4 (2003) 409–414.
[114] H.T. McMahon, I.G. Mills, COP and clathrin-coated vesicle budding: different pathways, common approaches, Curr. Opin. Cell Biol. 16 (2004) 379–391.
[115] J.R. Strating, G.J. Martens, The p24 family and selective transport processes at the ER–Golgi interface, Biol. Cell. 101 (2009) 495–509.
[116] M. Dominguez, K. Dejgaard, J. Fullekrug, S. Dahan, A. Fazel, J.P. Paccaud, D.Y. Thomas, J.J. Bergeron, T. Nilsson, gp25L/emp24/p24 protein family members of the cis-Golgi network bind both COP I and II coatomer, J. Cell Biol. 140 (1998) 751–765.
[117] V. Anantharaman, L. Aravind, The GOLD domain, a novel protein module involved in Golgi function and secretion, Genome Biol. 3 (2002) (research0023).
[118] G. Emery, J. Gruenberg, M. Rojo, The p24 family of transmembrane proteins at the interface between endoplasmic reticulum and Golgi apparatus, Protoplasma 207 (1999) 24–30.
[119] N. Jenne, K. Frey, B. Brugger, F.T. Wieland, Oligomeric state and stoichiometry of p24 proteins in the early secretory pathway, J. Biol. Chem. 277 (2002) 46504–46511.
[120] L.F. Ciufo, A. Boyd, Identification of a lumenal sequence specifying the assembly of Emp24p into p24 complexes in the yeast secretory pathway, J. Biol. Chem. 275 (2000) 8382–8388.
[121] T.A. Fligge, C. Reinhard, C. Harter, F.T. Wieland, M. Przybylski, Oligomerization of peptides analogous to the cytoplasmic domains of coatomer receptors revealed by mass spectrometry, Biochemistry 39 (2000) 8491–8496.
[122] M. Weidler, C. Reinhard, G. Friedrich, F.T. Wieland, P. Rosch, Structure of the cytoplasmic domain of p23 in solution: implications for the formation of COPI vesicles, Biochem. Biophys. Res. Commun. 271 (2000) 401–408.
[123] F.X. Contreras, A.M. Ernst, P. Haberkant, P. Bjorkholm, E. Lindahl, B. Gonen, C. Tischer, A. Elofsson, G. von Heijne, C. Thiele, R. Pepperkok, F. Wieland, B. Brugger, Molecular recognition of a single sphingolipid species by a protein's transmembrane domain, Nature 481 (2012) 525–529.
Q7 [124] R. Mahfoud, N. Garmy, M. Maresca, N. Yahi, A. Puigserver, J. Fantini, Identification of a common sphingolipid-binding domain in Alzheimer, prion, and HIV-1 proteins, J. Biol. Chem. 277 (2002) 11292–11296.
[125] D.G. Cook, J. Fantini, S.L. Spitalnik, F. Gonzalez-Scarano, Binding of human immunodeficiency virus type I (HIV-1) gp120 to galactosylceramide (GalCer): relationship to the V3 loop, Virology 201 (1994) 206–214.
[126] N. Yahi, J.M. Sabatier, S. Baghdiguian, F. Gonzalez-Scarano, J. Fantini, Synthetic multimeric peptides derived from the principal neutralization domain (V3 loop) of human immunodeficiency virus type 1 (HIV-1) gp120 bind to galactosylceramide and block HIV-1 infection in a human CD4-negative mucosal epithelial cell line, J. Virol. 69 (1995) 320–325.
[127] E. Fujita, S.I. Nishimura, Density dependent interaction of polymeric analogs of beta-galactosyl ceramide with GP120 of human immunodeficiency virus 1, Carbohydr. Lett. 4 (2000) 53–60.
[128] J. Fantini, How sphingolipids bind and shape proteins: molecular basis of lipid–protein interactions in lipid shells, rafts and related biomembrane domains, Cell. Mol. Life Sci. 60 (2003) 1027–1032.
[129] A. Chattopadhyay, Y.D. Paila, S. Shrivastava, S. Tiwari, P. Singh, J. Fantini, Sphingolipid-binding domain in the serotonin(1A) receptor, Biochem. Roles Eukaryot. Cell Surf. Macromol. 749 (2012) 279–293.
[130] P. Bjorkholm, A.M. Ernst, M. Hacke, F. Wieland, B. Brugger, G. von Heijne, Identification of novel sphingolipid-binding motifs in mammalian membrane proteins, Biochim. Biophys. Acta 1838 (2014) 2066–2070.
[131] A. Pralle, P. Keller, E.L. Florin, K. Simons, J.K.H. Horber, Sphingolipid–cholesterol rafts diffuse as small entities in the plasma membrane of mammalian cells, J. Cell Biol. 148 (2000) 997–1007.
[132] T. Harder, K. Simons, Caveolae, DIGs, and the dynamics of sphingolipid–cholesterol microdomains, Curr. Opin. Cell Biol. 9 (1997) 534–542.
[133] E. London, D.A. Brown, Insolubility of lipids in Triton X-100: physical origin and relationship to sphingolipid/cholesterol membrane domains (rafts), Biochim. Biophys. Acta Biomembr. 1508 (2000) 182–195.
[134] T. Rog, I. Vattulainen, Cholesterol, sphingolipids, and glycolipids: what do we know about their role in raft-like membranes? Chem. Phys. Lipids 184C (2014) 82–104.
[135] V. Horejsi, M. Hrdinka, Membrane microdomains in immunoreceptor signaling, FEBS Lett. 588 (2014) 2392–2397.
[136] S. Sonnino, A. Prinetti, Membrane domains and the “lipid raft” concept, Curr. Med. Chem. 20 (2013) 4–21.
[137] D.M. Owen, A. Magenau, D. Williamson, K. Gaus, The lipid raft hypothesis revisited—new insights on raft composition and function from super-resolution fluorescence microscopy, Bioessays 34 (2012) 739–747.
[138] W.A. Maltese, S. Wilson, Y. Tan, S. Suomensaari, S. Sinha, R. Barbour, L. McConlogue, Retention of the Alzheimer's amyloid precursor fragment C99 in the endoplasmic reticulum prevents formation of amyloid beta-peptide, J. Biol. Chem. 276 (2001) 20267–20279.
[139] Y. Ling, K. Morgan, N. Kalsheker, Amyloid precursor protein (APP) and the biology of proteolytic processing: relevance to Alzheimer's disease, Int. J. Biochem. Cell Biol. 35 (2003) 1505–1535.
[140] B.L. Tang, Alzheimer's disease: channeling APP to non-amyloidogenic processing, Biochem. Biophys. Res. Commun. 331 (2005) 375–378.
[141] Y.W. Zhang, R. Thompson, H. Zhang, H. Xu, APP processing in Alzheimer's disease, Mol. Brain 4 (2011) 3.
[142] T.L. Kukar, T.B. Ladd, P. Robertson, S.A. Pintchovski, B. Moore, M.A. Bann, Z. Ren, K. Jansen-West, K. Malphrus, S. Eggert, H. Maruyama, B.A. Cottrell, P. Das, G.S. Basi, E.H. Koo, T.E. Golde, Lysine 624 of the amyloid precursor protein (APP) is a critical determinant of amyloid β peptide length: support for a sequential model of γ-secretase intramembrane proteolysis and regulation by the amyloid β precursor protein (APP) juxtamembrane region, J. Biol. Chem. 286 (2011) 39804–39812.
[143] M. Takami, Y. Nagashima, Y. Sano, S. Ishihara, M. Morishima-Kawashima, S. Funamoto, Y. Ihara, gamma-Secretase: successive tripeptide and tetrapeptide release from the transmembrane domain of beta-carboxyl terminal fragment, J. Neurosci. 29 (2009) 13042–13052.
[144] K.D. Nadezhdin, O.V. Bocharova, E.V. Bocharov, A.S. Arseniev, Structural and dynamic study of the transmembrane domain of the amyloid precursor protein, Acta Nat. 3 (2011) 69–76.
[145] K.D. Nadezhdin, O.V. Bocharova, E.V. Bocharov, A.S. Arseniev, Dimeric structure of transmembrane domain of amyloid precursor protein in micellar environment, FEBS Lett. 586 (2012) 1687–1692.
[146] P.J. Barrett, Y.L. Song, W.D. Van Horn, E.J. Hustedt, J.M. Schafer, A. Hadziselimovic, A.J. Beel, C.R. Sanders, The amyloid precursor protein has a flexible transmembrane domain and binds cholesterol, Science 336 (2012) 1168–1171.
[147] S. Urban, Taking the plunge: integrating structural, enzymatic and computational insights into a unified model for membrane-immersed rhomboid proteolysis, Biochem. J. 425 (2010) 501–512.
[148] O. Pester, P.J. Barrett, D. Hornburg, P. Hornburg, R. Probstle, S. Widmaier, C. Kutzner, M. Durrbaum, A. Kapurniotu, C.R. Sanders, C. Scharnagl, D. Langosch, The backbone dynamics of the amyloid precursor protein transmembrane helix provides a rationale for the sequential cleavage mechanism of gamma-secretase, J. Am. Chem. Soc. 135 (2013) 1317–1329.
[149] P. Lu, X.C. Bai, D. Ma, T. Xie, C. Yan, L. Sun, G. Yang, Y. Zhao, R. Zhou, S.H. Scheres, Y. Shi, Three-dimensional structure of human gamma-secretase, Nature 512 (2014) 166–170.
[150] P. Osenkowski, W. Ye, R. Wang, M.S. Wolfe, D.J. Selkoe, Direct and potent regulation of gamma-secretase by its lipid microenvironment, J. Biol. Chem. 283 (2008) 22529–22540.
[151] Y. Song, E.J. Hustedt, S. Brandon, C.R. Sanders, Competition between homodimerization and cholesterol binding to the C99 domain of the amyloid precursor protein, Biochemistry 52 (2013) 5051–5064.
[152] Y. Song, K.F. Mittendorf, Z. Lu, C.R. Sanders, Impact of bilayer lipid composition on the structure and topology of the transmembrane amyloid precursor C99 protein, J. Am. Chem. Soc. 136 (2014) 4093–4096.
[153] C. Di Scala, H. Chahinian, N. Yahi, N. Garmy, J. Fantini, Interaction of Alzheimer's beta-amyloid peptides with cholesterol: mechanistic insights into amyloid pore formation, Biochemistry 53 (2014) 4489–4502.
[154] E. Arbely, I.T. Arkin, Experimental measurement of the strength of a C alpha-H…O bond in a lipid bilayer, J. Am. Chem. Soc. 126 (2004) 5362–5363.
[155] K.R. MacKenzie, J.H. Prestegard, D.M. Engelman, A transmembrane helix dimer: structure and implications, Science 276 (1997) 131–133.
[156] A.J. Beel, C.K. Mobley, H.J. Kim, F. Tian, A. Hadziselimovic, B. Jap, J.H. Prestegard, C.R. Sanders, Structural studies of the transmembrane C-terminal domain of the amyloid precursor protein (APP): does APP function as a cholesterol sensor? Biochemistry 47 (2008) 9428–9446.
[157] P.M. Gorman, S. Kim, M. Guo, R.A. Melnyk, J. McLaurin, P.E. Fraser, J.U. Bowie, A. Chakrabartty, Dimerization of the transmembrane domain of amyloid precursor proteins and familial Alzheimer's disease mutants, BMC Neurosci. 9 (2008) 17.
[158] P. Kienlen-Campard, B. Tasiaux, J. Van Hees, M. Li, S. Huysseune, T. Sato, J.Z. Fei, S. Aimoto, P.J. Courtoy, S.O. Smith, S.N. Constantinescu, J.N. Octave, Amyloidogenic processing but not amyloid precursor protein (APP) intracellular C-terminal domain production requires a precisely oriented APP dimer assembled by transmembrane GXXXG motifs, J. Biol. Chem. 283 (2008) 7733–7744.
[159] L.M. Munter, A. Botev, L. Richter, P.W. Hildebrand, V. Althoff, C. Weise, D. Kaden, G. Multhaup, Aberrant amyloid precursor protein (APP) processing in hereditary forms of Alzheimer disease caused by APP familial Alzheimer disease mutations can be rescued by mutations in the APP GxxxG motif, J. Biol. Chem. 285 (2010) 21636–21643.
[160] S. Takamori, M. Holt, K. Stenius, E.A. Lemke, M. Gronborg, D. Riedel, H. Urlaub, S. Schenck, B. Brugger, P. Ringler, S.A. Muller, B. Rammner, F. Grater, J.S. Hub, B.L. De Groot, G. Mieskes, Y. Moriyama, J. Klingauf, H. Grubmuller, J. Heuser, F. Wieland, R. Jahn, Molecular anatomy of a trafficking organelle, Cell 127 (2006) 831–846.

Please cite this article as: M. Stangl, D. Schneider, Functional competition within a membrane: Lipid recognition *vs.* transmembrane helix oligomerization, Biochim. Biophys. Acta (2015), http://dx.doi.org/10.1016/j.bbamem.2015.03.011

[161] K. Simons, R. Ehehalt, Cholesterol, lipid rafts, and disease, J. Clin. Invest. 110 (2002) 597–603.

[162] W.H. Evans, W.G. Hardison, Phospholipid, cholesterol, polypeptide and glycoprotein composition of hepatic endosome subfractions, Biochem. J. 232 (1985) 33–36.

[163] F. Zambrano, S. Fleischer, B. Fleischer, Lipid composition of the Golgi apparatus of rat kidney and liver in comparison with other subcellular organelles, Biochim. Biophys. Acta 380 (1975) 357–369.

[164] K. Mitra, I. Ubarretxena-Belandia, T. Taguchi, G. Warren, D.M. Engelman, Modulation of the bilayer thickness of exocytic pathway membranes by membrane proteins rather than cholesterol, Proc. Natl. Acad. Sci. U. S. A. 101 (2004) 4083–4088.

[165] A.Y. Andreyev, E. Fahy, Z. Guan, S. Kelly, X. Li, J.G. McDonald, S. Milne, D. Myers, H. Park, A. Ryan, B.M. Thompson, E. Wang, Y. Zhao, H.A. Brown, A.H. Merrill, C.R. Raetz, D.W. Russell, S. Subramaniam, E.A. Dennis, Subcellular organelle lipidomics in TLR-4-activated macrophages, J. Lipid Res. 51 (2010) 2785–2797.

[166] W.G. Wood, M. Cornwell, L.S. Williamson, High performance thin-layer chromatography and densitometry of synaptic plasma membrane lipids, J. Lipid Res. 30 (1989) 775–779.

[167] G. Daum, Lipids of mitochondria, Biochim. Biophys. Acta 822 (1985) 1–42.

[168] A. Radhakrishnan, J.L. Goldstein, J.G. McDonald, M.S. Brown, Switch-like control of SREBP-2 transport triggered by small changes in ER cholesterol: a delicate balance, Cell Metab. 8 (2008) 512–521.

[169] F.R. Maxfield, D. Wustner, Intracellular cholesterol transport, J. Clin. Invest. 110 (2002) 891–898.

[170] M. Zhou, N. Morgner, N.P. Barrera, A. Politis, S.C. Isaacson, D. Matak-Vinkovic, T. Murata, R.A. Bernal, D. Stock, C.V. Robinson, Mass spectrometry of intact V-type ATPases reveals bound lipids and the effects of nucleotide binding, Science 334 (2011) 380–385.

[171] M. Simons, P. Keller, B. De Strooper, K. Beyreuther, C.G. Dotti, K. Simons, Cholesterol depletion inhibits the generation of beta-amyloid in hippocampal neurons, Proc. Natl. Acad. Sci. U. S. A. 95 (1998) 6460–6464.

[172] S. Wahrle, P. Das, A.C. Nyborg, C. McLendon, M. Shoji, T. Kawarabayashi, L.H. Younkin, S.G. Younkin, T.E. Golde, Cholesterol-dependent gamma-secretase activity in buoyant cholesterol-rich membrane microdomains, Neurobiol. Dis. 9 (2002) 11–23.

[173] R. Ehehalt, P. Keller, C. Haass, C. Thiele, K. Simons, Amyloidogenic processing of the Alzheimer beta-amyloid precursor protein depends on lipid rafts, J. Cell Biol. 160 (2003) 113–123.

[174] S.J. Lee, U. Liyanage, P.E. Bickel, W. Xia, P.T. Lansbury Jr., K.S. Kosik, A detergent-insoluble membrane compartment contains A beta in vivo, Nat. Med. 4 (1998) 730–734.

[175] A.J. Beel, M. Sakakura, P.J. Barrett, C.R. Sanders, Direct binding of cholesterol to the amyloid precursor protein: an important interaction in lipid–Alzheimer's disease relationships? Biochim. Biophys. Acta Mol. Cell Biol. Lipids 1801 (2010) 975–982.

[176] H.P. Cheng, K.S. Vetrivel, P. Gong, X. Meckler, A. Parent, G. Thinakaran, Mechanisms of disease: new therapeutic strategies for Alzheimer's disease — targeting APP processing in lipid rafts, Nat. Clin. Pract. Neurol. 3 (2007) 374–382.

[177] G. Di Paolo, T.W. Kim, Linking lipids to Alzheimer's disease: cholesterol and beyond, Nat. Rev. Neurosci. 12 (2011) 284–296.

[178] I.J. Martins, T. Berger, M.J. Sharman, G. Verdile, S.J. Fuller, R.N. Martins, Cholesterol metabolism and transport in the pathogenesis of Alzheimer's disease, J. Neurochem. 111 (2009) 1275–1308.

[179] J.V. Rushworth, N.M. Hooper, Lipid rafts: linking Alzheimer's amyloid-beta production, aggregation, and toxicity at neuronal membranes, Int. J. Alzheimers Dis. 2011 (2010) 603052.

[180] S. Eggert, B. Midthune, B. Cottrell, E.H. Koo, Induced dimerization of the amyloid precursor protein leads to decreased amyloid-beta protein production, J. Biol. Chem. 284 (2009) 28943–28952.

[181] S. Scheuermann, B. Hambsch, L. Hesse, J. Stumm, C. Schmidt, D. Beher, T.A. Bayer, K. Beyreuther, G. Multhaup, Homodimerization of amyloid precursor protein and its implication in the amyloidogenic pathway of Alzheimer's disease, J. Biol. Chem. 276 (2001) 33923–33929.

[182] M. Marenchino, P.T. Williamson, S. Murri, G. Zandomeneghi, H. Wunderli-Allenspach, B.H. Meier, S.D. Kramer, Dynamics and cleavability at the alpha-cleavage site of APP(684–726) in different lipid environments, Biophys. J. 95 (2008) 1460–1473.

[183] J. Fiedor, M. Pilch, L. Fiedor, Tuning the thermodynamics of association of transmembrane helices, J. Phys. Chem. B 113 (2009) 12831–12838.

[184] V. Arluison, J. Seguin, J.P. Le Caer, J.N. Sturgis, B. Robert, Hydrophobic pockets at the membrane interface: an original mechanism for membrane protein interactions, Biochemistry 43 (2004) 1276–1282.

[185] J. Fantini, F.J. Barrantes, How cholesterol interacts with membrane proteins: an exploration of cholesterol-binding sites including CRAC, CARC, and tilted domains, Front. Physiol. 4 (2013).

[186] M.A. Hanson, V. Cherezov, M.T. Griffith, C.B. Roth, V.P. Jaakola, E.Y.T. Chien, J. Velasquez, P. Kuhn, R.C. Stevens, A specific cholesterol binding site is established by the 2.8 angstrom structure of the human beta(2)-adrenergic receptor, Structure 16 (2008) 897–905.

[187] C. Di Scala, N. Yahi, C. Lelievre, N. Garmy, H. Chahinian, J. Fantini, Biochemical identification of a linear cholesterol-binding domain within Alzheimer's beta amyloid peptide, ACS Chem. Neurosci. 4 (2013) 509–517.

[188] R. Mahfoud, N. Garmy, M. Maresca, N. Yahi, A. Puigserver, J. Fantini, Identification of a common sphingolipid-binding domain in Alzheimer, prion, and HIV-1 proteins, J. Biol. Chem. 277 (2002) 11292–11296.

[189] D.H. Murray, L.K. Tamm, Clustering of syntaxin-1A in model membranes is modulated by phosphatidylinositol 4,5-bisphosphate and cholesterol, Biochemistry 48 (2009) 4617–4625.

[190] C. Hunte, Specific protein–lipid interactions in membrane proteins, Biochem. Soc. Trans. 33 (2005) 938–942.

[191] J. Maupetit, P. Derreumaux, P. Tuffery, PEP-FOLD: an online resource for de novo peptide structure prediction, Nucleic Acids Res. 37 (2009) W498–W503.

[192] J. Maupetit, P. Derreumaux, P. Tuffery, A fast method for large-scale de novo peptide and miniprotein structure prediction, J. Comput. Chem. 31 (2010) 726–738.

[193] P. Thevenet, Y. Shen, J. Maupetit, F. Guyon, P. Derreumaux, P. Tuffery, PEP-FOLD: an updated de novo structure prediction server for both linear and disulfide bonded cyclic peptides, Nucleic Acids Res. 40 (2012) W288–W293.